

Imperial College of Science & Technology
University of London
Department of Electrical Engineering

THE SIX-PHASE TWO-CIRCUIT SYNCHRONOUS
GENERATOR AND ITS ASSOCIATED TRANSFORMER

By

Robert Alexander Hanna

B.Sc. (Eng.), M.Sc.

Thesis submitted for the degree of
Doctor of Philosophy in the Faculty
of Engineering

January, 1978

ABSTRACT

Six-phase stator windings have been proposed for two-pole generators above 700 MVA. The current per circuit is reduced when compared with a 3-ph machine, and the output coefficient is slightly higher.

In these machines each phase band is 30° wide and two 3-ph outputs are obtained separated by 30° in time phase. These are connected into the 3-ph power system through a star-delta/star transformer arrangement. Here tests on a 6-ph micro-generator are described. It is then tested in conjunction with a transformer arrangement designed and built in the course of the work.

Harmonic voltages and currents in the generator and the transformer are studied and their behaviour is accounted for theoretically. Fifth and seventh harmonics can be a problem, and recommendations are made to avoid this difficulty.

The difficulties of designing micro-transformers are discussed, and the equivalent circuits of the special transformer required are derived from first principles.

The harmonic effects are shown to be governed by expressions different from those for 3-ph machines. However, it is shown that with suitable design, including transformer tertiary windings, the harmonic currents can be made acceptably low.

ACKNOWLEDGEMENTS

The work in this thesis was carried out under the supervision of Dr. D.C. Macdonald, B.Sc. (Eng.), Ph.D., M.I.E.E., C.Eng., Lecturer in Electrical Engineering Department, Imperial College of Science and Technology, London. I wish to express my sincere gratitude to Dr. Macdonald for his helpful guidance, constant encouragement and keen interest during the preparation and completion of this project.

I also wish to express my sincere thanks to Dr. P.G.H. Allen, Senior Lecturer, Electrical Engineering Department, for his supervision in several aspects of this work.

I wish to acknowledge the valuable discussions I have had with Dr. B. Adkins and Mr. C.J. Carpenter throughout this work.

I wish to thank Mr. H.E. Pettitt, Chief Engineer, GEC Transformers Limited, Stafford, for reading and commenting on the micro-transformer design exercise.

I am grateful to the Ministry of Higher Education and Scientific Research of the Government of the Republic of Iraq for their financial support, which made this work possible.

Finally, I wish to extend appreciation to all my colleagues in the Power System Laboratory, especially Dr. A.Y. Hannalla, Mr. M.H.S. El-Markabi for many fruitful conversations, Mr. E. Horne and Dr. C.B. Giles for their assistance in the preparation of this thesis, and Mr. J.C. McDonald for skillful technical help in constructing the micro-transformers.

This project was supported by S.R.C.

To
my beloved parents
and Olive

	<u>Page</u>
3.3.3 Differential or air gap leakage reactance	66
3.3.3.1 Zigzag leakage reactance	67
3.3.3.2 Belt leakage reactance	68
3.4 Calculation of the magnetizing and leakage reactances for the laboratory micro-machine	70
<u>Chapter 4:</u> Experimental and Theoretical Investigation of Time Harmonic Currents in a Synchronous Machine connected in Six and Three Phases	78
4.1 Introduction	78
4.2 Description of the micro-generator model	78
4.3 Open circuit and short circuit tests	79
4.3.1 Determination of X_d and X_q	84
4.4 Theoretical analysis and computation	88
4.4.1 Calculation of open circuit harmonic voltages	89
4.4.2 Analysis and calculation of steady state short circuit harmonic currents	91
4.5 Comparison of experimental and computed results	93
4.6 Conclusions	97
<u>Chapter 5</u> Design, Construction and Testing of 6-ph/3-ph Micro-Transformer Bank	98
5.1 Introduction	98
5.2 Survey of proposed generator transformer arrangement	99
5.3 Description of the transformer arrangement presented by this work	107
5.4 Rating of the micro-transformer	110
5.5 Design of the micro-transformer	110
5.5.1 Determination of the winding dimensions	115
5.5.2 Losses in the micro-transformer	118
5.5.3 Required weight of copper	120
5.5.4 Magnetizing current	121
5.6 Micro-transformer construction	121
5.7 Micro-transformer testing	126
5.8 Conclusions	133

	<u>Page</u>
List of References	230
 <u>Appendices:</u>	
A. Calculation of the effective air gap length and the saliency effects on the m.m.f. waveform.	233
B. Listing of alternative micro-transformer designs.	238
C. Short circuit and open circuit test results for the micro-transformer.	240
D. Determination of the iron reluctances of the micro-transformer.	243

LIST OF SYMBOLS AND ABBREVIATIONSSYMBOLS

Capital Letters:

A	Area
B	Magnetic flux density, susceptance
C	Coefficient, capacitance
D	Air gap diameter, mean diameter of transformer winding
E	Induced voltage
F	Magnetomotive force
G	Effective air gap length, conductance
H	Magnetic field intensity
I	Current
J	Current density
K	Defined factor, coefficient
L	Effective core length, inductance
N	Number of turns
R	Resistance
S	Slots per phase
T	Number of turns per phase
V	Voltage
X	Reactance
Y	Admittance
Z	Impedance

Small Letters:

a	Ratio of actual to effective air gap length, cross-sectional area of conductor
f	Field, frequency
g	Actual air gap length
h	Order of stator space harmonic, slot depth, window height
i	Current
j	90° operator
k	Defined factor, coefficient
ℓ	Gross core length
m	Number of phases
n	Order of time harmonic
p	Number of pole pairs

q	Slots per pole per winding, slots per pole per phase
r	Winding radius
s	Slip, number of slots per pole
t	Radial thickness of winding, radial clearance between pair of windings
v	Voltage
w	Slot width
z	Number of series conductors per tier

GREEK LETTERS

α	Angle between divided rotor windings, stator slot angle
β	Rotor slot angle, separation angle between the rotor and stator reference lines at time $t = 0$
γ	Slot pitch in radiant
θ	Position angle
μ_0	Permeability of air = $4\pi \times 10^{-7}$ H/m
ν	Order of rotor space harmonic
ρ	Ratio of coil span to pole pitch or coil pitch, resistivity
τ	Pole pitch
Φ	Magnetic flux
φ	Time phase angle indicating the instant of the maximum of magnetomotive force
ω	Angular velocity

SUBSCRIPTS

a	Axial, armature
b	Belt
c	Connection
d	Distribution
e	Effective, end
f	Field
g	Gap
h	Order of stator space harmonic
i	Inner, iron
l	Leakage
m	Magnetizing, magnetic
n	Order of time harmonic

o	Outer
p	Pitch, peripheral
r	Reactive winding, rotor, resultant
s	Stator, skew, slot, search coil
t	Torque winding
w	Winding
z	Zigzag

ABBREVIATIONS

m.m.f.	Magnetomotive force
ph	Phase
l.v.	Low voltage
h.v.	High voltage
max	Maximum
md	Magnetic dual quantity
N_{ph}	Number of turns per phase

CHAPTER ONEINTRODUCTION1.1 GENERAL

The development and growth of electric power systems has led to a steady increase in the rating of generating plant. Economic considerations have provided the major incentive for building larger generators. The output of a generator at a given speed is proportional to the product of magnetic flux and stator ampere-turns. The largest ratings result from maximizing both of these variables. However, each has its typical effects on the generator design and gives rise to its own characteristic limitations.

At one extreme^{1,2}, if the magnetic flux per pole is not changed as ratings are increased, the same winding pattern and terminal voltage can be maintained, but the electromagnetic forces on the stator bars, pushing them to the bottom of the slots, will increase as the square of the ratings. Also, the generator efficiency and transient reactances will deteriorate rapidly.

If, however, the magnetic flux and hence generator size are increased and a fixed winding pattern is maintained, terminal voltage will increase in direct proportion. Consequently, more spacing is required for insulation, compounding the problems of providing electrical clearances. In addition, the active copper area and coolant space in the armature winding may tend to be reduced if the physical size of the machine has not been increased appreciably. This will increase losses and reduce the winding transient overload capability.

Instead, the tendency has been to increase flux per pole and armature m.m.f. together in some preferred ratio, thus avoiding excessive terminal voltage and producing only a linear increase of electromagnetic forces with rating. Various design techniques have been developed in order to achieve these objectives.

For a given magnetic flux, the important variable determining generator voltage is the number of turns connected in series per phase. For a double layer winding with single-turn coils, the latter is equal to the ratio of number of slots to the product of the number of parallel circuits per phase and the number of phases. The problem of reducing generator voltage is then resolved to obtaining the minimum practical value of this ratio. However, both the number of slots and the number of parallel circuits per phase are subjected to design limitations.

With a very small number of slots the current per slot and the corresponding electromagnetic forces on the stator bars are increased, pressing them into the slots. In addition, very wide slots will result in increased losses both in the rotor surface and the stator conductors.

On the other hand, the number of parallel circuits per phase in a conventional winding has been almost universally restricted so as not to exceed the number of field poles. Thus, large 2-pole generators have been constructed with two circuits to keep the generator voltage low. The logic behind this restriction is to keep all parallel circuits electrically identical and thus avoid circulating currents between them. If the winding could be subdivided further, the current per circuit would be reduced in proportion, and the

force acting on the bars in the slots, being dependent on the square of the current, would be very significantly reduced for a given rating. Alternatively, much higher outputs would be possible without exceeding a force level that has been proven to be acceptable.

Three basic methods are available to overcome the above-mentioned problems. The first, which is described by Holley and Willyoung¹, is to keep the number of slots large but to divide each phase band into two parallel circuits, giving a winding having four parallel paths per phase. This division of the voltage by an integer is sufficient to give a worthwhile reduction of insulation thickness with increased space factor and saving in cost. The distribution of the coils between two such phase bands requires very detailed analysis to ensure that the voltages generated in the two parallel circuits of each phase band are closely balanced. In addition, their reactances must be nearly equal to avoid harmful circulating currents and unbalanced loading between phase bands. The main disadvantage of these winding arrangements is that they involve complicated end connections to the coils.

The second¹ is to connect the generator internally in delta instead of star configuration. The application of this principle is, however, rather limited because of the constraints imposed on the winding design by the need to minimise harmonic circulating currents to avoid excessive parasitic losses, particularly in the rotor surface.

The third and by far most attractive method is to divide each phase band into two and to produce what is essentially a 12-phase machine, each circuit displaced 30° electrically from the

next, compared with the 60° displacement of the normal 6-phase double-layer winding of a two-pole machine. Every two circuits, which have their generated voltages 180° apart, are connected properly in parallel, thus producing what is called a "6-ph winding" comprising two separate sets of 3-ph windings displaced by 30° electrically. The 6-ph machine can then be connected to 3-ph busbars by choosing an appropriate transformer arrangement.

1.2 ADVANTAGES OF SIX-PHASE GENERATORS

The idea of providing a generator with more than one winding is at least forty years old. It was introduced in the early 1930's³ when sets rated at up to 160 MVA led to circuit breaker capacity problems. These were alleviated by providing two independent three-phase windings generating in-phase sets of voltages, each connected to the common busbars through its own circuit breaker. These machines proved adequate until the fault current problem was mitigated by connecting each generator to its own step-up transformer, with switching accomplished on the high voltage side. Today, however, the idea is being applied to secure improvement in the design and performance of the generator itself.

The use of a two-circuit 6-ph winding for building large generators has been proposed^{4,5} and is reported to be under construction in the USSR⁶. The basic advantages of increasing the number of generator winding phases are:

1. For a given size of machine the same output power can be obtained from 6 phases as from 3 phases, but at approximately half of the terminal voltage. Consequently, less insulation

thickness is required for the conductors in the slots and the available additional slot area may be used for other purposes. For example, both the conductor cross-sectional area and the current density may be increased provided that the forces on the conductors are kept within an acceptable limit. On the other hand, a larger number of slots can be used to reduce the forces on the conductors without causing excessive terminal voltage. Thus it can be said that for the same physical dimensions, a generator embodying the 6-ph winding may be rated to a higher power output than when it has a conventional 3-ph winding.

2. Space harmonics of the stator m.m.f. have orders $(2km \pm 1)$ where m is the number of winding phases and k is an integer. Thus, on going from 3 to 6 phases, 5th, 7th, 17th and 19th harmonics are eliminated, leaving only the 11th, 13th, 23rd and 25th. Since each harmonic magnitude is reduced by the reciprocal of its harmonic order times the harmonic winding factor, and the principal harmonics (11th and 13th) can be largely pitched out by using about 11/12 coil pitch, it is evident that this generator will have a very low harmonic m.m.f. content. Benefits accrue due to reduced rotor surface losses and hence higher efficiency^{7,8}. Such generators should be particularly attractive for feeding power to a d.c. transmission grid because of their reduced sensitivity to harmonics in the line current which will be introduced by the rectifier system.
3. The replacement of a 3-ph, 60° phase belt winding having 5/6 coil pitch by a 6-ph, 30° phase belt winding having

11/12 coil pitch increases the power output of the machine by nearly 6.0%. This means that for the same dimensions and power output, the ampere-turns will be reduced to the same extent and that losses varying with the load will be lower by 12%.

Cost penalties might be anticipated because six busbars are required instead of only three, and a special arrangement of three single unit transformer banks is necessary. This is not so, however, when the MVA rating of the transformer or the transmission voltage is sufficient to preclude the use of a low-cost three-phase single tank transformer. Estimating the true economic balance between the 3-ph and 6-ph machines is not straightforward and depends on many factors. The study presented in ref. 1 shows that the evaluated first cost of the generator-bus-transformer complex tends to be slightly higher for 6-ph system, relative to conventionally connected generators.

1.3 CONTENTS OF THE PRESENT WORK

The main objective of this thesis is to highlight some of the problems arising from the 6-ph machine winding arrangement and to provide sound solutions based on experimental and theoretical investigations. The studies made here can be broadly divided into three parts. These are:

- (i) a comparison between a 6-ph and a 3-ph machine with reference to the presence of harmonics (Chapters 2, 3 and 4);
- (ii) a transformer arrangement is described to couple a 6-ph machine to a 3-ph system and a "micro" version of it is designed, built, tested, and an equivalent circuit is

developed (Chapters 5 and 6);

- (iii) behaviour of harmonics in a 6-ph generator and its associated 6-ph/3-ph transformer bank when on open circuit and when delivering power to 3-ph system (Chapter 7).

In Chapter 2 a general expression is derived for the space harmonic m.m.f. produced by a 6-ph winding when carrying non-sinusoidal current. Special attention is paid to the behaviour of 3rd harmonic current in the new winding arrangement. A three-phase winding is considered as a special case of the general approach developed for a 6-ph winding. Formulae are given for obtaining the distribution factor for any 6-ph machine from that of the corresponding 3-ph machine which is normally available.

In Chapter 3 formulae are developed for the magnetizing and leakage reactances at each harmonic frequency for both 6-ph and 3-ph machines. Slot leakage reactance, which is the dominant component of the leakage reactance, is analysed in more detail. These expressions are used to obtain the harmonic reactances for the laboratory micro-machine when connected in 6 and 3 phases.

In Chapter 4 the results of open circuit and steady state short circuit tests are presented for the laboratory micro-machine connected in 6 and 3 phases. An analytical method is described for predicting the individual harmonic components of current at different excitation levels. Tables are shown comparing the calculated and measured harmonics to check the validity of the method developed.

In Chapter 5 the main methods so far proposed to couple a 6-ph generator to a 3-ph system are surveyed critically. In addition, a new transformer arrangement is described and the details of the design work for a "micro" version of it are included. The problems associated with building a micro-transformer to simulate a large generator transformer are discussed. Parameters of the micro-transformer are measured and compared with the calculated values to ensure that the design work is satisfactory.

In Chapter 6 a method is given whereby an equivalent circuit of a four-limb four-winding transformer is obtained. It contains as many branches as may be necessary for determining the performance of the transformer in the steady state. The main value of this approach is to derive an equivalent circuit so that the effect of any changes in transformer construction or in the method of exciting the windings can easily be recognized. The equivalent circuit is arranged to allow for series and parallel connections of high voltage winding sections. The parameters of the equivalent circuit are determined.

In Chapter 7 the behaviour of harmonics in a 6-ph generator and its associated 6-ph/3-ph transformer bank are investigated. The study includes the harmonics generated within the transformer in addition to those arising from non-sinusoidal generator voltage when delivering power to 3-ph busbars. The effect of the presence of a tertiary winding on the current and voltage waveforms is demonstrated for the high voltage winding sections connected in series and in parallel. It is shown that the magnitude of the current harmonics of order $n = 12k \pm 5$ ($k = 0, 1, 2, 3, \dots$) originating in the generator are dependent on the transformer winding arrangement. These harmonics are suppressed from either side of the transformer if the h.v. winding

sections are connected in series, but if they are put in parallel a closed path is provided for them to circulate and therefore they appear on the generator-transformer side. It is also shown that the equivalent circuit of the transformer derived in Chapter 6 for fundamental frequency current requires substantial modification to account for the behaviour of these harmonic currents. The performance of a two-limb transformer when subjected to these harmonics is compared with that of the four-limb transformer used.

1.4 CONTRIBUTIONS OF THE THESIS

It is thought that the following matters in the thesis are original contributions:

1. Sets of curves relating the slot leakage factor with respect to time harmonic currents versus coil pitch are derived for a 6-ph machine which differ from those already known for a 3-ph machine.
2. The behaviour of time harmonic currents in a 6-ph machine under steady state short circuit conditions is studied experimentally and a method is developed for predicting each of these harmonics, and it is shown that a coil pitch of $5/6$ gives the largest 5th and 7th harmonic currents.
3. A new transformer arrangement is described to couple a 6-ph machine to a 3-ph system; a "micro" version has been designed, constructed and tested which has 0.6% copper loss and 9.0% leakage reactance to simulate a large generator transformer.

4. A method is described for the development of an equivalent circuit for the multi-winding transformer tested here which contains as many branches as may be necessary for studying the performance of the transformer. The main feature of the approach used is that the non-linear elements in the magnetic circuit are represented by equivalent elements in the electric circuit.
5. It is shown that the use of tertiary windings with the 6-ph/3-ph transformer bank used here is essential if its h.v. winding sections are connected in series, but if they are put in parallel it is only necessary when the third harmonic current circulating between the h.v. windings would otherwise be excessive.
6. The presence of current harmonics of order $n = 12k \pm 5$ ($k = 0, 1, 2, 3, \dots$) originating in the generator depends on the connection mode of h.v. winding sections. Series connection eliminates them from either side of the transformer, but parallel connection provides a path for them to circulate and they therefore appear on the generator-transformer side. These harmonic currents do not produce fundamental space harmonic and thus their effect in a 6-ph machine is less harmful than they would be in a 3-ph machine.

CHAPTER TWOHARMONIC ANALYSIS OF M.M.F. IN A SYNCHRONOUS
MACHINE CONNECTED IN SIX AND THREE PHASES2.1 INTRODUCTION

Because the stator windings of multiphase machines consist of coils arranged in a finite number of slots and connected in a finite number of phases, the shape of the wave of travelling m.m.f. is not sinusoidal, even though the winding carries balanced sinusoidal polyphase currents.

The analysis of m.m.f. waveform shows that it contains a series of harmonics in addition to the fundamental whose pole pitch is determined by the number of pole pairs of the machine. The arrangement of the stator windings controls the harmonic content of the waveform and may even suppress some harmonics completely.

It is well established that the dominant m.m.f. space harmonics in a 3-ph winding with 60° phase belts are the fifth and seventh, and can normally be controlled by selecting a coil span of $5/6$. In this chapter, the space harmonics arising in 6-ph windings with 30° phase belts when carrying non-sinusoidal balanced currents are discussed with a view to the choice of the best pitch factor. Three-phase windings are considered as a special case of the general approach for a 6-ph winding.

2.2 HARMONICS IN THE AIRGAP FIELD OF A SYNCHRONOUS MACHINE

The air gap field of a synchronous machine includes, besides the fundamental, a multitude of harmonics with multiples of

the fundamental number of poles. These harmonics are usually objectionable, producing supplementary loss and distortion in the generator voltage waveform. They arise from two causes:

1. The winding is discontinuous and concentrated in slots and coil groups. Hence, the air gap m.m.f. which is produced by the stator and rotor windings is non-sinusoidal.
2. The permeance of the air gap is not constant. Permeance variation is caused by the stator and rotor slot openings, saliency and iron saturation.

The harmonics due to slot openings and saturation are ignored in this work but the effect of the saliency is discussed in Appendix A. The harmonics created under the first heading above are fully investigated in subsequent sections for a synchronous machine when connected in 6 and 3 phases.

2.3 HARMONICS M.M.F. PRODUCED BY ROTOR WINDING.

Constructionally, synchronous machine rotors are of two basic types: cylindrical rotors with distributed windings, and salient pole rotors with concentric windings. Only the first type is considered as it is used exclusively with high speed turbo-generators of large capacity where the diameter of the rotor must be kept small in order to avoid excessive centrifugal forces.

Although most cylindrical rotors have a single distributed winding, considerable interest is being taken in the divided-winding rotor (d.w.r.) for large generators, particularly because it offers an increase in the steady state stability limit and improves the

transient stability⁹. The d.w.r. machine is beyond the scope of this work, but it is briefly discussed here because the experimental laboratory micro-machine, the details of which are given in Section 4.2, has a rotor winding of this kind.

The rotor is slotted in the conventional way, but the rotor conductors are divided into separate sections, as shown in Fig. 2.1, to provide two windings, the direct axis being between the two winding axes, and inclined at an angle of less than 90° electric from each other. This angle is preferably about 60° electrical because, in practice, it is not feasible, on economic grounds, to slot more than two-thirds of the rotor periphery as this will increase the magnetic saturation in the poles. The benefits arise because the direction of the rotor m.m.f. is no longer rigidly related to the angular position of the rotor, but can be varied by adjusting the currents in the two sections of the winding, thereby eliminating the time delay otherwise involved in accelerating or decelerating the high inertia rotor system of the set.

The space harmonic m.m.f. produced by the rotor winding has an important effect on the induced voltage waveform of the stator winding and, therefore, is investigated first.

Assuming that the coil m.m.f. is concentrated at slot openings of negligible width, the m.m.f. distribution of each winding of the divided-winding rotor carrying a direct current will be as shown in Fig. 2.1(a). By the well-known Fourier method of analysis, the stepped m.m.f. distribution may be represented as the sum of a series of sine waves. Thus the m.m.f. F_r (see Fig. 2.1(b)), at any angular position θ_r from the d-axis, is:

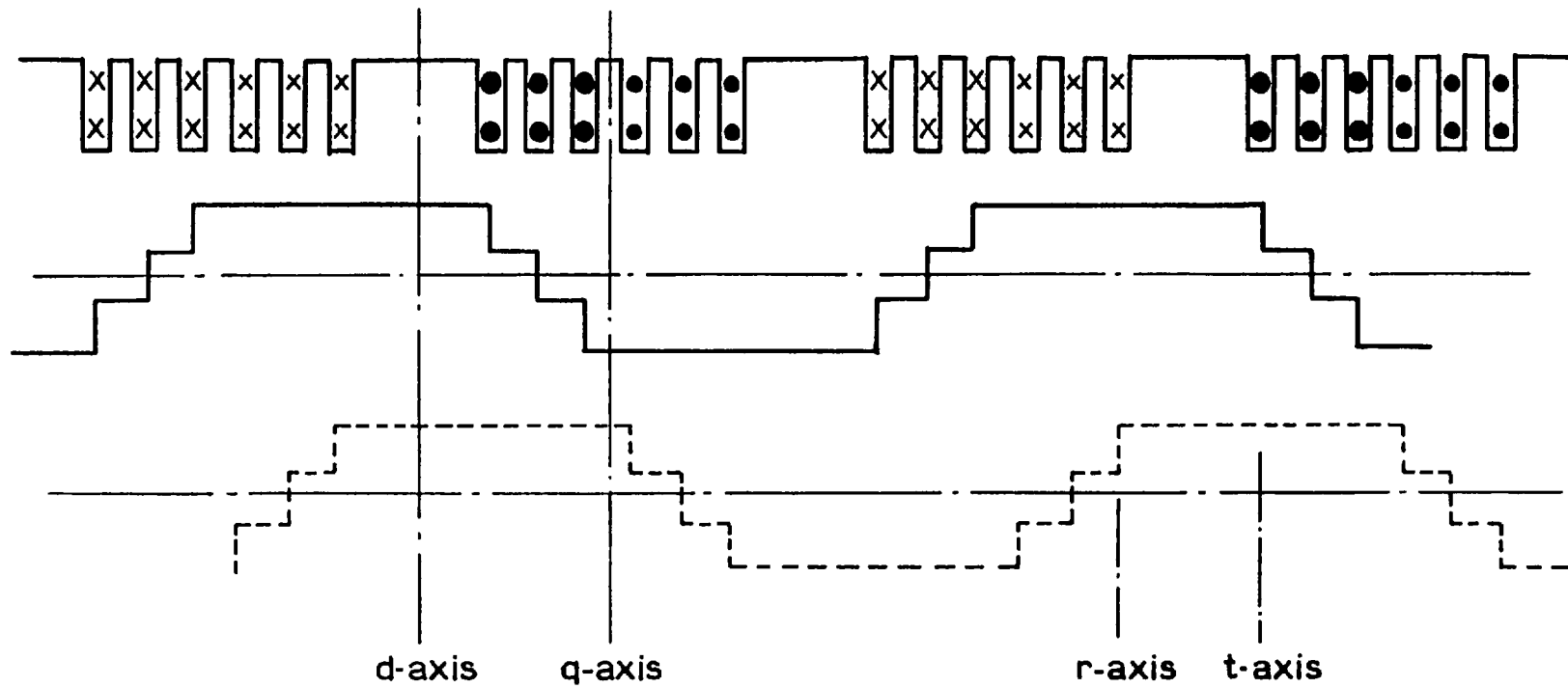


Fig. 2-1(a) Divided-winding rotor and its m.m.f. distribution. Number of slots/pole/winding=6

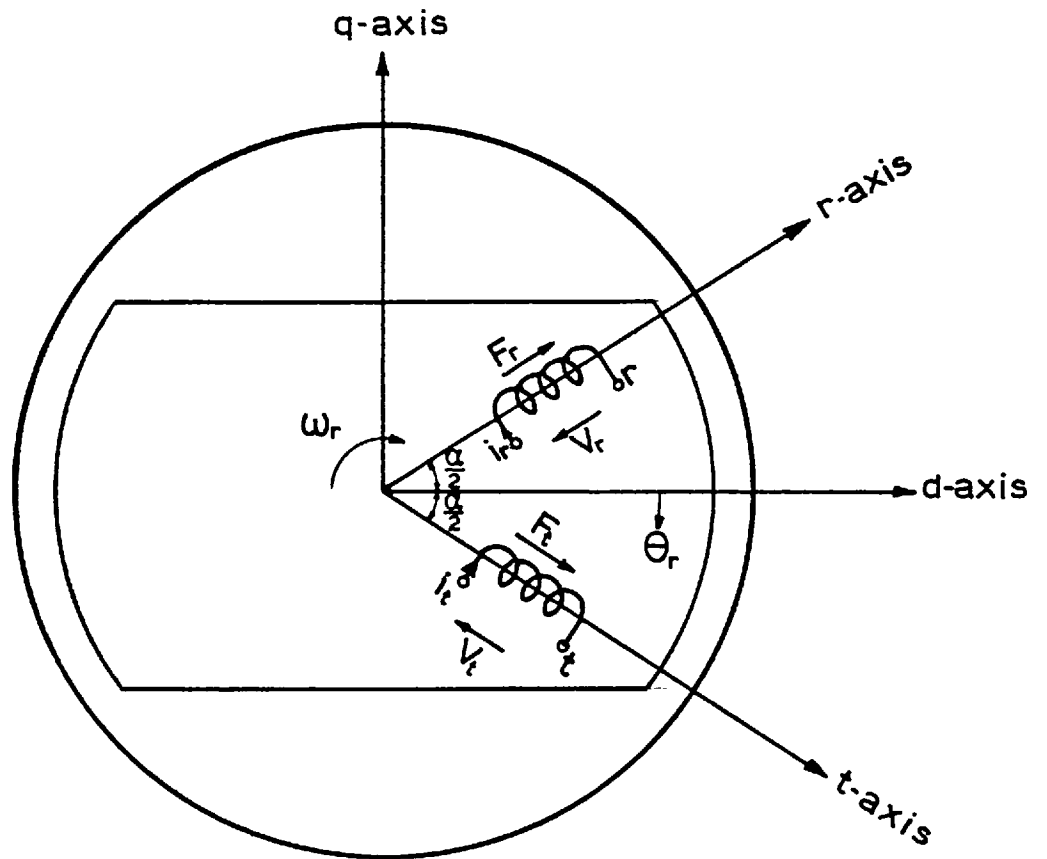


Fig. 21(b) Schematic layout of divided-winding rotor.

$$F_r = \frac{4}{\pi} \frac{N_r q}{2} I_r \sum_{V=1}^{\infty} \frac{K_{dV}}{V} \cos V(\theta_r + \frac{\alpha}{2}) \quad (2.1.a)$$

and

$$F_t = \frac{4}{\pi} \frac{N_t q}{2} I_t \sum_{V=1}^{\infty} \frac{K_{dV}}{V} \cos V(\theta_r - \frac{\alpha}{2}) \quad (2.1.b)$$

where,

N_r, N_t : r and t winding number of turns,

I_r, I_t : r and t winding currents,

q : slots/pole/winding,

V : order of space harmonic which is an odd integer because the m.m.f. waveform is repetitive at intervals of π for the regular windings considered here,

$\alpha/2$: angle between each winding axis and the d-axis,

K_{dV} : distribution factor for V^{th} harmonic = $\frac{\sin Vq \beta/2}{q \sin V \beta/2}$

β : rotor slot angle.

The resultant field m.m.f. F_f is the summation of the two components

$$F_f = \frac{2}{\pi} q \sum_{V=1}^{\infty} \frac{K_{dV}}{V} \left[N_r I_r \cos V(\theta_r + \frac{\alpha}{2}) + N_t I_t \cos V(\theta_r - \frac{\alpha}{2}) \right] \quad (2.2)$$

It can be seen that the position of F_f depends on the m.m.f. magnitude and direction of each winding. When, for example, the number of turns $N_t = N_r = N_f$, and the windings carry equal and positive current $I_t = I_r = I_f$, equation (2.2) becomes

$$F_f = \frac{4}{\pi} q I_f \sum_{V=1}^{\infty} \frac{K_{dV}}{V} \cos V \frac{\alpha}{2} \cos V \theta_r \quad (2.3)$$

This equation, which has its maximum along the d-axis, shows that the resultant field m.m.f. contains fundamental as well as space harmonics. The space harmonics have a fixed position with respect

to the fundamental, travel at the same speed as the fundamental and have ν times as many poles as the fundamental. Therefore, they induce harmonic e.m.f.'s in the stator winding, the frequency of which is n times the fundamental frequency ($n = \nu$).

2.4 ARMATURE M.M.F. DUE TO BALANCED CURRENT TIME HARMONICS IN 6-PH WINDING

The arrangement of windings in a 6-ph machine is illustrated in Fig. 2.2. It consists of two 3-ph windings separated by 30° in space. The magnetic axis of phase A is assigned to be the zero stator reference position ($\theta_s = 0$) whereas the direct-axis is assigned to be the zero rotor reference position ($\theta_r = 0$). If β is the separation angle of the two reference lines when $t = 0$, and ω_r is the rotor angular velocity in rad/s, then the relationship between the two references can be expressed as:

$$\theta_s = \theta_r + \theta \quad (2.4.a)$$

$$\text{where } \theta = \beta + \omega_r t \quad (2.4.b)$$

F_{hA} , the h^{th} harmonic m.m.f. due to phase A at angle θ_s from the reference axis at time t is¹⁰:

$$F_{hA} = F_n \cos(n\omega t - \varphi_n) \cos(h\theta_s) \quad (2.5)$$

where,

F_n : the maximum amplitude of the h^{th} space harmonic of m.m.f. produced by the n^{th} time harmonic of current in phase A and is given by the equation:

$$F_n = \frac{2\sqrt{2}}{\pi h} \frac{1}{p} T_{e_h} I_n \quad (2.6)$$

T_{e_h} : effective number of turns/phase = $K_{w_h} N_{ph}$,

N_{ph} : number of series turns/phase,

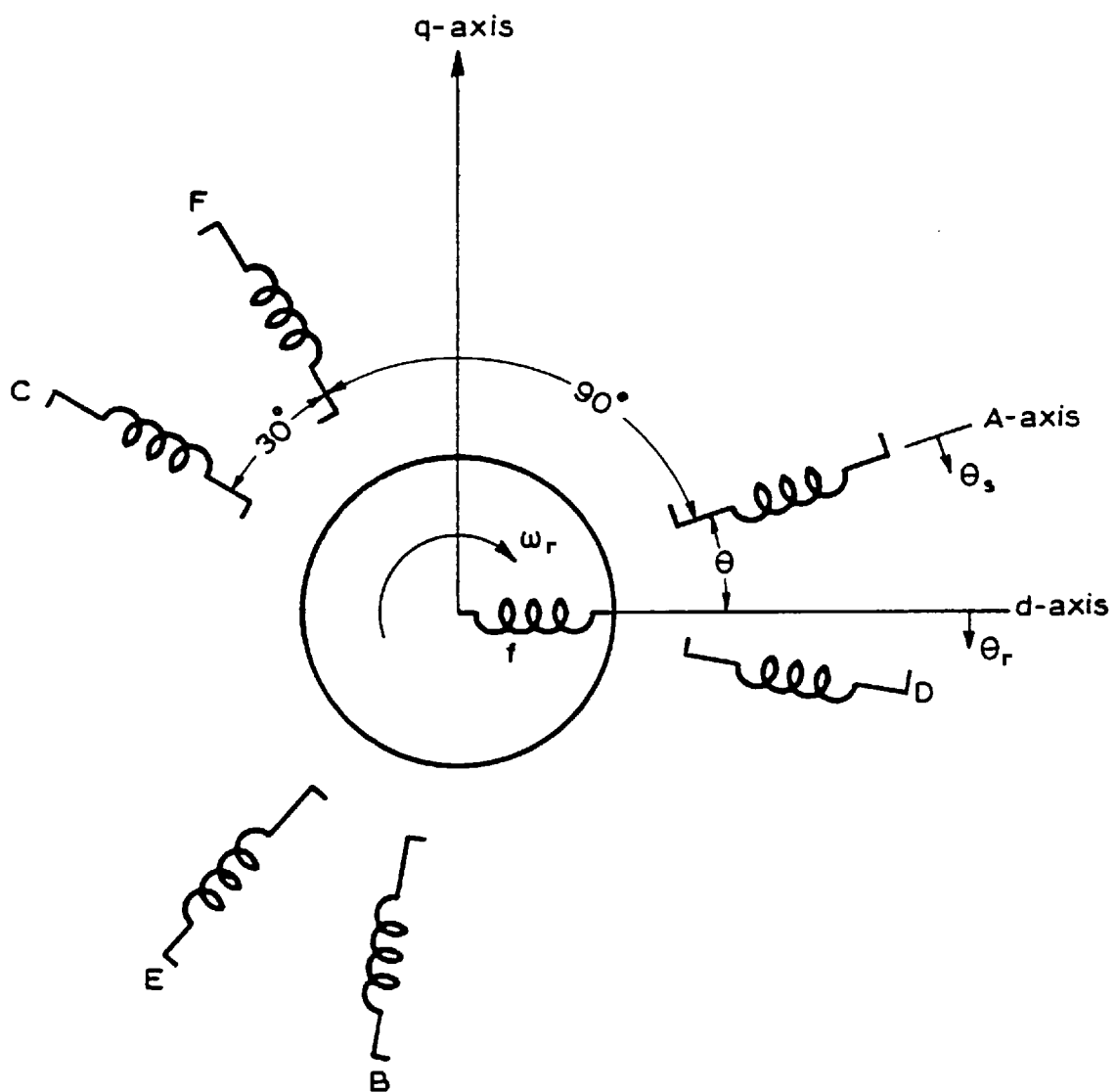


Fig. 2-2 Schematic diagram of 6-ph generator

- K_{w_h} : winding factor for h^{th} harmonic = $K_{d_h} K_{p_h} K_{s_h}$,
 K_{d_h} : distribution factor for h^{th} harmonic = $\frac{\sin(hq\alpha/2)}{q\sin(h\alpha/2)}$
 K_{p_h} : pitch factor for h^{th} harmonic = $\sin(h\rho\pi/2)$
 K_{s_h} : skew factor for h^{th} harmonic = $\frac{\sin(h\gamma/2)}{h\gamma/2}$
 q : slots/pole/phase,
 α : stator slot angle,
 ρ : ratio of coil span to pole pitch,
 γ : slot pitch in radians,
 p : number of pole pairs,
 I_n : r.m.s. value of time harmonic current,
 φ_n : time phase angle indicating the instant of the maximum of F_{h_A} ,

The h^{th} harmonic m.m.f. for the other phases can similarly be written by considering the space angle between the windings and the time angle between the currents of two adjacent phases, viz.,

$$F_{h_B} = F_n \cos [n(\omega t - 120) - \varphi_n] \cos [h(\theta_s - 120)] \quad (2.7)$$

$$F_{h_C} = F_n \cos [n(\omega t - 240) - \varphi_n] \cos [h(\theta_s - 240)] \quad (2.8)$$

$$F_{h_D} = F_n \cos [n(\omega t - 30) - \varphi_n] \cos [h(\theta_s - 30)] \quad (2.9)$$

$$F_{h_E} = F_n \cos [n(\omega t - 150) - \varphi_n] \cos [h(\theta_s - 150)] \quad (2.10)$$

$$F_{h_F} = F_n \cos [n(\omega t - 270) - \varphi_n] \cos [h(\theta_s - 270)] \quad (2.11)$$

Adding together the expressions for all the six phases, the sum will give the resultant distribution due to the entire winding. It will be noted that each term in this summation contains a product of the form $\cos\alpha\cos\beta$, which can be written as

$$\cos\alpha\cos\beta = \frac{1}{2}\cos(\alpha \mp \beta)$$

Hence, the resultant distribution of the h^{th} harmonic is

$$\begin{aligned}
 F_{h_r} = & \frac{F_n}{2} \cos [(n\omega t - \varphi_n) \mp h\theta_s - 0] \\
 & + \cos [(n\omega t - \varphi_n) \mp h\theta_s - 120(n \mp h)] \\
 & + \cos [(n\omega t - \varphi_n) \mp h\theta_s - 240(n \mp h)] \\
 & + \cos [(n\omega t - \varphi_n) \mp h\theta_s - 0 - 30(n \mp h)] \\
 & + \cos [(n\omega t - \varphi_n) \mp h\theta_s - 120(n \mp h) - 30(n \mp h)] \\
 & + \cos [(n\omega t - \varphi_n) \mp h\theta_s - 240(n \mp h) - 30(n \mp h)] \\
 & \qquad \qquad \qquad (2.12)
 \end{aligned}$$

Equation (2.12) is sufficiently general to permit the determination of the magnitude and distribution of any space harmonic of m.m.f. produced by any time harmonic in the current wave, except in the particular case when $n = 3$, which requires modification depending on the winding connection, and this is considered in Section 2.4.1. An inspection of equation (2.12) shows that there is a phase difference of $30(n \mp h)$ electric deg. between the resultant m.m.f. produced by the first set of 3-ph winding (A-B-C) and the second set of 3-ph winding (D-E-F). Zero resultant m.m.f. is produced by the two sets of windings for any space and time harmonic combination which does not give a phase shift equal to 360° or its multiples. This can be stated as

$$F_{h_r} = 0 \text{ unless } (n \mp h) = 0 \text{ or } 2km_1 \quad (2.13)$$

where k is any integer, and

m_1 is the number of phases, 6 in this case.

Equation (2.13) is the criterion for the existence of the h^{th} harmonic from which equation (2.12) reduces to

$$F_{h_r} = 6 \cdot \frac{F_n}{2} \cos [(n\omega t - \varphi_n) \mp h\theta_s]$$

Replacing F_n by its equivalent from equation (2.6), then

$$F_{h_r} = \frac{6\sqrt{2}}{\pi} \frac{I_n}{hp} \cos [(n\omega t - \varphi_n) \mp h\theta_s] \quad (2.14)$$

This is a simple and compact expression for any possible harmonic m.m.f. in the 6-ph machine winding. It may be interpreted as a cosine wave travelling in one direction or the other with respect to the stator at an angular velocity given by the derivative of the cosine argument w.r.t. time,

$$\begin{aligned} \frac{d}{dt} [(n\omega t - \varphi_n) \mp h\theta_s] &= 0 \\ \frac{d\theta_s}{dt} &= \pm \frac{n}{h} \omega \end{aligned} \quad (2.15)$$

In equation (2.15) and in later expressions, the upper sign indicates that the wave is rotating in the forward direction, that is, the same direction as the fundamental, and the lower sign indicates that the wave is rotating in backward direction.

The velocity of the space harmonic of m.m.f. can be referred to the rotor by using the transformation of equation (2.4)

$$\begin{aligned} \frac{d}{dt} [\theta_r + \beta + \omega_r t] &= \pm \frac{n}{h} \omega \\ \frac{d\theta_r}{dt} &= \pm \frac{n}{h} \omega - \omega_r \end{aligned} \quad (2.16)$$

The slip w.r.t. the harmonic is

$$s_{n_h} = \frac{\pm \frac{n}{h} \omega - \omega_r}{\pm \frac{n}{h} \omega}$$

For a synchronous machine $\omega = \omega_r$, therefore

$$s_{n_h} = \left(1 \mp \frac{h}{n}\right) \quad (2.17)$$

Equation (2.17) shows that the slip of the rotor w.r.t. each harmonic is zero when $h = n$, and that otherwise currents are induced in rotor circuits of frequencies determined by the relationship

$$\begin{aligned} f_{n_h} &= n f_1 s_{n_h} \\ &= (n \mp h) f_1 \end{aligned} \quad (2.18)$$

Any space harmonic of order $h = n$ is stationary with respect to the rotor and interacts with any rotor harmonic of the same order to produce synchronous torque in a similar manner to the interaction of the fundamental components of stator and rotor m.m.f.'s.

The foregoing harmonic analysis is general from which the following case is selected as an example. Consider the condition when balanced fundamental currents flow in the 6-ph winding ($n = 1$); this will give rise to space harmonics the order of which is obtained from equation (2.13)

$$h = 1, 11, 13, 23, 25, \dots$$

Substituting for each space harmonic in equation (2.14) and adding up all the components, the resultant m.m.f. then is

$$\begin{aligned} F_r = \frac{6\sqrt{2}}{\pi} \frac{I_1}{p} \left\{ T_{e_1} \cos(\omega t - \varphi_1 - \theta_s) + \frac{T_{e_{11}}}{11} \cos(\omega t - \varphi_1 + 11\theta_s) \right. \\ \left. + \frac{T_{e_{13}}}{13} \cos(\omega t - \varphi_1 - 13\theta_s) + \dots + \frac{T_{e_h}}{h} \cos(\omega t - \varphi_1 \mp h\theta_s) \right\} \end{aligned} \quad (2.19)$$

It is interesting to observe that the lowest space harmonics, namely the 3rd, 5th and 7th, do not exist in the armature m.m.f. distribution.

Therefore a pitch factor can be selected on the basis of weakening of the 11th and 13th harmonics in the armature m.m.f. A coil span of 11/12 is therefore recommended for winding with 12 slots/pole. Also, equation (2.19) shows that the space harmonics rotate slower than the fundamental wave as they have higher number of poles. They therefore induce currents in rotor circuits the frequency of which are given by equation (2.18). Thus for $n = 1$

h	1	11	13	23	25
f_{1_h}	0	$12f_1$	$12f_1$	$24f_1$	$24f_1$

Similarly, the analysis can be applied to find the m.m.f. space harmonics produced by time harmonic currents. The results are summarized in Table 2.1(A), the number indicating the speed at which the armature field moves relative to the armature winding, and the sign indicating the direction.

TABLE 2.1(A)

Speed and directions of rotation of components of armature m.m.f. of 6-ph winding.
Synchronous speed is when $n = 1, h = 1$.

Order of space harmonic h	Order of time harmonic, n				
	1	5	7	11	13
1	+1			$-\frac{11}{1}$	$+\frac{13}{1}$
3					
5		+1	$-\frac{7}{5}$		
7		$-\frac{5}{7}$	+1		
9					
11	$-\frac{1}{11}$			+1	$-\frac{13}{11}$
13	$+\frac{1}{13}$			$-\frac{11}{13}$	+1

2.4.1 Third Harmonic m.m.f. and Current in 6-ph Winding

The existence of third harmonic current and its odd multiples (for brevity termed the triplen harmonics¹¹) depends on the way in which the two 3-ph winding sets are connected. There can be no triplen harmonic currents flowing in each of the 3-ph winding set if its neutral point is isolated externally. However, it is likely that each star point would be earthed in use, and thus they are interconnected. The method of interconnection of the line terminals then controls the flow of triplen harmonic currents. Two methods of connection are considered here in which the two 3-ph winding sets can be electrically coupled so as to furnish a path for triplen harmonic currents to flow. Any practical connection to a power system may provide connections of either type.

A short circuit across the 6-ph winding is considered first (case 1). The connection diagram is given in Fig. 2.3, where switch 1 is closed and switch 2 is open. This situation is also identical to a 6-ph generator feeding two balanced 3-ph loads with neutrals joined together. The triplen harmonic currents produced in one set of windings complete their path via the other set of windings; therefore the equations for 3rd harmonic current, for example, are

$$I_A = I_B = I_C = \sqrt{2} I_3 \cos(3\omega t - \varphi_3) \quad (2.20)$$

$$I_D = I_E = I_F = -\sqrt{2} I_3 \cos(3\omega t - \varphi_3) \quad (2.21)$$

The resultant h^{th} harmonic m.m.f. due to the 3rd harmonic current is the sum of the components,

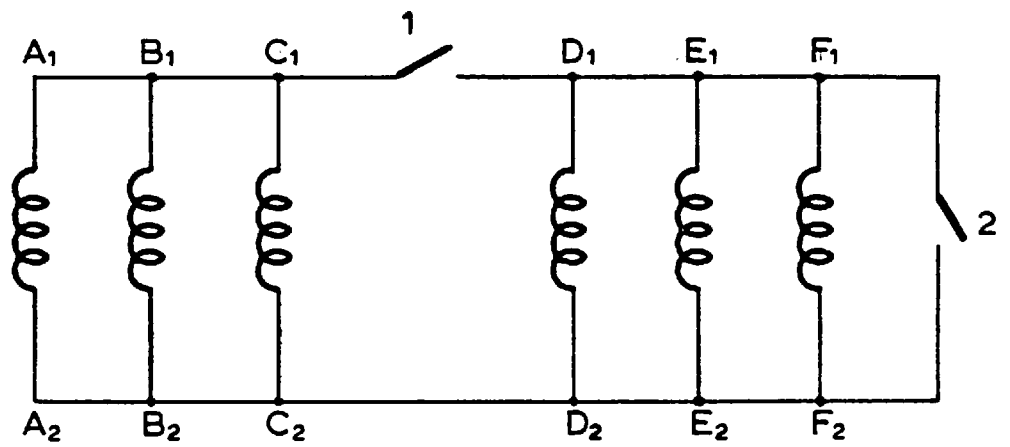


Fig. 2-3 Two possible ways for connecting two 3-ph windings to allow for 3rd. harmonic currents to flow.

$$\begin{aligned}
F_{h_r} &= F_{h_A} + F_{h_B} + F_{h_C} + F_{h_D} + F_{h_E} + F_{h_F} \\
&= \frac{2\sqrt{2}}{\pi} \frac{T_e h}{hp} I_3 \cos(3\omega t - \varphi_3) \left\{ \left[\cos(h\theta_s) + \cos(h(\theta_s - 120)) \right. \right. \\
&\quad \left. \left. + \cos(h(\theta_s - 240)) \right] - \left[\cos(h(\theta_s - 30)) + \cos(h(\theta_s - 150)) \right. \right. \\
&\quad \left. \left. + \cos(h(\theta_s - 270)) \right] \right\} \quad (2.22)
\end{aligned}$$

Equation (2.22) sums to zero for $h = 6k + 1$, where $k = 0$ or any positive integer, and for $h = 6k + 3$ it becomes

$$F_{h_r} = \frac{6\sqrt{2}}{\pi} \frac{T_e h}{hp} I_3 \cos(3\omega t - \varphi_3) \left[\cos(h\theta_s) - \cos(h(\theta_s - 30)) \right]$$

Making use of the trigonometric expressions,

$$\cos \alpha - \cos \beta = -2 \sin \frac{\alpha + \beta}{2} \sin \frac{\alpha - \beta}{2}$$

and,

$$\cos \alpha \cos \beta = \frac{1}{2} \left[\cos(\alpha - \beta) + \cos(\alpha + \beta) \right],$$

the above expression can be written as

$$F_{h_r} = \frac{6\sqrt{2}}{\pi} \frac{T_e h}{hp} \sin(15h) I_3 \cos \left\{ (3\omega t - \varphi_3) \mp \left[h(\theta_s - 15) + 90 \right] \right\} \quad (2.23)$$

This represents two waves of equal magnitude travelling relative to the winding in opposite directions at a speed of $3/h$ times the synchronous speed. If $h = 3$, then one of them is stationary with respect to the rotor, the other moves at twice synchronous speed in the backward direction. The other possible space harmonics with this connection are given in Table 2.1(B).

When both switches 1 and 2 of Fig. 2.3 are closed (case 2), the 3rd harmonic current in one set of windings is 90° out of phase

with that in the other set, and the sum of the two components flow in the path provided by switch 2. The 3rd harmonic current equations are:

$$I_A = I_B = I_C = \sqrt{2} I_3 \cos(3\omega t - \varphi_3)$$

$$I_D = I_E = I_F = \sqrt{2} I_3 \cos(3\omega t - \varphi_3 - 90)$$

Proceeding as before, it can be shown that only space harmonics of order $h = 3, 9, 15, \dots$ are present in the resultant armature m.m.f. waveform, which can be expressed as:

$$F_{h_r} = \frac{6\sqrt{2}}{\pi} \frac{e_h^T}{hp} I_3 \left\{ \cos(3\omega t - \varphi_3) \cos(h\theta_s) + \cos(3\omega t - \varphi_3 - 90) \cos(h(\theta_s - 30)) \right\} \quad (2.24.a)$$

$$= \frac{6\sqrt{2}}{\pi} \frac{e_h^T}{hp} I_3 \left\{ \cos(3\omega t - \varphi_3) \cos(h\theta_s) \pm \sin(3\omega t - \varphi_3) \sin(h\theta_s) \right\}$$

$$= \frac{6\sqrt{2}}{\pi} \frac{e_h^T}{hp} I_3 \cos \left[(3\omega t - \varphi_3) \mp (h\theta_s) \right] \quad (2.24.b)$$

Equation (2.24.a) is made up of two equal waves which are in quadrature in time and in space, each being stationary with respect to the winding; in other words, this is similar to the resultant armature m.m.f. produced by 3rd harmonic current flowing in a two-phase winding. It can also be seen that equation (2.24.b) is the same as equation (2.14) for $n = 3$, showing that the above result could have been obtained from the general approach described in section 2.4. The upper sign in equation (2.24.b) is associated with space harmonics of order $h = 6k+3$, $k = 0, 2, 4, 6, \dots$, and the lower sign is related to harmonics of order $h = 6k+3$, $k = 1, 3, 5, \dots$. As an example, the 3rd space harmonic ($h = 3$) rotates in a forward direction at synchronous speed and therefore is stationary relative to the rotor.

The analysis described above for each method of connection applies to all harmonics which are odd multiples of 3, i.e. triplen harmonics. Table 2.1(B) gives the speed and direction of the harmonics of normal interest.

TABLE 2.1(B)

Speed and directions of rotation of components of armature m.m.f. of 6-ph winding carrying 3rd harmonic current. Synchronous speed is when $n = h = 3$.

Order of space harmonic h	3rd harmonic currents $n = 3$	
	Case 1	Case 2
3	± 1	+1
9	$\pm \frac{1}{3}$	$-\frac{1}{3}$
15	$\pm \frac{1}{5}$	$+\frac{1}{5}$

2.5 ARMATURE M.M.F. PRODUCED BY NON-SINUSOIDAL BALANCED CURRENTS IN 3-PH WINDING

Any 6-ph machine may be converted to a 3-ph machine by connecting each phase of one group (A, B and C) in series with its neighbour from the second group (D, E and F respectively). Under the same excitation conditions, the current time harmonics flowing in 3-ph winding are normally different from those in 6-ph winding, for the harmonic reactances are not the same and this is investigated in Chapter 3. However, for the sake of comparison it is here assumed that the time harmonics of currents are the same for each

connection. Hence, the m.m.f. equations for the 3-ph winding can readily be derived from equations (2.5) and (2.7)-(2.11) inclusive.

$$F_{h_{AD}} = F_n \cos(n\omega t - \varphi_n) [\cos(h\theta_s) + \cos(h(\theta_s - 30))] \quad (2.25)$$

$$F_{h_{BE}} = F_n \cos[n(\omega t - 120) - \varphi_n] [\cos(h(\theta_s - 120)) + \cos(h(\theta_s - 150))] \quad (2.26)$$

$$F_{h_{CF}} = F_n \cos[n(\omega t - 240) - \varphi_n] [\cos(h(\theta_s - 240)) + \cos(h(\theta_s - 270))] \quad (2.27)$$

Substituting for F_n from equation (2.6), and summing up the above three equations, the result after simplifications can be shown to be,

$$\begin{aligned} F_{h_r} = \frac{2\sqrt{2}}{\pi} \frac{T e_h}{hp} I_n \cos(15h) \left\{ \cos[(n\omega t - \varphi_n) + h(\theta_s - 15)] \right. \\ \left. + \cos[(n\omega t - \varphi_n) + h(\theta_s - 15) - 120(n+h)] \right. \\ \left. + \cos[(n\omega t - \varphi_n) + h(\theta_s - 15) - 240(n+h)] \right\} \quad (2.28) \end{aligned}$$

Equation (2.28) represents a general formula for the h^{th} harmonic armature m.m.f. of the machine connected in 3 phases, taking into account the space and time harmonics. Each term in equation (2.28) may be considered as a phasor in which the angle between them is $120(n+h)$ degree. The resultant armature m.m.f. vanishes except when

$$(n+h) = 0 \text{ or } 2km_2 \quad (2.29)$$

where: k = any integer,

and m_2 = number of phases = 3.

Thus equation (2.28) reduces to

$$F_{h_r} = \frac{6\sqrt{2}}{\pi} \frac{T e_h}{hp} K_{c_h} I_n \cos[(n\omega t - \varphi_n) + h(\theta_s - 15)] \quad (2.30)$$

where: $K_{c_h} =$ connection factor for h^{th} harmonic $= \cos(15h)$.

Comparison of equation (2.30) with (2.14) shows that there is a phase shift of $(15h)$ elec. deg. between the h^{th} harmonic component for the machine connected in 3 and 6 phases. Moreover, the ratio of the amplitude of the h^{th} harmonic m.m.f. is

$$\frac{(F_h)_{\max 6\text{-ph}}}{(F_h)_{\max 3\text{-ph}}} = \frac{1}{K_{c_h}}, \quad h = 1, 3 \text{ (case 2)}, 5, 7, 11, 13, \dots \quad (2.31)$$

Note that this relationship is correct only when both the 6-ph and 3-ph machine carry the same currents. As the connection factor is less than unity, the amplitude of h^{th} harmonic m.m.f. for machine connected in 6 phases will always be greater than that in 3 phases.

Consider, as an example, a 3-ph winding carrying sinusoidal current. Equation (2.29) yields the harmonics

$$h = 1 \qquad 5 \qquad 7 \qquad 11 \qquad 13$$

Substituting for each harmonic in equation (2.30) and summing up, the resultant armature m.m.f. can be obtained.

$$\begin{aligned} F_r = & \frac{6\sqrt{2}}{\pi} \frac{I_1}{p} \left\{ T_{e_1} K_{c_1} \cos [(\omega t - \varphi_1) - (\theta_s - 15)] + \frac{T_{e_5}}{5} K_{c_5} \cos [(\omega t - \varphi_1) \right. \\ & + 5(\theta_s - 15)] + \frac{T_{e_7}}{7} K_{c_7} \cos [(\omega t - \varphi_1) - 7(\theta_s - 15)] \\ & + \frac{T_{e_{11}}}{11} K_{c_{11}} \cos [(\omega t - \varphi_1) + 11(\theta_s - 15)] \\ & \left. + \frac{T_{e_{13}}}{13} K_{c_{13}} \cos [(\omega t - \varphi_1) - 13(\theta_s - 15)] + \dots + \right\} \quad (2.32) \end{aligned}$$

In like manner, the investigation can be carried out to obtain any space harmonic of m.m.f. produced by any time harmonic of

current, including the triplen harmonics. The results are listed in Table 2.2, which is constructed on a basis similar to Table 2.1.

TABLE 2.2

Speed and directions of rotation of components of armature m.m.f. of three-phase winding. Synchronous speed is obtained when $n = 1$, $h = 1$.

Order of space harmonic h	Order of time harmonic, n					
	1	3	5	7	11	13
1	+1		-5	+7	-11	+13
3		± 1				
5	$-1/5$		+1	$-7/5$	$+11/5$	$-13/5$
7	$+1/7$		$-5/7$	+1	$-11/7$	$+13/7$
9		$\pm 1/3$				
11	$-1/11$		$+5/11$	$-7/11$	+1	$-13/11$
13	$+1/13$		$-5/13$	$+7/13$	$-11/13$	+1

From comparison of Tables 2.1 and 2.2 several main differences can be observed:

- a) The arrangement of the winding in 6 phases suppresses more space harmonics of m.m.f. than are in 3 phases. There is no 5th or 7th space harmonic in the resultant m.m.f. waveform of a 6-ph winding when excited with fundamental current, whereas they do exist in the m.m.f. waveform of a 3-ph winding.
- b) Since the 5th and 7th space harmonics are absent in 6-ph winding, the machine designer is allowed to choose freely the winding pitch greater than 5/6 which is normally required for 3-ph winding. A typical winding pitch for a 6-ph winding is 11/12.

c) As a result of the above, the stray losses in the rotor surface of a 6-ph winding are likely to be smaller than those of a 3-ph winding. The advantage of the 6-ph winding, from the point of view of reducing the stray losses in the rotor surface, is investigated in refs. 7 and 8.

2.6 RELATIONSHIP BETWEEN THE DISTRIBUTION FACTORS FOR MACHINES CONNECTED IN 6 AND IN 3 PHASES

The distribution factor for h^{th} harmonic is

$$K_{d_h} = \frac{\sin(h q \frac{\alpha}{2})}{q \sin(h \frac{\alpha}{2})}$$

When a 6-ph machine is converted to a 3-ph, then it will have twice the number of slots per pole per phase; therefore

$$\frac{(K_{d_h})_{6\text{-ph}}}{(K_{d_h})_{3\text{-ph}}} = \frac{1}{\cos(h q \frac{\alpha}{2})}$$

where, $q\alpha$: the phase belt and is equal to 30° for 6-ph winding.

$$\begin{aligned} \frac{(K_{d_h})_{6\text{-ph}}}{(K_{d_h})_{3\text{-ph}}} &= \frac{1}{\cos(15h)} && (2.33) \\ &= \frac{1}{\cos 15} = 1.035 && \text{for } h = 1, 11, 13, 23, 25, \dots \\ &= \frac{1}{\cos 45} = 1.414 && \text{for } h = 3, 9, 15, 21, \dots \\ &= \frac{1}{\cos 75} = 3.863 && \text{for } h = 5, 7, 17, 19, \dots \end{aligned}$$

The above relationships clearly indicate that a 6-ph machine has a better distribution factor as far as the fundamental component is concerned, but unfortunately worse distribution factors for all harmonics. This means that for the same field flux density waveform, the harmonic voltages in the 6-ph machine will be higher than in the 3-ph machine. These harmonic voltages and their effects on the winding are later investigated in Chapter 4.

The result of equation (2.33) is the same as that derived for equation (2.31). Thus,

$$\frac{(F_{h \max})_{6\text{-ph}}}{(F_{h \max})_{3\text{-ph}}} = \frac{(K_{d_h})_{6\text{-ph}}}{(K_{d_h})_{3\text{-ph}}} \quad (2.34)$$

Equation (2.33) may be used to determine the distribution factor for any 6-ph machine from the distribution factor for the corresponding 3-ph machine, which is normally available¹². Figure 2.4 shows the distribution factors for 3-ph¹² and 6-ph machines. The curves are valid for integer slots per pole per phase.

2.7 CONCLUSIONS

The resultant armature m.m.f. of n^{th} time harmonic current has been obtained for machine connected in 6 and 3 phases, tables indicating the space harmonics produced by each machine being given. It has also been shown that:

1. The 5th and 7th space harmonics are missing in the armature m.m.f. waveform of a 6-ph machine when excited with fundamental current.
2. The 6-ph machine has a better fundamental pitch and distribution factor than that of a 3-ph machine. In other words, the output power of 6-ph machine as compared to a conventional 3-ph machine having the same overall size is increased by a factor of

$$\left(\frac{.988 \times .991}{.955 \times .966} - 1 \right) \times 100 = 6.0\%$$

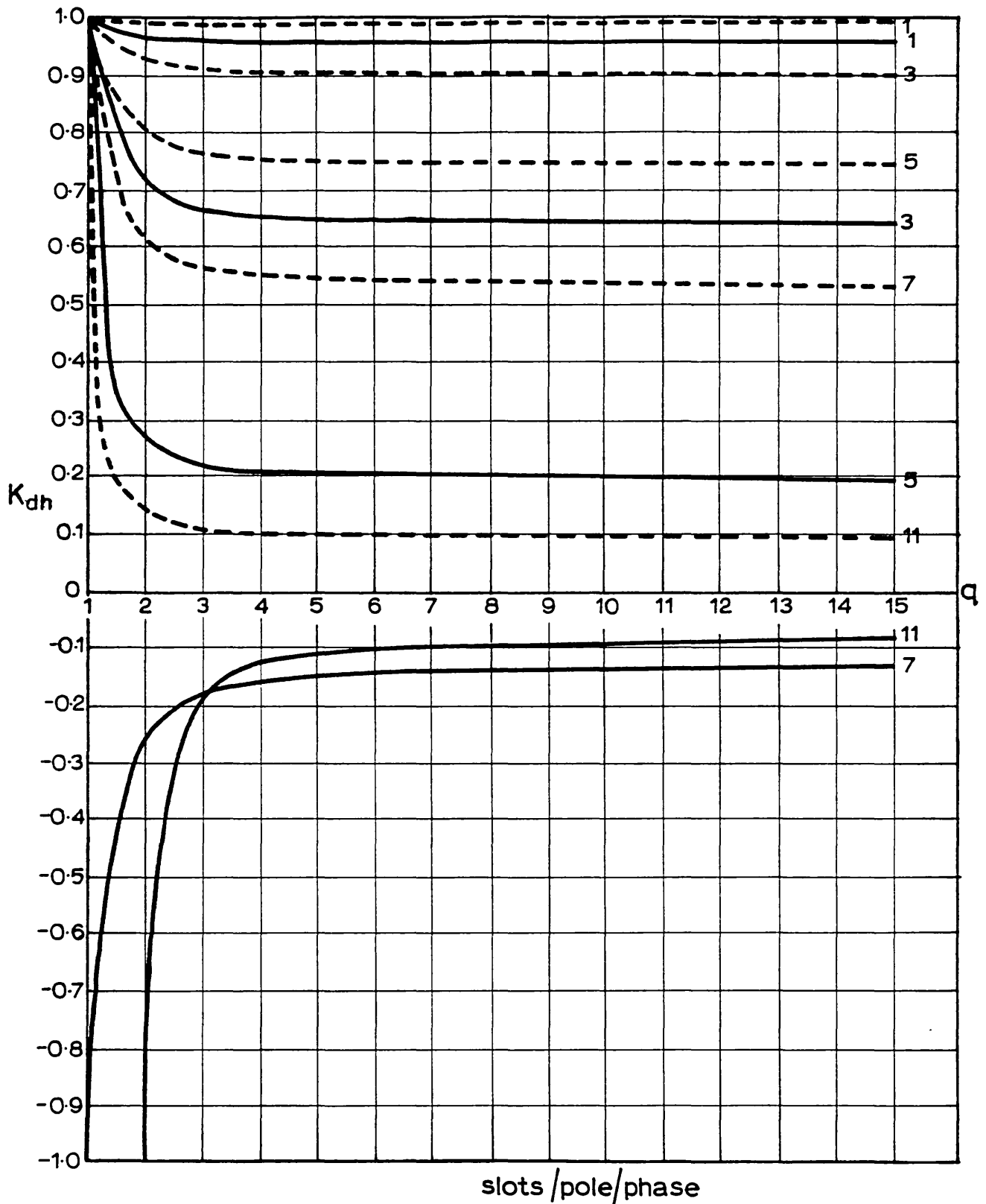


Fig. 2.4 Distribution factors

— Machine connected as 3-ph
 - - - Machine connected as 6-ph

THE DETERMINATION OF THE MAGNETIZING
AND LEAKAGE REACTANCES WITH RESPECT TO
nTH HARMONIC CURRENT

3.1 INTRODUCTION

The calculation of the magnitude of time harmonic currents flowing in any machine will require a knowledge of the machine magnetizing and leakage reactances at each frequency. In this chapter these parameters are obtained for a machine connected in 6 and 3 phases. The definitions of the reactances are based on those given by Alger¹³ and Liwschitz¹⁴ but have been modified to include time harmonic effects. The influence of the number of phase belts, and of fractional pitch on the machine reactances, particularly on the slot leakage reactance component, is considered. The effect of rotor damping on the reduction of space harmonics is discussed. Formulae and curves are given for the reactances. These are applied to obtain the reactances of the laboratory micro-machine connected in 6 and 3 phases.

3.2 MAGNETIZING REACTANCE WITH RESPECT TO THE HARMONIC $h = n$

The magnetizing reactance associated with each time harmonic of current (n) is defined as that of the airgap space harmonic (h) of the same order. When $h = n$, the resultant m.m.f. is stationary with respect to the rotor and any flux it gives rise to in the airgap induces no voltage in the rotor circuits. Defined in this way magnetizing reactance for each harmonic corresponds with the normal definition for fundamental m.m.f. However, each space harmonic has its own pole pitch ($\frac{1}{h}$ that of the fundamental) and

winding factor, and the expression must take this into account. The airgap space harmonics resulting from the time harmonics of current for which $h \neq n$ contribute to the leakage reactance.

The amplitude of the h^{th} harmonic m.m.f. due to n^{th} time harmonic current of an m -ph machine is (see equation (2.14))

$$F_{h_{\max}} = \frac{\sqrt{2} m}{\pi} \frac{e_h}{h p} I_n \quad \text{At/pole} \quad (3.1)$$

The corresponding maximum flux density in an airgap of effective length G_d on the direct-axis is therefore,

$$B_{h_{\max}} = \frac{\mu_0}{G_d} K C_{d_h} \cdot F_{h_{\max}} \quad \text{T} \quad (3.2)$$

where K is a factor (less than unity) which takes into account that part of the m.m.f. which is consumed in the iron part of the flux path. In this case K is made equal to unity, i.e. all the m.m.f. is consumed in the airgap. Moreover, the influence of slot openings on the harmonic fluxes is the same as on the fundamental wave, that is, the same permeance of the airgap has been used for the fundamental and the harmonics. G_d and C_{d_h} are given in Appendix A. The flux per pole corresponding to the h^{th} harmonic is

$$\bar{\Phi}_h = \frac{2}{\pi} B_{h_{\max}} \frac{\tau L}{h} \quad (3.3)$$

where, τ : pole pitch = $\frac{\pi D}{2p}$,

D : airgap diameter,

L : effective core length,

τ , D and L are measured in metres.

The e.m.f. induced by this flux is

$$E_n = \sqrt{2} \pi n f T_{e_h} \bar{\Phi}_h \quad (3.4)$$

On substituting for $\bar{\Phi}_h$ from (3.3), for $B_{h_{\max}}$ from (3.2), and for $F_{h_{\max}}$ from (3.1) into equation (3.4), then E_n becomes

$$E_n = \frac{4m}{\pi} n f \mu_o \frac{C_{d_h} \tau L}{G_d p} \left(\frac{e_h}{h}\right)^2 I_n \quad (3.5)$$

By definition, the magnetizing reactance with respect to n^{th} time harmonic current is the ratio of E_n to I_n at $h = n$. Hence

$$X_{m_n} = \frac{X_{m_1}}{h} \left(\frac{K_{w_h}}{K_{w_1}}\right)^2 \quad \Omega/\text{ph} \quad (3.6)$$

where X_{m_1} is the magnetizing reactance at fundamental frequency and is equal to

$$X_{m_1} = \frac{4m}{\pi} f \mu_o \frac{C_{d_1} \tau L}{G_d p} K_{w_1}^2 N_{\text{ph}}^2 \quad \Omega/\text{ph} \quad (3.7)$$

Equation (3.6) shows that the higher the order of the harmonic, the lower is the magnetizing reactance.

3.3 LEAKAGE REACTANCE OF SYNCHRONOUS MACHINES WITH NON-SINUSOIDAL EXCITATION

The leakage reactance of synchronous machines can be considered as four components:

- a. Slot leakage reactance,
- b. End leakage reactance,
- c. Zigzag leakage reactance, and
- d. Belt leakage reactance.

c and d together constitute the airgap leakage, or differential leakage reactance, due to harmonics of the airgap field. It is assumed here that the saturation of the iron has negligible effect on the leakage paths.

3.3.1 Slot Leakage Reactance

This comprises all of the flux crossing the slots due to the armature current, but does not include flux passing from tooth to tooth in the airgap space. Evidently, there is a slight error here because the flux lines near the opening of the slot do not pass straight across, but bulge outward into the gap. The slot leakage reactance of the fundamental current is equal to the product:

$2\pi f \times \text{slots per phase} \times \text{total slot inductance in henrys,}$

or

$$X_{\text{slot}_1} = 2\pi f S L_s \quad \Omega/\text{ph} \quad (3.8)$$

The total slot inductance consists of the self inductance of each coil side and the mutual inductance for each of them. Consider, for example, a full pitch double layer winding in which the upper and lower coil sides carry identical in-phase current. The total slot inductance is

$$L_s = L_A + L_B + 2L_{AB}$$

The values of these inductances depend on the slot configuration. For a fractional pitch winding, the currents in the two coil sides in some slots are not in phase, and in order to take this time phase shift into account, the above must be written as

$$L_s = L_A + L_B + 2K_r L_{AB} \quad (3.9)$$

The correction factor K_r is smaller than 1 for fractional pitch winding, and is equal to 1 for full pitch winding. Also, if all the slots were alike, as in a full-pitch, or a 3-ph, $\frac{2}{3}$ pitch winding, a single value of K_r could be used in equation (3.9). In

the general case, however, when there are at least two kinds of slots carrying coil sides of different phases, the effective value of K_r for the entire winding is determined from the expression¹⁴

$$K_r = \frac{1}{2q} \sum_{2q} \cos \alpha \quad (3.10)$$

where α is the time phase shift between the current in the upper coil side and the current in the lower coil side of the same slot, and q is the number of slots per pole per phase. To obtain results comparable with those given by Alger¹³, K_r is replaced by slot leakage factor K_s where

$$K_s = \frac{1 + K_r}{2} \quad (3.11)$$

On substituting for L_s from equation (3.9), for K_r from (3.10) and for K_s from (3.11) into equation (3.8), then

$$X_{\text{slot}_1} = 2\pi f.S [L_A + L_B + 2L_{AB}(2K_s - 1)] \quad (3.12)$$

Equation (3.12) can be modified to represent the slot leakage reactance of the n^{th} time harmonic current by

1. Evaluating the reactances at the harmonic frequency nf .
2. Calculating the slot leakage factor K_s for each harmonic current.

Hence, with respect to the n^{th} harmonic current equation (3.12) may be written as

$$X_{\text{slot}_n} = 2\pi nf.S [L_A + L_B + 2L_{AB}(2K_{s_n} - 1)] \quad (3.13)$$

Knowing the value of K_{s_n} for each harmonic current enables

X_{slot_n} to be obtained in the same way as the fundamental frequency slot leakage reactance.

3.3.1.1 Slot leakage factor for a 6-ph machine

- a) Slot leakage factor with respect to the harmonic current of order $n = 12k \pm 1$ ($k = 0, 1, 2, \dots$):

Consider the case in which fundamental balanced current is flowing in a 6-ph winding. The example given below takes the particulars of the laboratory micro-machine, the details of which are given in Section 4.2, as a means of illustrating the principles by which the slot leakage factor is obtained. The fundamental current phasor diagram as well as a schematic diagram for the winding distribution is shown in Fig. 3.1(a). As the 6-ph winding has 48 slots, 2 slots per pole per phase and a coil pitch of 5/6, all slots will have mixed phases. The correction factor using equation (3.10) is

$$\begin{aligned} K_{r_1} &= \frac{1}{2 \times 2} [4 \times \cos 30] \\ &= \frac{\sqrt{3}}{2} \end{aligned}$$

and

$$K_{s_1} = \frac{1 + \frac{\sqrt{3}}{2}}{2} = .933$$

It can be shown that the harmonic current, the order of which is determined by the expression $12k \pm 1$ ($k = 1, 2, 3, \dots$) will have the same current direction in the upper and lower coil sides depending on coil pitch as the fundamental current; Table 3.1 shows the phase sequence of harmonic currents. Consequently, the slot leakage factor for these harmonics is the same as for the fundamental current. The values of K_s for other coil pitches can be obtained similarly.

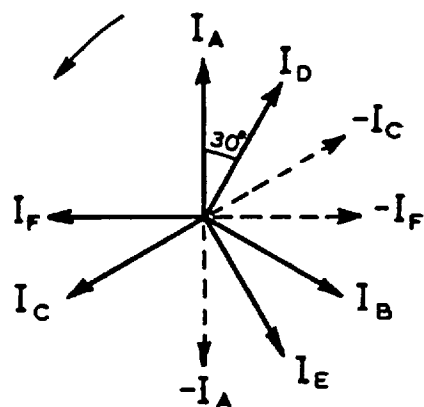
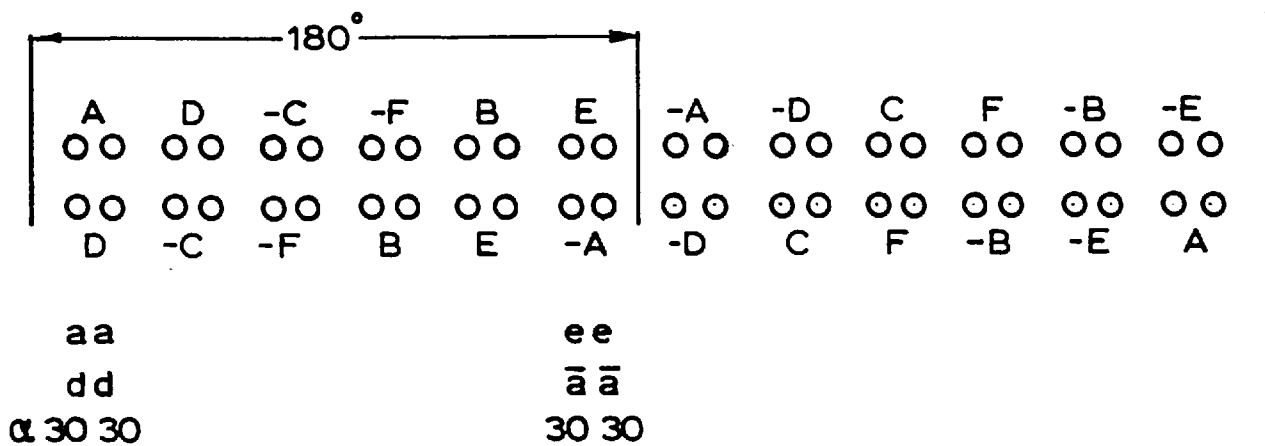


Fig.31(a) Determination of the slot leakage factor (K_s) for a 6-ph winding, with $q=2$ and $\rho = 5/6$

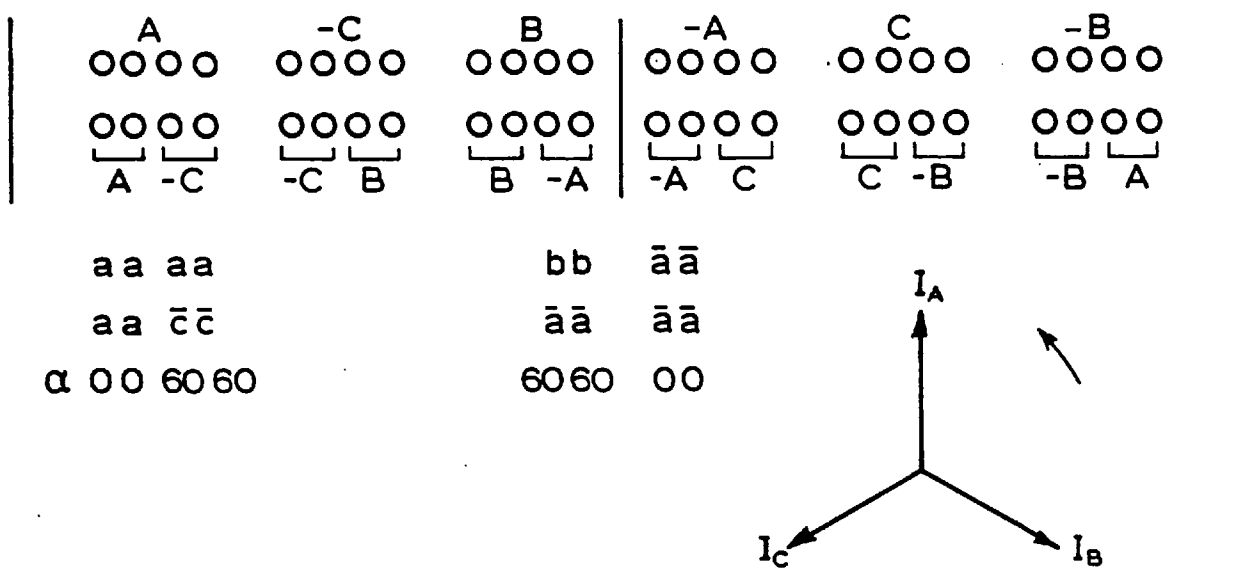


Fig.31(b) Determination of K_s for a 3-ph winding, with $q=4$ and $\rho = 5/6$

TABLE 3.1

The phase sequence of harmonic currents in
6-ph and 3-ph machine.
 $k = 0$ or any positive integer.

6-ph machine	3-ph machine
<p>For $n = 12k + 1$, the phase sequence is $I_A, I_D, I_B, I_E, I_C, I_F$.</p> <p>For $n = 12k - 1$, the phase sequence is $I_A, I_F, I_C, I_E, I_B, I_D$.</p>	<p>For $n = 6k + 1$, the phase sequence is I_A, I_B, I_C.</p> <p>For $n = 6k - 1$, the phase sequence is I_A, I_C, I_B.</p>
<p>For $n = 12k + 5$, the phase sequence is $I_A, I_E, I_C, I_D, I_B, I_F$.</p> <p>For $n = 12k - 5$, the phase sequence is $I_A, I_F, I_B, I_D, I_C, I_E$.</p>	
<p>For $n = 6k + 3$, the currents in each 3-ph group are in time phase.</p>	<p>For $n = 6k + 3$ the currents are in time phase.</p>

The results are given in Table 3.2 and plotted in Fig. 3.2, curve 1. For intermediate values of coil pitch, K_s can be obtained by the following equations:

$$K_s = \frac{3}{2}(2 - \sqrt{3})\rho \quad \text{if } 0 \leq \rho \leq \frac{1}{6}$$

$$K_s = \frac{3}{2}(-1 + \sqrt{3})\rho + \frac{3 - 2\sqrt{3}}{4} \quad \text{if } \frac{1}{6} \leq \rho \leq \frac{2}{6}$$

$$K_s = \frac{3}{2}\rho - \frac{1}{4} \quad \text{if } \frac{2}{6} \leq \rho \leq \frac{4}{6}$$

$$K_s = \frac{3}{2}(-1 + \sqrt{3})\rho + \frac{7 - 4\sqrt{3}}{4} \quad \text{if } \frac{4}{6} \leq \rho \leq \frac{5}{6}$$

$$K_s = \frac{3}{2}(2 - \sqrt{3})\rho + \frac{6\sqrt{3} - 8}{4} \quad \text{if } \frac{5}{6} \leq \rho \leq 1$$

It can be seen that the slot leakage factor varies linearly with the coil pitch; breaks are observed only at points with $\rho = \frac{5}{6}, \frac{4}{6}, \frac{2}{6}$ and $\frac{1}{6}$.

The slot leakage reactance is maximum when all the slots carry in phase currents ($K_s = 1$), and it has a minimum value when they carry antiphase currents ($K_s = 0$). Figure 3.3 shows the flux density distribution as a result of the above current conditions.

b) Slot leakage factor with respect to the harmonic currents of order $n = 12k + 5$:

The phase sequence for this set of current harmonics is given in Table 3.1. The appropriate values of K_s can readily be derived using the method employed in part (a). The values of slot leakage factors for the entire winding, from curve 2, Fig. 3.2, are:

$$K_s = \frac{3}{2}(2 + \sqrt{3})\rho \quad \text{if } 0 \leq \rho \leq \frac{1}{6}$$

$$K_s = -\frac{3}{2}(1 + \sqrt{3})\rho + \frac{3 + 2\sqrt{3}}{4} \quad \text{if } \frac{1}{6} \leq \rho \leq \frac{2}{6}$$

TABLE 3.2

Values of K_{s_n} for 6-ph machine.

Order of time harmonic currents	Winding Pitch						
	0	1/6	2/6	3/6	4/6	5/6	1
	α and K_{s_n}						
$n = 1, 11,$ $13, \dots$	180	150	120	90	60	30	0
$12k \pm 1$	0	.067	.25	.5	.75	.933	1
$n = 5, 7,$ $17, \dots$	180	30	120	90	60	150	0
$12k \pm 5$	0	.933	.25	.5	.75	.067	1
$n = 3, 9,$ $15, \dots$	180		0		180		0
$6k + 3$	0		1		0		1

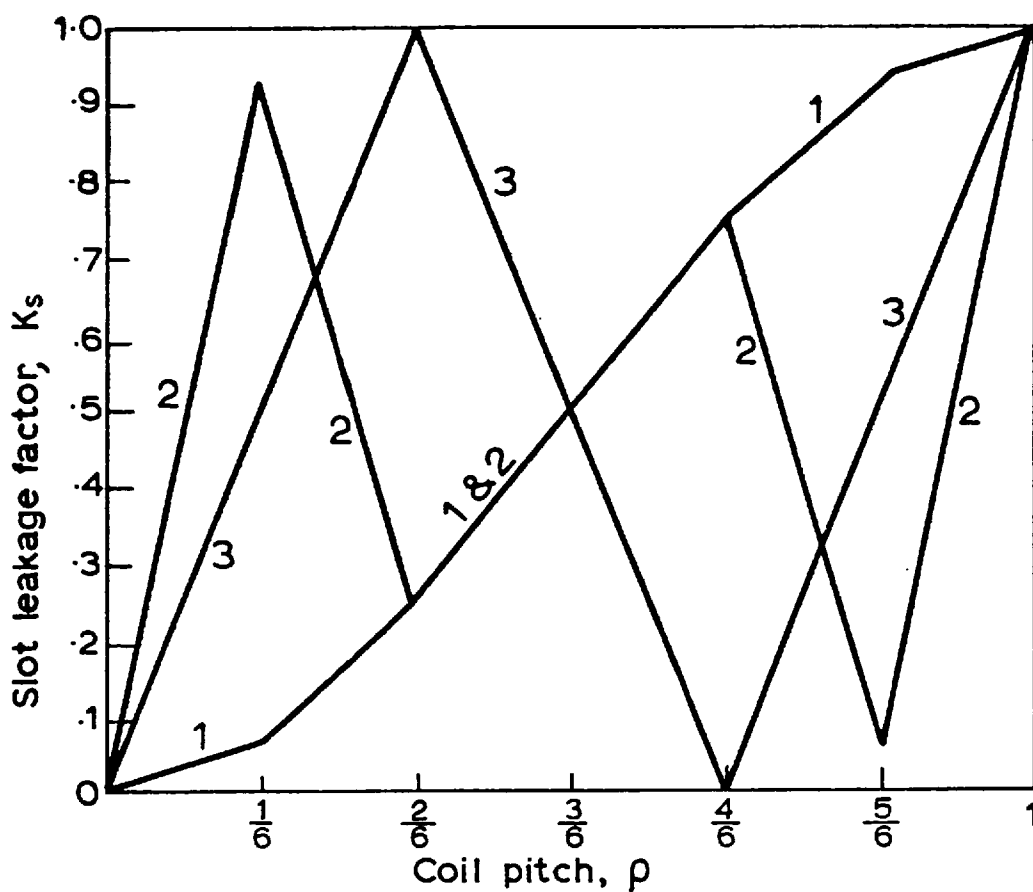
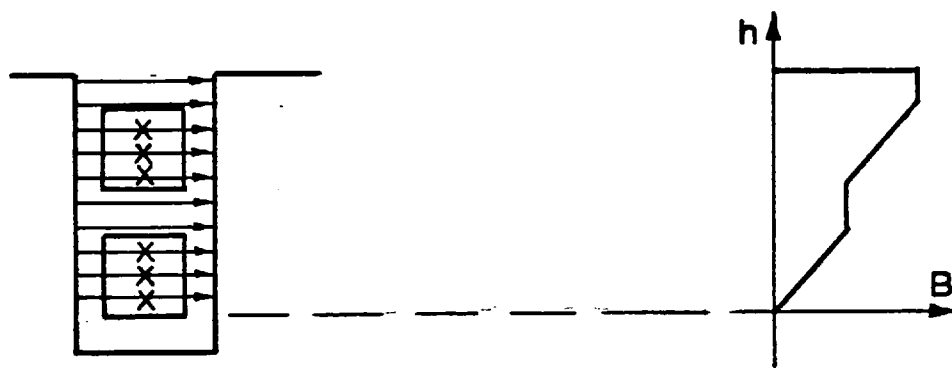


Fig. 3-2 Slot leakage factor for 6-ph machine with 30° phase belt.

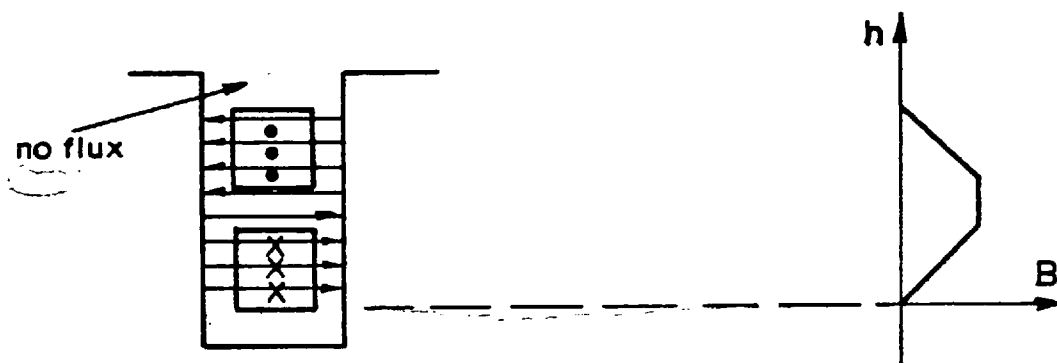
1. Harmonic currents of orders $12K \pm 1$
2. " " " " $12K \pm 5$
3. " " " " $6K + 3$

$$K = 0, 1, 2, \dots$$

Curve 3 applies to either connection of section 2·4·1



(a) Currents in phase



(b) Currents in antiphase

Fig.3.3 Flux density distribution in a slot carrying in phase or antiphase currents.

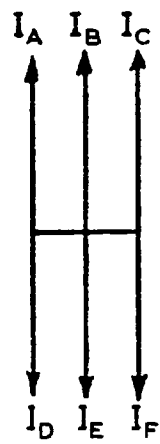
$$\begin{aligned}
 K_s &= \frac{3}{2}\rho - \frac{1}{4} && \text{if } \frac{2}{6} \leq \rho \leq \frac{4}{6} \\
 K_s &= -\frac{3}{2}(1 + \sqrt{3})\rho + \frac{7 + 4\sqrt{3}}{4} && \text{if } \frac{4}{6} \leq \rho \leq \frac{5}{6} \\
 K_s &= \frac{3}{2}(2 + \sqrt{3})\rho - \frac{8 + 6\sqrt{3}}{4} && \text{if } \frac{5}{6} \leq \rho \leq 1
 \end{aligned}$$

It can be seen from curve 2 that the slot leakage factor is very small at a coil pitch of 5/6. This means that the mutual slot reactance with respect to the harmonic currents of order $12k \pm 5$ will have a relatively high value but with negative sign. The slot leakage reactance is, therefore, very small.

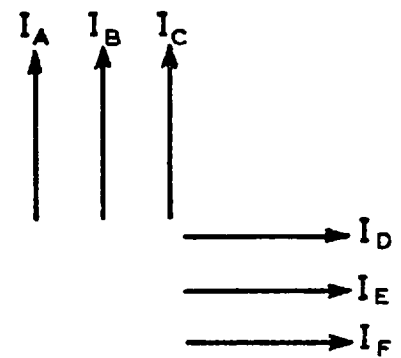
- c) Slot leakage factor with respect to the harmonic currents of order $n = 6k + 3$:

This applies when the currents in each 3-ph group are equal and in time phase, but the currents in the two groups are either in antiphase or in quadratura (see Section 2.4.1). The current phasor diagram for both winding connections which provide a path for third harmonic current to flow is shown in Fig. 3.4. The slot leakage factor for either connection is found by making $\cos \alpha = 1$ for coil sides in slots carrying in phase currents, and those carrying that are 120° out of phase; and $\cos \alpha = -1$ for coil sides in slots carrying current 60° out of phase; since with this connection alternate phase belts carry equal but opposite currents. The results obtained show that the value of slot leakage factor is the same for both connections. These are given in Table 3.2 and plotted in Fig. 3.2. The values of the slot leakage factor for the entire winding are:

$$\begin{aligned}
 K_s &= 3\rho && \text{if } 0 \leq \rho \leq \frac{2}{6} \\
 K_s &= -3\rho + 2 && \text{if } \frac{2}{6} \leq \rho \leq \frac{4}{6} \\
 K_s &= 3\rho - 2 && \text{if } \frac{4}{6} \leq \rho \leq 1
 \end{aligned}$$



Case 1



Case 2

Fig. 3-4 Current phasor diagram for triplen harmonics in 6-ph generator.

3.3.1.2 Slot leakage factor for a 3-ph machine

The method of derivation of slot leakage factor is similar to that already described in subsection 3.3.1.1. The results are given in Table 3.3 and plotted in Fig. 3.5. From curve 1, the values of slot leakage factor with respect to harmonic currents of order $n = 6k \pm 1$ are

$$\begin{aligned}
 K_s &= \frac{3}{4}\rho && \text{if } 0 \leq \rho \leq \frac{2}{6} \\
 K_s &= \frac{3}{2}\rho - \frac{1}{4} && \text{if } \frac{2}{6} \leq \rho \leq \frac{4}{6} \\
 K_s &= \frac{3}{4}\rho + \frac{1}{4} && \text{if } \frac{4}{6} \leq \rho \leq 1
 \end{aligned}$$

The following main points can be observed when comparing Figs. 3.2 and 3.5:

1. The variation of K_s with winding pitch is the same for current harmonics of order $n = 12k \pm 1$ and $n = 12k \pm 5$ in 3-ph machine. Consequently, the slot leakage reactance with respect to these harmonics is n times that of fundamental current, or

$$X_{\text{slot}_n} = n X_{\text{slot}_1} \quad n = 6k \pm 1 \quad k = 0, 1, 2, \dots$$

However, this relationship is incorrect in the 6-ph machine except when $\frac{2}{6} \leq \rho \leq \frac{4}{6}$, for at this region curve 1 and curve 2 coincide with each other.

2. It is clear that the value of slot leakage reactance for currents of order $12k \pm 5$ in the 6-ph machine is very much smaller than in the 3-ph machine at a coil pitch of $\frac{5}{6}$. Therefore, if, as is normally the case, the slot leakage

TABLE 3.3

Values of K_{s_n} for 3-ph machine.

Order of time harmonic currents	Winding pitch			
	0	1/3	2/3	1
	α and K_{s_n}			
$n = 1, 5, 7, 11,$	180	120	60	0
$6k \pm 1$	0	.25	.75	1
$n = 3, 9, 15,$	180	0	180	0
$6k + 3$	0	1	0	1

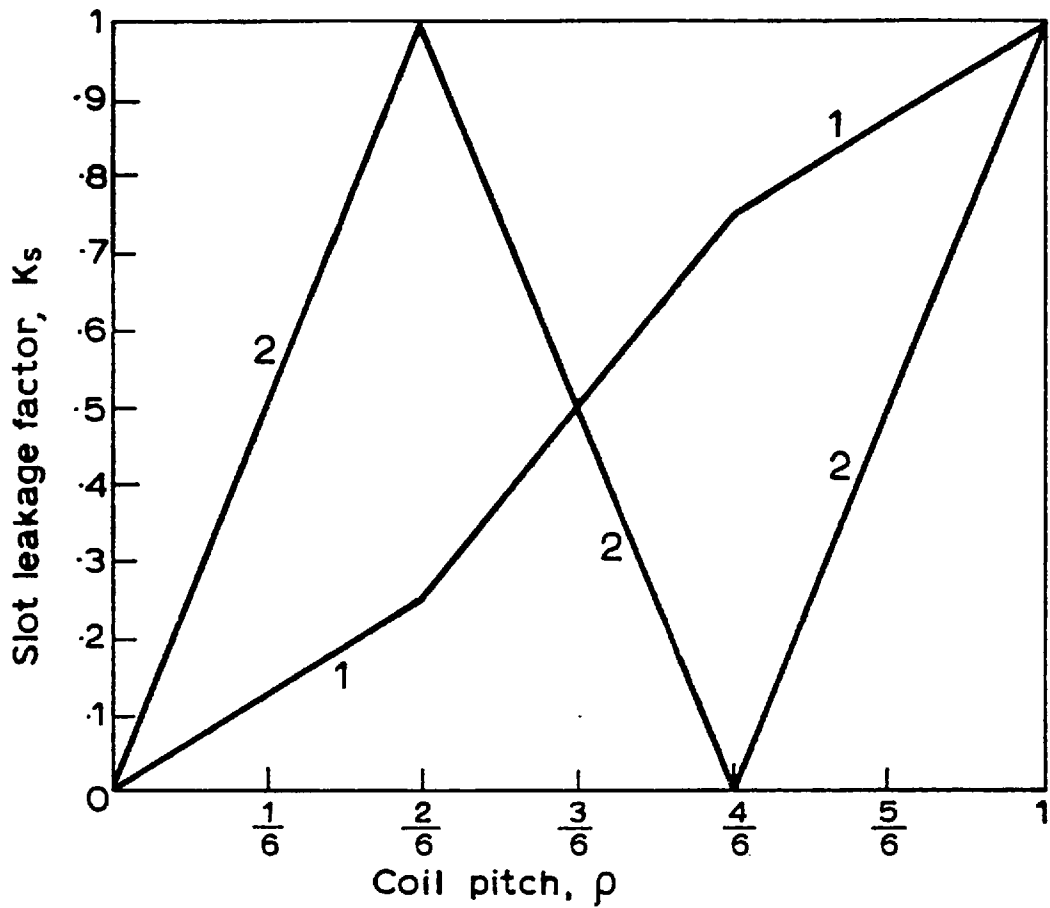


Fig.3-5 Slot leakage factor for 3-ph machine with 60° phase belt.

1. Harmonic currents of orders $6K \pm 1$
2. " " " " " $6K \pm 3$

$$K = 0, 1, 2, \dots$$

reactance is the dominant component of leakage reactance, relatively large harmonic current of order $n = 12k \pm 5$ might flow in a 6-ph machine. Even if a coil pitch of 11/12 is selected, it is likely that the harmonic current with 6-ph will be greater than with three.

3. The slot leakage factor for triplen harmonic currents is the same in 6-ph and 3-ph machine.

In view of the above, it can be said that the determination of slot leakage factor depends on winding pitch, winding connection (whether it is 6-ph or 3-ph) and on the order of the harmonic current. However, it is independent of the number of slots per pole per phase as clearly shown from all the expressions for K_s .

3.3.2 End Leakage Reactance

- a) End leakage reactance with respect to the fundamental current.:

This reactance is due to that flux linking the end turns which induces fundamental frequency voltages in the conductors.

Alger¹³ has analyzed this component of leakage reactance as due to two sets of currents:

1. The axial currents flowing parallel to the shaft, and
2. the peripheral currents flowing circumferentially.

He finds, after some approximations, that the end leakage reactance due to the axial currents is

$$X_{ea1} = \frac{0.197 f m N_{ph}^2 D_1 K_1^2}{p^2 \times 10^5} \tan \xi \left[\frac{\rho \pi - \sin \rho \pi}{\pi} \right] \Omega / \text{ph} \quad (3.14)$$

and the end leakage reactance due to peripheral currents is

$$X_{ep_1} = \frac{0.8fmN_{ph}^2 K_{p_1}^2 K_{d_1}^2}{p^2 \times 10^6} D_1 \left[\ln\left(\frac{4D_1}{r}\right) - 1.75 \right] \Omega/ph \quad (3.15)$$

where: r = the mean radius of the imaginary circular coil in which the peripheral stator end winding current flows. It is suggested that the value of r should be taken as one-half the depth of the stator slot.

Angle ξ and D_1 are shown in Fig. 3.6, from which

$$\tan \xi = \frac{Y}{2y_s}$$

where: $y_s = \frac{\pi D_1}{2p} \rho$

The total end leakage reactance is found by adding equations (3.14) and (3.15):

$$X_{e_1} = X_{ea_1} + X_{ep_1} \quad (3.16)$$

b) End leakage reactance with respect to the harmonic currents of order $n = h$:

For each time harmonic current, the end leakage reactance can be calculated by applying equations (3.14) and (3.15) with the following amendments:

1. Put K_{d_h} and K_{p_h} in place of K_{d_1} and K_{p_1} .
2. Put $h\rho$ instead of ρ .
3. Replace p by hp .
4. Multiply the fundamental frequency by order of time harmonic current.

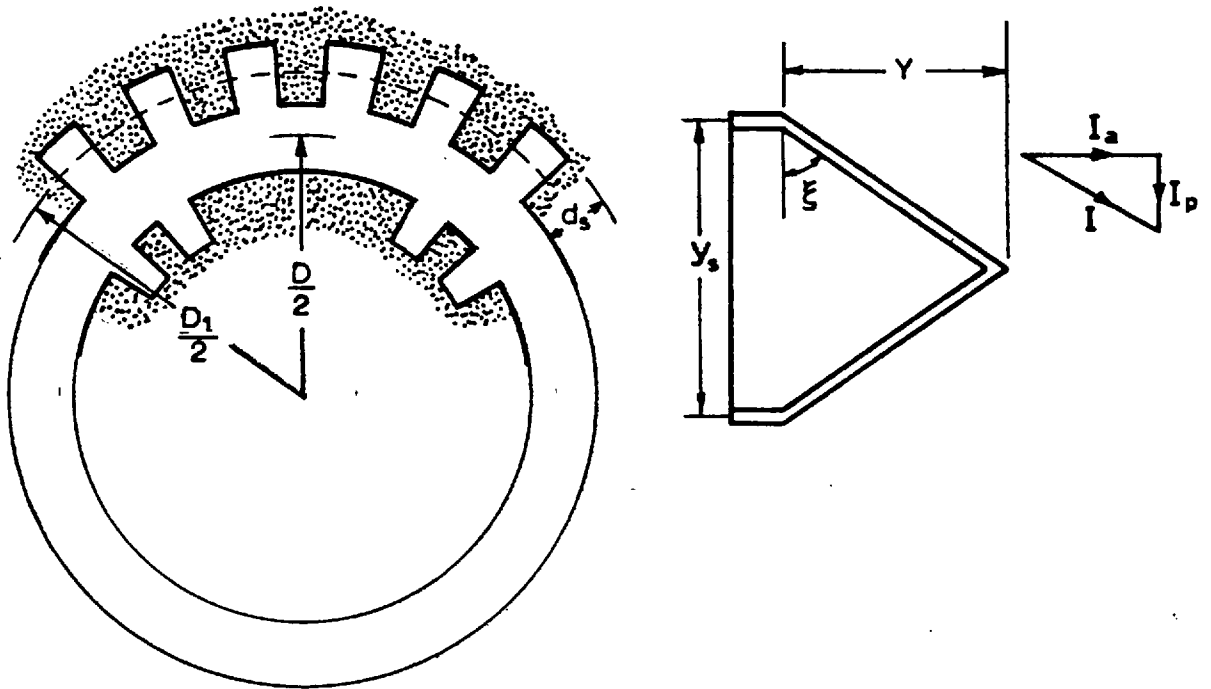


Fig.3-6 End winding configuration

Equations (3.14) and (3.15) may, therefore, be written as:

$$X_{ea_n} = \frac{0.197 \text{ nf } mN_{ph}^2 K_{dh}^2}{h^2 p^2 \times 10^5} D_1 \tan \xi \left[\frac{h\rho\pi - \sin(h\rho\pi)}{\pi} \right] \Omega/\text{ph} \quad (3.17)$$

and

$$X_{ep_n} = \frac{0.8 \text{ nf } mN_{ph}^2 K_{ph}^2 K_{dh}^2}{h^2 p^2 \times 10^6} D_1 \left[\ln\left(\frac{4D_1}{r}\right) - 1.75 \right] \Omega/\text{ph} \quad (3.18)$$

3.3.3 Differential or Airgap Leakage Reactance

As shown by equation (2.14) for the 6-ph winding, or equation (2.30) for the 3-ph winding, the airgap field contains harmonics which may be classified into four types:

1. A fundamental sine wave, stationary on the rotor, inducing fundamental frequency voltages, e.g. $n = h = 1$.
2. A series of harmonics moving with respect to the rotor and also including fundamental frequency voltages, e.g. $n = 1$, $h = 11, 13, 23, 25, \dots$
3. A sine wave, produced by the n^{th} harmonic current, stationary with respect to the rotor, inducing n times fundamental frequency voltages, e.g. $n = h = 5$.
4. A series of harmonics due to n^{th} harmonic current, moving with respect to the rotor and also including n times fundamental frequency voltages in the armature, e.g. $n = 5$, $h = 7, 19, 29, \dots$

Of these, (1) is the magnetizing reactance at fundamental frequency (see equation (3.7)), (2) constitutes an element of leakage

reactance at fundamental frequency and is called the differential leakage reactance, (3) is the magnetizing reactance calculated at n times fundamental frequency (see equation (3.6)), and (4) contributes to the differential leakage reactance with respect to n^{th} harmonic current.

For convenience, the differential leakage reactance is considered as the sum of two elements, the zigzag and the belt leakage. The zigzag leakage is defined by Alger¹³ as that due to all the airgap harmonics that would be produced if the winding had one slot per pole per phase, i.e. if each slot formed a complete phase belt and each slot carried the same current, equally spaced apart in time as well as space phase. The belt leakage reactance is the additional reactance due to the actual phase belts, which may be several slots wide.

3.3.3.1 Zigzag leakage reactance

a) Zigzag leakage reactance due to the fundamental current:

This accounts for slot harmonics which are of orders $2ks+1$, where s = slots per pole, and k is any integer.

The expression for zigzag leakage reactance is fully described by Alger¹³. He gives different expressions depending on the approximations made, but the recommended one which considers the effect of slot openings is

$$X_{z_1} = \frac{\pi^2 X_{m_1} K_{s_1}}{12 K_{w_1}^2} \left[\frac{6a - 1}{5 s^2} \right] \quad \Omega/\text{ph} \quad (3.19)$$

where, a : g/G ,

g : actual airgap length,

- G : effective airgap length,
 s : number of slots per pole.

It can be seen from equation (3.19) that the zigzag leakage reactance is greatly influenced by the number of slots and it is zero if this number is large.

- b) Zigzag leakage reactance with respect to the time harmonic currents:

This accounts for the slot harmonics of orders $2ks \pm n$ and can be found directly from equation (3.19).

$$X_{z_n} = \frac{\pi^2}{12} X_{m_h} \frac{K_{s_h}}{K_{w_h}^2} \left[\frac{6a - 1}{5s^2} \right] \quad n = h$$

But, $X_{m_h} = \frac{X_{m_1}}{h} \left(\frac{K_{w_h}}{K_{w_1}} \right)^2$ from equation (3.6), hence

$$X_{z_n} = \frac{\pi^2}{12} \frac{X_{m_1}}{h} \frac{K_{s_h}}{K_{w_1}^2} \left[\frac{6a - 1}{5s^2} \right] \quad (3.20)$$

K_{s_h} can be obtained from Figs. 3.2 and 3.5 for the 6-ph and 3-ph machine respectively.

3.3.3.2 Belt leakage reactance

The belt leakage reactance is due to the increase in differential leakage caused by reducing the number of phase belts to a small number. The harmonic fields corresponding to the belt leakage are of lower orders than those of zigzag leakage, as the former are primarily due to the phase belts which extend over several of the slots to which the latter are due. The derivation of the belt

leakage reactance is similar to that of the magnetizing reactance described in Section 3.2. It can be shown that the belt leakage reactance with respect to n^{th} harmonic current is

$$X_{b_n} = \frac{X_{m1}}{K_{w1}^2} \sum_{h \neq n}^{\infty} \left(\frac{K_{wh}}{h} \right)^2 \quad \Omega/\text{ph} \quad (3.21)$$

The belt leakage harmonics can be determined by the expression $h = 2km \pm n$ (see equation (2.13)). For the 6-ph machine ($m = 6$) carrying fundamental currents, the possible space harmonics are $h = 11, 13, \dots$, from which

$$X_{b_1} = \frac{X_{m1}}{K_{w1}^2} \left[\left(\frac{K_{w11}}{11} \right)^2 + \left(\frac{K_{w13}}{13} \right)^2 + \dots \right] \quad \Omega/\text{ph}$$

and for 3-ph machine ($m = 3$),

$$X_{b_1} = \frac{X_{m1}}{K_{w1}^2} \left[\left(\frac{K_{w5}}{5} \right)^2 + \left(\frac{K_{w7}}{7} \right)^2 + \left(\frac{K_{w11}}{11} \right)^2 + \dots \right] \quad \Omega/\text{ph}$$

Likewise, if a 5^{th} time harmonic current is flowing in 6-ph winding, then

$$X_{b_5} = \frac{X_{m1}}{K_{w1}^2} \left[\left(\frac{K_{w7}}{7} \right)^2 + \left(\frac{K_{w19}}{19} \right)^2 + \dots \right] \quad \Omega/\text{ph}$$

It can be seen that the per unit belt leakage reactance of 6-ph winding is smaller than that of 3-ph winding, for the former winding produces less space harmonics.

Belt leakage reactance was derived as being due to stator currents acting alone, and without considering rotor effects. The belt leakage harmonics will induce voltages in the opposing winding, causing opposing circulating currents, which reduce the effective

reactance. The calculation of the belt leakage reactance taking into account the damping effects of the rotor is well analyzed by Liwschitz¹⁵.

Here, the belt leakage reactance (X_{b_n}) is assumed to be zero because the values of X_{b_n} determined by equation (3.21) are already very small and are further reduced by the damper bars in the laboratory machine.

3.4 CALCULATION OF THE MAGNETIZING AND LEAKAGE REACTANCES FOR THE LABORATORY MICRO-MACHINE

The leakage reactance due to the n^{th} time harmonic current of a synchronous machine with integral slots per pole, and with a squirrel cage winding has been determined by equations (3.13), (3.17), (3.18) and (3.20) to be

$$X_{l_n} = X_{\text{slot}_n} + X_{e_n} + X_{z_n} \quad (3.22)$$

The belt leakage reactance given by equation (3.21) should be added when the machine has no squirrel cage winding and is laminated. The formulae of the above equations together with equation (3.6) are applied here to calculate the reactances of the laboratory micro-machine. The details of this micro-machine are given in Section 4.2.

a) Magnetizing reactance:

Consider, for example, when a fundamental current is flowing in the micro-machine connected in 6 phases. Substituting the following values, $f_1 = 50\text{Hz}$, $m = 6$, $\mu_0 = 4\pi \times 10^{-7} \text{ H/m}$, $C_{d_1} = .97$ and $G_d = .733 \times 10^{-3} \text{ m}$ (given in Appendix A), $\tau = .18 \text{ m}$, $L = .132 \text{ m}$, $K_{w_1} = .955$, $p = 2$ and $N_{\text{ph}} = 48$ in equation (3.7) gives:

$$X_{m_1} = 15.7 \quad \Omega/\text{ph}$$

Likewise, the magnetizing reactance with respect to the n^{th} harmonic current can be obtained from equation (3.6) by substituting for X_{m_1} and an appropriate value for K_{w_h} from Table 3.4. The results of X_{m_n} for machine connected in 6 and 3 phases are given in Table 3.5.

b) Slot leakage reactance:

The slot self and mutual inductances are obtained first as they depend on the slot configuration. Figure 3.7 shows the dimensions of the slot which contains two tiers in a double layer winding. Each pair of tiers belongs to one coil side and therefore carries in phase current. The total slot inductance is made up of the self inductance of each tier and twice the mutual inductance between them.

$$L_s = L_{a_1} + L_{a_2} + L_{b_1} + L_{b_2} + L_{a_1 a_2} + 2L_{b_1 b_2} + 2(2K_{s_n} - 1)(L_{a_1 b_1} + L_{a_1 b_2} + L_{a_2 b_1} + L_{a_2 b_2}) \quad (3.23)$$

K_{s_n} is the slot leakage factor with respect to n^{th} harmonic current and can be obtained from Figs. 3.2 and 3.5.

The self inductance of each tier is

$$L_{a_1} = \mu_0 z^2 \ell \left[\frac{h_1}{w_1} + \frac{h_2}{w_2} + \frac{h_3}{3w_2} \right]$$

where, z : the number of series conductors per tier = $N_{\text{ph}}/2S$,

S : the number of slots/phase,

and ℓ : the gross core length.

$$L_{a_2} = \mu_0 z^2 \ell \left[\frac{h_1}{w_1} + \frac{h_2 + h_3 + h_4}{w_2} + \frac{h_5}{3w_2} \right]$$

TABLE 3.4(A)

Pitch, skew, distribution and winding factors for the micro-machine connected in 3 phases. $K_{w_h} = K_{p_h} K_{skew_h} K_{d_h}$.

h	1	3	5	7	9	11	13	15
K_{p_h}	.966	-.707	.2588	.2588	-.707	.966	-.966	.707
K_{skew_h}	.997	.9745	.93	.8658	.784	.688	.583	.4705
K_{d_h}	.9576	.6533	.2053	-.1575	.271	-.126	.126	.271
K_{w_h}	.922	-.45	.0494	-.0353	.15	-.0837	.0709	.09

TABLE 3.4(B)

Micro-machine connected in 6 phases. The pitch and skew factors are the same as in 3 phases.

h	1	3	5	7	9	11	13	15
K_{d_h}	.9914	.9238	.7933	.6087	.3827	.1305	-.1305	-.3827
K_{w_h}	.9547	-.6364	.1909	-.1363	.212	-.0866	.0734	-.1273

TABLE 3.5

Magnetizing reactance with respect to the n^{th} harmonic current. Values are in Ω/ph .

h	Machine as 3-ph	Machine as 6-ph
	$X_{m_n}, n = h$	$X_{m_n}, n = h$
1	29.2	15.7
3	3.28	1.64 Case 1 2.32 Case 2
5	.0168	.125
7	.0061	.046
11	.022	.0117
13	.0133	.0071

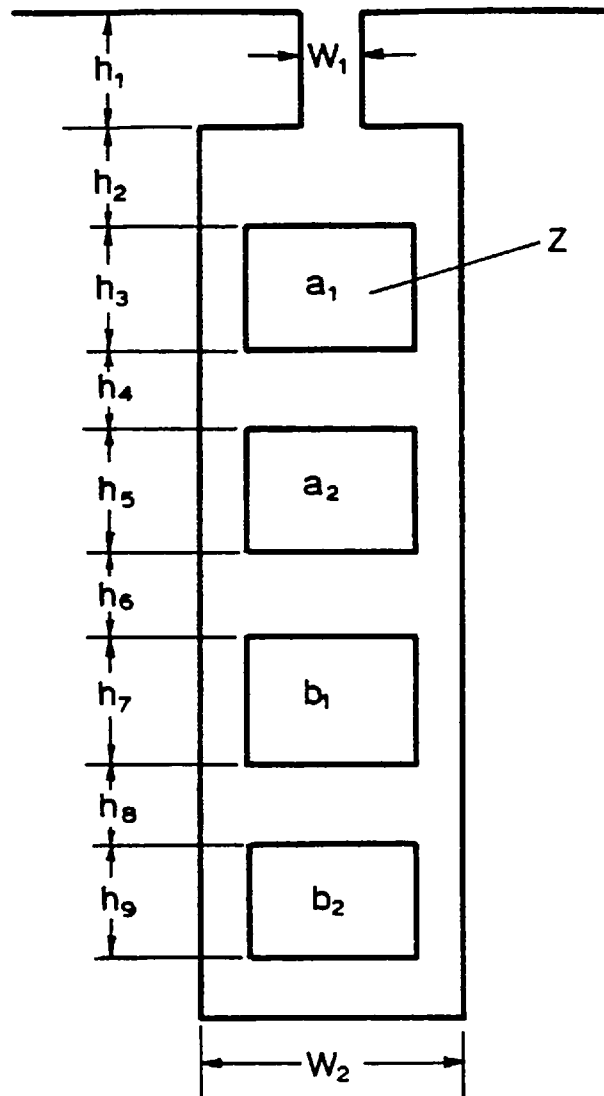


Fig. 3-7 Slot dimensions

$$h_3 = h_5 = h_7 = h_9 = 10.16 \text{ mm}$$

$$h_4 = h_6 = h_8 = 1.74 \text{ mm}$$

$$h_2 = 4.07 \text{ mm}$$

$$h_1 = 12.7 \text{ mm}$$

$$W_1 = 1.53 \text{ mm}$$

$$W_2 = 10.92 \text{ mm}$$

$Z = \text{no. of series conductors/tier}$

$$L_{b_1} = \mu_0 z^2 \ell \left[\frac{h_1}{w_1} + \frac{h_2 + h_3 + h_4 + h_5 + h_6}{w_2} + \frac{h_7}{3w_2} \right]$$

$$L_{b_2} = \mu_0 z^2 \ell \left[\frac{h_1}{w_1} + \frac{h_2 + h_3 + h_4 + h_5 + h_6 + h_7 + h_8}{w_2} + \frac{h_9}{3w_2} \right]$$

Notice that $L_{b_2} > L_{b_1} > L_{a_2} > L_{a_1}$.

The mutual inductance between the tiers is

$$L_{a_1 a_2} = L_{a_1 b_1} = L_{a_1 b_2} = \mu_0 z^2 \ell \left[\frac{h_1}{w_1} + \frac{h_2}{w_2} + \frac{h_3}{2w_2} \right]$$

$$L_{a_2 b_1} = L_{a_2 b_2} = \mu_0 z^2 \ell \left[\frac{h_1}{w_1} + \frac{h_2 + h_3 + h_4}{w_2} + \frac{h_7}{2w_2} \right]$$

$$L_{b_1 b_2} = \mu_0 z^2 \ell \left[\frac{h_1}{w_1} + \frac{h_2 + h_3 + h_4 + h_5 + h_6}{w_2} + \frac{h_7}{2w_2} \right]$$

Inserting into equation (3.23) these expressions for the inductances, simplifying and substituting for h and w from Fig. 3.7, the slot leakage inductance is

$$L_s = \mu_0 \ell \frac{N_{ph}^2}{S^2} \left[1.48 + 38.72 K_{s_n} \right]$$

On substituting for L_s in equation (3.8) and allowing for the order of harmonic, the slot leakage reactance becomes

$$X_{slot_n} = 2\pi f n \mu_0 \ell \frac{N_{ph}^2}{S} \left[1.48 + 38.72 K_{s_n} \right] \quad (3.24)$$

Consider, for example, when the micro-machine is connected in 6 phases and carrying fundamental current. Substituting the

following values, $f = 50\text{Hz}$, $n = 1$, $\mu_0 = 4\pi \times 10^{-7} \text{H/m}$, $\ell = .14\text{m}$,

$N_{ph} = 48$, $S = 8$ and K_{s_1} is obtained from Fig. 3.2 as .933 at $\rho = 5/6$ in equation (3.24) gives:

$$X_{slot_1} = 0.6 \quad \Omega/\text{ph}$$

The slot leakage reactance with respect to n^{th} harmonic current can similarly be obtained by substituting for K_{s_n} from Figs. 3.2 and 3.5. The results of X_{slot_n} for machine connected in 6 and 3 phases are given in Table 3.6. Also, it is shown the relationship between the slot leakage reactances for the two machine connections.

c) End and zigzag leakage reactance:

Consider, as before, when a fundamental current is flowing in the micro-machine connected in 6 phases. Inserting these values, $D_1 = 0.293$ m, $\tan \xi = .933$, $r = .032$ m, $s = 12$, together with those given in part (b), in equations (3.17), (3.18) and (3.20) give

$$X_{e_1} = .1309 \Omega/\text{ph}, \quad \text{and} \quad X_{z_1} = .0822 \Omega/\text{ph}$$

The other values with respect to time harmonic currents are given in Table 3.6. Also, the relationship between the leakage reactance components for machines connected in 6 and 3 phases is shown. It can be seen that the end and zigzag leakage reactances with respect to the n^{th} time harmonic current are small compared with the slot leakage reactance and may, therefore, be ignored.

TABLE 3.6

Leakage reactance components for the laboratory machine. Values are given in Ω/ph .

Reactances	3-ph connection	6-ph connection	Relationships between the reactances of machine connected in 3 and 6 phases
X_{slot_1}	1.125	.6	$(X_{\text{slot}_n})_{3\text{-ph}} = n(X_{\text{slot}_1})_{3\text{-ph}}$ for $n = 1, 5, 7, 11, 13, \dots$ $n \neq 3, 9, 15$ $(X_{\text{slot}_n})_{6\text{-ph}} = n(X_{\text{slot}_1})_{6\text{-ph}}$ for $n = 1, 11, 13, \dots$ $n \neq 3, 5, 7$
X_{slot_3}	2.0	1.0	
X_{slot_5}	5.625	.3245	
X_{slot_7}	7.875	.5	
$X_{\text{slot}_{11}}$	12.375	6.6	
$X_{\text{slot}_{13}}$	14.625	7.8	
X_{e_1}	.2443	.1309	$(X_{e_n})_{6\text{-ph}} = \frac{1}{2} \frac{(K_{d_h})_{6\text{-ph}}^2}{(K_{d_h})_{3\text{-ph}}^2} (X_{e_n})_{3\text{-ph}}$ for $n = 1, 5, 7, 11, 13, \dots$
X_{e_5}	.0064	.0476	
X_{e_7}	.004	.03	
$X_{e_{11}}$.0027	.00146	
$X_{e_{13}}$.00267	.0014	
X_{z_1}	.154	.0822	$(X_{z_n})_{3\text{-ph}} = \frac{(X_{z_1})_{3\text{-ph}}}{n}$ $n = 1, 5, 7, 11, 13$ $(X_{z_n})_{6\text{-ph}} = \frac{(X_{z_1})_{6\text{-ph}}}{n}$ $n = 1, 11, 13$ $n \neq 5, 7$ $(X_{z_n})_{6\text{-ph}} = .533(X_{z_n})_{3\text{-ph}}$ $n = 1, 11, 13, \dots$ $n \neq 5, 7$
X_{z_5}	.0308	.0012	
X_{z_7}	.022	.0008	
$X_{z_{11}}$.014	.0075	
$X_{z_{13}}$.0118	.0063	
X_{l_1}	1.52	.812	
X_{l_3}	2.0	1.0	
X_{l_5}	5.66	.373	
X_{l_7}	7.9	.531	
$X_{l_{11}}$	12.39	6.587	
$X_{l_{13}}$	14.625	7.774	

CHAPTER FOUREXPERIMENTAL AND THEORETICAL INVESTIGATION OF TIME
HARMONIC CURRENTS IN A SYNCHRONOUS MACHINE CONNECTED
IN SIX AND THREE PHASES4.1 INTRODUCTION

The experimental work shows that the steady state short circuit current waveform of the micro-machine is very rich in harmonics when connected in 6 phases, and is almost sinusoidal with 3-ph connection. This result highlights the need to know the cause of the harmonics, and to develop a method of analysis for predicting them. No previous publications have attempted to study the experimental results or to calculate the harmonic currents in a 6-ph machine; Chutorezkij and Woronov⁸ alone have concentrated on the study of losses in 6-ph machine due to harmonic currents.

The theoretical approach described in this chapter is similar to that used by refs. 15 and 16 to study the 3-ph induction machine having a non-sinusoidal supply but modifications to make it suitable for the synchronous machine have been made.

The calculated results are verified by test data which include a measurement of the individual harmonic components of current at different excitation levels, and a comparison of these with the calculated values. From the results obtained, recommendations are made for the design of a 6-ph machine.

4.2 DESCRIPTION OF THE MICRO-GENERATOR MODEL

The power system laboratory possesses a twelve phase belts per pole pair micro-generator, manufactured by Maudsleys Ltd. rated

at 3 kVA, consisting of that company's stator number 3 and rotor number 5. This micro-generator is specially designed to give a range of parameters on a per unit basis similar to a large generator of rating up to 1500 MVA; also, its twelve terminal windings are available externally to allow for either a six-phase or three-phase connection, as shown in Fig. 4.1. The stator specifications when connected as six-phase are given in Table 4.1.

The cylindrical rotor has four poles with 24 slots, having a full pitch double layer winding, divided, the axes of the two halves being displaced by approximately 67.5° from each other. For this case, however, the two winding sections are connected in series so as to obtain the conventional field winding which has its m.m.f. axis coincident with the direct-axis.

The constructional details in a 2-dimensional cross-sectional area of this micro-machine are given in Appendix A, Fig. A.1.

4.3 OPEN CIRCUIT AND SHORT CIRCUIT TESTS

The open circuit characteristics of the machine connected in 6 and 3 phases were obtained simultaneously, first by measuring, for example, between the terminals A_1A_2 , and then between D_1A_2 (see Fig. 4.1(b)). The recording of open circuit phase voltage as well as the short circuit phase current are shown in Figs. 4.2 and 4.3. It is very interesting to see that, although the current waveform of the machine connected in 3 phases is sinusoidal, that of 6-ph machine is highly distorted, in which the 3rd, 5th and 7th are the principal harmonics. When the 3rd harmonic current was eliminated (see Subsection 2.4.1, Case 1), the current waveform slightly

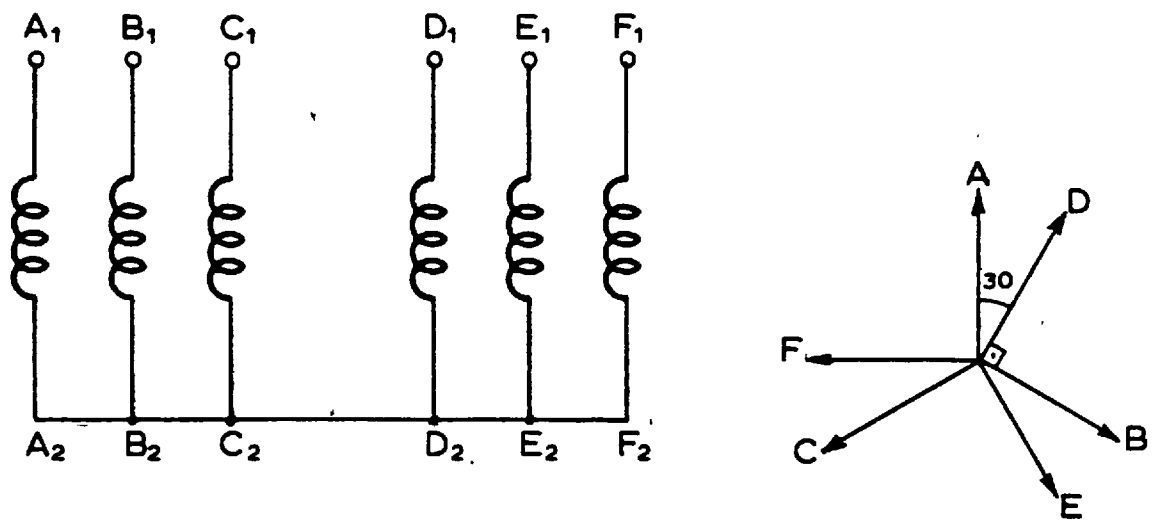


Fig.4.1a Stator winding connected as 6-ph and its voltage phasor diagram.

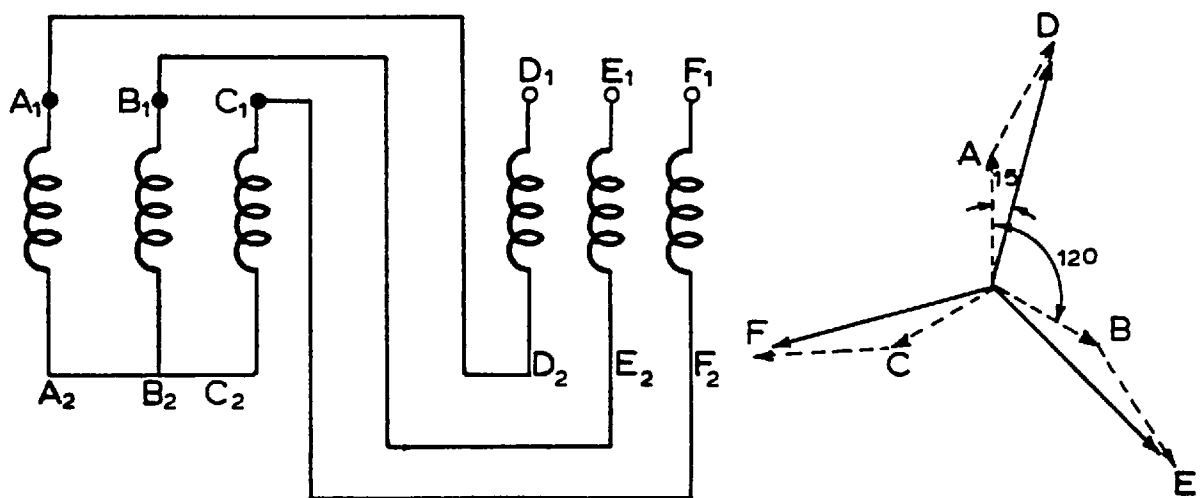
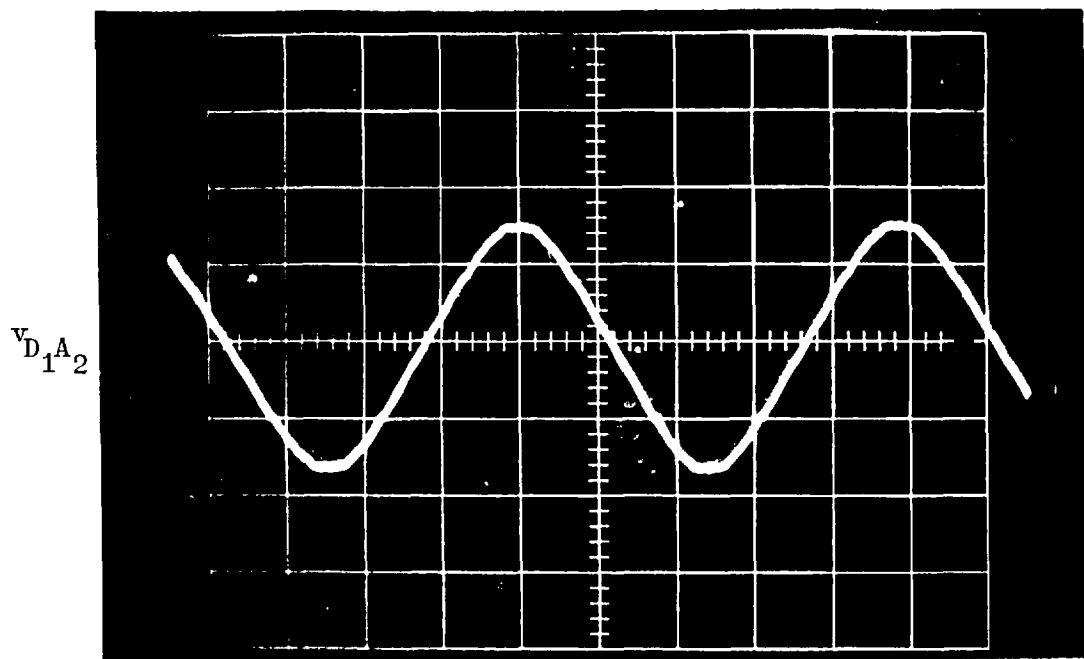


Fig.4.1b 3-ph connection and its voltage phasor diagram

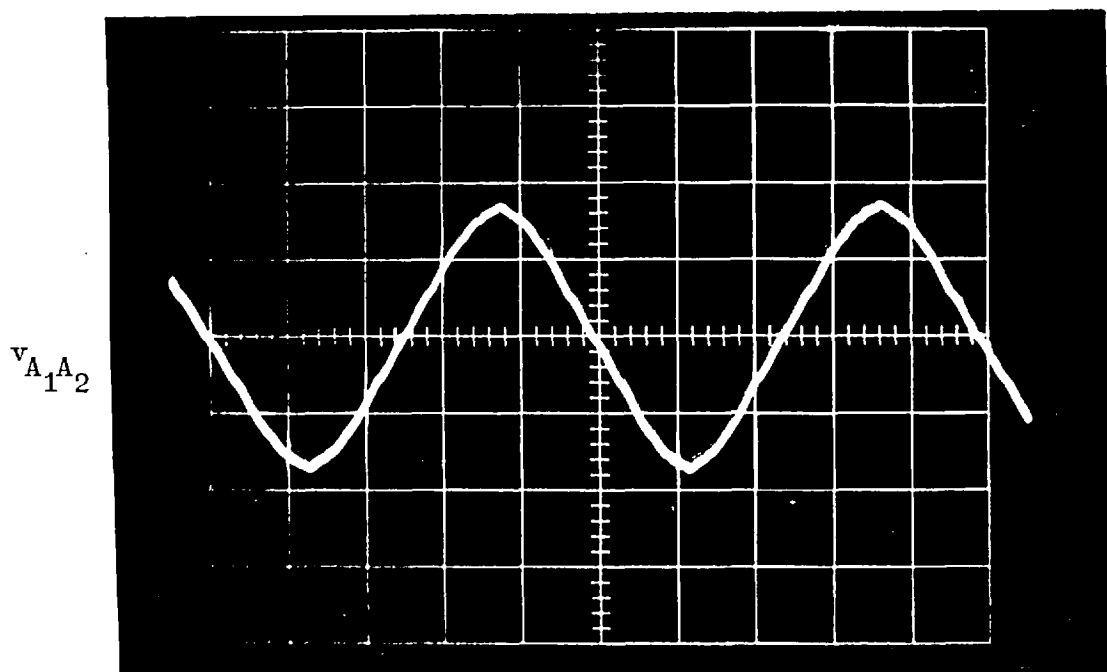
TABLE 4.1

Particulars of stator number 3.
Winding connected in 6 phases.

Phase voltage	62 V
Full load phase current	8.0 A
Number of poles	4
Frequency	50 Hz
Number of slots	48
Number of conductors per slot	12
Number of turns per phase	48
Conductor size (copper)	2 (10 mm. x 1.25 mm.)
Type of winding	2-tier, double layer
Coil pitch	10/12
Winding factor	.955
Length of mean turn	40" (102 cm.)
Phase resistance, 15 deg. C	.035 Ω
Slot skew	1 slot pitch
Axial length, gross	5.5" (14 cm.)
Axial length, effective	5.2" (13.2 cm.)



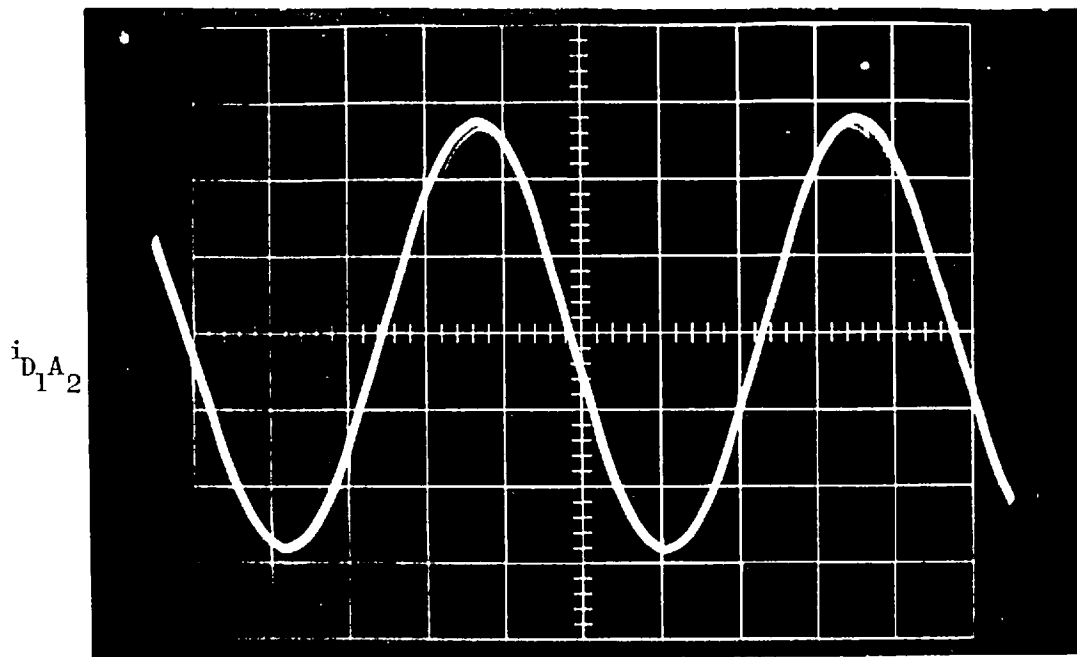
(a) Micro-machine connected in 3 phases.



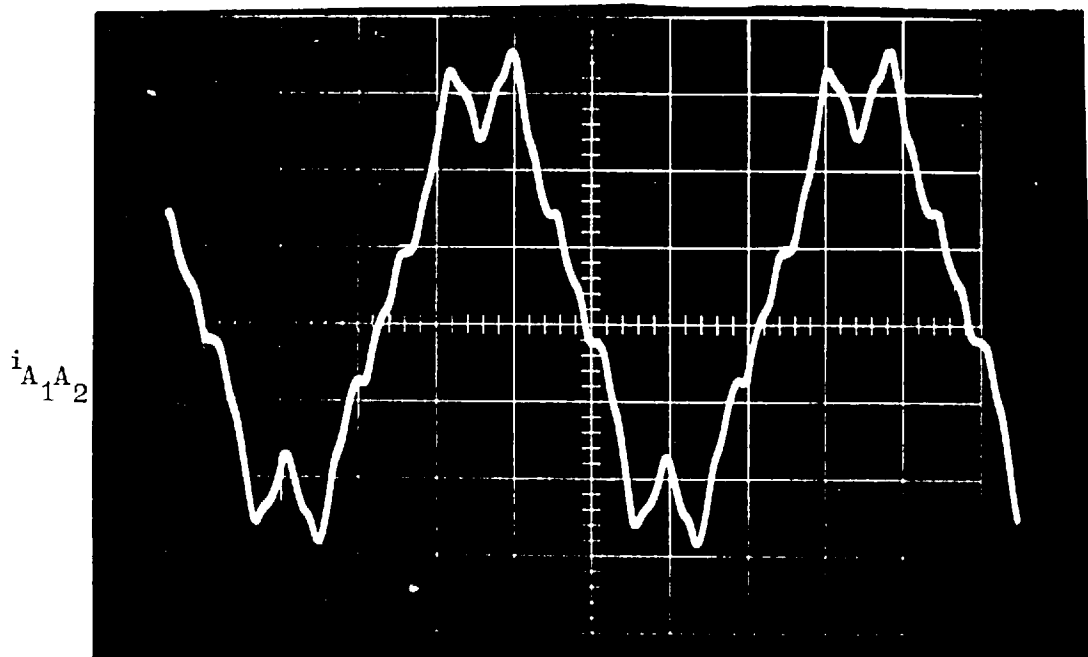
(b) Micro-machine connected in 6 phases.

FIG. 4.2

Open circuit phase voltage.
Excitation current = 0.8 A.



(a) Micro-machine connected in 3 phases.



(b) Micro-machine connected in 6 phases.

FIG. 4.3 Steady state short circuit phase current.
Excitation current = 1.8 A.

changed, and the magnitudes of the 5th and 7th harmonic currents remain the same because, under balanced conditions, they only circulate between the phases in the same way as the fundamental current. This shows that the dip in the current waveform is mainly due to the 5th and 7th harmonics.

The harmonic components in the current waveform were measured using a FR A2 Radiometer wave analyzer. This is essentially a sensitive and selective vacuum-tube voltmeter which can be tuned to any frequency between 5 and 1600 Hz, and which can be given any sensitivity between 100 μ V and 1000 V (full scale deflection). The fundamental components of the phase voltage and current are plotted versus the excitation current as shown in Fig. 4.4.

4.3.1 Determination of X_d and X_q

The direct axis synchronous reactance may be found from Fig. 4.4 as a quotient of the no-load voltage taken from the airgap line at some excitation and the sustained short circuit current value taken from the short circuit characteristic at the same excitation current. The value of X_d determined in such a way corresponds to an unsaturated state of the machine.

$$X_d = \frac{60}{3.6} = 16.7 \quad \Omega/\text{ph}$$

for machine connected in 6 phases, and

$$X_d = \frac{116}{3.8} = 30.5 \quad \Omega/\text{ph}$$

for machine connected in 3 phases.

The quadrature axis synchronous reactance may be obtained

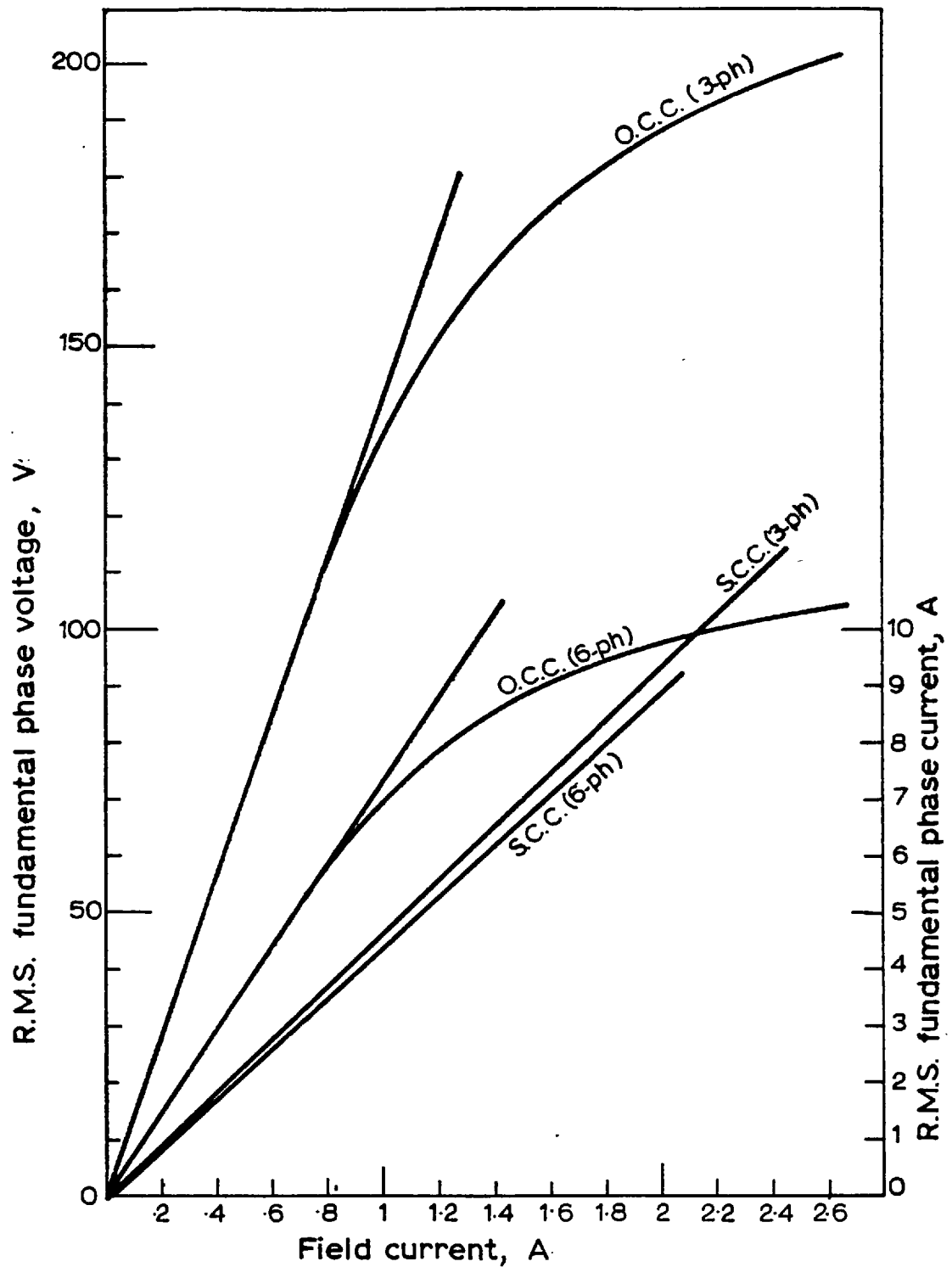


Fig.4-4 Open circuit and short circuit characteristics for the micro-machine connected as 6-ph and 3-ph. Field along d-axis.

from curves similar to those given for calculating X_d , but with machine excited on the q-axis. The rotor of the tested machine has divided windings (see Fig. 2.1) which can be connected and energized so that the field m.m.f. axis is along the q-axis. From Fig. 4.5

$$X_q = \frac{36}{2.3} = 15.6 \text{ } \Omega/\text{ph}$$

for machine connected in 6 phases, and

$$X_q = \frac{70}{2.45} = 28.6 \text{ } \Omega/\text{ph}$$

for machine connected in 3 phases.

The validity of this method was confirmed by finding X_q from a load test. The test was conducted with the machine delivering power to a dead resistive load and excited on its direct-axis. The measurements of fundamental phase current and voltage, and load angle (the angle between the terminal voltage and e.m.f.) were taken. The load angle was measured by electronic phase meter (type 406L) which measures the angle between two signals, one from the terminals of two-phase tachogenerator and the other from the machine terminals. A phasor diagram for machine connected in 6 and 3 phases was constructed, from which the values of X_q were found which were similar to those given above.

The value of X_q was not determined from a slip test because a 6-ph machine would require a 6-ph supply, which was not available at that time. This, however, is not a problem any more, as a 6-ph/3-ph transformer was constructed, the details of which will be given in Chapter 5, and which could be used to perform the slip test.

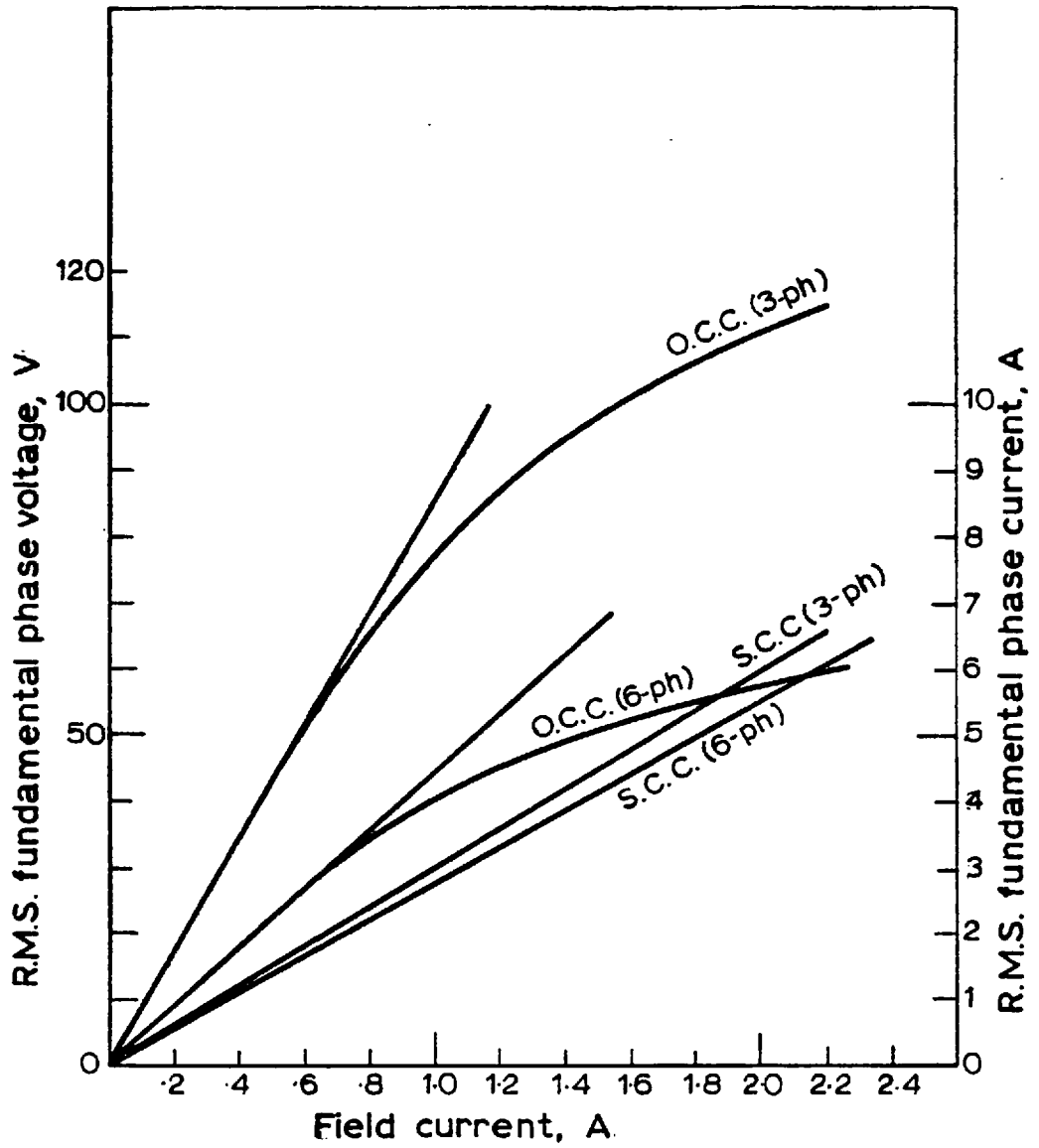


Fig. 4.5 Open circuit and short circuit characteristics for the micro-machine connected as 6-ph and 3-ph. Field along the q -axis.

4.4 THEORETICAL ANALYSIS AND COMPUTATIONS

The general method of calculating the harmonic voltages and currents may be summarized in the following steps:

1. The rotor winding produces fundamental and harmonic m.m.f.'s.
2. Depending on the airgap permeance, the winding distribution, and the pitch factor, harmonic voltages are induced.
3. Harmonic voltages act on the stator winding impedance to give circulating harmonic currents, the magnitude of which depends on the winding configuration, harmonic reactances, and the rotor damping effect.

To simplify the analysis, the following assumptions are made:

1. No saturation, i.e. the iron has infinite permeability. The harmonic voltages are, therefore, linearly proportional to the excitation current.
2. The influence of the slot opening on the harmonic fluxes is the same as on the fundamental wave. Moreover, the same permeance of the airgap, μ_o/G_d , has been used for the fundamental and the harmonics.
3. The excitation current contains no ripples. This was confirmed by exciting the machine with accumulators instead of the normal 3-ph rectifier unit. It was found that the harmonic content of the terminal voltage and the current waveform remained unchanged.

4. The machine windings are symmetrical.
5. The armature resistance is ignored, being much smaller than the leakage reactance.

4.4.1 Calculation of Open Circuit Harmonic Voltages

As shown by equation (2.3), the main field m.m.f. includes, besides the fundamental sine wave, a series of harmonic waves with multiples of the fundamental number of poles, revolving at the rotor speed. Therefore, each space harmonic induces time harmonic voltage, the frequency of which is n times the fundamental frequency ($n = \nu$, see Section 2.3). These harmonic voltages can be obtained from equation (3.4), if the armature m.m.f. is replaced by the main field m.m.f. which is given by equation (2.3) as

$$F_f = \frac{4}{\pi} N_f q I_f \sum_{\nu=1}^{\infty} \frac{K_{d\nu}}{\nu} \cos \nu \frac{\alpha}{2} \cos \nu \theta_r$$

The distribution and $\cos \nu \frac{\alpha}{2}$ factors for rotor space harmonics of the micro-machine are

ν	1	3	5	7	11	13
$K_{d\nu}$.95	.588	.0782	-.2826	.0782	.588
$\cos \nu \frac{\alpha}{2}$.8315	-.195	-.9807	-.555	.9807	.195

Substituting for $K_{d\nu}$ and $\cos \nu \frac{\alpha}{2}$ and putting $Nq = 300$ turns/winding, then

$$F_f = I_f \left[301.5 \cos \theta_r - 14.63 \cos 3\theta_r - 5.84 \cos 5\theta_r + 8.56 \cos 7\theta_r + 2.66 \cos 11\theta_r + 3.37 \cos 13\theta_r + \dots \right] \text{ At/pole} \quad (4.1)$$

Thus equation (3.4) becomes

$$E_{f_n} = \sqrt{2} \pi n f_1 T_e \bar{\Phi}_{f_n} \quad \text{V/ph} \quad (4.2)$$

where
$$\bar{\Phi}_{f_n} = \frac{2}{\pi} (B_{f_n \max}) \frac{\tau L}{h}$$

The n^{th} harmonic and the fundamental e.m.f. components may be related by

$$\frac{E_{f_n}}{E_{f_1}} = \frac{K_{w_n} (B_{f_n \max})}{K_{w_1} (B_{f_1 \max})} \quad (4.3)$$

It is not difficult to show that the relationship between the harmonic e.m.f. of the machine connected in 6 and 3 phases is

$$\frac{(E_{f_n})_{6\text{-ph}}}{(E_{f_n})_{3\text{-ph}}} = \frac{1}{2} \frac{(K_{d_n})_{6\text{-ph}}}{(K_{d_n})_{3\text{-ph}}}$$

The ratio of the distribution factors for n^{th} harmonic is given by equation (2.33)

$$\frac{(E_{f_n})_{6\text{-ph}}}{(E_{f_n})_{3\text{-ph}}} = \frac{1}{2} \frac{1}{\cos(15h)} \quad (4.4)$$

Calculated values of harmonic components of e.m.f. as a function of excitation current for the micro-machine connected in 6 and 3 phases are listed in Table 4.2, and are in V/ph.

TABLE 4.2

Machine connection	$\frac{E_{f_1}}{I_f}$	$\frac{E_{f_3}}{I_f}$	$\frac{E_{f_5}}{I_f}$	$\frac{E_{f_7}}{I_f}$	$\frac{E_{f_{11}}}{I_f}$	$\frac{E_{f_{13}}}{I_f}$
6-phase	76.71	2.481	0.297	.31	.061	.066
3-phase	148.2	3.510	0.153	.16	.118	.127

4.4.2 Analysis and Calculation of Steady State Short Circuit Harmonic Currents

The method of analysis is based on the conventional synchronous machine equivalent circuit but includes modifications to the conventional theory necessary to account for time harmonic effects. These modifications involve recalculating the open circuit voltages, leakage reactance and the magnetizing reactance with respect to different harmonics.

The classical way of calculating the sinusoidal armature current under steady state short circuit condition is from the synchronous machine equivalent circuit as given in Fig. 4.6(b). However, when the induced voltage waveform is distorted, the same equivalent circuit may still be implemented but with different parameters. The non-sinusoidal waveform can be expressed as a Fourier series containing only odd harmonics, and therefore the analysis of the synchronous machine can proceed as if there were a series of independent sources all connected in series as shown in Fig. 4.6(a). Since each harmonic current will be independent of all the others, a series of independent equivalent circuits, one for each harmonic, can be used to calculate the steady state performance for that specific harmonic current. The equivalent circuit for the n^{th} harmonic is shown in Fig. 4.6(c), from which

$$I_{a_n} = \frac{E_{f_n}}{X_{\ell_n} + X_{m_n}} \quad \text{A/ph} \quad (4.4)$$

The values of open circuit voltage, magnetizing and leakage reactances with respect to n^{th} harmonic current can be obtained from Tables 4.2, 3.5 and 3.6 respectively. The results are given in Table 4.3 as the ratio of harmonic current component and the field current.

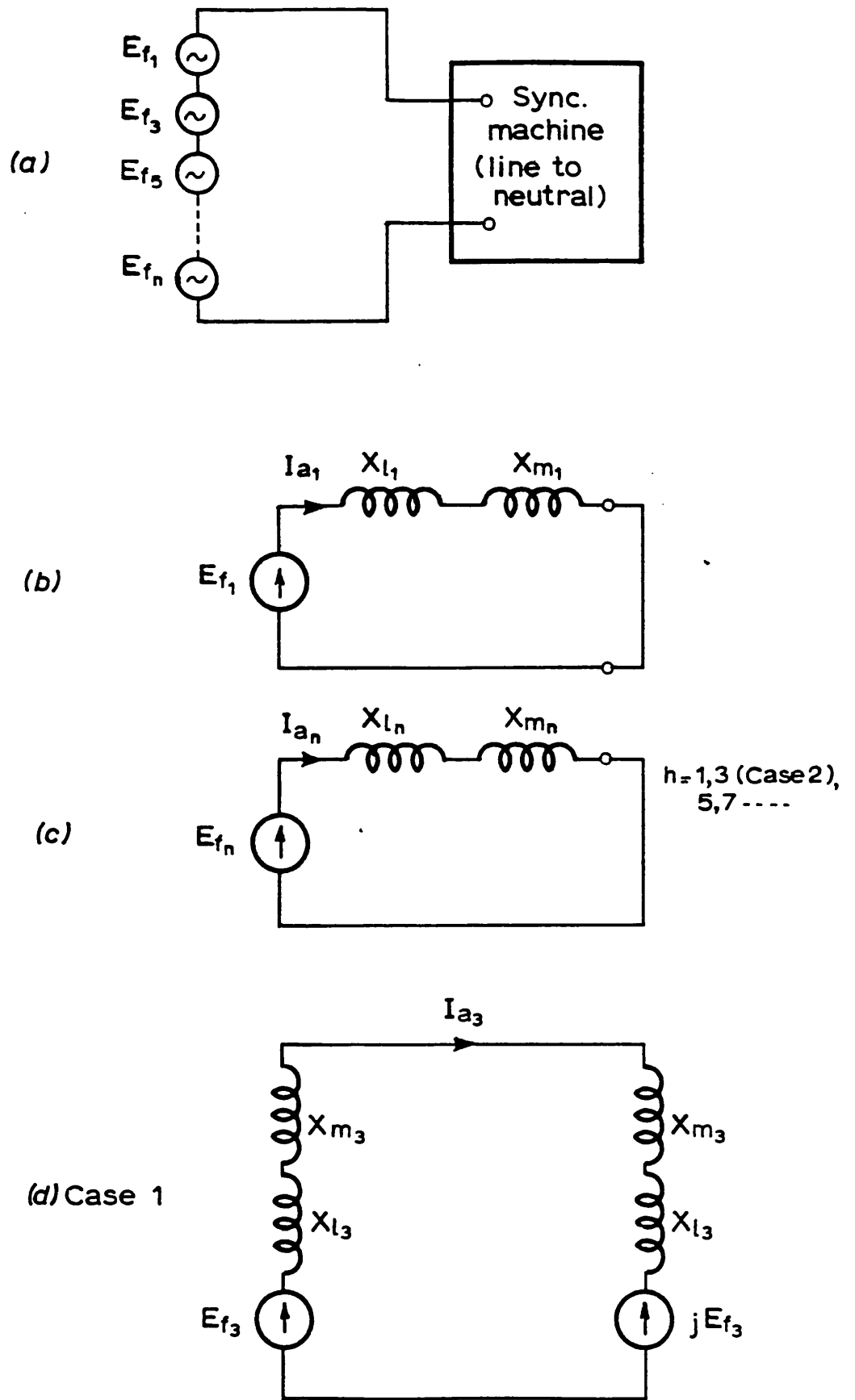


Fig.46 Equivalent circuit for synchronous generator with nonsinusoidal excitation.

Machine connection	$\frac{I_{a1}}{I_f}$	$\frac{I_{a3}}{I_f}$	$\frac{I_{a5}}{I_f}$	$\frac{I_{a7}}{I_f}$	$\frac{I_{a11}}{I_f}$	$\frac{I_{a13}}{I_f}$
6-phase	4.66	.66 case 1 .75 case 2	.59	.54	.009	.0085
3-phase	4.8	.66	.027	.02	.0095	.0087

4.5 COMPARISON OF EXPERIMENTAL AND COMPUTED RESULTS

Tables 4.4(A) and 4.4(B) give a comparison between the tested and calculated values of harmonic current in the micro-machine connected in 6 and 3 phases. The following observation can be made after studying the differences between the measured and computed results:

1. The calculated values of fundamental currents agree reasonably with the test ones.
2. There is a discrepancy of less than 10% in the values of 5th and 7th harmonic currents with the machine connected in 6 phases.
3. There is a difference of less than 15% in the values of the 3rd harmonic currents in machine connected in 6 and 3 phases.

Nevertheless, the overall agreement between the predicted and experimental results is such as to indicate that the adopted method of analyzing the time harmonic currents with the machine connected in 6 and 3 phases is basically sound.

I_f	I_{a1}		I_{a3}		I_{a5}		I_{a7}		I_{a11}		I_{a13}	
	m	c	m	c	m	c	m	c	m	c	m	c
1	4.5	4.66	.6	.66*	.56	.59	.5	.54	.03	.009	.022	.0085
			.7	.75**								
1.2	5.4	5.6	.7	.79	.66	.71	.6	.65	.036	.011	.026	.01
			.81	.9								
1.4	6.2	6.5	.81	.924	.75	.82	.7	.76	.042	.013	.031	.012
			.95	1.05								
1.6	7.1	7.5	.92	1.05	.86	.944	.79	.865	.049	.014	.035	.014
			1.1	1.2								
1.8	8	8.4	1.05	1.2	.96	1.06	.89	.97	.055	.016	.04	.015
			1.21	1.35								
2	8.9	9.32	1.15	1.32	1.1	1.18	.99	1.08	.06	.018	.044	.017
			1.35	1.5								

* Case 1

** Case 2

TABLE 4.4(A)

Comparison between computed and measured harmonic currents in micro-machine connected in 6 phases at different excitation current. Values in A.

I_f	I_{a1}		I_{a3}		I_{a5}		I_{a7}		I_{a11}		I_{a13}	
	m	c	m	c	m	c	m	c	m	c	m	c
1	4.63	4.8	.6	.66	.026	.027	.02	.0203	.008	.0095	.01	.0087
1.2	5.6	5.76	.7	.79	.032	.032	.024	.024	.01	.011	.012	.01
1.4	6.45	6.72	.81	.92	.036	.038	.027	.028	.011	.013	.014	.012
1.6	7.4	7.68	.92	1.1	.043	.043	.032	.0325	.012	.015	.017	.014
1.8	8.3	8.64	1.04	1.2	.047	.048	.036	.0365	.014	.017	.02	.0156
2	9.3	9.6	1.15	1.32	.053	.054	.04	.041	.016	.019	.022	.0173

TABLE 4.4(B)

Same as Table 4.4(A), but with the micro-machine connected in 3 phases.

The main reasons for the discrepancy between the tested and predicted results are thought to be:

1. Excluding the belt leakage reactance component and assuming that the damper bars completely suppress all the harmonic m.m.f.'s which are in motion relative to the rotor. This is not absolutely true for each harmonic m.m.f. has its own damping factor as illustrated in ref. 15.
2. All the leakage reactance components with respect to the 3rd harmonic current were ignored except for the slot leakage reactance component.
3. All the foregoing considerations are based on the assumption that the harmonic induced voltages are directly proportional to the excitation current. This is not entirely correct, because of the machine having slight residual magnetism which forced some of the harmonic voltages first to decrease and then to increase with the excitation.

It was difficult to measure the magnitude of harmonic voltages or currents when they were only about 0.5% of the fundamental component. Also, the harmonic voltages varied in magnitude from phase to phase, presumably reflecting mechanical imperfections. However, harmonic currents were similar in each phase and that is why the comparison between measured and calculated values has been made for them rather than for the voltages.

The measured 11th and 15th harmonic current magnitudes indicated in Tables 4.4(a) and (b) are not accurate values and it is possible that they are widely out. Values fluctuated from one instant to the next and the measurement is very suspect.

In this chapter the analysis of harmonic currents in synchronous generator connected in 6 and 3 phases and under steady state short circuit conditions was studied. The time harmonic currents have been measured and a method of calculation devised. Correlation between individual measured and computed values of harmonic currents is within 10% over a range of excitation.

The main conclusions arrived at on the basis of the studies made here and in the previous two chapters are as follows:

1. A coil pitch of $5/6$ should not be chosen for a 6-ph machine. At this coil pitch the leakage reactance with respect to 5^{th} and 7^{th} harmonic currents is minimal and therefore the corresponding harmonic currents are maximal.
2. The 5^{th} and 7^{th} harmonic currents in a 6-ph machine can be reduced by selecting a coil pitch of $11/12$. The laboratory micro-generator was given a coil pitch of $5/6$ so that it could also be used as a 3-ph machine.
3. The harmonic voltages will always be larger in a 6-ph winding, as compared to a 3-ph one, because of the poor distribution factors for harmonics.
4. The existence of third harmonic current depends on the way in which the two 3-ph winding sets of a 6-ph machine are connected. There can be no such harmonic current flowing in either of the 3-ph winding sets if the neutral point is isolated externally.

CHAPTER FIVEDESIGN, CONSTRUCTION AND TESTING
OF 6-PH/3-PH MICRO-TRANSFORMER BANK5.1 INTRODUCTION

This chapter surveys critically the main methods so far proposed to couple a 6-ph generator to a 3-ph system. In addition, a new transformer arrangement is described and the details of the design work for a "micro" version are included. As a micro-generator is designed to have small per unit copper loss and high per unit reactances to model a large turbo-generator, so a micro-transformer must also be designed to have per unit parameters similar to those of a large one.

For a given rating of transformer, certain rules and tables are used to initiate the design of a conventional transformer. In generator transformers, it is desirable to keep the total loss down to obtain better efficiency, the leakage reactance being specified according to system requirement. The higher the rating of the transformer, the lower the per unit copper loss and with higher transmission voltages high leakage reactance is unavoidable because more insulation and spacing is needed. A 1200 MVA 3-ph generator transformer might have:

1. A percentage copper loss in the range of 0.25% at full load.
2. A leakage reactance of approximately 15%.
3. Core loss of about one-fifth of the copper loss and a magnetizing current 0.5% of full load current.

4. An operating flux density of $B_{\max} = 1.7 \text{ T}$.

It was hoped, therefore, to design and build a micro-transformer which would have equivalent per unit parameters close to an actual 1200 MVA transformer.

Tests were carried out to compare the measured and calculated parameters of the model transformer actually built. Reasonable agreement indicates the soundness of the design method used.

5.2 SURVEY OF PROPOSED GENERATOR TRANSFORMER ARRANGEMENTS

In order to combine the double 3-ph windings to a single 3-ph system, a special transformer arrangement is necessary to offset the 30° phase shift between the two windings. There are many ways which can be adopted for obtaining a phase adjustment of voltages in the transformer system, but not all of these are suitable. The main requirements for such a unit generator transformer are:

1. The fundamental voltages and currents in one set of phases are shifted by 30° or both are shifted by 15° .
2. The output current is drawn equally from both sets of windings. That is, the low voltage (l.v.) windings of the transformer must present the generator with equal leakage reactances.
3. A sufficiently high impedance is provided between the two l.v. windings to minimize the circulation of harmonic currents and consequent additional losses in both stator and rotor.

The basic methods so far proposed are covered by two

British patents^{18,19}, No. 1 107 704 and No. 1 104 844. In a recent article²⁰, Allen and Macdonald have surveyed critically these proposals and put forward an alternative. For the sake of completeness, the methods proposed by the two patents as well as by ref. 20 are summarized here to point out the difficulties and the possibilities of each. Another transformer arrangement is described fully in Section 5,3 and this was tested in the present work.

Examination of the methods proposed by the two patents shows that unbalanced voltages must either be tolerated or be eliminated at the expense of a slightly increased rating. Figure 5.1 gives a diagrammatic survey of the main proposals embodied in the two patents, in ref. 20, and in this work. They fall into five categories, here designated as A, B, C, D and E, each with its own problems and advantages. There are two possible difficulties presented by A, B and C:

1. The two l.v. windings are star-delta connected and hence their voltages differ by a factor of $\sqrt{3}$. If, as in B, they both share a core limb with a common high voltage (h.v.) winding, their turns must be in this ratio, which can only be obtained approximately. Unable to satisfy the requirements of both applied voltages simultaneously, the main flux takes up an intermediate value giving a small unbalanced voltage in both l.v. windings and consequently higher current is drawn from the generator.

In A and C, however, the two l.v. windings are not located on the same limb, and the ratio can be obtained more closely. This could be done by making the turns ratio close to a factor of $\sqrt{3}$ and adjusting the core dimensions so that

30° phase displacement only

Arbitrary phase displacement

Zero-phase displacement

one l.v. winding
star connected

one l.v. winding
delta connected

h.v. winding
star connected

one l.v. winding
zigzag delta connected

one l.v. winding
delta connected

h.v. winding
star
connected

two l.v. windings
delta connected } one h.v. winding
star connected

Two separate 3-ph
transformers
↓
Six 1-ph
transformers

Single transformer
each limb with two
l.v. windings, one
common h.v.
winding

Three doubly-fed
transformers, each
inner limb with one
l.v. winding and
half of l.v. winding

Single transformer
each limb with one
plus two part l.v.
windings, one common
h.v. winding.

Three double-fed trans-
formers, each outer limb
with one l.v. winding
and one h.v. winding
embracing both adjacent
inner limbs.

↑
A

Three
single-phase
transformers

↑
B

↑
C

↑
D

↑
E

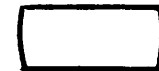
Covered by Patent No. 1 107 704



Covered by Patent No. 1 104 844



Tested in the present work



Suggested in reference 20



Figure 5.1

Classification of the generator transformer arrangement to couple a 6-ph generator to 3-ph bus bars.

the ratio between the induced e.m.f.'s in both l.v. windings was equal to $\sqrt{3}$. In this case, of course, the two h.v. winding sections cannot be connected in parallel unless they have the same number of turns. If, on the other hand, it is impractical to adjust the core dimensions, the parallel connection will inevitably furnish a path for currents to circulate. The problems associated with whether to connect the h.v. winding sections in parallel or series is fully investigated for design C in Chapter 7.

2. In order that the two sets of 3-ph generator windings operate at the same power factor, it is essential that the leakage reactances seen by each set of 3-ph windings are the same. The leakage reactance, as given by equation (5.1) in Section 5.5, is shown to depend on the number of turns to which the reactance is referred, core and winding section geometries. In design category B, it is difficult to achieve equal leakage reactance since the l.v. windings of both sets share a h.v. winding on common limbs and so cannot occupy the same cross-section. To overcome this, a method is suggested here for altering the radial location of both l.v. windings so that the leakage reactances become the same. Figure 5.2 shows the new arrangement in which both l.v. windings are divided into two halves and then cross-connected. Design according to A and C, however, offers some hope since for these cases the h.v. winding sections can have equal number of turns. Provided that, in addition, core and winding section geometries are the same, leakage reactances will be equal. As the currents in the unequal windings will differ by a factor of $\sqrt{3}$ and inversely as the turns, there should be little difficulty in assigning the different number of turns to occupy the same cross-section.

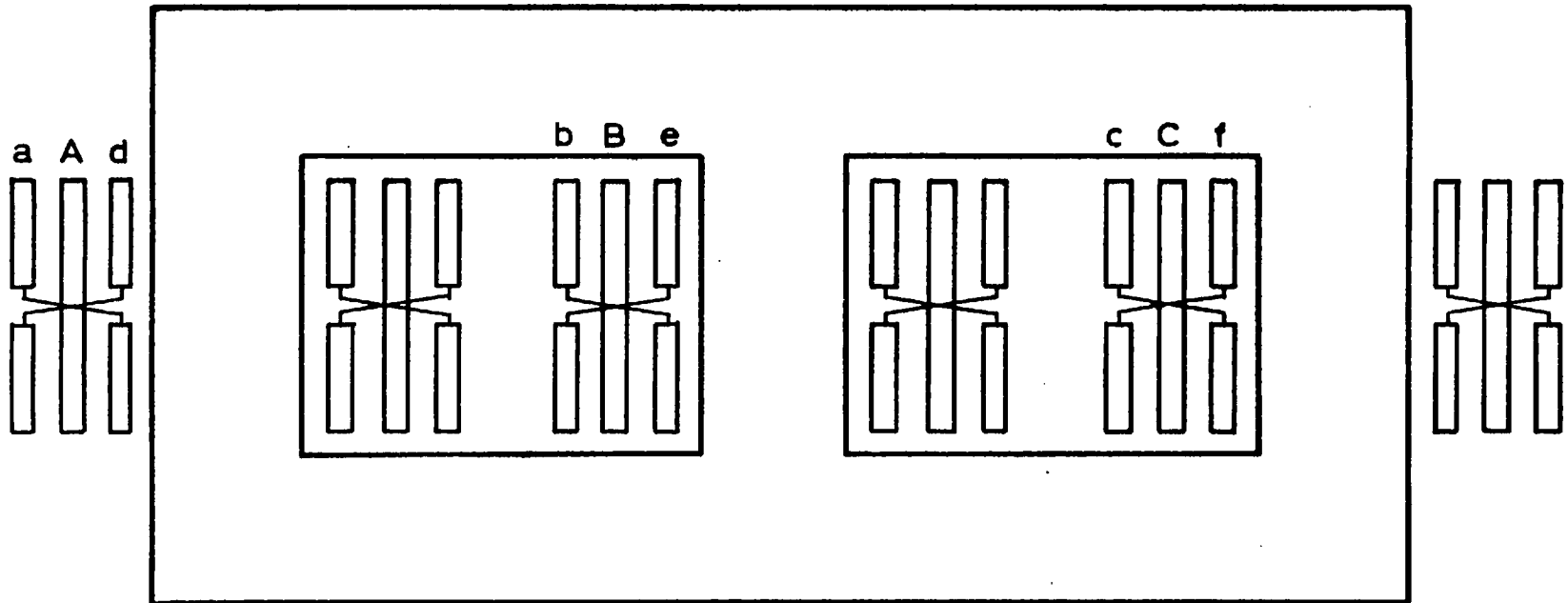


Fig.5-2 6-ph/3-ph generator transformer with its low voltage windings divided into two halves and cross-connected, and a common high voltage winding.

- a-b-c star connected low voltage winding*
- d-e-f delta connected low voltage winding*
- A-B-C star connected high voltage winding*

Design categories D and E offer freedom from any turns ratio out of balance, at least when used to combine sets of voltages displaced by 30° . This, unfortunately, is obtained at the expense of increasing the number of turns and therefore the cost of the transformer. Figure 5.3 gives the transformer arrangement in D and it can readily be seen that in the zigzag delta half of the l.v. winding, about 16% more turns are needed due to phasor addition of series voltages displaced by 60° .

Figure 5.4 shows another alternative which is suggested in ref. 20 and specified here as design category E. This has an identical l.v. winding on each outer limb and a single h.v. winding embracing both adjacent inner limbs. With the l.v. windings supplied with voltages of the same amplitude but at 30° phase displacement, the voltage induced in the output winding is the phasor sum of these multiplied by the turns ratio. To compensate for the phase difference between voltages, about 3.5% more turns are needed in the h.v. winding. The advantages, on the other hand, are believed to be:

1. The l.v. windings will automatically have equal leakage impedances to the h.v. winding due to their symmetrical disposition.
2. A closed path for the third harmonic of magnetizing current is readily provided by delta connection of both set of l.v. windings.

To appreciate fully the technical problems associated with each of these designs requires a deeper investigation and considerable experimental work. To facilitate this for the method presented here, a model transformer has been constructed and is described in the next section.

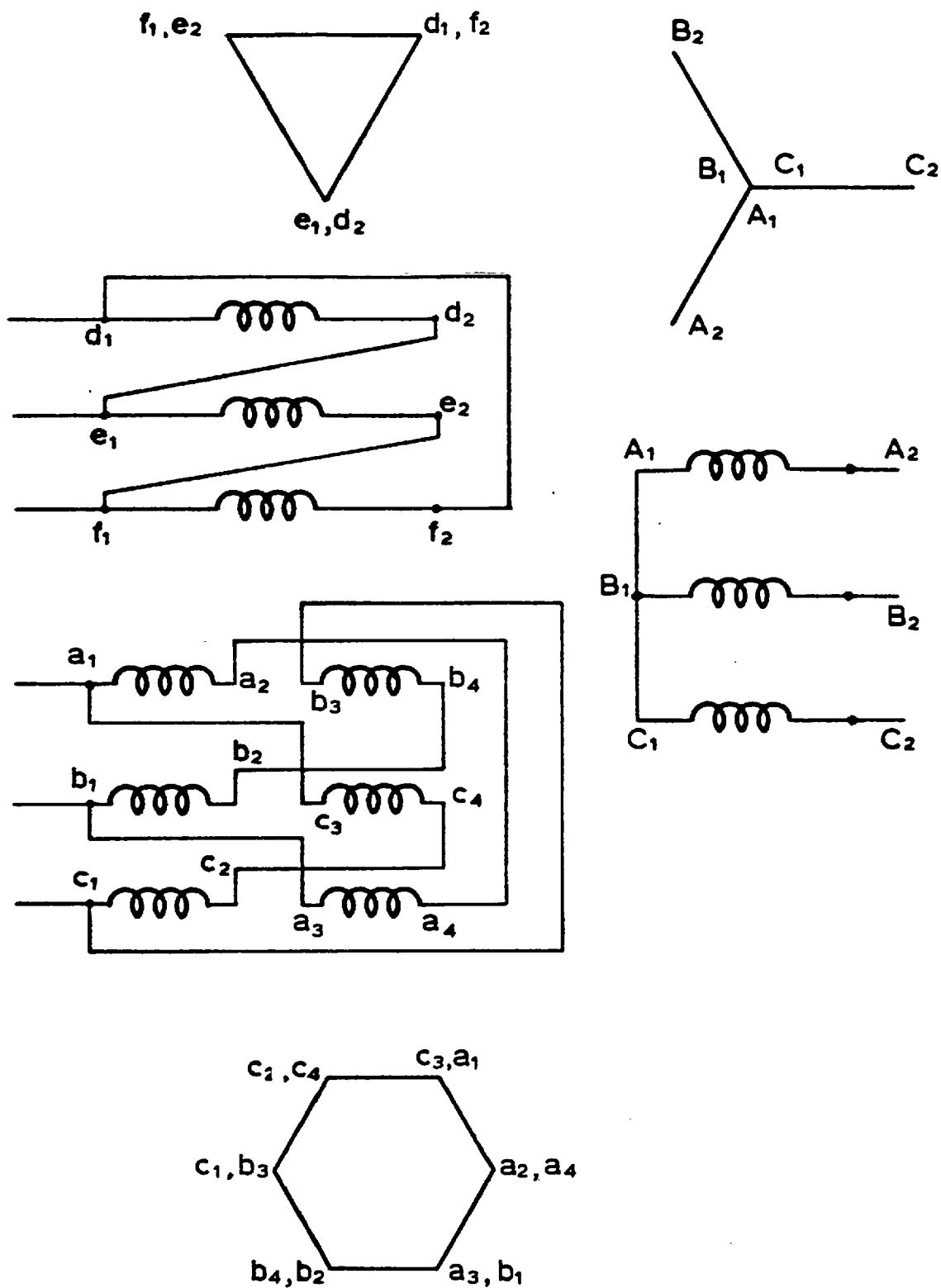


Fig.5-3 Winding connection and phasor diagram for zigzag delta - delta/star arrangement.

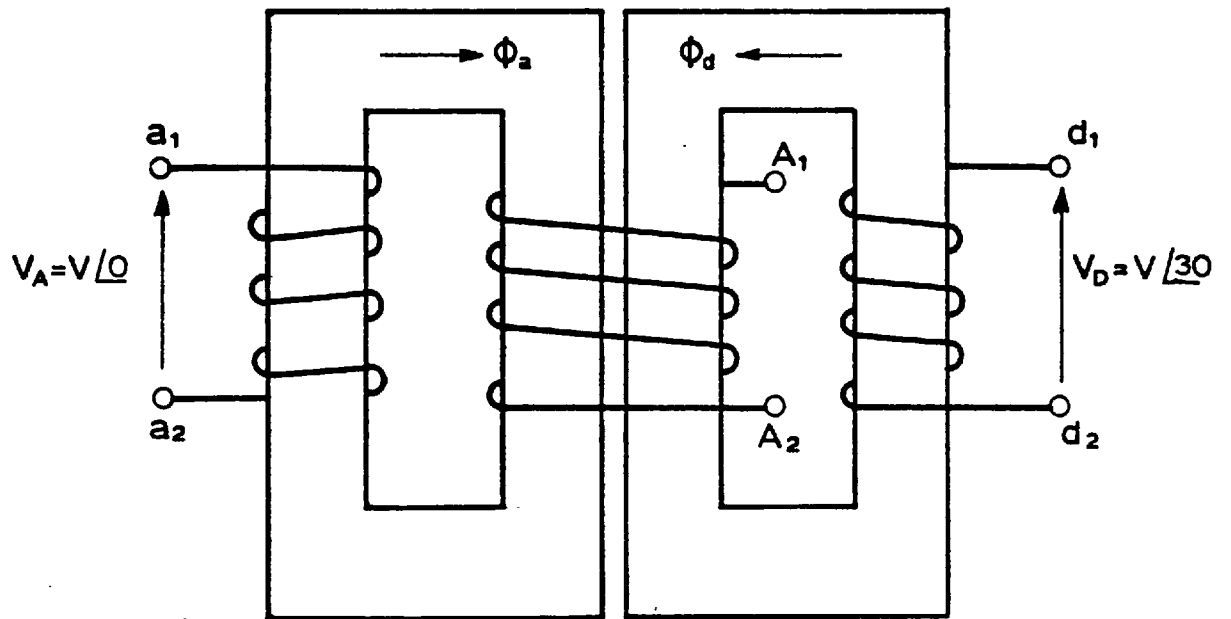


Fig. 5-4 Single unit of a 6-ph/3-ph transformer bank.

5.3 DESCRIPTION OF THE TRANSFORMER ARRANGEMENT PRESENTED BY THIS WORK

For very large transformers, it is important to reduce the height of the active part because of transportation limitations. The height of the yokes, which are an appreciable percentage of the total active height, can be reduced by using either a greater number of limbs which provide appropriate paths for the flux or a bank of single unit transformers, or both.

Here an arrangement with two main limbs and two return limbs is used for each single unit of the three-transformer bank, with yokes 50% of the height compared with the conventional two limb arrangement as shown in Figs. 5.5(a) and (b). Each transformer unit has two low voltage windings and one high voltage winding split into two sections. The windings, as shown in Fig. 5.5(c), are placed concentrically around the main limbs in which the l.v. windings are adjacent to the core.

The circuit diagram of the 6-ph generator connected to 3-ph busbars is shown in Fig. 5.6. Three of the l.v. windings, that is, one from each transformer, are in star connection and connected to the first set of three phase windings of the generator. The remaining three l.v. windings are in delta connection and connected to the other set of three phase windings of the generator. The three h.v. windings are in star connection and connected to the 3-ph system. Each phase of the h.v. is split into two sections which can be connected in series (as shown in Fig. 5.6) or in parallel. The l.v. and h.v. windings of the same transformer are drawn parallel to each other. The tertiary windings, which provide, amongst other

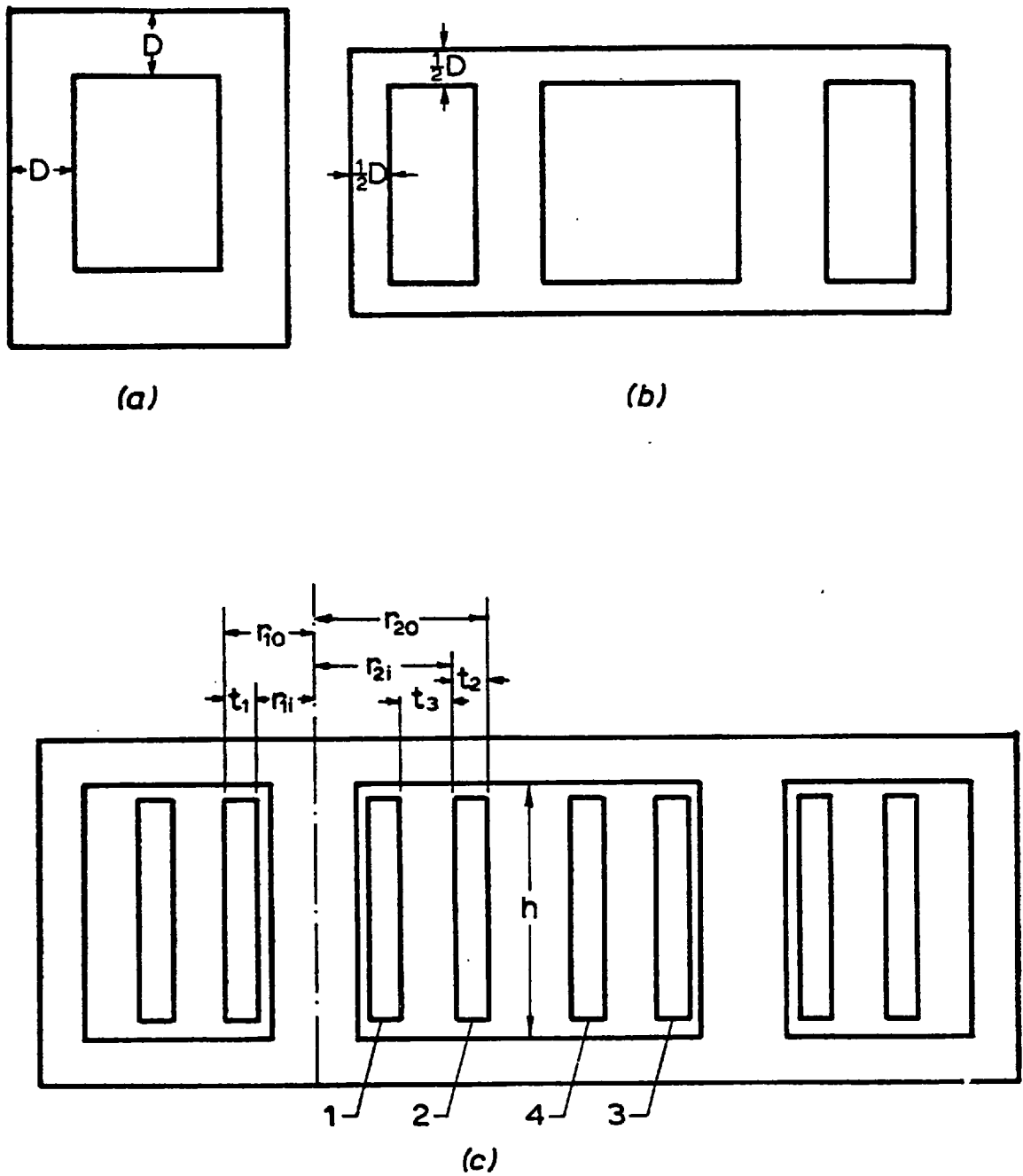


Fig. 5-5 Single unit transformer having :-
 (a) two limbs
 (b) four limbs
 (c) four windings in which 1 & 3 are low voltage,
 2 & 4 are high voltage

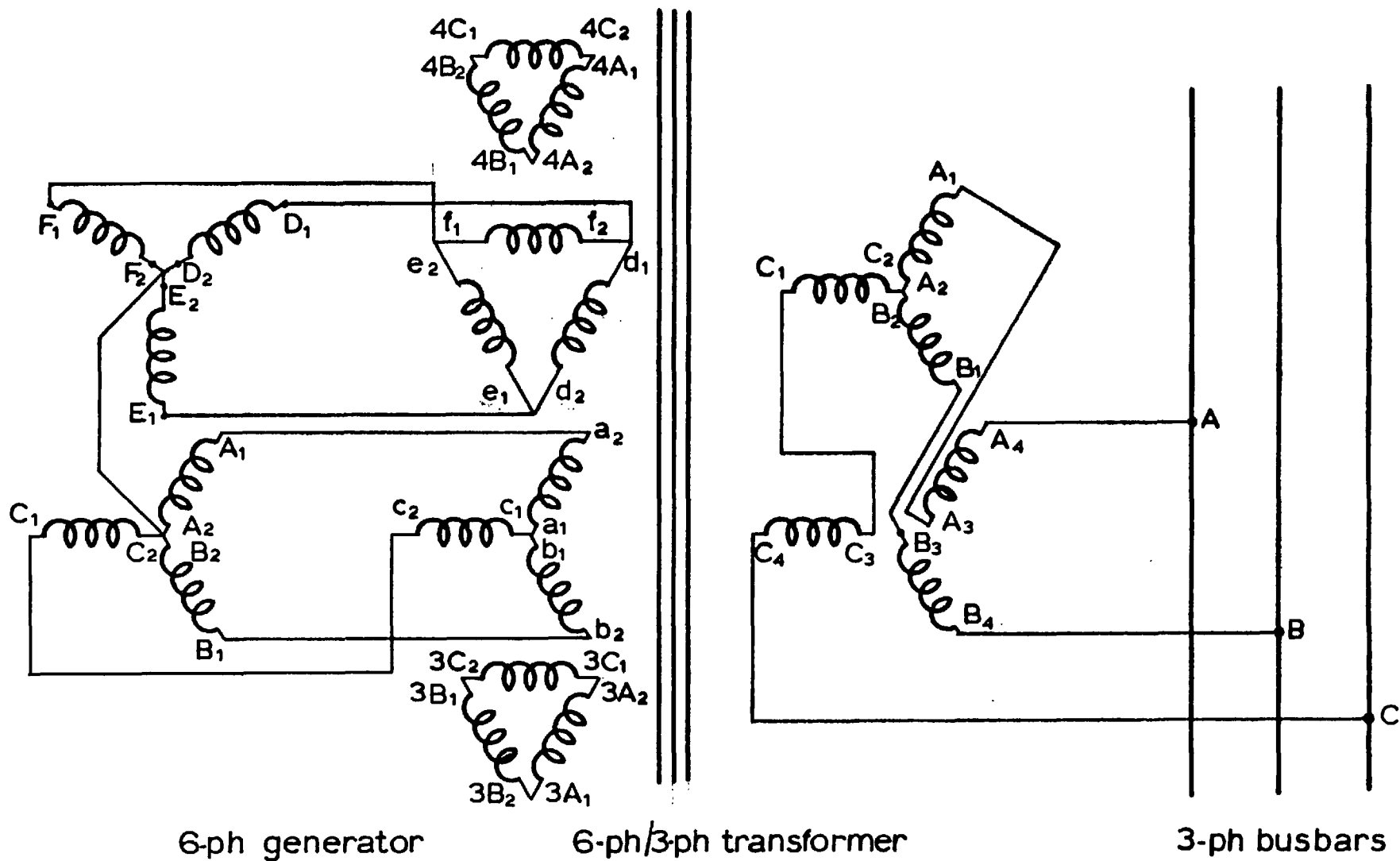


Fig. 5.6 Circuit diagram of 6-ph generator connected to 3-ph busbars through a special transformer arrangement. H.V. winding sections are connected in series. Tertiary windings are also shown.

advantages, a path for third harmonic current to circulate, are also shown. The effects of including or excluding the tertiary windings on the transformer behaviour is investigated in Chapter 7.

It can be seen from the circuit diagram that the 30° phase shift provided by a star-delta winding on the l.v. side is used to reduce the 6-ph generator output to 3-ph. Also, the voltages generated by the windings on a single transformer are all in phase.

5.4 RATING OF THE MICRO-TRANSFORMER

The micro-transformer bank was designed to have the same rating as the 6-ph micro-generator. The terminal voltage of each section of the h.v. winding was, for convenience, selected as 120 V. Thus, when the h.v. winding sections are connected in series, the transformer can be coupled directly to the 3-ph busbars which has a line voltage of 415 V. The rating of the micro-transformer bank is 3 kVA, 50 Hz, $104 Y - 104 \Delta / 208 Y - 208 Y.V.$

In order to model a 1200 MVA transformer bank, 3 units were designed as far as possible so as to have the per unit values given in Section 5.1, i.e.

- 0.25% copper loss
- 15% leakage reactance
- 1.7 T peak flux density.

5.5 DESIGN OF THE MICRO-TRANSFORMER

To obtain the required parameters simultaneously, it was necessary to study the mathematical expression for each and to

examine closely the factors affecting them. For the sake of simplicity, the following assumptions are normally made when deriving a formula for the leakage reactance between a pair of windings in a core-type transformer:

1. Circular symmetry about the core limb.
2. The core iron has infinite permeability relative to the media in the window.
3. Ampere-turns balance.
4. Both windings have the same axial length.
5. Magnetix flux lines are purely axial.
6. The current is uniformly distributed over the winding cross-section.

Then the leakage reactance X_{12} between an inner winding 1 and outer winding 2 referred to the terminals of winding 1 is

$$X_{12} = \frac{4\pi^2 f \mu_o N_1^2}{h} \left[\left(\frac{r_{1i}}{3} + \frac{t_1}{4} \right) t_1 + \left(r_{10} + \frac{t_3}{2} \right) t_3 + \left(\frac{r_{20}}{3} + \frac{t_2}{4} \right) t_2 \right] \quad (5.1)$$

This formula is as given in ref. 21 in unrationalized M.F.S. units. The factors in equation (5.1) are clearly defined in Fig. 5.5. To obtain X_{21} the leakage reactance between the same two windings referred to winding 2, N_2 replaces N_1 .

It can also be shown that a winding resistance in terms of its dimensions may be expressed as

$$R = \frac{\rho \times \pi DN}{a} \quad (5.2.A)$$

or,

$$R = \frac{2\rho lDN^2}{A_w K_w} \quad (5.2.B)$$

where: ρ = resistivity of copper = $1.724 \times 10^{-6} \Omega \cdot \text{cm}$ at $20^\circ\text{C}.$,

D = mean diameter of the winding,

N = number of turns,

a = cross-sectional area of the conductor,

A_w = net window area,

K_w = space factor of window.

Careful examination of equations (5.1) and (5.2) indicates that:

1. Low copper loss is obtained by:
 - a. minimising number of turns,
 - b. using larger core section,
 - c. reducing the number of layers and hence smaller D ,
 - d. using a narrower spacing between the windings.

2. High leakage reactance is achieved if:
 - a. number of turns is maximized,
 - b. the core is smaller,
 - c. number of layers is increased, i.e. height of window decreased,
 - d. the spacing between the winding is widened.

It is obvious that the conditions in (1) can only be fulfilled at the expense of those in (2). When different designs were tested (details of alternative designs are given in Appendix B), it was found that it is not feasible to obtain simultaneously both 0.25% copper loss and 15% leakage reactance. Hence, it was more practical and

economical to design a micro-transformer with approximately 0.6% copper loss and 9% leakage reactance. The leakage reactance may later be increased to 15% by inserting iron packets in the spacing between the l.v. and h.v. windings while making sure that the laminations do not form a closed magnetic circuit. Moreover, it is imperative that this iron does not saturate below the short circuit current level. Let

$$A_i = \text{net core section, mm}^2,$$

$$B_m = \text{maximum flux density, T,}$$

$$J = \text{current density, A/mm}^2,$$

$$E_t = \text{e.m.f. per turn, V,}$$

$$N = \text{number of turns,}$$

$$a = \text{conductor cross-sectional area, mm}^2,$$

Subscript 1 = star-connected l.v. winding,

2 = star connected half of h.v. winding,

3 = delta connected l.v. winding,

4 = star connected other half of h.v. winding.

The e.m.f. per turn can be expressed as:

$$\begin{aligned} E_t &= 4.44 f B_m A_i \times 10^{-6} & (5.3) \\ &= 4.44 \times 50 \times 1.7 \times 40 \times 40 \times .96 \times 10^{-6} = 0.58 \text{ V/turn} \end{aligned}$$

The area was chosen by trial and error.

The number of turns for each winding is

$$N_1 = \frac{60}{0.58} = 103.5 \approx 104$$

$$N_2 = N_4 = \frac{120}{0.58} = 207$$

$$N_3 = \frac{104}{.58} = 179.4 \approx 180$$

In the design of a conventional transformer, the conductor cross-section is chosen according to the current rating of the winding, but for micro-transformer, as the copper loss must be very small with respect to its rating, the conductor is greater. From the preferred wire tables specified in B.S. 4516: Part 2, a rectangular enamelled (Lewmex Grade 1) high conductivity copper conductor of cross-sectional area 49.85 mm^2 and sizes of $3.15 \text{ mm} \times 16.0 \text{ mm}$ was found to be adequate for the winding that carries the highest current rating, namely 8.36 A . This current density (of 0.1677 A/mm^2) is very small as in the micro-generator. Assume the same current density in l.v. and h.v. windings to obtain minimum copper loss. Then

$$a_2 = \frac{4.18}{0.1677} = 24.92 \text{ mm}^2, \quad a_3 = \frac{4.83}{0.1677} = 28.8 \text{ mm}^2$$

The nearest standard rectangular conductor sizes listed in the wire tables are 24.65 mm^2 ($3.15 \text{ mm} \times 8 \text{ mm}$) and 27.8 mm^2 ($3.15 \text{ mm} \times 9 \text{ mm}$). The amended current densities are therefore $J_2 = 0.1695 \text{ A/mm}^2$, and $J_3 = 0.1737 \text{ A/mm}^2$.

Careful selection of the number of layers was essential for the reasons explained earlier in this section. Eight layers were considered appropriate. Hence

$$\text{turns/layer for winding 1} = \frac{104}{8} = 13$$

$$\text{winding 3} = \frac{180}{8} = 22.5 \approx 23$$

$$\text{winding 2 or 4} = \frac{207}{8} = 25.87 \approx 26$$

One and four dummy turns are needed for windings 2 and 3, respectively.

$$\text{Height of winding 1} = (13 + 1) \times 16 = 244 \text{ mm}$$

$$3 = (23 + 1) \times 9 = 216 \text{ mm}$$

$$2 \text{ or } 4 = (26 + 1) \times 8 = 216 \text{ mm}$$

(1 added in order to compensate for the spacing required because of winding helix.) A gap of 10 mm is left above and below each winding for insulation purposes. The height of the window becomes = $220 + 20 = 240$ mm.

5.5.1 Determination of the Winding Dimensions

For the sake of simplicity, the two inner limbs have been chosen of square cross-section, each being 40 mm x 40 mm, whilst the outer limbs have rectangular section 20 mm x 40 mm. Dimensions of all the windings are given in Fig. 5.7. Each inner limb has three laminated cotton fabric based tubes (Lantex) which carry three circular windings: (i) the tertiary, (ii) the low voltage, and (iii) the high voltage windings. The circular diameter around the square core is = $40/.71 = 56.3 \text{ mm} = 2.218''$ rounded off for constructional convenience to $2.25''$ (57.15 mm).

The diameter of the first base cylinder is fixed by the core section, that of the second is determined by the number of layers of tertiary winding and its conductor size, and that of the third is dependent on the spacing between the l.v. and the corresponding h.v. winding, the number of layers of l.v. winding and its conductor size. Obviously it would be easier and cheaper if the cylinder diameters are the same as those preferred by the manufacturer.

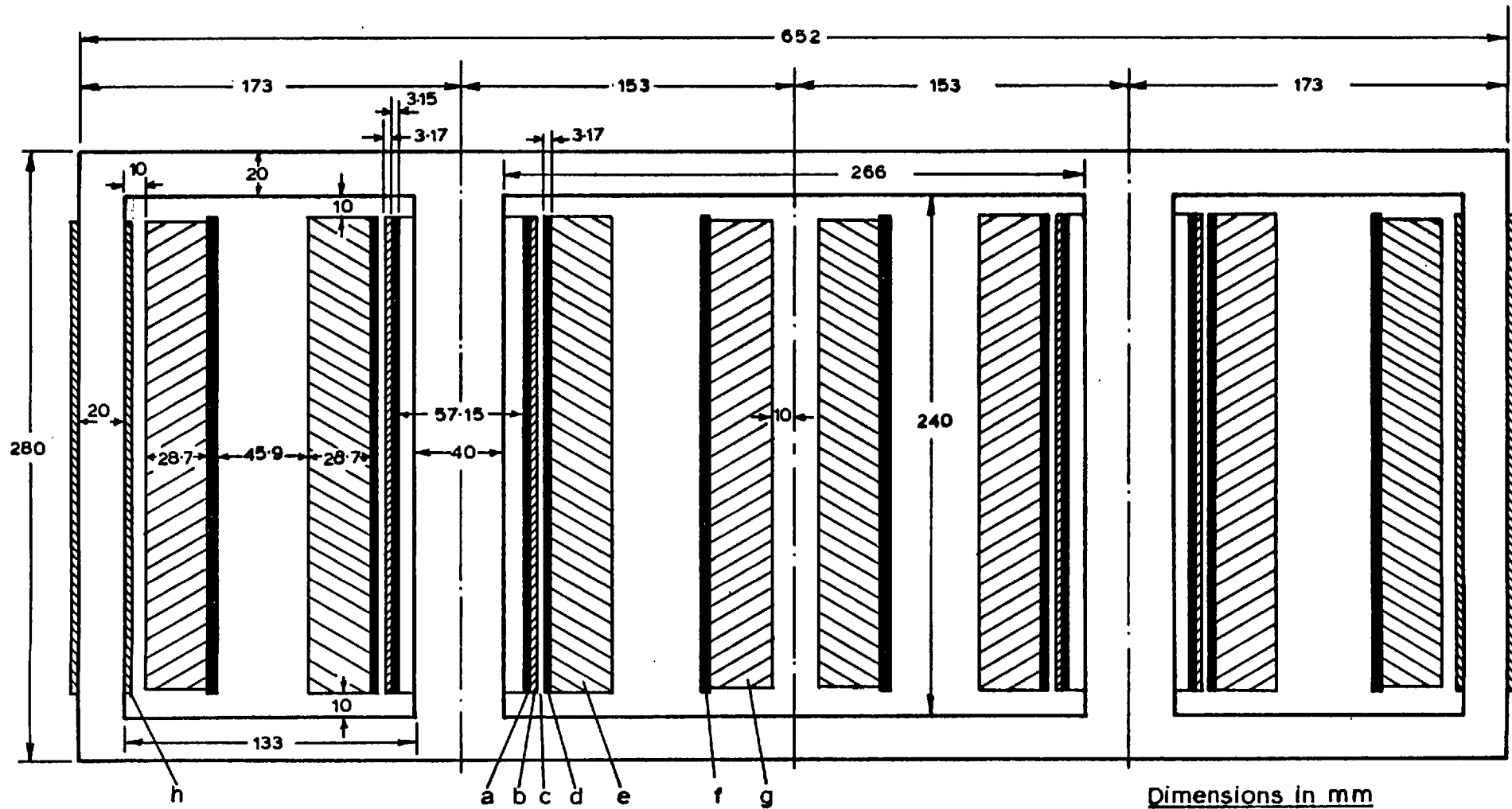


Fig.5.7 Design of 1000 VA single unit micro-transformer with four windings.
*a - First base cylinder b - Tertiary winding c - Spacing for cooling the tertiary, d - Second base cylinder
 e - First low voltage winding f - Third base cylinder g - Half h.x winding h - Search coil*

A single layer of 26 turns and a conductor size of 3.15 mm x 8 mm were found suitable for the tertiary winding. It can be seen that the tertiary winding was wound on both limbs despite one of the l.v. windings being delta connected. This is done in order to produce the same winding configuration on both limbs and hence achieve equal leakage reactance between each l.v. and its corresponding h.v. winding. The thickness of each l.v. or half h.v. winding = $8 \times 3.15 + 7 \times .5 = 28.7$ mm, where 0.5 mm is the thickness of the wrapping paper on each layer.

The nearest standard sizes for the first and second base cylinders are (from ref. 22): $2\frac{1}{4}$ " i.d. x $\frac{1}{8}$ " wall and $2\frac{7}{8}$ " i.d. x $\frac{1}{8}$ " wall, respectively. The transformer is designed to have 9.25% leakage reactance between the l.v. and its corresponding h.v. winding and its ohmic value when referred to the l.v. star connected winding = $0.09 \times \frac{60}{8.36} = 0.664 \Omega$. On substituting in equation (5.1) the following parameters: $X_{12} = 0.664 \Omega$, $f = 50$ Hz, $N_1 = 104$ turns, $h = 240$ mm, $\mu_0 = 4\pi \times 10^{-10}$ H/mm, $t_1 = 28.7$ mm, $r_{1i} = 39.68$ mm, $r_{10} = 68.38$ mm, $t_{12} = x$ mm, $t_2 = 28.7$ mm, $r_{2i} = x + r_{10} = x + 68.38$, $r_{20} = x + 97.08$ mm, and simplifying it becomes

$$x^2 + 15.6x - 92.6 = 0$$

$x = 45.91$ mm, the spacing between each l.v. winding and its corresponding h.v. winding.

The outside diameter of the third base cylinder = $2 \times (68.38 + 45.91) = 228.6$ mm = 9.0". The nearest standard size for the third base cylinder as given by ref. 22 is $8\frac{1}{8}$ " i.d. x $\frac{7}{16}$ " wall.

5.5.2 Losses in the Micro-Transformer

a) Copper loss:

The resistance of a winding, as given by equation (5.2 A) is

$$R = \frac{\rho \times \pi DN}{a}$$

The mean diameter of the first l.v. winding

$$= 2 \times \left(r_{li} + \frac{t_1}{2} \right) = 108 \text{ mm}$$

Therefore

$$R_1 = \frac{1.724 \times 10^{-6} \times \pi \times 108 \times 10^{-1} \times 104}{49.85 \times 10^{-2}} = 0.0122 \Omega$$

Likewise,

$$R_2 = R_4 = 0.117 \Omega, \text{ and } R_3 = 0.038 \Omega.$$

The percentage copper loss of each unit transformer

$$\begin{aligned} &= \frac{R_1 I_1^2 + R_2 I_2^2 + R_3 I_3^2 + R_4 I_4^2}{\text{VA rating}} \times 100 \\ &= \frac{0.0122 \times (8.36)^2 + 2 \times 0.117 \times (4.18)^2 + 0.0379 \times (4.83)^2}{1000} \times 100 \\ &= 0.58\% \end{aligned}$$

Allowing 20% for extra loss to represent the eddy losses in the high voltage, low voltage and tertiary windings, the total copper loss = 0.68%.

b) Core loss:

Since the yoke cross-sectional area is half that of the limb, it can be assumed that the flux density is roughly the same

in all parts of the transformer.

$$\text{Volume of inner limb} = 4 \times 4 \times 24 = 384 \text{ cm}^3$$

$$\text{Volume of outer limb} = 2 \times 4 \times 24 = 192 \text{ cm}^3$$

$$\text{Volume of upper yoke} = 2 \times 4 \times 65.2 = 521.6 \text{ cm}^3$$

$$\text{Total volume of iron} = 2(384+192+521.6) = 2195.2 \text{ cm}^3$$

$$\text{The iron density} = 7650 \text{ Kg/m}^3$$

Therefore the iron weight of each unit transformer

$$= 7650 \times 2195.2 \times 10^{-6} = 16.8 \text{ Kg}$$

The steel grade used to construct the core is, as suggested by the transformer manufacturer, grain oriented electrical steel with 0° to the rolling direction and is supplied under the trade names of "Unisil" or "Alphasil". A steel thickness of 0.3 mm was considered adequate and already available in stock. The core loss can generally be estimated from curves showing the relationship between the specific total loss in W/Kg and the peak magnetic flux density in Tesla. These curves, which are obtained from a 25 cm double lap joint Epstein square and are described in the revised edition of B.S. 601 (Part 5), are normally supplied by electric steel manufacturers, as in this case by the British Steel Corporation²³. The core loss at $B_{\text{max}} = 1.7 \text{ T}$ and $f = 50 \text{ Hz}$ is given as 1.32 W/Kg.

The percentage core loss of each transformer =

$$\frac{16.8 \times 1.32}{1000} \times 100 = 2.2\%$$

5.5.3 Required Weight of Copper

$$\text{Volume of a winding} = 2 \pi t h R_{av}$$

where: t , h and R_{av} are the thickness, height and the average radius of the winding, respectively.

$$\begin{aligned} \text{Volume of first l.v. winding} &= 2 \pi \times 28.7 \times 22.4 \times 5.403 \\ &= 2182.75 \text{ cm}^3. \end{aligned}$$

$$\text{Volume of wrapping paper used between the layers} = 7 \times 2 \pi \times .05 \times 22.4 \times 5.403 = 266 \text{ cm}^3.$$

$$\text{Net copper volume} = 2182.75 - 266.19 = 1917 \text{ cm}^3.$$

Copper density = $8.9 \times 10^{-3} \text{ Kg/cm}^3$. Copper weight of first low voltage winding = $1917 \times 8.9 \times 10^{-3} = 17 \text{ Kg}$.

The weights of other windings can be found similarly and are given in Table 5.1.

TABLE 5.1

Total required copper weight for the micro-transformer bank.

Winding	Nominal cross-section	Weight, Kg
First l.v. winding	3.15 mm x 16 mm	52
Second l.v. winding	3.15 mm x 9 mm	52
H.V. winding	3.15 mm x 8 mm	237
Tertiary winding	3.15 mm x 8 mm	9

For reasons of economy, it was found to be advantageous to use two parallel 3.15 mm x 8 mm windings instead of 3.15 mm x 16 mm winding. This has an additional benefit in that eddy losses are reduced, and it is easier to wind.

5.5.4 Magnetizing Current

The magnetizing current can be evaluated from the curves relating the specific apparent power in VA/Kg and the peak magnetic flux density in Tesla. The data of these curves are also obtained from the Epstein test and are given in ref. 23. At $B_{\max} = 1.7 \text{ T}$ and steel thickness of 0.3 mm, the required specific apparent power = 3.25 VA/Kg. The total apparent power = $3.25 \times 16.8 = 54.6 \text{ VA}$. As the transformer is doubly excited, the apparent power consumed in each l.v. winding is half that of the total. Hence

$$I_{m1} = \frac{54.6/2}{60} = 0.455 \text{ A} \quad \text{magnetizing current in first star connected l.v. winding}$$

Percentage magnetizing current

$$= \frac{0.455}{8.36} \times 100 = 5.44\% \text{ of full load current.}$$

5.6 MICRO-TRANSFORMER CONSTRUCTION

The main constructional elements are the core, comprising limbs, yokes and clamping devices; l.v., h.v. and tertiary windings, search coils, insulating base cylinders and terminals.

The core of each micro-transformer was made of rectangular strips cut from sheets of silicon steel which were assembled in the manner shown in Fig. 5.8. The butt joints between the strips, consisting of any one layer, were overlapped by the strips of the next layer, thus minimising the reluctance introduced into the magnetic circuit by the joints. Since the lamination plates were supplied unperforated, which made their assembly on pins impossible, a wooden jig was built to hold the plates in position and to ensure

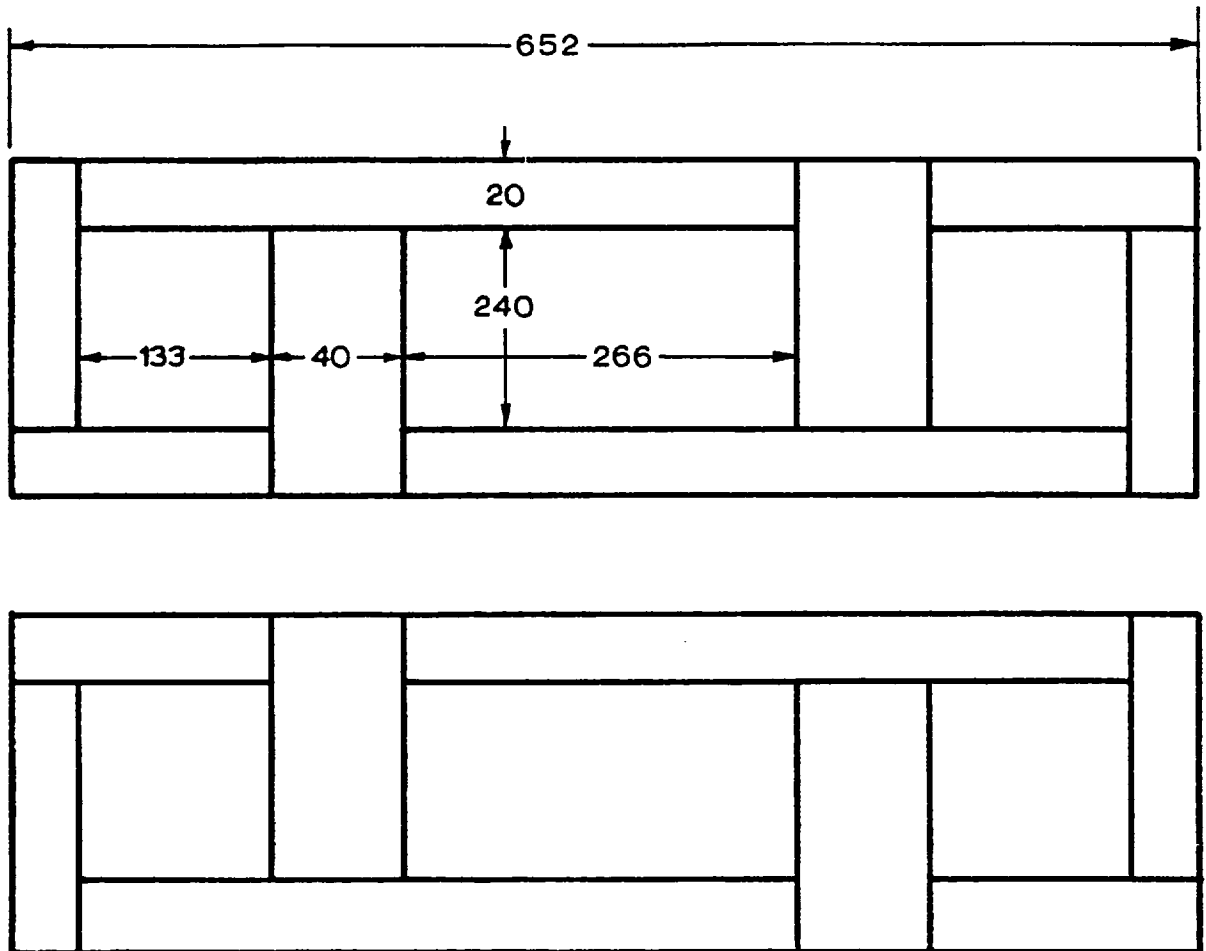


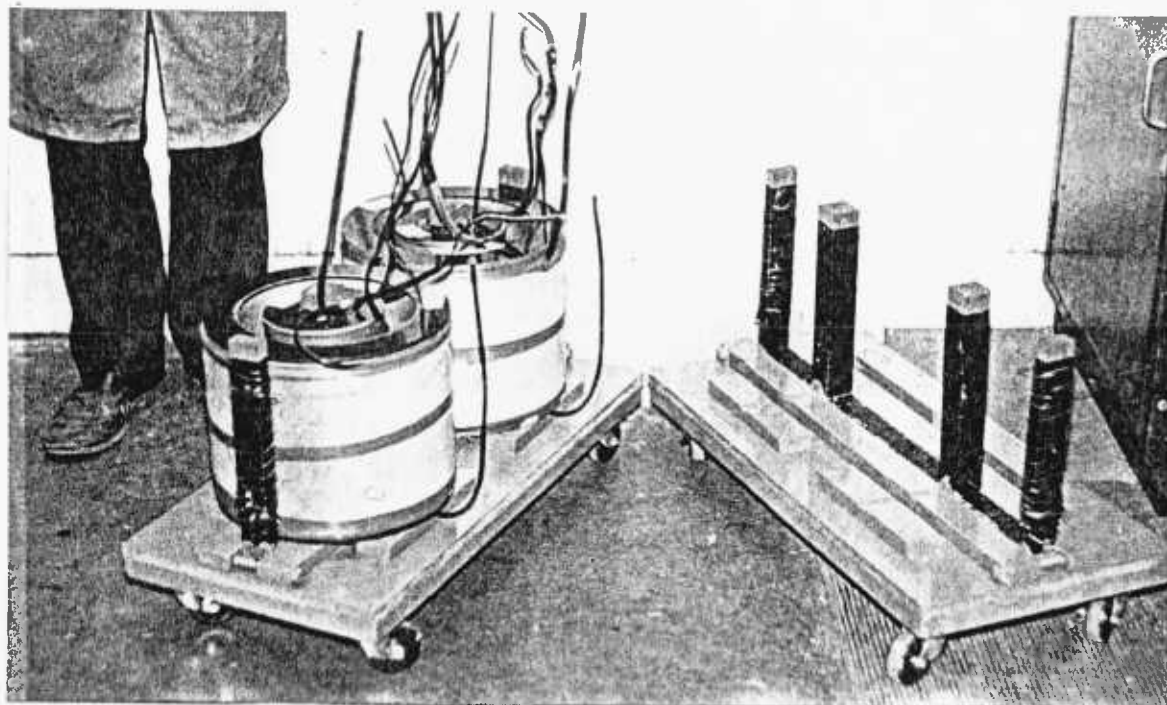
Fig.5-8 Successive layers of laminations. Dimensions in mm.

correct registration. The assembly was carried out by stacking the strips comprising the legs and their lower connection, after which the core (as shown in Fig. 5.9(a)) was lifted upright and the temporary cotton webbing replaced by a strong tape. (As a guide for future practice, it was found important to specify core thickness by number of laminations needed rather than by a linear dimension.)

Cylindrical concentric helical windings, commonly employed for core-type transformers, were wound onto the fabric tube, which facilitate erection and form a strong foundation for winding the coils. A special low speed lathe was used for making the windings in which they all were wound in the same direction and the start and finish terminals were clearly marked to ensure the correct polarity as well as simplifying their connections. Particular attention was paid to winding the two paralleled 3.15 mm x 8 mm copper strips for which an end transposition was required for each layer, as shown in Fig. 5.10.

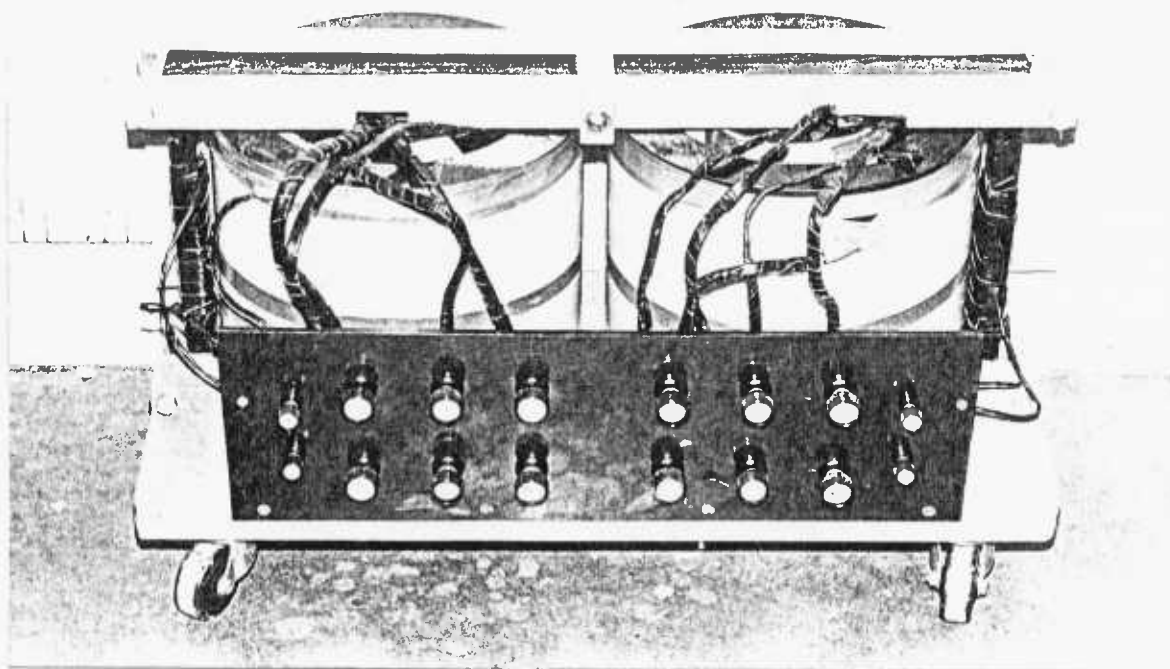
Each preformed winding and its insulating tube was slipped into place (see Fig. 5.9(b)), and the top portion of the core was then built to close the magnetic circuit as shown in Fig. 5.9(c). The top and bottom yokes were each compressed by two wooden members. The upper was permanently clamped by an aluminium G-clamp. The lower yoke was compressed temporarily by a G-clamp and then screwed down to the baseboard.

A search coil with 104 turns was wound onto each outer limb over a layer of insulation for measurement and observing of the flux behaviour. After the three transformers were completely assembled it was found that some turns of the search coils on transformer C were



(B)

(A)



(c)

FIG. 5.9 Core construction of a core-type single unit transformer (one of the three units).

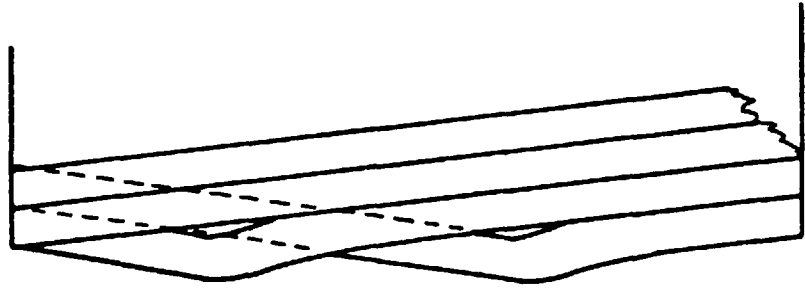


Fig.5-10 Conductors transposition to ensure uniform current density.

shorted to the iron. Consequently, these coils had to be rewound in situ, and because of the limited accesses only half the number of turns (52) was wound on this transformer. In addition to these search coils, another one was wound on the upper yoke of transformer C which also has 52 turns.

The leads from the tops and bottoms of the windings were brought out and connected to the terminal board. The rating plates and the terminal markings were made according to British Standard specification 171-1970 in which the l.v. winding has been given a small letter and the h.v. winding a capital letter. Figure 5.11 shows the markings on the winding terminals of micro-transformer B.

5.7 MICRO-TRANSFORMER TESTING

Tests were carried out to verify the details of the design work, in particular to check the value of the losses and the leakage reactance. The three single unit micro-transformers are, for convenience, called A, B and C, and were tested individually. Because the test results were found to be approximately the same for each of them, only those of transformer B are given in full.

Preliminary tests were first conducted to check the polarity and turns ratio of all windings; obtaining correct polarity is of vital importance as each transformer is doubly fed, has multiple windings and the flux is not confined to a single path. The turns ratio between the windings not on the same limb was found by energising the h.v. winding sections connected in parallel to rated voltage, thus making certain that a common flux was linking them. Typical test results for the turns ratio are given in Appendix C.1

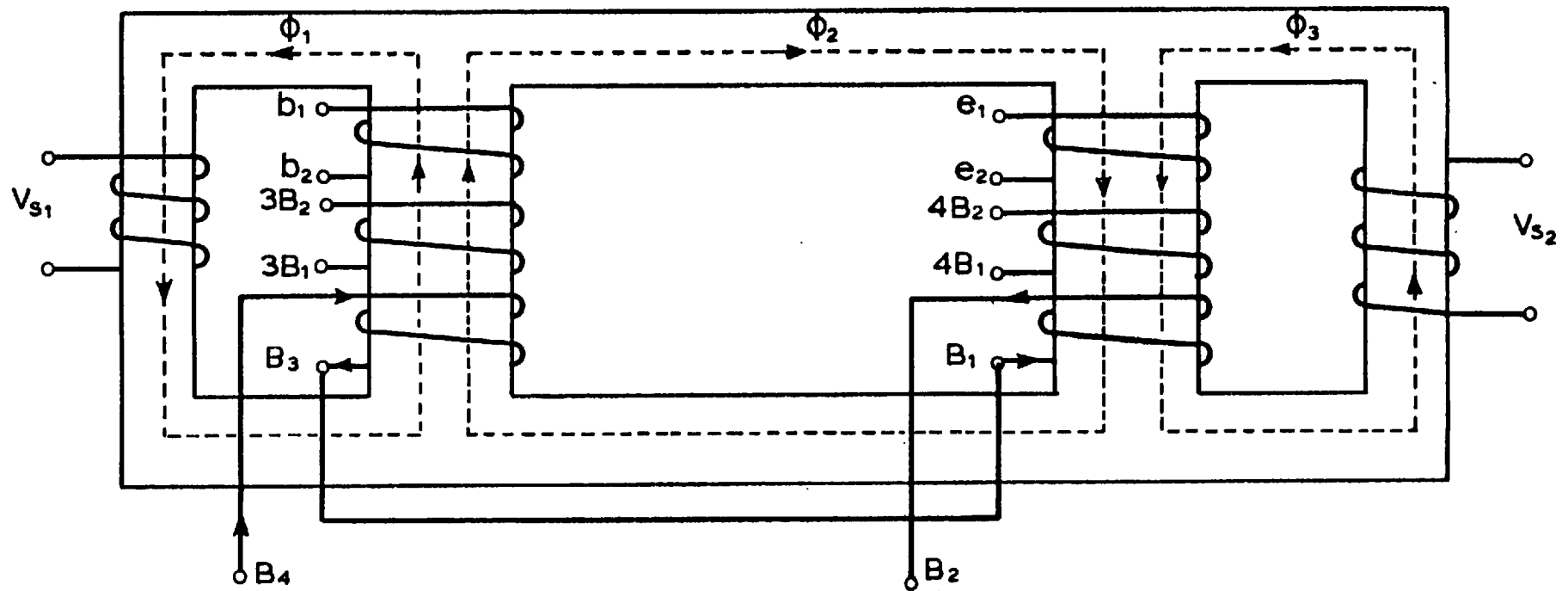


Fig. 5.11 Single unit transformer winding arrangement. High voltage winding sections are connected in series. Dotted lines represent the flux lines.

together with the design values. A good correlation (1.5%) between these values can be seen.

The other routine tests which were performed on the micro-transformer are summarized below.

1. D.C. resistance:

This was measured using a low resistance Kelvin bridge. Appendix C.2 gives the measured and calculated values of resistances for comparison, the measured values being up to 5% more than the design values.

2. Leakage reactance and copper loss:

The leakage reactance between each l.v. winding and its corresponding h.v. winding was determined by short circuiting one of them and sufficiently energising the other to circulate full rated current. Simultaneously, the copper loss was measured and found to have a typical value of .7%, which agrees reasonably with the design value (0.68%). It can be seen from the results given in Appendix C.2 that the actual leakage reactance is 90% of the value calculated using equation (5.1). This discrepancy is probably because the leakage flux path was assumed to be wholly axial.

3. Magnetizing current and core loss:

An open circuit test was made to obtain the magnetizing current and core loss. In performing such a test, care was taken to ensure a distribution of flux as shown in Fig. 5.11 because it was possible to sustain the same terminal voltage with flux in the outer part of iron circuit only. A typical set of measurements for the power loss, voltages and magnetizing current is given in Appendix C.3

at different excitation levels. Figs. 5.12 and 5.13 show curves relating specific total loss and specific apparent power versus peak flux density for transformers A, B and C. A typical actual value of magnetizing current required to produce a flux density of 1.7 T in the inner limbs of each transformer is 20% of full rated current and the core loss is 2.3% of the transformer rating. For the sake of comparison, typical curves supplied by British Steel Corporation catalogue²³ are also included. The following observations can be inferred after studying the differences between the tested and the typical steel manufacturer results.

1. A discrepancy of less than 5% between the core loss.
2. A difference of about 280% in the values of the magnetizing current.

Nevertheless, the overall agreement between the tested characteristics of transformers A, B and C is such as to indicate that they are almost identical in their construction and behaviour.

The main reasons for such a large deviation in the magnetizing current are:

1. The flux density is not equal in all parts of the iron core:

As the flux in the micro-transformer is not confined to a single path, it therefore divides according to the reluctances of the magnetic circuit, namely the characteristics of iron and the airgap joints. It is not possible to develop a test for such a core arrangement in which the flux density can be made uniform so as

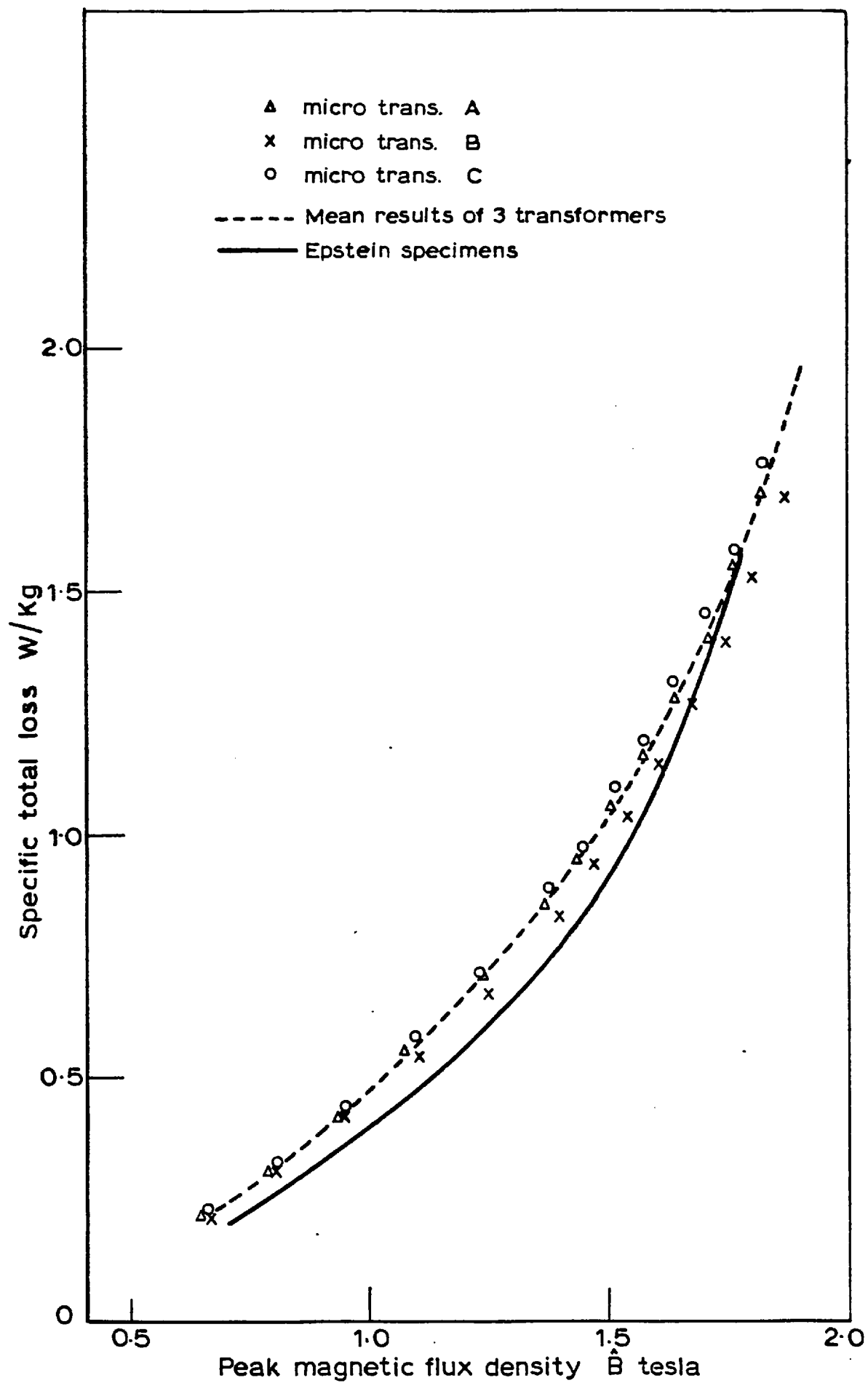


Fig.5.12 Specific total loss

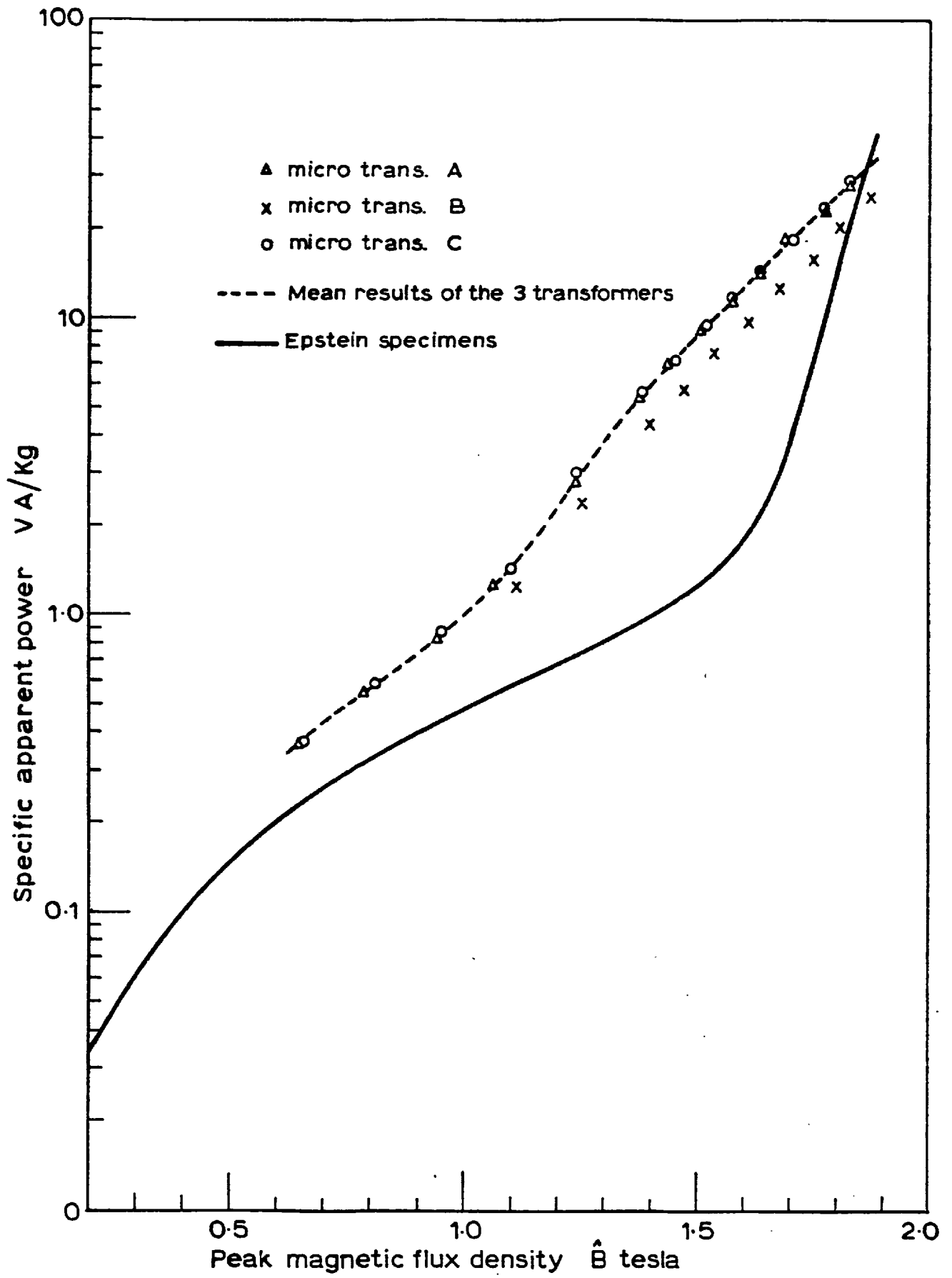


Fig. 5.13 Specific apparent power

to simulate the Epstein test. Evidently, the flux in the yokes of a transformer built in the manner shown in Fig. 5.8 will exceed that in the outer limbs because of differences in path reluctances. Therefore the yokes tend to saturate before the other parts, causing higher magnetizing current to be drawn from the supply. Another consequence of the uncertainty in the flux distribution pattern complicates the construction of the specific apparent power curve. In other words, each part of the transformer which has a different value of flux density would require its own curve. As an approximation, the flux density in the inner limbs is only considered and assumed that the other transformer parts will have the same value.

2. The joints have appreciable influence on the magnetic circuit calculation:

The Epstein specimen is assembled in such a way as to minimize the joint effect and thereby the applied m.m.f. will be fully utilized in magnetizing the iron. Although, on the other hand, considerable care was taken to design the transformer with minimum number of joints (see Fig. 5.8), the effect of airgap was unavoidable because not only were the joints of butt type, but also the laminations were supplied unperforated. It can be seen from Fig. 5.13 that the joint effects are significant when operating at flux densities below 1.5 T. However, it is interesting to observe that as the excitation is increased, the deviation between the curves is reduced because the iron begins to saturate and its reluctance becomes comparable with that of the airgap. At about $B = 1.86$ T the curves meet, which indicates that the magnetic circuit reluctances can now be determined by the iron effects only. In Section 6.4, a method of analysis is developed to consider the joint effect on the magnetic circuit calculation.

5.8 CONCLUSIONS

The design studies made revealed that it is not economical and may not be possible to design a micro-transformer which will have the same per unit parameters as a 1200 MVA generator transformer. Therefore, instead, a micro-transformer of 0.6% copper loss and 9% leakage reactance was designed and built.

The joints between the laminations in the micro-transformer were found to have a significant effect in increasing the magnetizing current on a per unit basis when compared with a large transformer. This occurs because although both transformers are working at the same flux density, scaling effects work to increase the significance of airgaps in the joints. In other words, the gap will be of the same order of magnitude in both transformers, but with the micro-transformer having much shorter lamination lengths.

CHAPTER SIXEQUIVALENT CIRCUITS FOR THE
MULTI-LIMB MULTI-WINDING TRANSFORMER6.1 INTRODUCTION

Complex systems of electrical elements are commonly analysed in terms of equivalent circuits. These circuits contain components representing the significant effects which dictate the performance. The equivalent circuit is thus a simplified mathematical model of the real system. Having developed an adequate equivalent circuit, the well-known techniques of electric circuit analysis are then employed to determine its behaviour. The accuracy with which the solution for the behaviour of the electric circuit represents the performance of the real system is limited only by the adequacy of the equivalent circuit model.

Certain established equivalent circuits for transformers have been developed from linear circuit theory. For example, the treatment of a two-winding transformer as a linear four-terminal network has resulted in the familiar equivalent tee circuit. The limitations of these equivalent circuits often arise from the fact that non-linear elements in the magnetic circuit are not represented by equivalent elements in the electric circuit, and it is often difficult to compensate for non-linearity.

The object of the chapter is to build up a circuit model containing as many branches as may be necessary for determining the performance of a transformer in the steady state. The fundamental assumptions for the method of developing an equivalent circuit are introduced in reducing the magnetic field system to a

magnetic circuit of lumped reluctances. The approach to the equivalent circuit is based on Carpenter's method²⁴, which was previously used to solve eddy current problems. This method is extended here to cover a multi-circuit transformer. The essence of the method is to form two separate, but coupled, circuit models, one magnetic and one electric, of the various flux and current flow paths and then to examine the linkages between these two circuits. In order to define a unique potential function in the magnetic circuit, the linkages between the circuits must be transferred from meshes to the branches which can be done by using the tearing principle. Once this has been done, the equivalent electric circuit is developed from the magnetic circuit by the use of a topological duality technique.

The method of analysis, which is outlined in Section 6.2, is first applied to a two-winding transformer to afford as an illustrative simple example. Equivalent circuits are then developed for a four-winding transformer (the details of which were given in Section 5.3), and further transformations are introduced to allow for series and parallel connections of high voltage winding sections. Finally, the parameters of the equivalent circuit are determined to predict the performance of the transformer in service.

6.2 METHOD OF ANALYSIS

Carpenter²⁴ has developed a method of solving magnetic field problems in electrical devices in which the field quantities are replaced by two separate, but coupled, networks, one magnetic and one electric. Because the network approach provides a direct

topological description of the problem it gives a means of visualising and gaining insight into the behaviour of the device. The central feature of the problem in this approach is the mutual linkages between the two networks, and it is helpful to examine their effect first in networks of few elements. Consider, for example, the two-winding transformer shown in Fig. 6.1(a), for which a magnetic circuit of lumped reluctances is formed from its magnetic field using the techniques described in ref. 25. The assumptions made in developing the magnetic circuit are given in Section 6.3. The iron path elements, as shown in Fig. 6.1(b), are shaded to distinguish them, since they are both non-linear and lossy. This can be further reduced, without changing the linkages between the magnetic and electric circuit, by folding about the centre to three magnetic branches as shown in Fig. 6.1(c).

A most important consequence of the linkage between the magnetic and electric circuits is that the potential difference between any two nodes depends on the path by which it is evaluated. The magnetic potential $(\Omega_1 - \Omega_3)$, for example, takes one value when $(\Omega_1 - \Omega_2)$ is added to $(\Omega_2 - \Omega_3)$ and another when $(\Omega_1 - \Omega_4)$ is added to $(\Omega_4 - \Omega_3)$, i.e. the potential drops do not sum to zero round a mesh. To overcome this difficulty each mesh source in Fig. 6.1(b) or Fig. 6.1(c) must be replaced by an equivalent branch source, or m.m.f. generator. The branch source can be inserted into any branch in which it will ensure the correct mesh m.m.f. condition. A convenient general rule for placing the equivalent branch generators is as follows. If the linkages are removed by tearing them apart, then into each of the intersected branches, in both circuits, a "linkage element" of N turns carrying a current I is

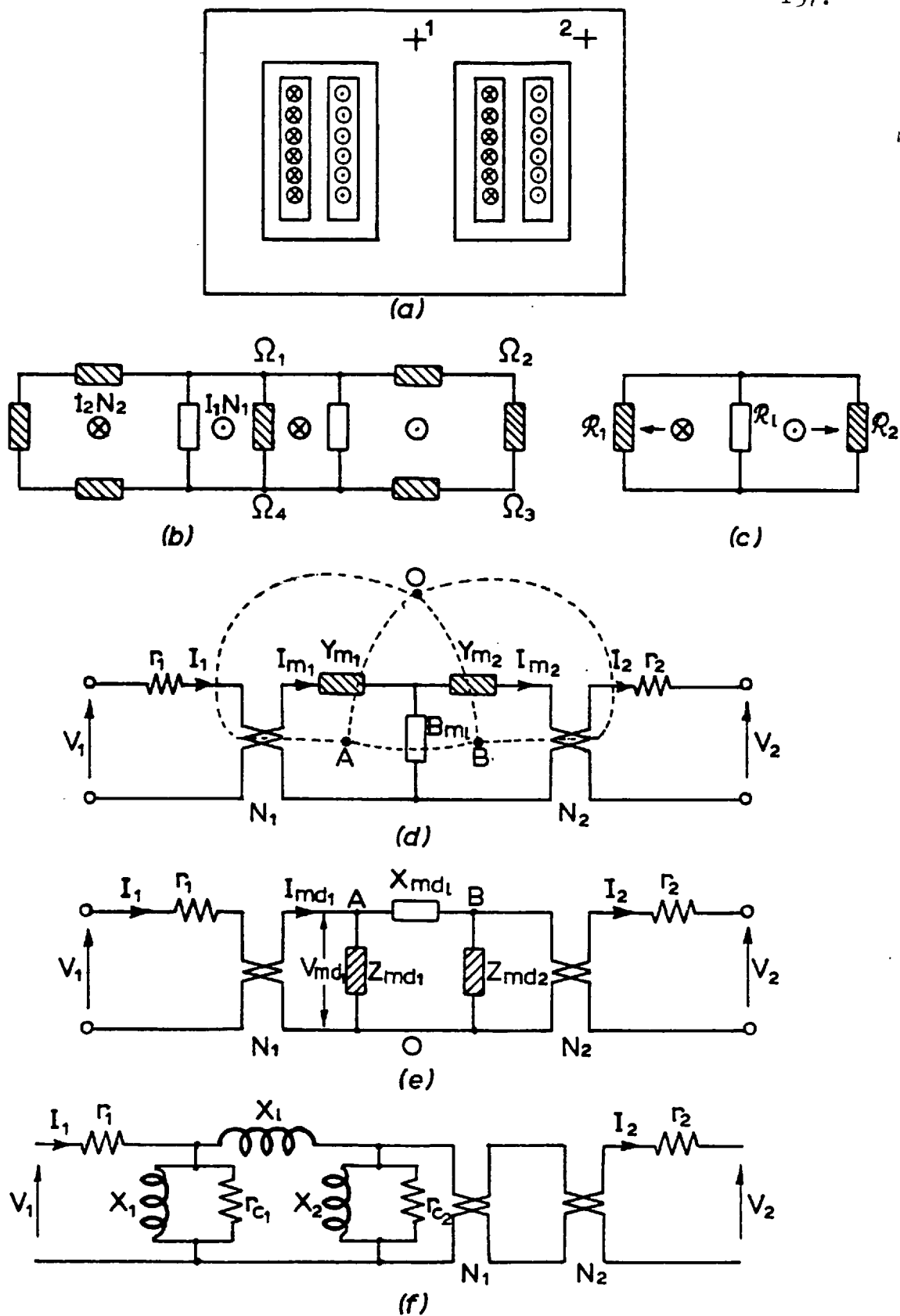


Fig.6.1 Development of equivalent circuit of a two winding transformer.

- (a) Transformer
- (b) Discrete model
- (c) Reduced model
- (d) Equivalent circuit and topological development
- (e) Circuit with magnetic dual
- (f) Equivalent circuit including Ideal transformer

inserted. In this example, as shown in Fig. 6.1(d), the l.v. winding linkage is N_1 and the h.v. winding is N_2 . Before proceeding with the analysis, it is useful to examine the characteristics of these coupled elements. The linkage element has four terminals, two electric and two magnetic. The applied electric voltage is

$$V = N \frac{d\bar{\Phi}}{dt} \quad (6.1)$$

and the m.m.f. which appears across the magnetic terminals is

$$V_m = Ni \quad (6.2)$$

in which it is convenient to regard m.m.f. as "magnetic voltage" and hence use the suffix m. If $d\bar{\Phi}/dt$, instead of $\bar{\Phi}$, is considered as the magnetic equivalent of current, equation (6.1) can be written as

$$V = Ni_m \quad (6.3)$$

Examination of equations (6.2) and (6.3) shows that the linkage element is a symmetrical and reciprocal one in which the output voltage is proportional to the input current. Notice that since magnetic current (i_m) is $d\bar{\Phi}/dt$, then $\bar{\Phi}$ corresponds to charge and, although this picture is less familiar, it has many advantages in comparing electric and magnetic quantities.

Suppose a reluctance \mathcal{R} is connected across magnetic terminals; this is now equivalent not to a resistor but to a capacitor C_m^{26} , i.e.

$$\begin{aligned} \mathcal{R} &= V_m / \bar{\Phi} \\ &= V_m / \int i_m dt = 1/C_m \end{aligned} \quad (6.4)$$

This is entirely appropriate, since the reluctances do not dissipate energy but store it. However, there may also be losses associated with the magnetization, so that the element can be regarded more generally as a magnetic admittance, defined in terms of r.m.s. quantities

$$Y_m = G_m + jB_m = I_m/V_m \quad (6.5)$$

It is not possible to refer the elements shown in Fig. 6.1(d) from one circuit to another without first taking the dual, because, as explained above, the relationships between voltage on one side and currents on the other is an inverted one. To obtain results comparable with ordinary transformer theory, the dual of the magnetic, not the two electric circuits, is taken as shown in Fig. 6.1(d), and quantities in it are denoted by the suffix md. A node is marked within each mesh of the magnetic circuit, and a reference node is marked outside the circuit. These nodes are then joined by branches (shown dotted here), one of which passes through each element in the magnetic circuit. The magnetic capacitors are replaced by inductors (or, more exactly, an admittance by an impedance for non-linear elements and a capacitive susceptance by an inductive reactance for the leakage path) which are numerically equal, and the magnetic voltages and currents are interchanged so that the linkage equations (6.2) and (6.3) in terms of r.m.s. quantities become

$$I_{md} = NI \quad (6.6)$$

$$V = NV_{md} \quad (6.7)$$

All the magnetic impedances in Fig. 6.1(e) can now be transferred from the magnetic to the electric circuit by merely changing their

magnitude by N^2 because, from equations (6.6) and (6.7)

$$V/I = Z = N^2 V_{md}/I_{md} = N^2 Z_{md} \quad (6.8)$$

In this example, as shown in Fig. 6.1(f), the elements are referred to the left hand electric circuit, and they are also shown more explicitly, for comparison with the familiar results. The two coupling elements which are connected back to back form the ideal transformer.

It can be seen that the resultant equivalent circuit is not identical to the conventional one. It is a Π and not a tee equivalent circuit. It is possible, of course, to obtain the tee from the Π by a star-delta transformation, but the reactances which are obtained have no direct physical interpretation, nor are they linear, whereas the series reactance, X_g , in Fig. 6.1(f) is. This approach as well as that of ref. 25 shows that the magnetizing, and not the leakage, reactance should be split into two components.

6.3 DEVELOPMENT OF EQUIVALENT CIRCUIT FOR DOUBLY-FED FOUR-LIMB TRANSFORMER

The method of analysis described in the previous section is used here to derive an equivalent circuit for the four-limb transformer structure shown in Fig. 6.2(a). The method could be applied to any transformer arrangement if its magnetic circuit is planar²⁷. If it is not planar, it is not possible to obtain the dual.

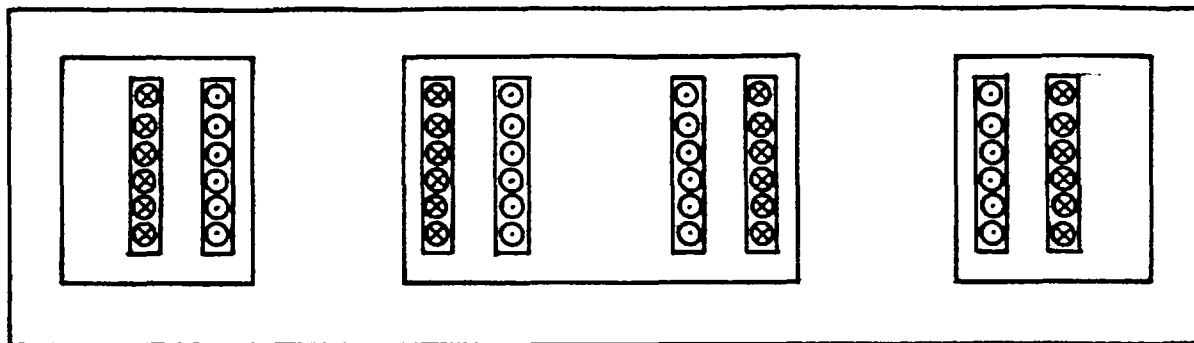
The first and most difficult step in developing an equivalent circuit for a transformer (or any other electric device) is the reduction of its magnetic field into a magnetic circuit of lumped reluctances. All the necessary assumptions can be introduced

at this stage where their significance is most easily visualized. With each set of assumptions, a different equivalent circuit is obtained, and therefore there is no unique simple equivalent circuit for a magnetic system. Here, in constructing a discrete network model of the magnetic field, the following assumptions have been made:

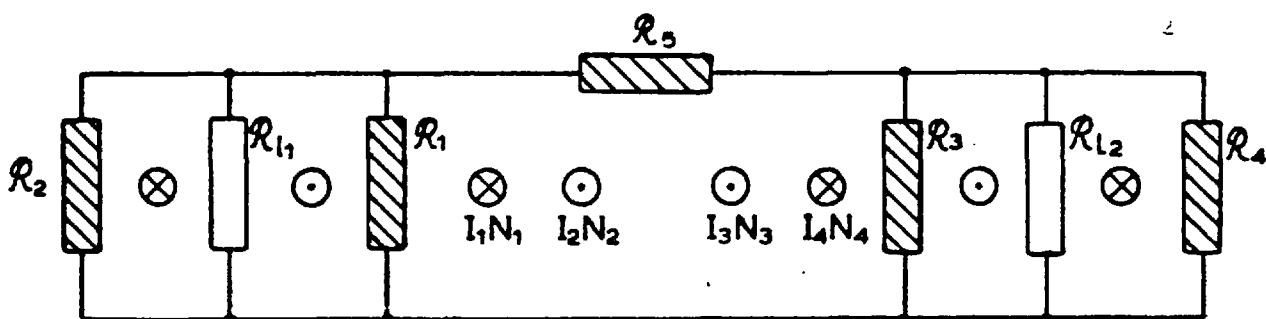
1. The main leakage flux path between the pairs of windings is represented by its reluctances.
2. The flux path confined to the iron is represented by its reluctance.
3. The leakage and core fluxes meet at the same node.
4. The reluctance of each iron element is represented by a curve relating its flux and its m.m.f., i.e. the permeability is not constant.

Figure 6.2(b) shows the magnetic equivalent circuit that results from the foregoing assumptions. It has five non-linear and two linear elements.

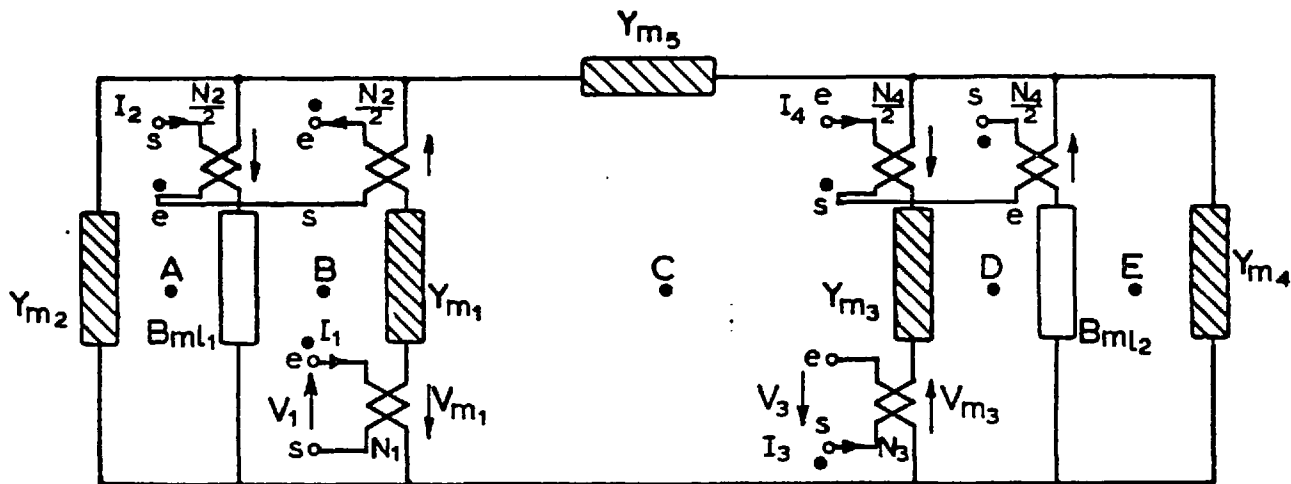
The first step of simplification is to replace the mesh sources by branch sources using the tearing principle as shown in the previous section. There are many possible ways of doing this, but the simplest one is to pull the electric circuit upwards, thus ensuring minimum intersections. Representing each intersection by a branch coupling element gives the linked circuit arrangement shown in Fig. 6.2(c). The l.v. winding linkages are N_1 and N_3 , and the h.v. winding linkages are N_2 and N_4 .



(a)



(b)



(c)

Fig.6-2 Development of equivalent circuit of four winding transformer

(a) Transformer (b) Discrete model (c) Equivalent circuit and topological development (d) Circuit with magnetic dual (e) Equivalent circuit
 $I_1/I_3 = \sqrt{3}$ $N_3/N_1 = \sqrt{3}$ $N_2 = N_4$

(Continued on next page)

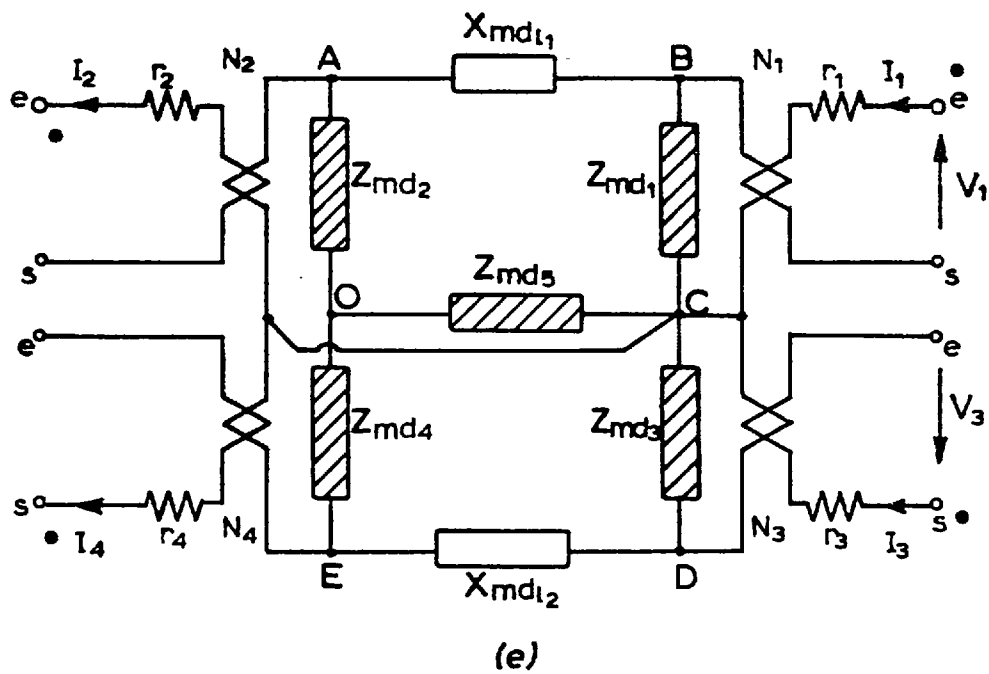
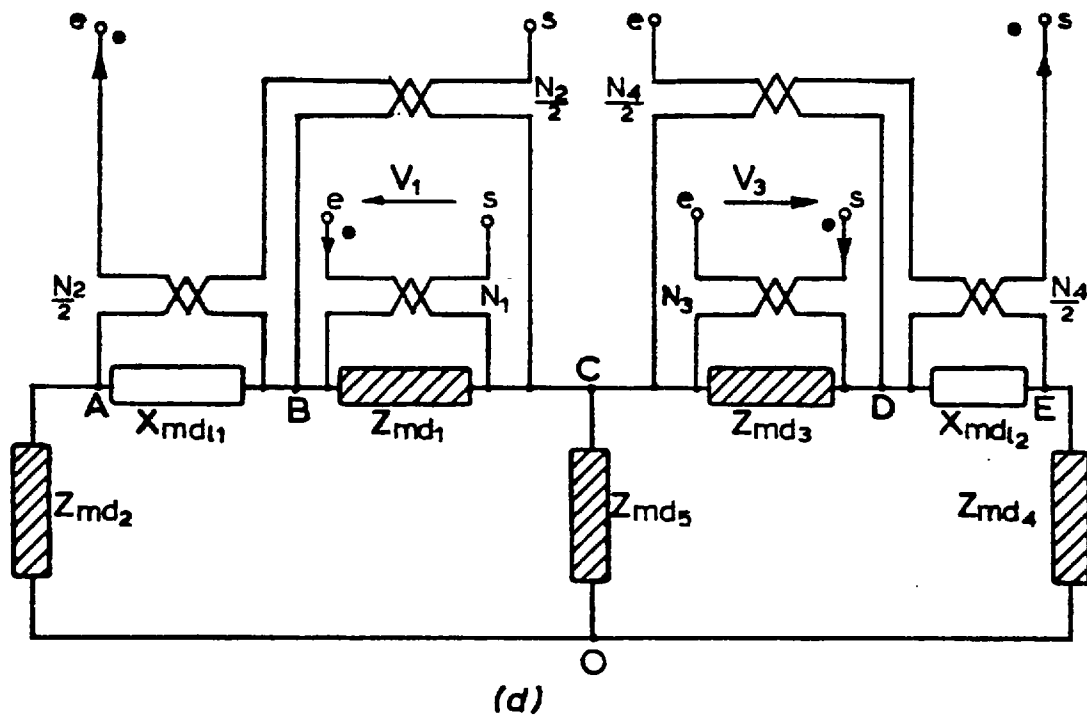


Fig.6-2 (continued)

The sign convention adopted is that of Skilling²⁸ in which the dots are placed so that a current entering the dot marked terminal of electric circuit will produce a m.m.f. in the same direction around the magnetic circuit.

The linked circuits could be solved numerically, but they are more easily dealt with, and visualised, if combined into one. This can be done by taking the dual of the magnetic circuit, since it is assumed to be planar, and the result is shown in Fig. 6.2(d), in which the linkage elements are "half transformers" as defined by equations (6.6) and (6.7). Since the linkage element N_2 is divided into two sections which are connected in series on the electric side, the corresponding sections on the magnetic side can be regarded as being connected in series too. Therefore, the magnetic terminal of each section at node B can be disconnected and combined together to form a single linkage element N_2 as shown in Fig. 6.2(e). Similarly, the two sections of the linkage element N_4 can be replaced by one. The resulting equivalent circuit consists of two Π 's with a common element between them, and for convenience the l.v. winding linkages are arranged on one side. Having obtained the dual, it is possible now to reflect not only single "impedances" but entire circuits from one "winding" to the other.

The essential feature of this approach is that the non-linear elements in the magnetic circuit are represented by equivalent elements in the electric circuit. Moreover, any variation in the transformer construction or in the method of excitation can easily be recognized. For example, the effect of exciting the transformer so that the flux path is confined to the outer limbs can be indicated

in the equivalent circuit by merely short circuiting the common impedance Z_{md5} . Further applications of the equivalent circuit regarding the harmonics are considered in Section 7.4.

The apparent complexity of the system in Fig. 6.2(e) arises because it represents a multi-limb four-winding transformer with no electric connection between any of its windings. Although this transformer could be operated with four independent windings, it is only used here with the h.v. winding sections either connected in series or in parallel. It is shown below that with simple assumptions Fig. 6.2(e) may be reduced to a simple single equivalent π -circuit for either of the two connections.

Figure 6.3(a) shows the equivalent circuit that applies with h.v. winding sections connected in series, and the star connection about O to A, C and E being replaced by its equivalent delta. If it is assumed that the magnetic circuit is symmetrical ($\mathcal{R}_1 = \mathcal{R}_3, \mathcal{R}_2 = \mathcal{R}_4$ and $\mathcal{R}_{l_1} = \mathcal{R}_{l_2}$), the resultant current flowing in (Z_{md})_{AE} is zero because the components are equal in magnitude but in opposite direction. Therefore, this impedance can be removed without affecting the current distribution. The remaining magnetic dual equivalent circuit consists of two π 's which are similar. If, in addition, symmetry is maintained on the electric sides too, that is, the machine windings are balanced and the load is shared equally by each half of the transformer, then it is sufficient to consider half of the equivalent circuit and to replace Fig. 6.3(a) by Fig. 6.3(b). It can be seen that the upper π circuit is, for example, considered and is reflected to its corresponding right hand electric circuit by changing each element magnitude by N_1^2 . Comparison of Figs. 6.2(e) and 6.3(b) shows that the former is suitable for studying any

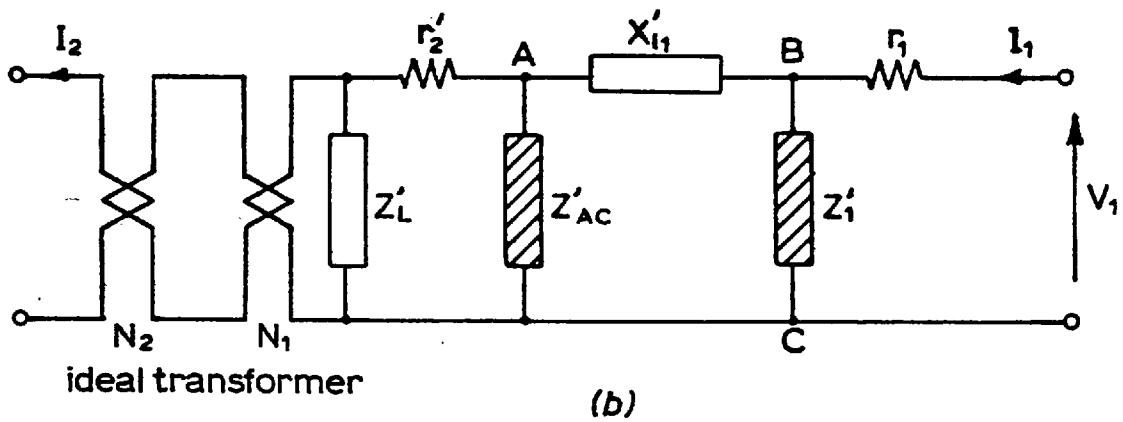
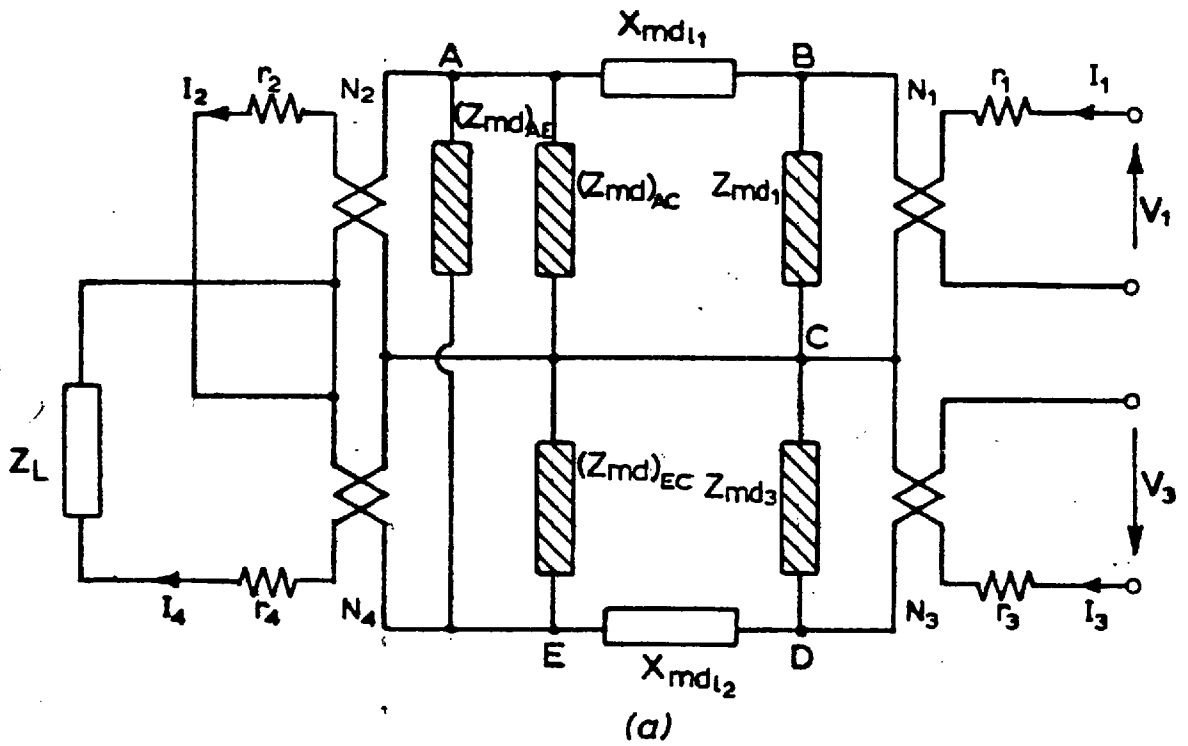


Fig. 6-3 (a) Equivalent circuit with high voltage winding sections connected in series, $I_2 = I_4$

(b) Simplified equivalent circuit

$$X'_{11} = N_1^2 X_{md11}, Z'_{AC} = N_1^2 (Z_{md})_{AC} \quad Z'_L = \left(\frac{N_1}{N_2}\right)^2 \frac{Z_L}{2}$$

imbalance in the magnetic circuit, whereas the latter is appropriate for power system studies.

When the h.v. winding sections are connected in parallel, as shown in Fig. 6.4(a), the voltages across the two electric "windings" are the same, and so are the voltages across their corresponding magnetic "windings". Thus nodes A and E will have the same potential and can be joined together. Consequently adding the impedances Z_{md_2} and Z_{md_4} in parallel and the combination in series with Z_{md_5} , the equivalent circuit becomes as given in Fig. 6.4(b). It is possible to simplify this configuration further by using the assumptions made above. From these assumptions, the potentials at nodes B and D are equal and in consequence the magnetic dual circuit can be reduced to a simple Π equivalent circuit as shown in Fig. 6.4(c). It should be noted that although the magnetic "windings" of the coupling elements N_1 and N_3 are now connected in parallel, their corresponding electric "windings" are not, because the voltages are different by a factor of $\sqrt{3}$.

6.4 DETERMINATION OF THE EQUIVALENT CIRCUIT PARAMETERS

It is desirable to determine the parameters of the equivalent circuit shown in Fig. 6.2(e) so that the transformer performance in service may be predicted. This section is devoted to the calculation of the magnetizing elements; the leakage reactances and the winding resistance have been discussed already in Section 5.7. The following points must be considered:

1. The magnetizing impedances are non-linear, their values varying widely with the excitation.

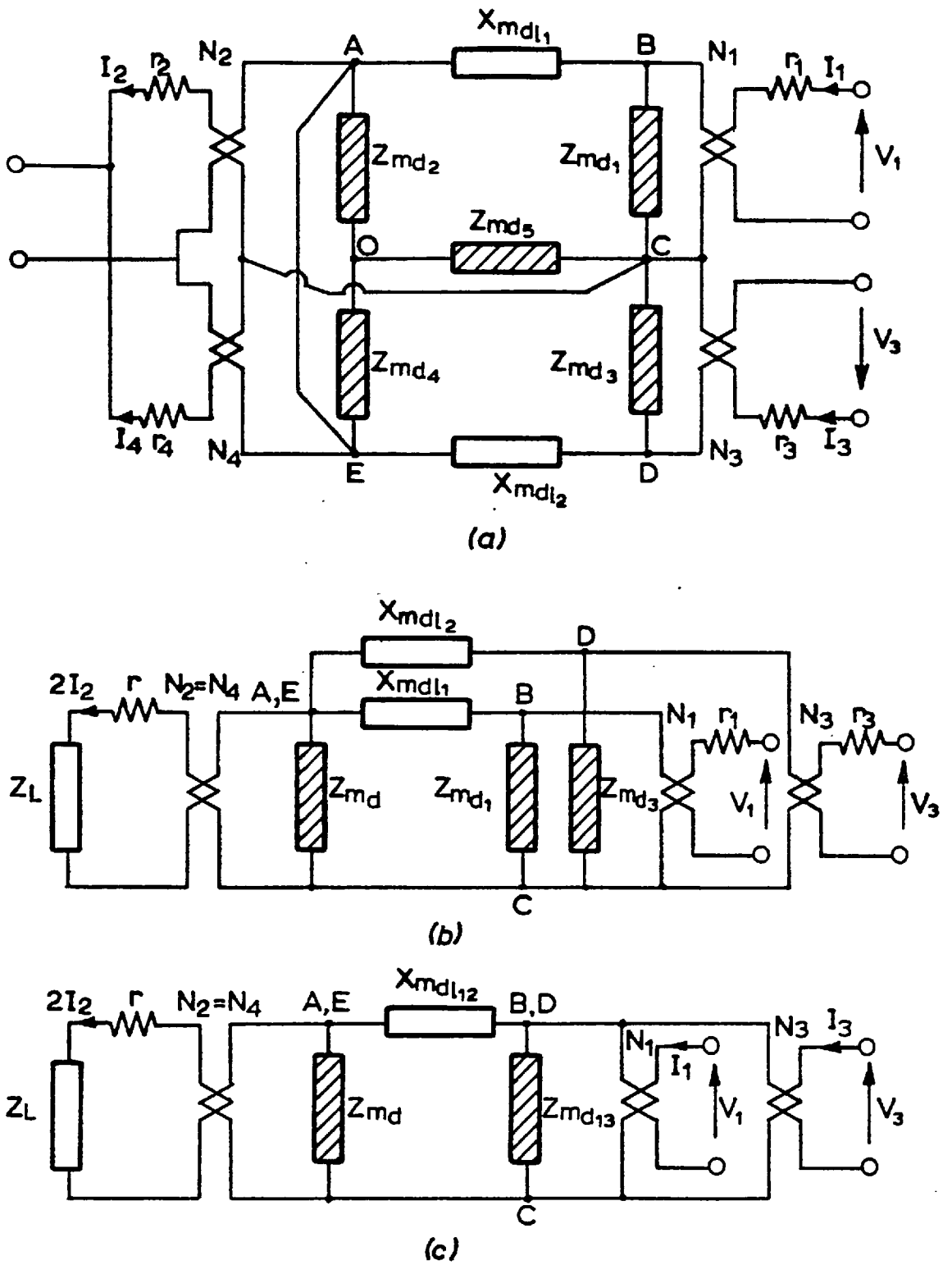


Fig:6-4 (a) Equivalent circuit with high voltage winding sections connected in parallel, $V_2=V_4$

(b) Rearrangement of the equivalent circuit

(c) Simplified equivalent circuit

$$X_{md12} = X_{md1} \parallel X_{md2} \quad Z_{md13} = Z_{md1} \parallel Z_{md3}$$

2. It is not possible to measure directly and exactly in an open circuit test the magnetizing impedances because of the core structure and the winding location.

3. Although the total core loss or the loss associated with each magnetizing branch can be found from published data of the power loss in the iron, the corresponding resistive component cannot.

Therefore an approximate method has been devised which ignores the resistive component, and combines the test results with the analytical solution of the magnetic circuit to find the magnetizing reactances at a particular excitation voltage. Any appreciable changes in the excitation can then be taken into account by adjusting the values of the magnetizing reactances accordingly. From the test results given in Section 5.7 it was decided to calculate the magnetizing reactances at a voltage which is less than the design rated value for two reasons:

1. To reduce the harmonic effect introduced by the transformer core saturation.
2. To permit the investigation of the effect of the transformer arrangement on the harmonic voltages produced by the machine (the details of which are given in Section 7.4).

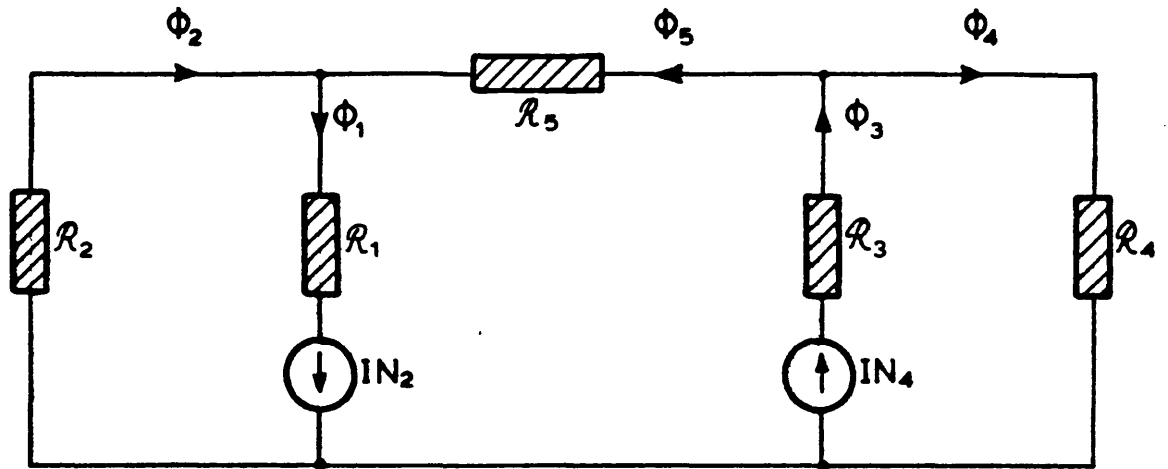
In other words, transformer harmonic effects are minimised by working at low flux densities and this enables the effect of the machine harmonic voltages to be studied on their own. For this reason, the magnetizing reactances were calculated at a working flux density of 1.5 T in the inside limbs and not at 1.7 T as originally designed.

The same open circuit test described in Section 5.7 was repeated here except that a wave analyser was used to measure the fundamental components of the magnetizing current and induced voltages; the results are given in Appendix D where the iron reluctances are calculated.

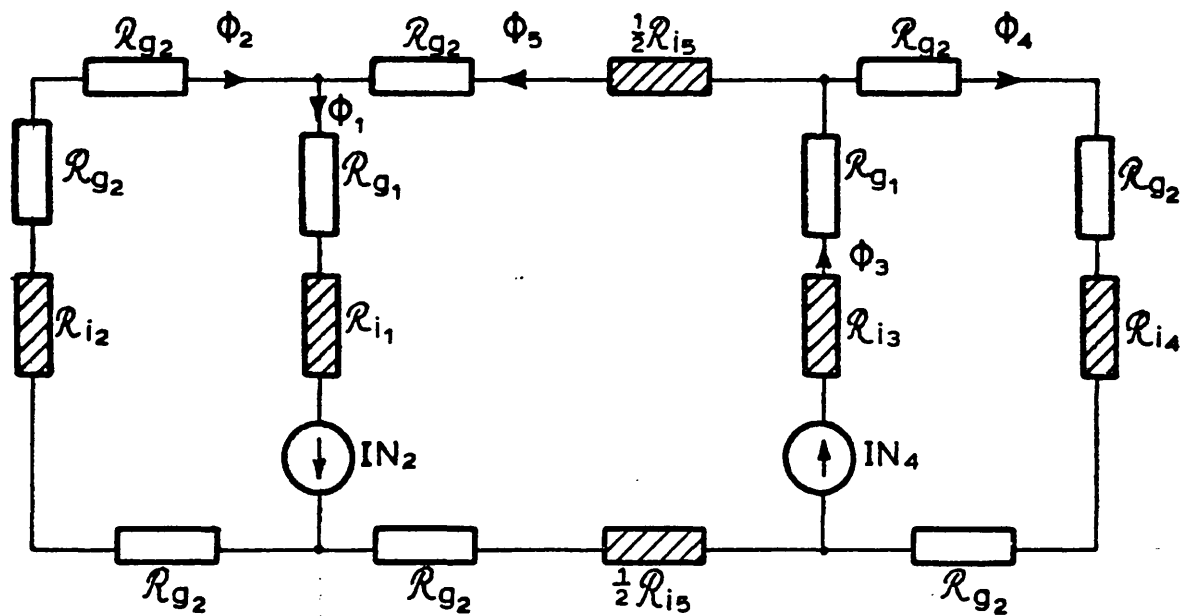
The magnetic equivalent circuit of the micro-transformer is shown in Fig. 6.5(a) with the leakage paths omitted. In a test values of the flux in the branches and the m.m.f. sources are known but the reluctances are not. In solving this circuit it is not possible to obtain unique values for the reluctances because there are three independent loop equations and five unknown reluctances. The task is to develop a method by which consistent values of these reluctances can be found. Since the magnitude of the flux is not only controlled by the iron reluctance but also by the airgap joint reluctance, then the equivalent circuit of Fig. 6.5(a) can be rearranged as shown in Fig. 6.5(b). When deriving this equivalent circuit it has been assumed that the joints between the laminations (see Fig. 5.8) of the same width may be represented by a single reluctance. As shown in Appendix D, the iron reluctances can be approximately found if the flux density and the normal magnetizing curve are given. Inserting these values in the equivalent circuit and solving the loop equations the result is that,

$$\mathcal{R}_{g_1} = 26602 \quad \text{and} \quad \mathcal{R}_{g_2} = 7759.$$

It can be seen that the reluctance with respect to the joints is comparable with that of the iron, and it would have been incorrect just to consider the iron reluctance in the magnetic circuit calculation. Summing where possible the iron and air reluctances, the



(a)



(b)

Fig. 6-5 (a) A magnetic equivalent circuit for the transformer.

(b) A magnetic equivalent circuit showing the reluctances with respect to iron and air gap joints separately.

value of five reluctances becomes (see Fig. 6.5(a))

$$\mathcal{R}_1 = \mathcal{R}_3 = 29921, \mathcal{R}_2 = 34926, \mathcal{R}_4 = 35466 \text{ and } \mathcal{R}_5 = 52930.$$

Having obtained the magnetic reluctances it is now possible to find the magnetic impedances of Fig. 6.2(e) using the formulae which are already given in Section 6.2. Since in this analysis the reluctance has been assumed lossless, then

$$L_{\text{md}} = \frac{1}{j\omega} \frac{\dot{V}_{\text{md}}}{I_{\text{md}}} = \frac{1}{\mathcal{R}} \quad (6.9)$$

Thus the values of the magnetic reactances are

$$\begin{aligned} X_{\text{md}_1} = X_{\text{md}_3} &= 1.05 \times 10^{-2} \Omega, & X_{\text{md}_2} &= 0.9 \times 10^{-2} \Omega, \\ X_{\text{md}_4} &= .89 \times 10^{-2} \Omega \text{ and } & X_{\text{md}_5} &= .6 \times 10^{-2} \Omega. \end{aligned}$$

It should be remembered that when referring these quantities to the appropriate electric current their magnitude must be multiplied by the number of turns squared (see equation (6.8)).

The magnetic leakage reactance (X_{md_ℓ}) can be determined from the measured value of the leakage reactance given in Appendix C.2 in the manner shown below.

The measured value of leakage reactance between windings 1 and 2 but referred to 1 is $= 0.0833 \times \frac{60}{8.36} = 0.6 \Omega$, and between windings 3 and 4 but referred to 3 is $= 0.0833 \times \frac{104}{4.83} = 1.8 \Omega$.

Hence

$$X_{\text{md}_{\ell 1}} = \frac{X_{\ell 12}}{N_1^2} = \frac{.6}{(104)^2} = .55 \times 10^{-4} \Omega$$

and,

$$X_{\text{md}_{\ell 2}} = \frac{X_{\ell 34}}{N_3^2} = \frac{1.8}{(180)^2} = .55 \times 10^{-4} \Omega$$

6.5 CONCLUSIONS

In this chapter a method has been described and demonstrated whereby the steady state equivalent circuit of a four-limb, four-winding transformer may be developed. The flux and current flow paths in the transformer are represented by two separate but coupled circuit models, one magnetic and one electric. Linkages between them are transferred from the meshes to the branches so as to define a single potential function in the magnetic circuit. The two circuits are combined into one by taking the dual of the magnetic side. Since all the elements in the dual circuit are directly proportional to elements in the magnetic circuit, the effects of non-linearity are preserved. This feature is generally not obtained with the equivalent circuits, which are derived using the linear concept of mutual coupling between the windings of the system.

Although the approach permits the derivation of equivalent circuits of varying accuracy and complexity, it is shown that its magnetizing branches cannot always be determined in a simple and direct way. This problem was encountered in the case of the four-winding transformer and an approximate solution was obtained. It is felt that the equivalent circuits derived are adequate for qualitative studies.

THE HARMONICS IN SIX-PHASE GENERATOR AND
ITS ASSOCIATED TRANSFORMER BANK7.1 INTRODUCTION

Following the consideration of the harmonics produced in a 6-ph generation in earlier chapters, the behaviour of the generator and its associated transformer is described in this chapter. Harmonics arise from within the machine and from the transformer. Those from the transformer are considered first.

Extensive test results are given, which cover the transformer on open circuit, short circuit and loaded at various power factors. In all these tests the waveforms of the induced voltages in the main windings and in search coils, and the line currents were obtained and the harmonic content of each waveform is presented. The observed harmonic behaviour is explained both physically and mathematically.

The harmonic content of the currents depends on whether the high voltage (h.v.) output winding sections of the transformers are connected in series or in parallel, and both connections are considered. It is shown that a transformer tertiary winding is essential if the h.v. winding sections are connected in series, but if they are put in parallel it is only necessary when the third harmonic current circulating between the h.v. winding sections would otherwise be excessive.

The transformer-generated harmonics are ignored in the consideration of the paths that the transformer connection provides for the generator harmonics, but may be added afterwards.

It is shown that the harmonic voltages and currents of order $n = 12k \pm 5$ ($k = 0, 1, 2, 3, \dots$) originating in the generator require special treatment because they behave differently from the fundamental and those of order $n = 12k \pm 1$. Harmonic voltages of order $12k \pm 5$ produce a flux pattern in the transformer which is confined to the outer limbs, and the corresponding harmonic currents are dependent on the transformer winding arrangement. If the h.v. winding sections are connected in series these harmonic currents do not appear in the lines on either side of the transformer. Parallel connection gives a closed circulating path for them and they appear in the generator-transformer lines, but not in h.v. output lines. Consequently, the equivalent circuits derived in Section 6.3 cannot be directly used to determine the behaviour of the harmonic currents of the above order by merely multiplying its impedances by the order of harmonics but requires certain modifications. A comparison is made which shows that a four-limb transformer has no significant advantage over a two-limb one in limiting the circulating harmonic currents of order $n = 12k \pm 5$ because their magnitudes depend on the leakage reactance between the windings and not on the magnetizing impedances.

7.2 EXCITATION PHENOMENA IN STAR-DELTA/STAR CONNECTED TRANSFORMER BANK

The excitation current of a 3-ph transformer depends on the arrangement of the winding connections and the flux paths provided. In a bank transformer where three single phase units are used, each phase is responsible for the magnetizing current of its transformer, whereas a 3-ph 3-limb transformer provides magnetic

linkage between the phases. The behaviour of these transformers with Δ/Δ , Y/Δ and Y/Y connection is well documented^{21,29,30}.

The bank of three 4-limb transformers considered here provides a new situation in that the six-phase arrangement and the $Y-\Delta/Y$ connection has not been used before. The following investigation was therefore made to obtain the excitation characteristics and to devise a method by which the flux in the inner limbs of the transformers may be made identical.

Harmonics arise in the magnetizing current when sinusoidal driving voltage is connected to an inductor, the core of which has a saturating magnetizing characteristic (Appendix D). The magnetizing current normally contains only odd harmonics if hysteresis is negligible, those of order 3 and 5 being most significant. These harmonics can give rise to an additional I^2R loss arising from circulating currents, additional core loss and interference with communication and protective circuits.

The transformer arrangement used here is considered with the h.v. winding sections connected in series and then in parallel. The effect of a tertiary winding is shown to be beneficial. It is also shown that the mode of connection has a strong effect on the odd harmonics, particularly the third and the odd multiples of the third (the triplen harmonics). The applied voltages are assumed to be balanced and sinusoidal, and the individual transformers are taken to have identical excitation characteristics.

7.2.1 High Voltage Winding Sections connected in Series

In Fig. 7.1 (which is Fig. 5.6) the circuit diagram for the 6-ph generator and its transformer is shown with the h.v. winding sections connected in series. Windings which belong to the same transformer are drawn parallel to each other. As the low voltage (l.v.) windings are differently connected, three being in star and three in delta, the excitation current in the lines from the generator will be different. However, this difference can be reduced by connection of the tertiary winding.

The excitation characteristic may be understood by study of the waveforms of Fig. 7.2 obtained for the circuit of Fig. 7.1. These are the generator terminal voltages, the transformer magnetizing currents, the h.v. winding voltages and the voltage in search coils on the outer limbs of the transformers. The harmonic content of these waveforms is shown in Table 7.1, having been measured with the wave analyser described previously in Section 4.3. Since the voltage and current waveforms of each set of 3-ph windings were found to be similar, only those of a typical phase are given. Figures 7.2(a) and 7.2(c) show respectively oscillograms of the time variation of generator voltage and exciting currents in lines A and D. It can be seen that for the same almost sinusoidal applied voltages, the waveforms of the exciting currents in the lines of the two low voltage windings differ greatly from each other. The delta connected winding draws a fundamental magnetizing current which is about one and a half times larger than that of the star connected winding. This means that the inner limb of each transformer carrying the delta l.v. winding is more saturated than that with the starred l.v. winding. The uneven nature of the flux pattern is indicated by

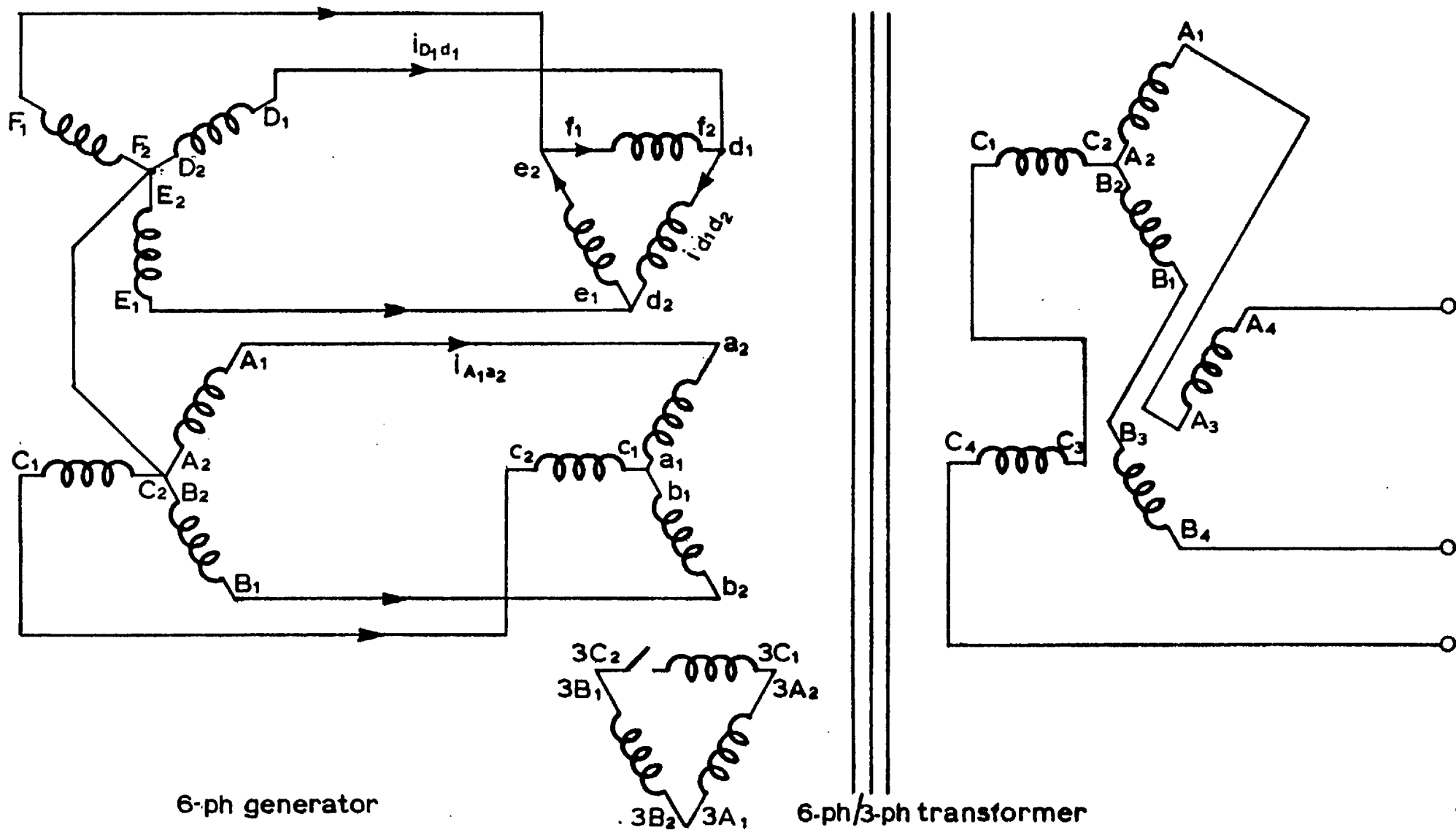


Fig. 7-1 Circuit diagram of 6-ph generator and its associated star-delta/star transformer bank. High voltage winding sections are connected in series. Tertiary winding is also shown.

TABLE 7.1

Harmonics content in the voltage and current waveforms of Figs. 7.2(a) to 7.2(h) inclusive. Harmonic voltages are given in V, and harmonic currents in A.

Fig. No.	Tertiary condition	Parameters	Definitions	Star or Delta	1st	3rd	5th	7th
a	open	$v_{A_1A_2}$	generator voltage L-N	S	53	3	.08	.34
a	open	$v_{D_1D_2}$		D	53	3	.16	.5
b	closed	$v_{A_1A_2}$		S	53	3	1.3	.58
b	closed	$v_{D_1D_2}$		D	53	3	1	.88
c	open	$i_{A_1a_2}$	generator line current	S	.75	.054	.26	.069
c	open	$i_{D_1d_1}$		D	1.13	.035	.22	.017
d	closed	$i_{A_1a_2}$		S	1.03	.031	.116	.036
d	closed	$i_{D_1d_1}$		D	.98	.017	.113	.013
e	open	$v_{A_1A_2}$	transformer output voltages	D	108	1	.7	.7
e	open	$v_{A_4A_3}$		S	108	50	2.7	1.6
f	closed	$v_{A_1A_2}$		D	108	.5	2.3	1.8
f	closed	$v_{A_4A_3}$		S	108	1	2.7	1
g	open	v_{s_1}	induced voltages in search coils		11	7.4	2.35	.8
g	open	v_{s_2}			11	4.5	3.4	.93
h	closed	v_{s_1}			11	2.4	3.0	1.15
h	closed	v_{s_2}			11	2.4	2.9	1.15

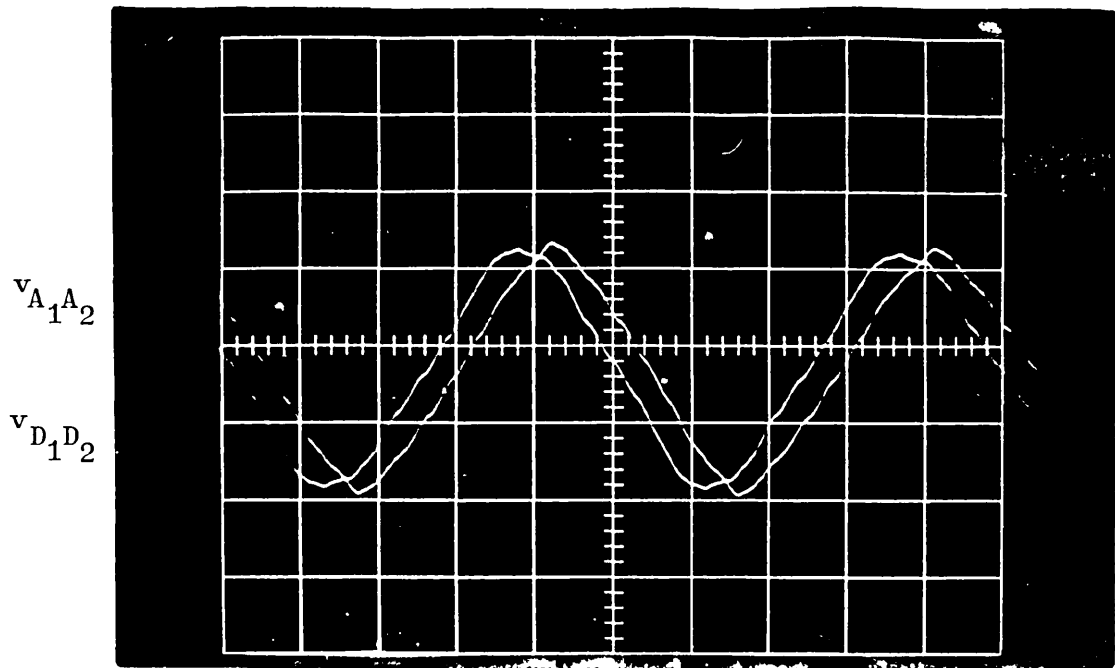


Fig. 7.2(b) The same, but tertiary winding closed.

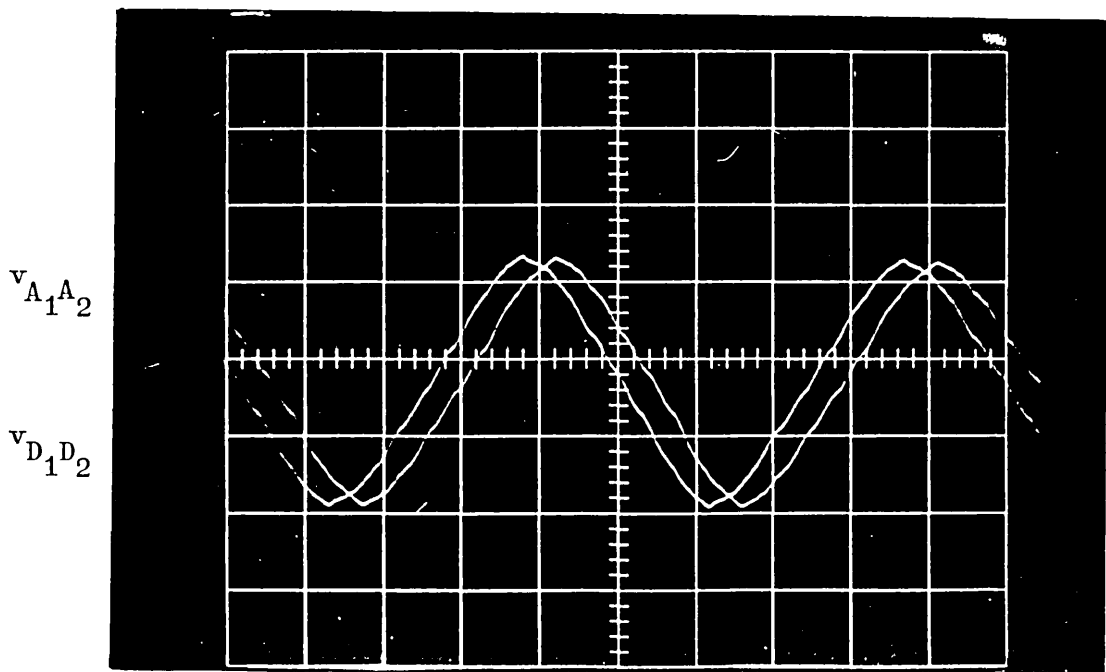


Fig. 7.2(a) Line to neutral generator voltages.
Tertiary winding open.

FIG. 7.2 6-ph generator connected to star-delta/star transformer bank. High voltage winding sections connected in series and on open circuit.

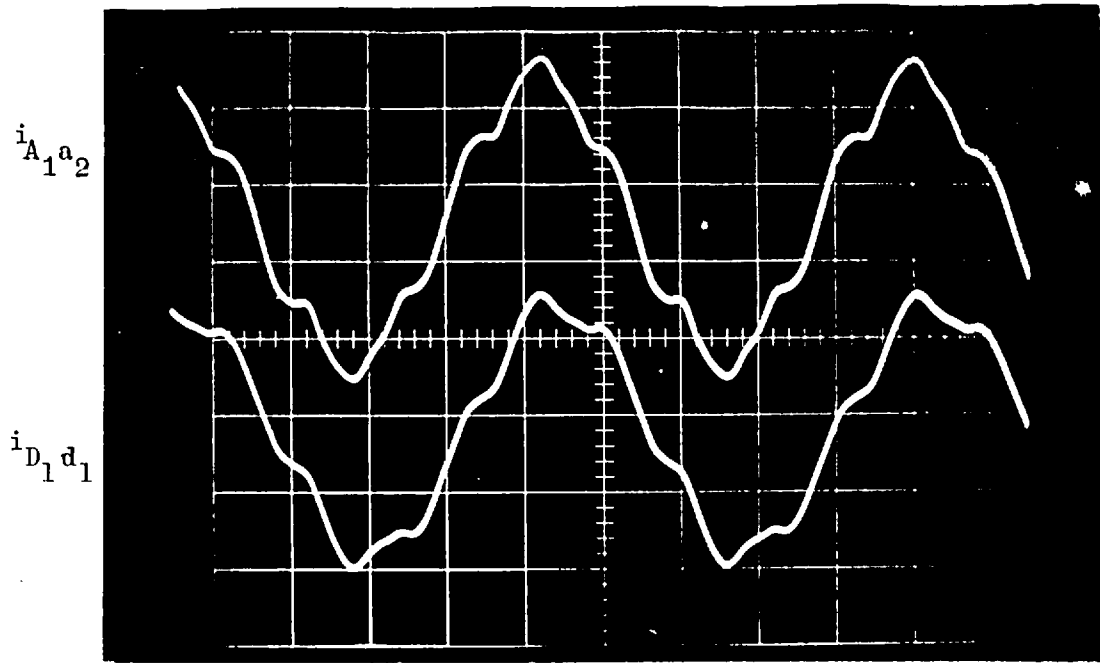


Fig. 7.2(d) The same, but tertiary winding closed.

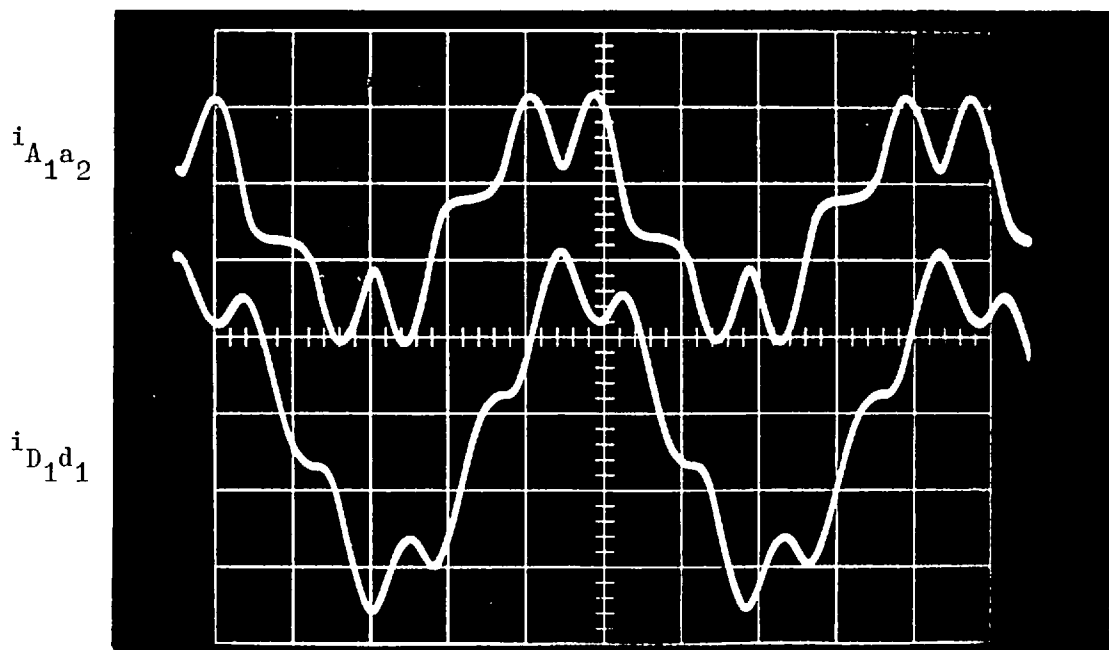


Fig. 7.2(c) Exciting currents in lines A and D.
 $i_{A_1 a_2}$ is for star connected winding, and $i_{D_1 d_1}$
 is for delta connected winding. Tertiary
 winding open.

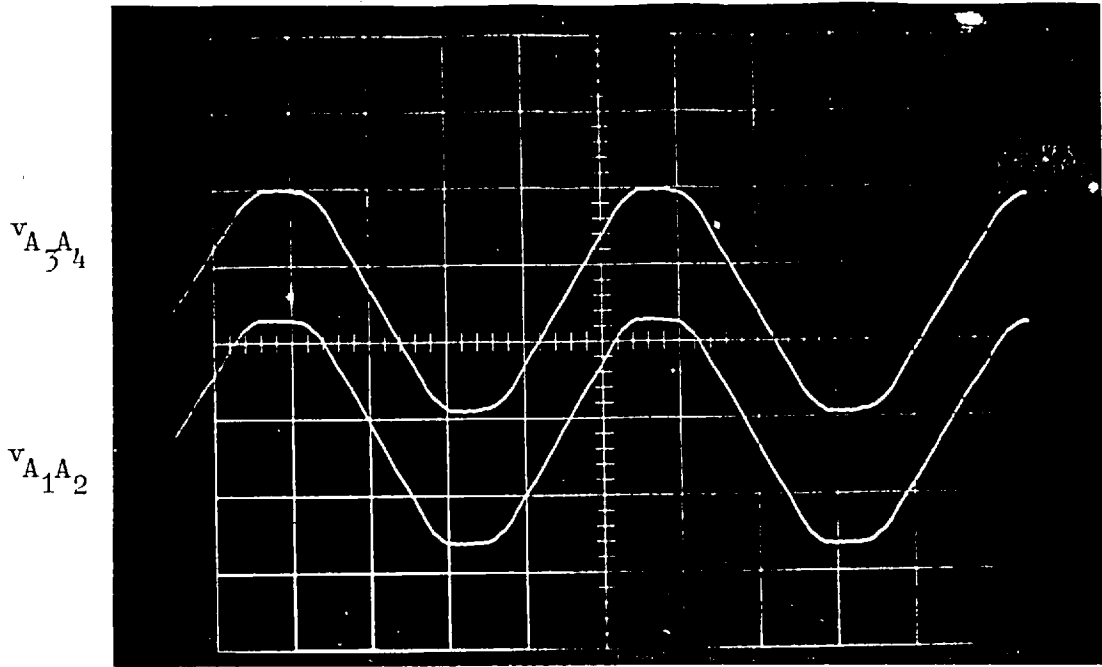


Fig. 7.2(f) The same, but tertiary winding closed.

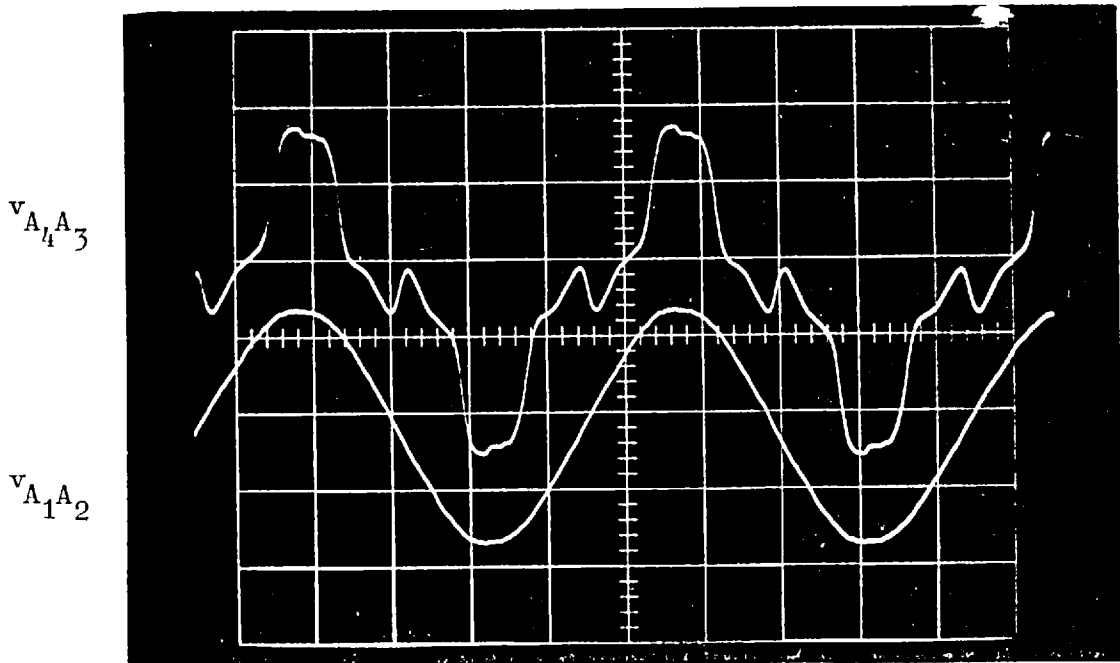


Fig. 7.2(e) Induced voltages in both h.v. winding sections. Tertiary winding open.

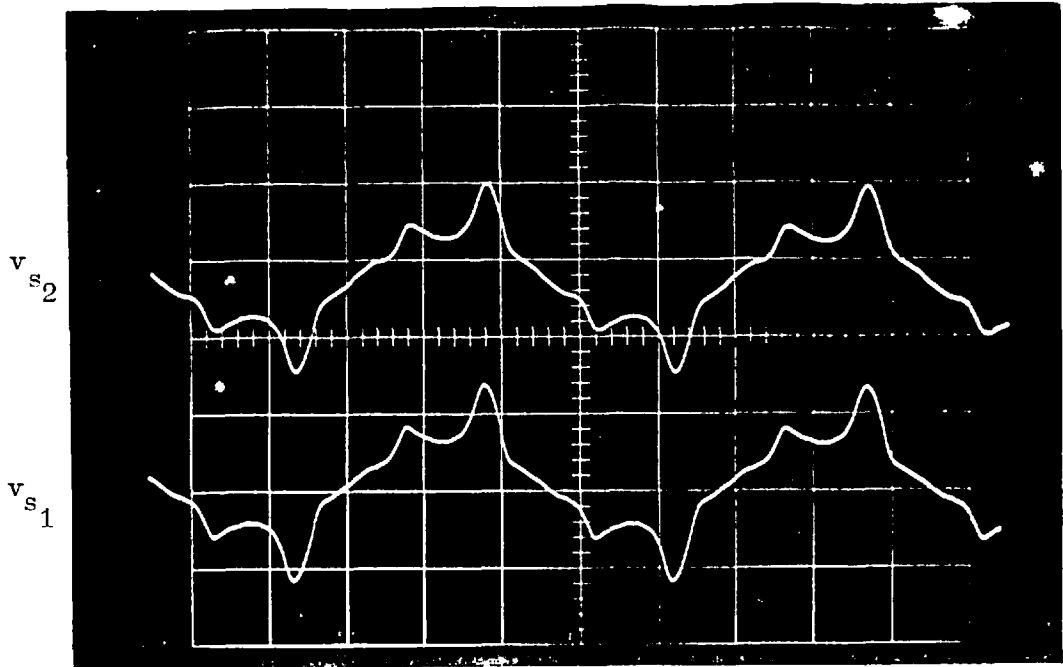


Fig. 7.2(h) The same, but tertiary winding closed.

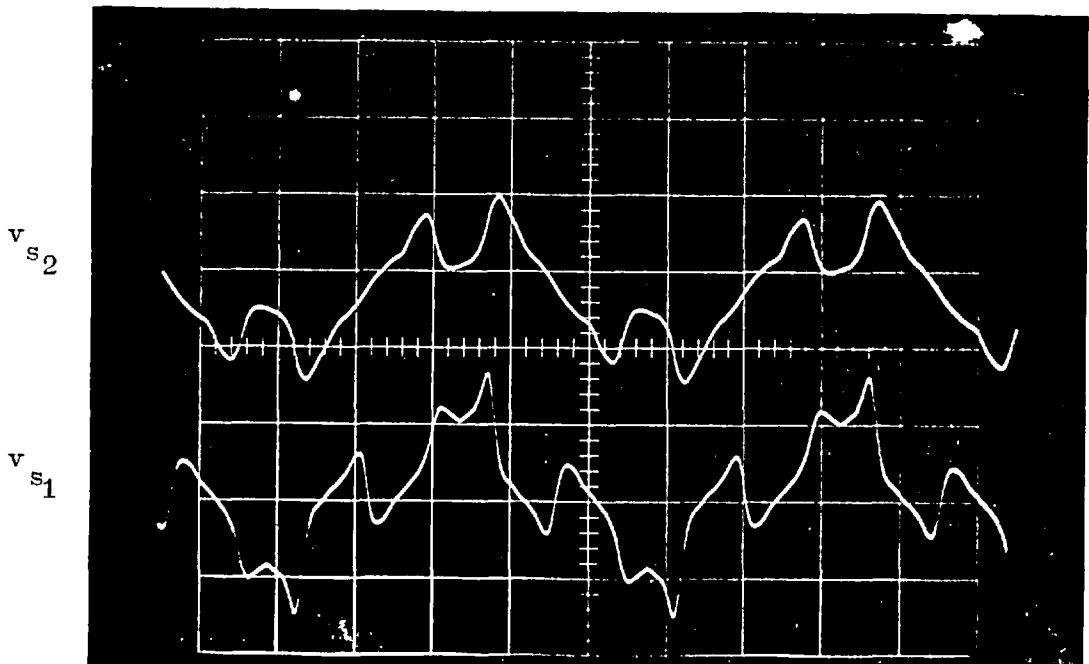


Fig. 7.2(g) Induced voltages in search coils wound on the outer limbs. v_{s1} is induced voltage in the left outer limb, and v_{s2} in the right outer limb (see Fig. 5.11). Tertiary winding open.

the waveforms of the induced voltages in the h.v. windings and in the search coils on the outer limbs (Figs. 7.2(e) and (g)). The reason for this assymetry is discussed below.

7.2.1.1 Triplen harmonics

The discussion is divided into two parts, one concerning the star connected l.v. winding and its corresponding h.v. winding, and the other concerning the delta-connected l.v. winding and its corresponding h.v. winding. Simultaneously, the effect of the magnetic link between the windings of each transformer is considered.

First consider the excitation currents supplied to the star connected winding. With balanced applied voltages and under identical excitation characteristics of the three transformers, there can be no triplen harmonic components in the excitation currents of a star connected winding with isolated neutral. Triplen harmonic currents are in time phase and flow in the same relative direction in the phases at the same instant. Consequently, the waveform of the exciting currents differs from that required to permit the very nearly sinusoidal variation of flux in the limbs with which these phases are associated. Since the third harmonic exciting currents necessary for nearly sinusoidal variation of flux are completely suppressed, the non-linear relationship between excitation and flux results in third harmonic components of core flux which induce third harmonic voltages in the line to neutral of the l.v. winding and its corresponding h.v. winding. Since the third harmonic components in the three line to neutral voltages of the l.v. windings (or its corresponding h.v. windings) are in phase and equal in

magnitude, there can be no third harmonic components between lines under balanced conditions. Fig. 7.2(e) shows a typical waveform of the induced voltage $v_{A_4 A_3}$ being very distorted, and with a very prominent third harmonic component which makes it more peaky than a sinusoid.

A peaky induced voltage waveform indicates generally that third harmonic is in opposition to the fundamental, the positive maximum of fundamental and harmonic wave occurring at the same instant. Also, it means that the flux waveform producing it is more flat-topped than a sinusoid because the induced voltage is proportional to the rate of change of the flux waveform. However, a flux waveform which is flat-topped indicates the presence of a third harmonic in phase with the fundamental, the harmonic having a negative maximum coincident with the positive maximum of the fundamental, and therefore the maximum density is reduced. In other words, a flux waveform which is more flat-topped than a sinusoid when reflected on a magnetizing characteristic gives rise to a smaller, magnetizing current than that of a sinusoid.

The exciting current in the lines of the delta connected l.v. winding is not equal to the corresponding phase current but is the phasor sum of currents in two phases. They differ from each other not only in magnitude but also in wave shape. The chief reason for this discrepancy is that third harmonic currents (if they exist) can only flow in the closed mesh and are missing from the lines under balanced conditions.

Since the impedance offered to third harmonic currents by the delta winding is normally low, a small deviation of flux from a

perfect sine wave is sufficient to produce a large third harmonic magnetizing current. The voltage induced in the delta connected winding by third harmonic flux does not appear at the terminals of the delta, because it is absorbed by its own leakage impedance drop, whereas the voltage induced in the corresponding star connected winding $v_{A_1A_2}$ contains a small component of third harmonic voltage between the line and neutral (see Fig. 7.2(e)).

When comparing the flux waveforms in limbs associated with the delta connected low voltage winding and with the star connected low voltage winding, it can be concluded that for the same applied voltages the former is nearly sinusoidal while the latter is flat-topped. Since the amplitude of the fundamental sine wave is greater than that of the corresponding flat-topped wave, then when reflecting both waveforms or the magnetization curve, the sine wave gives rise to higher magnetizing current.

The small third harmonic component measured in the line currents is mainly caused by inequalities in the excitation characteristics of the three transformers.

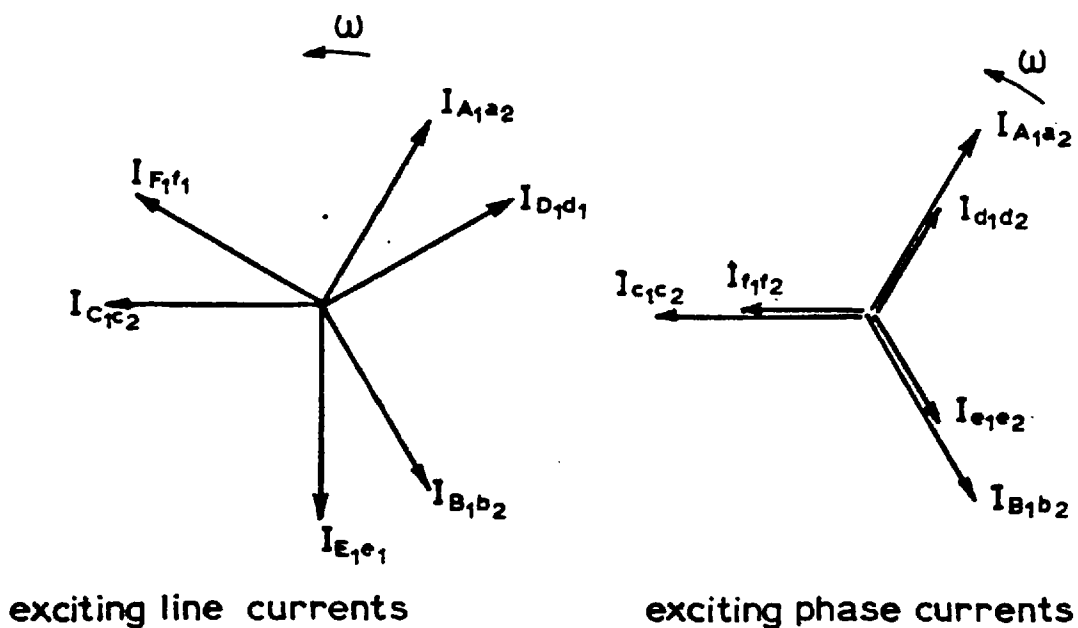
The path of other odd harmonic currents such as 5th and 7th are not restricted by the winding connection and they flow in phases as well as in lines like the fundamental current. Close examination of Fig. 7.2(c) shows that the principal harmonic component in the current waveform is the fifth, which causes the two peaks. The effects of these harmonics on the current waveform are further discussed in Subsection 7.2.1.3.

7.2.1.2 Tertiary winding

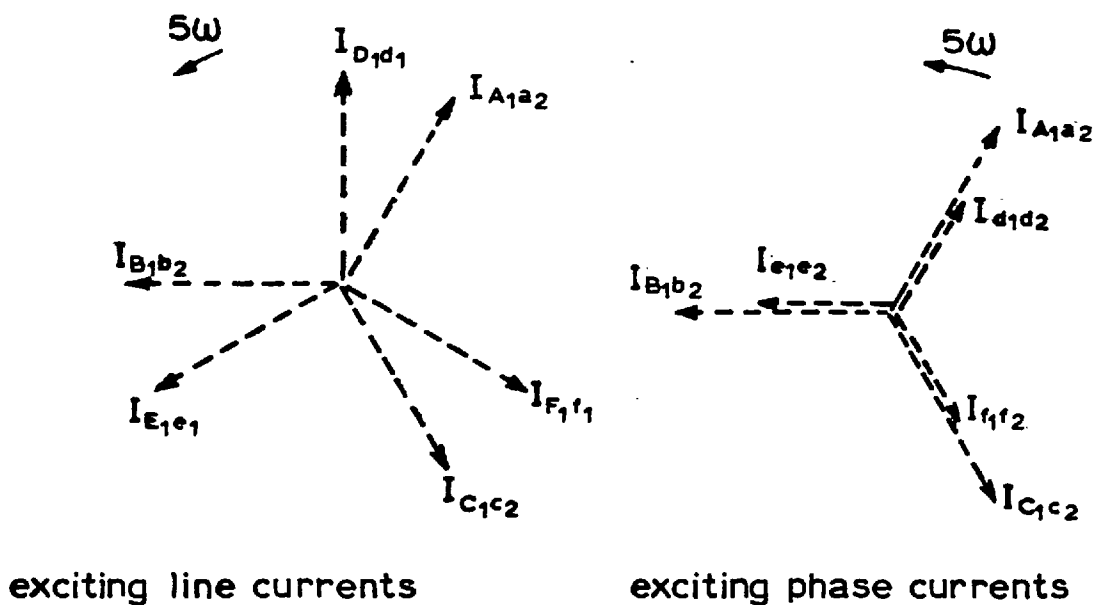
One method of reducing the problem of inequality in the exciting currents and achieving a nearly sinusoidal variation of flux in the inner limbs enclosed by the star-connected l.v. winding is to provide them with a tertiary winding. As its name implies, a tertiary winding is simply an additional winding in the form of closed delta and is normally associated with a transformer bank in which its windings are in star/star connection. The tertiary winding provides a path for triplen harmonic magnetizing currents which are necessary to permit a sinusoidal variation of flux in the limbs enclosed by the tertiary winding. Figures 7.2(d), 7.2(f) and 7.2(h) show clearly the advantages of having a tertiary winding with this arrangement.

7.2.1.3 Harmonic components of order $6k \pm 1$ ($k = 0, 1, 2, 3, \dots$) in the exciting current

It is interesting to observe that in Fig. 7.2(d) the waveform of line currents $i_{A_1 a_2}$ and $i_{D_1 d_1}$ are not similar despite their harmonic contents being in the same proportion. The chief reason for this is the phase relationship of their fifth harmonic current. These are not in phase for the following reason. Consider Fig. 7.3, in which the phasor diagrams of fundamental and fifth harmonic components of the phase and line currents in both low voltage windings are given. The phase sequence of fifth harmonics is the reverse (or in the terminology of symmetrical components is the negative) of the phase sequence of the fundamentals. The fundamental components of exciting current in the star and in the delta windings are in phase for any two phases which are shown parallel to each



(a)



(b)

Fig. 7-3 Phasor diagram for phase and line currents in low voltage winding of a 6-ph/3-ph transformer bank.
 (a) fundamental phasor diagram
 (b) fifth harmonic phasor diagram

other (see Fig. 7.1). For example, $I_{A_1a_2}$ and $I_{d_1d_2}$ are in phase but differ in magnitude by a factor of $\sqrt{3}$. The corresponding fundamental components in lines are now equal in magnitude but differ in phase shift. The fundamental component $I_{D_1d_1}$ lags behind $I_{A_1a_2}$ by 30° electric. It is worth pointing out that for the delta winding the phasor diagram of line currents differs from that of phase currents whereas in the star winding the phasor diagram is the same. The phasor diagram for fifth harmonic components (shown dotted) in phase currents is derived from its corresponding phasor diagram of fundamental components by taking phase A as a reference. It can be seen that, for example, the fifth harmonic and fundamental components in the delta current $I_{d_1d_2}$ are in phase with each other whereas the fifth harmonic component leads the fundamental component in line D by 60° electric. However, the phase relation between the fifth and fundamental component of the star current $I_{A_1a_2}$ remains the same in phases and in lines.

Thus, in brief: the phase relation between the fundamental and fifth harmonic components of the line currents for the delta winding differs from the phase relation between these components for the star winding and, although the line currents for delta and star windings contain fundamental and fifth harmonic components in the same proportions, their waveforms differ because of this phase shift.

The above argument is valid for any harmonic the order of which is given by the expression $6k - 1$, where k is any integer. However, harmonics of order $6k + 1$ have the same phase sequence as the fundamental and therefore the phase relation between these harmonics and fundamental components of phase and line current remains the same.

7.2.1.4 Induced voltages in search coils

One strange feature of a four-limb transformer is that the actual flux paths in the outer limbs or yokes are uncertain, and calculation of the core loss is likewise uncertain. Figure 7.2(h) shows the induced voltage in the search coils in which they are distorted despite those in the main windings being almost sinusoidal. This happens because the iron reluctances are non-linear and not equal, and that the sinusoidal flux emanating from the inner limbs divides according to the iron reluctances of the two available paths given equal magnetic potential drop in each. Higher flux tends to flow in the yokes because of their lower reluctances. This situation is identical to that in a 3-ph five-limb transformer³¹ in which the flux in the outer limbs and yokes is of non-sinusoidal nature.

The problem of the uncertainty of the flux paths in a four-limb transformer bank has been tackled in the past³² by having three additional windings for each transformer, two of which have equal number of turns and located on the two inner limbs and the other has double number of turns and is located on any of the two outer limbs. The flux emanating from the inner limbs can be divided into equal halves by connecting the three windings in parallel. The resultant winding of each of the three transformers are then connected together to form a tertiary winding.

7.2.1.5 Micro-transformer as a means to study the behaviour of large transformer

A comparison of voltage and current waveforms obtained from the 6-ph/3-ph micro-transformer bank and those of a typical 3-ph

transformer bank²¹ clearly shows that the micro-transformer can be a useful means for understanding and predicting the behaviour of large transformers. For example, the following waveforms of $i_{D_1 d_1}$ in Fig. 7.2(c) and i_{ϕ_A} in Fig. 1 in ref. [21], $i_{A_1 a_2}$ in Fig. 7.2(c) and i_{ϕ_A} in Fig. 8(b), $i_{A_1 a_2}$ in Fig. 7.2(d) and i_{ϕ_A} in 7(b) and finally $v_{A_4 A_3}$ in Fig. 7.2(e) and v_{AN} in 8(b) show a close resemblance.

7.2.2 High Voltage Winding Sections connected in Parallel

It has been suggested that it is cheaper to connect the h.v. winding sections in parallel rather than in series because then one end of each winding is at ground potential and requires less insulation. The main concern here is not the insulation problem but to investigate which of these connections produces lower harmonic circulating currents in the windings. For this reason, the studies of excitation phenomena made in Section 7.2.1 are repeated but with both h.v. winding sections connected in parallel. The main aspects of connecting both sections in parallel are:

1. Fluxes in the inner limbs of each transformer are forced to be the same.
2. A path is provided for third harmonic current to circulate even when the tertiary winding is open.

These aspects are discussed in more detail below. In Fig. 7.4 the oscillograms of exciting currents in the six lines and that circulating in the h.v. winding sections are shown. It can be seen that the exciting currents are neither equal nor identical. The appreciable discrepancy in the exciting current waveforms is due to

the fundamental components being unequal. Table 7.2 gives the harmonic contents of each waveform. An effort is made here to explain this peculiar excitation phenomena in the 6-ph/3-ph transformer bank with its h.v. winding sections connected in parallel.

In order to connect two windings in parallel their voltages must be equal in magnitude and in phase, otherwise a large current would circulate depending on the impedance of the closed loop to compensate for the difference. In Section 7.2.1 it was shown that with the tertiary winding open, the induced voltages in the h.v. winding sections were not similar.(see Fig. 7.2(e)). Therefore, if one tries to parallel these two sections, circulating current is inevitable. Figure 7.4(d), which shows the waveform of the circulating current, mostly consists of third harmonic component because the induced voltages mainly differ in this respect. Since parallel connection provides a path for third harmonic current to circulate, unlike series connection, it was found that including or excluding the tertiary winding had no significant effect on the exciting current or induced voltage waveforms. However, as shown in Fig. 7.4(e), the presence of the tertiary winding reduces the magnitude of third harmonic current circulating in the parallel connected h.v. sections. The induced voltage waveforms in the h.v. winding and the search coils are the same as those shown earlier in Figs. 7.2(f) and 7.2(h), and therefore not given in this section.

In view of the above, it is thought that the main reasons for the imbalance in the line currents regardless of whether the tertiary winding is open or closed are:

TABLE 7.2

Harmonics content in the current waveforms
of Figs. 7.4(a) to 7.4(e) inclusive.
The values are given in A.

Fig. No.	Tertiary connection	Parameters	Definitions	Star or Delta	1st	3rd	5th	7th
a	open or closed	$i_{A_1 a_2}$	Gen. line currents	S	1.52	.022	.094	.076
a	open or closed	$i_{D_1 d_1}$	Gen. line currents	D	.78	.013	.148	.04
b	open or closed	$i_{B_1 b_2}$	Gen. line currents	S	1.02	.077	.093	.075
b	open or closed	$i_{E_1 e_1}$	Gen. line currents	D	.70	.070	.143	.047
c	open or closed	$i_{C_1 c_2}$	Gen. line currents	S	1.22	.056	.102	.083
c	open or closed	$i_{F_1 f_1}$	Gen. line currents	D	1.04	.056	.130	.047
d	open	i_{Cir}	Circulating currents		.17	.28	.016	.026
d	closed	i_{Cir}	Circulating currents		.15	.04	.016	.024

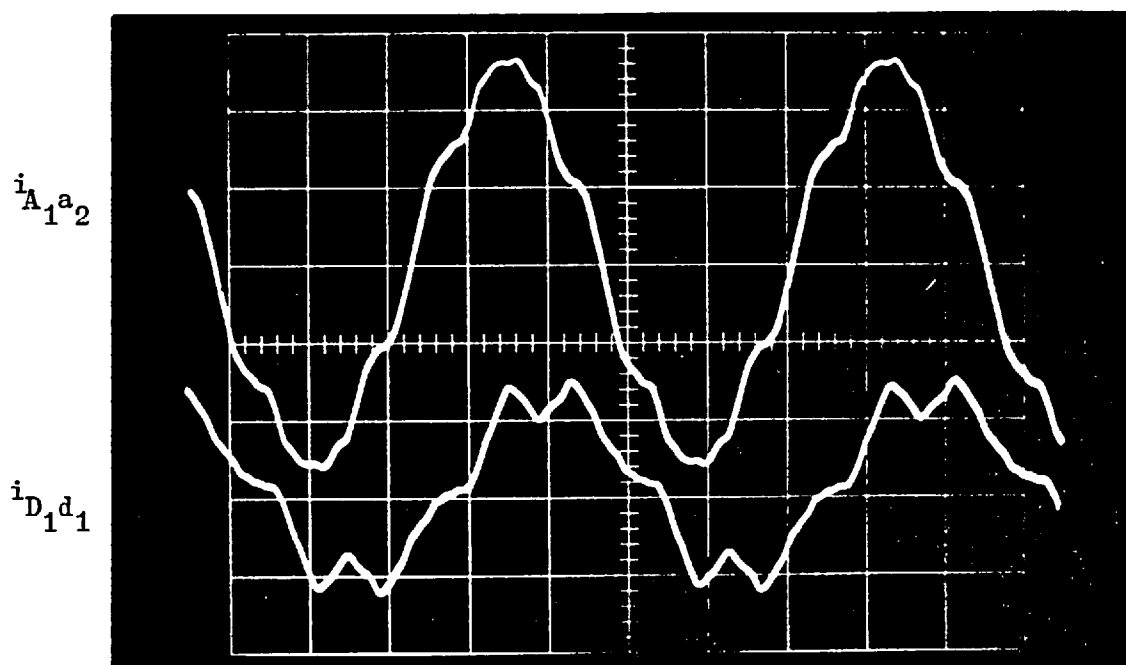


Fig. 7.4(a) Exciting currents in lines A and D.
Tertiary winding is ineffective.

FIG. 7.4

6-ph generator connected to star-delta/star transformer bank. High voltage winding sections connected in parallel.

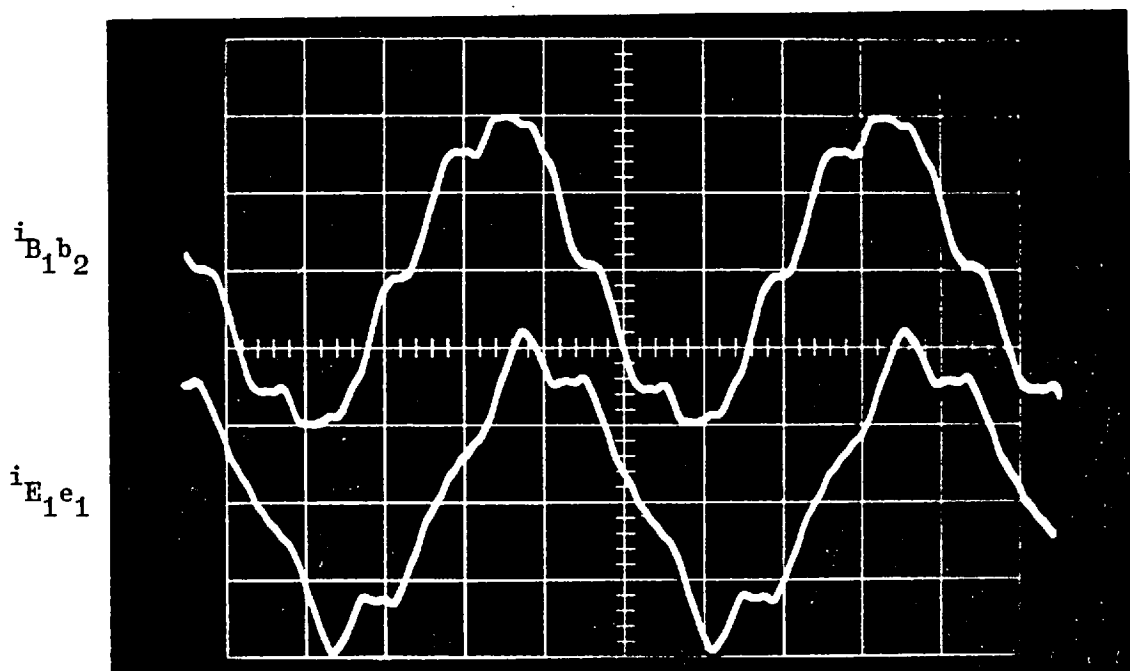


Fig. 7.4(b) Exciting currents in lines B and E.
Tertiary winding is ineffective.

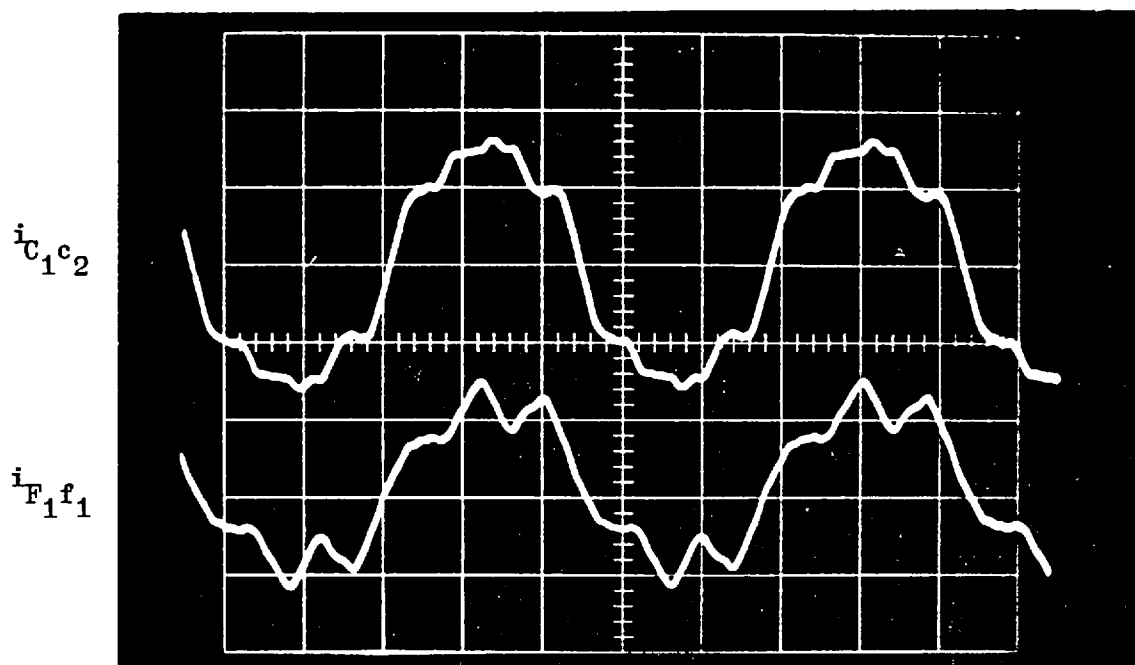


Fig. 7.4(c) Exciting currents in lines C and F.
Tertiary winding is ineffective.

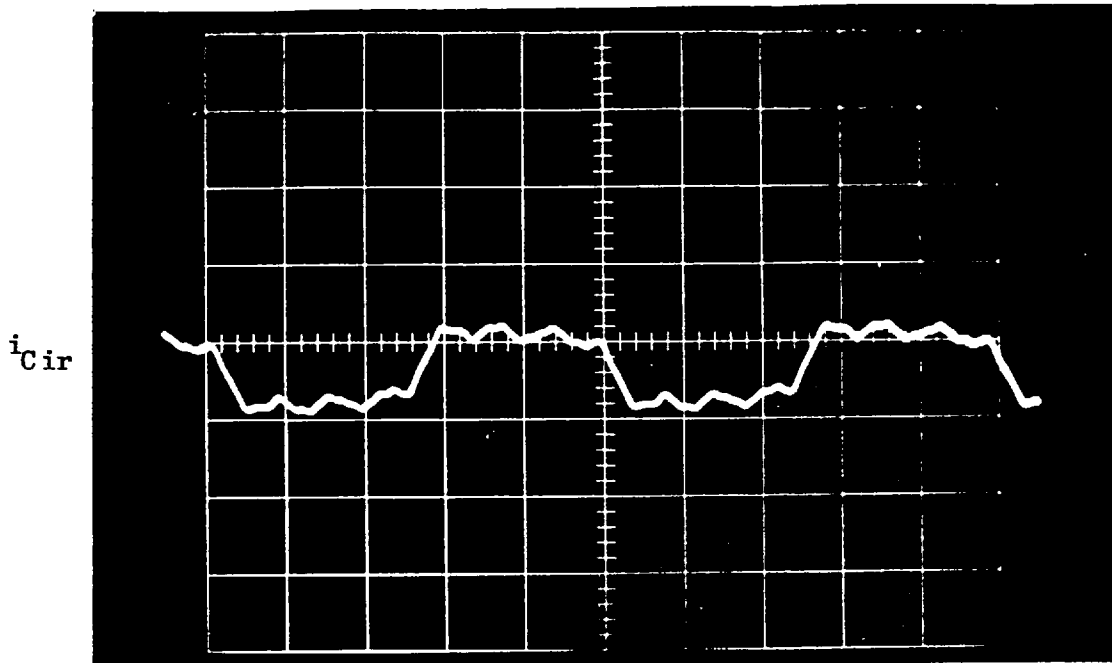


Fig. 7.4(e) The same, but tertiary winding closed.

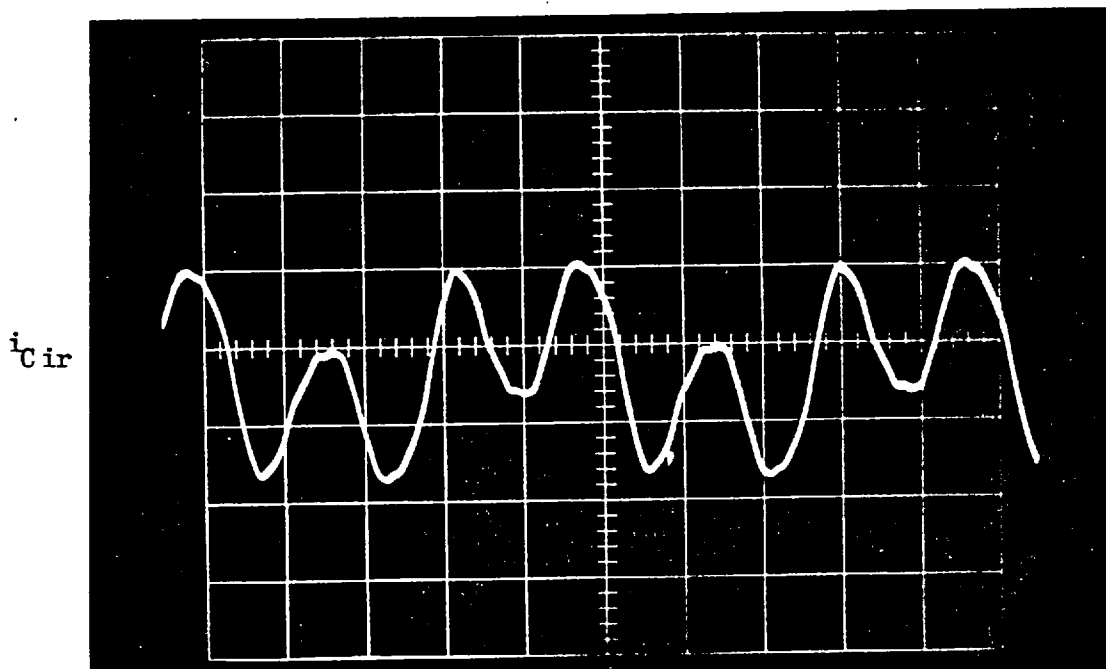


Fig. 7.4(d) Circulating current in high voltage winding.
Tertiary winding open.

1. The equal fluxes emanating from the inner limbs of each transformer do not divide in the same proportion. Experimental work showed that although the induced voltages in the search coils on the outer limbs of the three transformers were of the same nature, their magnitudes were slightly different not only in one transformer but between the three transformers also. In other words, the magnetic reluctances (iron plus joints) of the two outer flux paths of each transformer are not exactly the same, and furthermore these reluctances are not identical for the three transformers. The combined effect of equal fluxes in the inner limbs and the slight inequality in the magnetic reluctances probably caused the imbalance in the line currents. It is noteworthy that this imbalance is exaggerated in the micro-transformers because, as shown previously in Section 6.4, the joints between the laminations are very important. This effect is likely to be much less significant in a large transformer.

2. Although the applied voltages across the two l.v. windings differ by a factor of $\sqrt{3}$, their induced voltages cannot differ by this ratio, even when the same flux is linking both windings. This is because it is impossible to satisfy exactly a turnsratio of $\sqrt{3}$ between the windings. Therefore, any slight inequality between the applied and induced voltages causes more current to be drawn from the generator in which its value depends on the voltage difference and on the generator and transformer impedances.

7.3 STEADY STATE SHORT CIRCUIT TEST ON THE HIGH VOLTAGE WINDING

In Section 4.3 the short circuit test result on the 6-ph generator was given, from which the current waveform was found to be greatly distorted. The same test was repeated here on h.v. side of the transformer. A 3-ph short circuit was applied on the h.v. side, and the generator was excited to circulate full rated current. As shown in Fig. 7.5, the waveform of line currents of phases A and D are free of harmonics. This is because the transformer leakage reactance is directly proportional to the order of the harmonics and therefore their values, as compared to that of the generator, are sufficiently high to suppress the harmonic currents. The test result also showed that the current waveforms were sinusoidal for both series and parallel connection of high voltage winding sections.

7.4 EFFECT OF TRANSFORMER CONNECTION ON THE HARMONIC VOLTAGES PRODUCED BY THE SIX-PHASE GENERATOR

In Section 7.2, the output voltages of a 6-ph generator were assumed sinusoidal, and the harmonics generated within the transformer were considered. Here, the behaviour of the transformer is discussed when energised from a non-sinusoidal source. To simplify the analysis, the transformer is treated as a linear device which produces no harmonics. The n^{th} harmonic output voltage of a 6-ph generator, of which the circuit diagram was given in Fig. 7.1, can be expressed as

$$(V_{A_1 A_2})_n = V_n \sin(n\omega t + \alpha_n) \quad (7.1)$$

$$(V_{B_1 B_2})_n = V_n \sin [n(\omega t - 120) + \alpha_n] \quad (7.2)$$

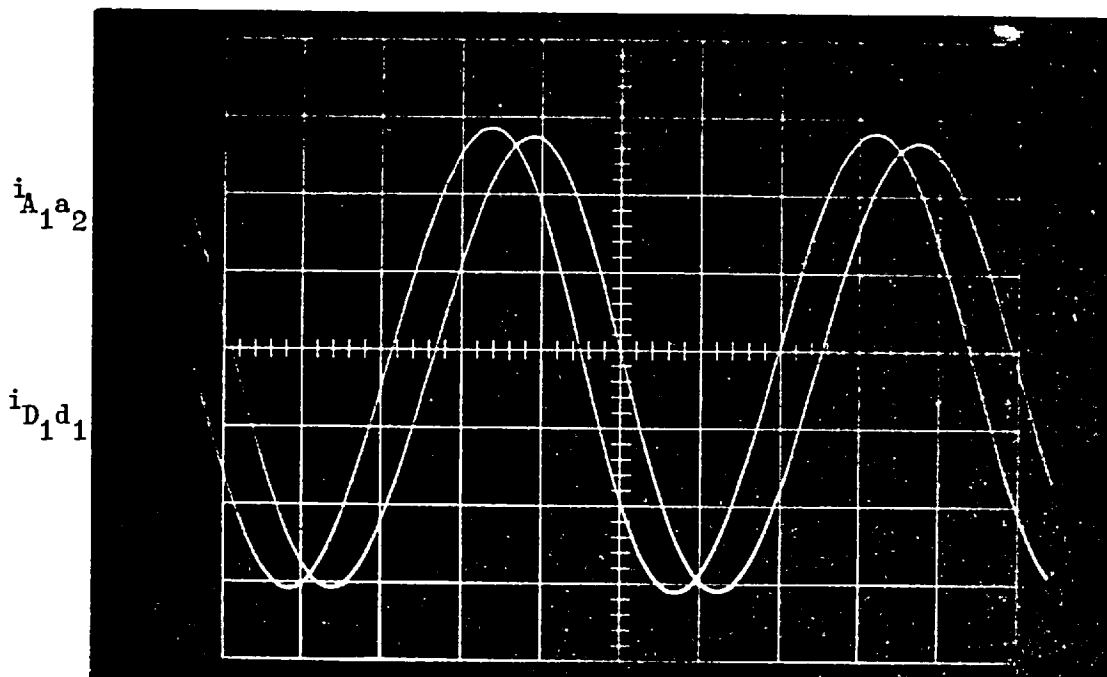


FIG. 7.5

Current waveforms of phase A and D when applying a study 3-ph short circuit on the high voltage winding.

$$(V_{C_1 C_2})_n = V_n \sin [n(\omega t - 240) + \alpha_n] \quad (7.3)$$

$$(V_{D_1 D_2})_n = V_n \sin [n(\omega t - 30) + \alpha_n] \quad (7.4)$$

$$(V_{E_1 E_2})_n = V_n \sin [n(\omega t - 150) + \alpha_n] \quad (7.5)$$

$$(V_{F_1 F_2})_n = V_n \sin [n(\omega t - 270) - \alpha_n] \quad (7.6)$$

where,

n : order of time harmonic, and an odd integer.

The voltages across the l.v. windings of the star-delta/star-transformer are:

$$(V_{a_2 a_1})_n = (V_{A_1 A_2})_n = V_n \sin(n\omega t + \alpha_n) \quad (7.7)$$

$$(V_{b_2 b_1})_n = (V_{B_1 B_2})_n = V_n \sin [n(\omega t - 120) + \alpha_n] \quad (7.8)$$

$$(V_{c_2 c_1})_n = (V_{C_1 C_2})_n = V_n \sin [n(\omega t - 240) + \alpha_n] \quad (7.9)$$

$$(V_{d_1 d_2})_n = (V_{D_1 D_2})_n - (V_{E_1 E_2})_n \quad (7.10)$$

$$(V_{e_1 e_2})_n = (V_{E_1 E_2})_n - (V_{F_1 F_2})_n \quad (7.11)$$

$$(V_{f_1 f_2})_n = (V_{F_1 F_2})_n - (V_{D_1 D_2})_n \quad (7.12)$$

Substituting for $(V_{D_1 D_2})_n$, $(V_{E_1 E_2})_n$ and $(V_{F_1 F_2})_n$ from equations (7.4), (7.5) and (7.6) respectively, it can be shown that:

$$(V_{d_1 d_2})_n = 2V_n \sin(60n)\sin(90n)\sin(n\omega t + \alpha_n) \quad (7.13)$$

$$(V_{e_1 e_2})_n = 2V_n \sin(60n)\sin(90n)\sin [n(\omega t - 120) + \alpha_n] \quad (7.14)$$

$$(V_{f_1 f_2})_n = 2V_n \sin(60n)\sin(90n)\sin [n(\omega t - 240) + \alpha_n] \quad (7.15)$$

It can be seen that the arguments of equations (7.13), (7.14) and (7.15) are similar to those of equations (7.7), (7.8) and (7.9)

respectively for any time harmonic. However, the magnitude of these two sets of voltages differs by a factor of $\sqrt{3}$, and this factor can be either positive or negative depending on the order of the time harmonic of voltage. When $n = 12k \pm 1$, where $k = 0$ or a positive integer, then equations (7.13)-(7.15) reduce to

$$(V_{d_1 d_2 n}) = \sqrt{3} V_n \sin(n\omega t + \alpha_n) \quad (7.16)$$

$$(V_{e_1 e_2 n}) = \sqrt{3} V_n \sin [n(\omega t - 120) + \alpha_n] \quad (7.17)$$

$$(V_{f_1 f_2 n}) = \sqrt{3} V_n \sin [(\omega t - 240) + \alpha_n] \quad (7.18)$$

At any single frequency, equations (7.16)-(7.18) and (7.7)-(7.9) can be represented by a phasor diagram as shown in Fig. 7.6(a).

For the case when $n = 12k \pm 5$, the phasor diagram of equations (7.13)-(7.15) is shown in Fig. 7.6(b) together with that of equations (7.7)-(7.9).

Finally, for the case when $n = 6k + 3$, equations (7.13)-(7.15) become $(V_{d_1 d_2 n}) = 0$, $(V_{e_1 e_2 n}) = 0$, and $(V_{f_1 f_2 n}) = 0$. Equations (7.7)-(7.9) reduce to three phasors which are equal in magnitude and in phase as shown in Fig. 7.6(c).

The following points can be made after studying the phasor diagrams of Fig. 7.6:

1. The fundamental and harmonic voltages of order $n = 12k \pm 1$ across the star winding are in phase with those across the delta winding.
2. The harmonic voltages of order $n = 12k \pm 5$ across the star winding are in antiphase with those across the delta winding.

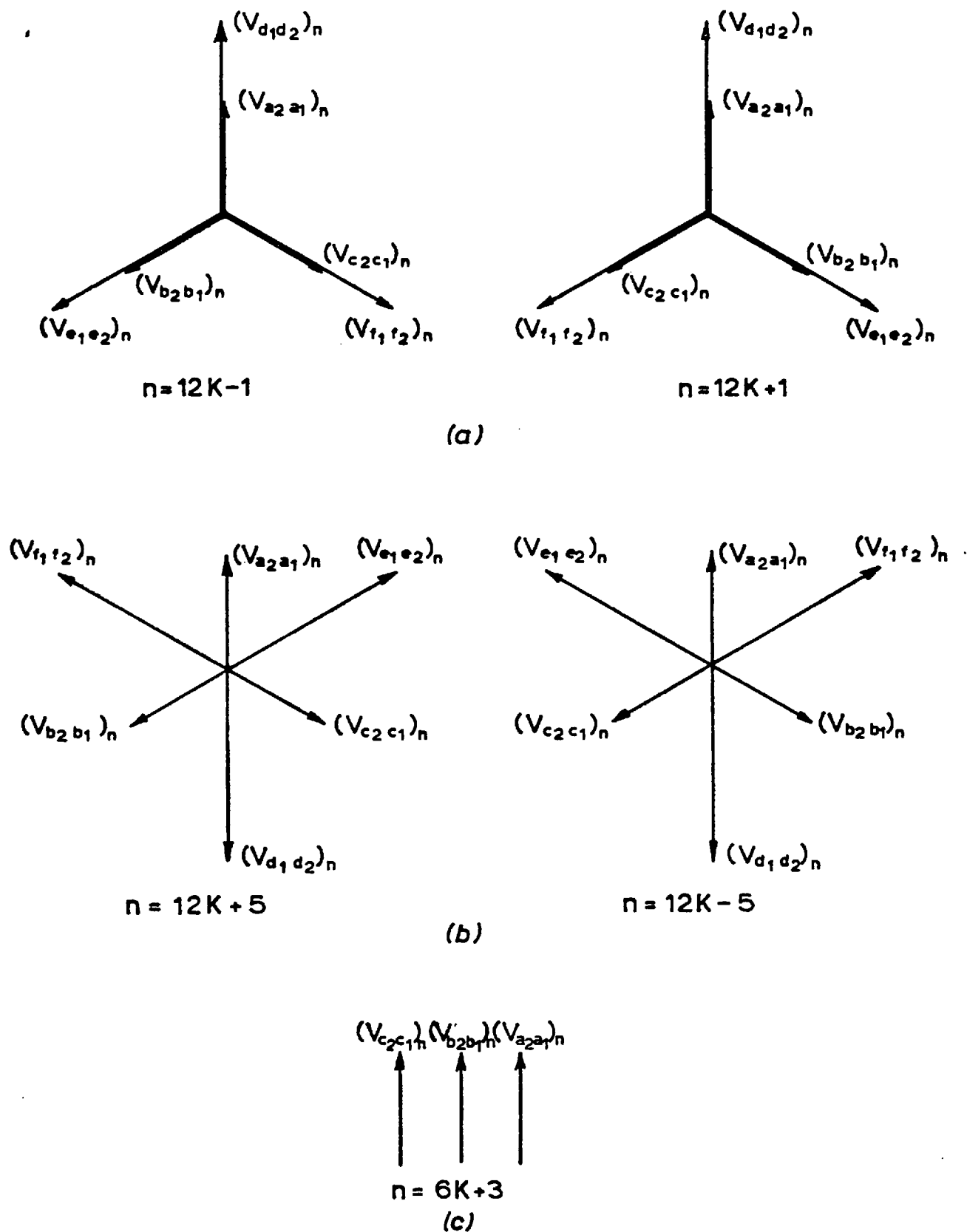


Fig. 7.6 Phasor diagrams for applied harmonic voltages on star-delta low voltage winding connection of a 6-ph/3-ph transformer bank.

- (a) Applied harmonic voltages of order $12K \pm 1$
 (b) " " " " " $12K \pm 5$
 (c) " " " " " $6K + 3$

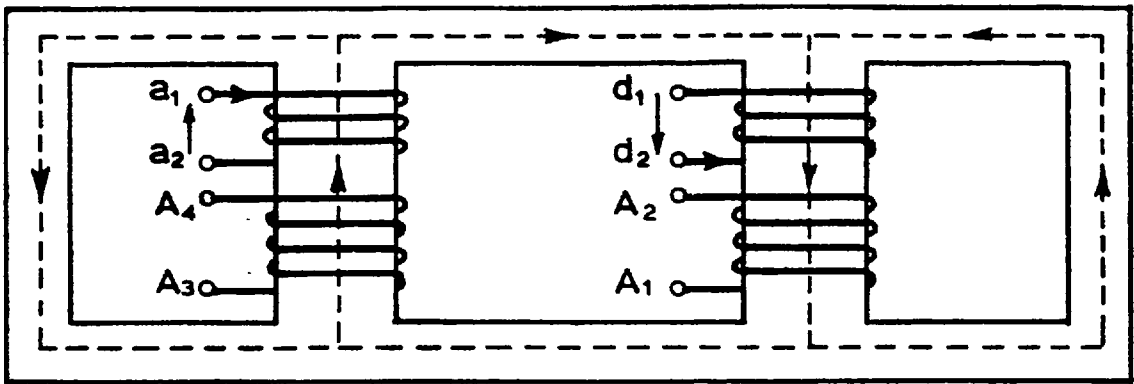
3. Harmonic voltages of order $6k + 3$ appear only across the star winding between each line and neutral.

Each of the above harmonic voltage types determines its own particular flux pattern as shown in Fig. 7.7. Therefore, the equivalent circuit of the transformer will differ according to the harmonic voltage types. Since the harmonic voltages of order $12k \pm 1$ produce the same flux pattern as the fundamental, then the equivalent circuit previously derived in Section 6.3 and given in Fig. 6.2(e) can be applied directly but with the reactance values scaled by the harmonic order. For harmonic voltages of order $12k \pm 5$, the following modifications must also be made:

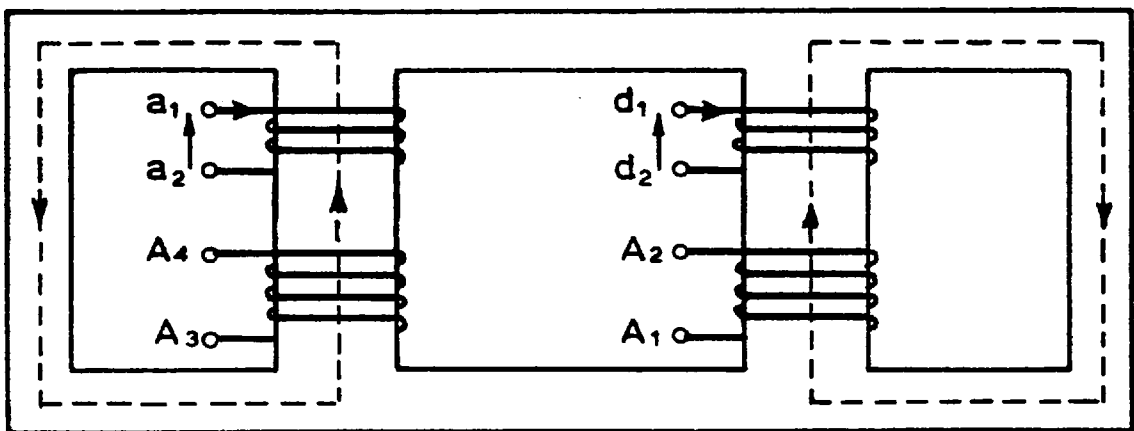
1. The magnetic branch \mathcal{R}_5 of Fig. 6.2(b) is set on open circuit because, under symmetrical conditions, no flux flows in it. Therefore, the corresponding impedance Z_{md_5} in Fig. 6.2(e) is short circuited.
2. The applied voltage on one of the l.v. windings is reversed.

The equivalent circuit of Fig. 6.2(e) then reduces to that shown in Fig. 7.8(a), in which the h.v. winding sections are assumed equally loaded. If, in addition, the assumptions made in Section 6.3 regarding the symmetry of the magnetic current are used here, i.e. $\mathcal{R}_1 = \mathcal{R}_3, \mathcal{R}_2 = \mathcal{R}_4$ and $\mathcal{R}_{l_1} = \mathcal{R}_{l_2}$, the resultant current in line OC is zero. Therefore, it is sufficient to consider half of the equivalent circuit which is shown in Fig. 7.8(b).

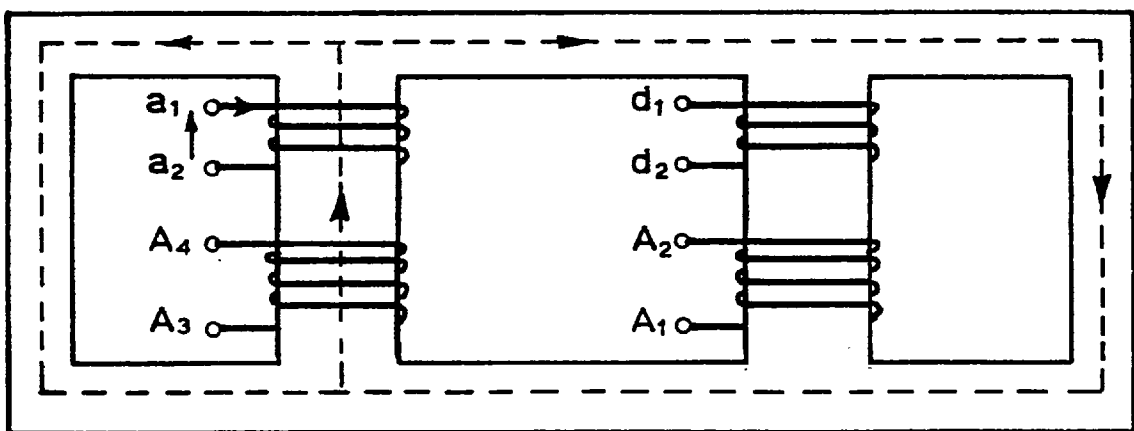
It is important to point out that the above situation is unlike that of a 3-ph transformer bank in which the applied harmonic



(a) Applied harmonic voltages of order $n = 12k \pm 1$



(b) Applied harmonic voltages of order $n = 12k \pm 5$



(c) Applied harmonic voltages of order $n = 6k + 3$

Fig. 7-7 Flux pattern in the transformer core with respect to n^{th} harmonic voltage. Dotted lines represent flux paths.

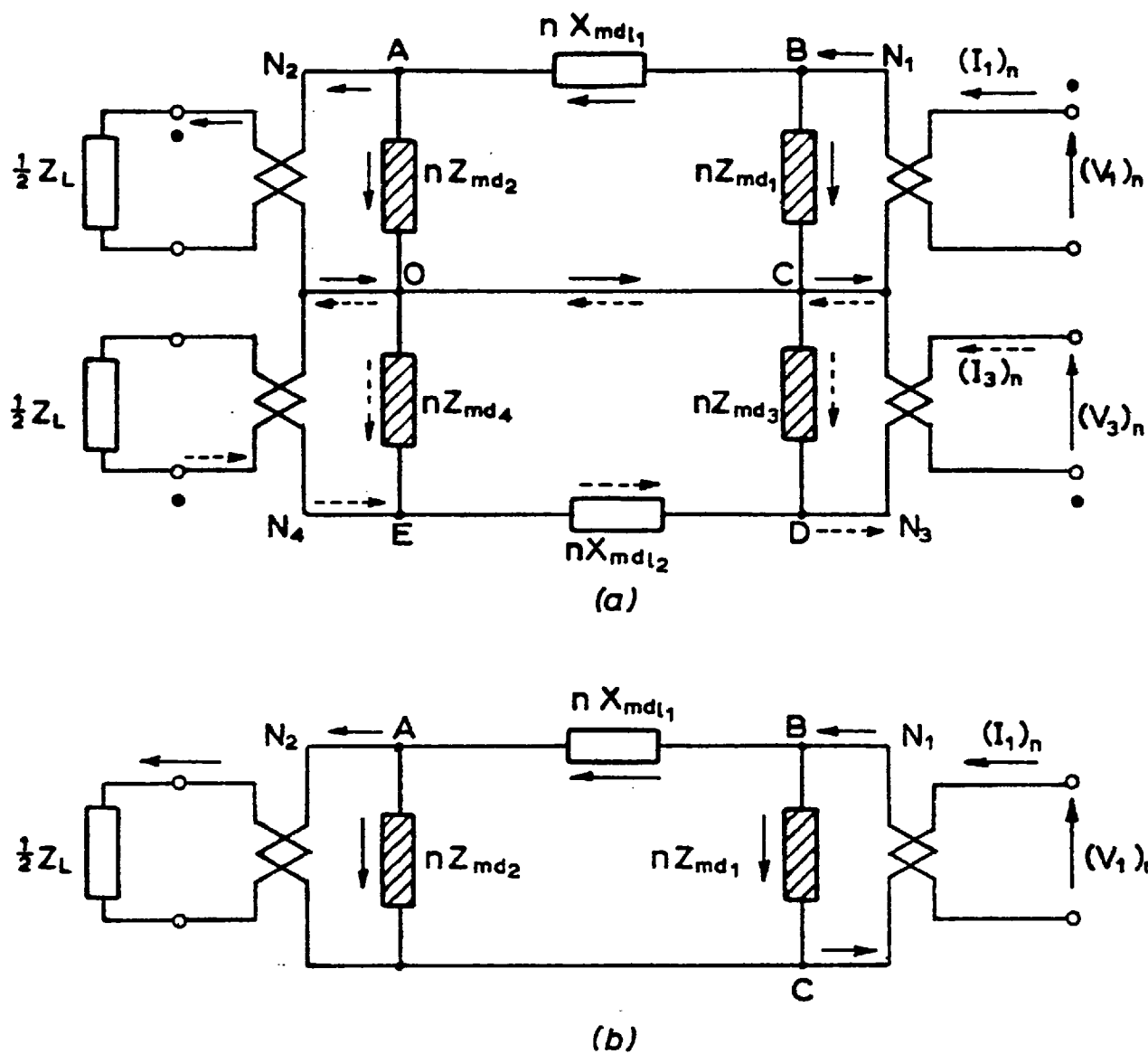


Fig. 7-8 Equivalent circuit of a four-limb, four-winding transformer subjected to a harmonic voltage of order $n = 12K \pm 5$ ($K = 0, 1, 2, \dots$).

voltages of order $12k \pm 1$ and of order $12k \pm 5$ produce the same flux pattern and thus the same equivalent circuit can be used.

Next, the behaviour of each harmonic voltage type in the h.v. winding sections is analysed. The induced voltages on the h.v. side can be derived from the voltage-turn relationship

$$\frac{(V_{A_1 A_2})_n}{(V_{d_1 d_2})_n} = \frac{N_{A_1 A_2}}{N_{d_1 d_2}}$$

Substituting for $(V_{d_1 d_2})_n$ from equation (7.13), then

$$(V_{A_1 A_2})_n = \frac{N_{A_1 A_2}}{N_{d_1 d_2}} \cdot 2V_n \sin(60n) \sin(90n) \sin(n\omega t + \alpha_n) \quad (7.19)$$

Likewise, $(V_{B_1 B_2})_n$, $(V_{C_1 C_2})_n$, $(V_{A_4 A_3})_n$, $(V_{B_4 B_3})_n$ and $(V_{C_4 C_3})_n$ can be found.

Consider first when the h.v. winding sections are connected in series (see Fig. 7.1). It follows that

$$\begin{aligned} (V_{A_4 A_2})_n &= (V_{A_4 A_3})_n + (V_{A_1 A_2})_n \\ &= \frac{N_{A_4 A_3}}{N_{a_2 a_1}} \cdot V_n \sin(n\omega t + \alpha_n) + \frac{N_{A_1 A_2}}{N_{d_1 d_2}} \cdot 2V_n \sin(60n) \\ &\quad \sin(90n) \sin(n\omega t + \alpha_n) \end{aligned} \quad (7.20)$$

Similarly

$$\begin{aligned} (V_{B_4 B_2})_n &= \frac{N_{B_4 B_3}}{N_{b_2 b_1}} \cdot V_n \sin [n(\omega t - 120) + \alpha_n] + \frac{N_{B_1 B_2}}{N_{e_1 e_2}} \cdot 2V_n \\ &\quad \sin(60n) \sin(90n) \sin [n(\omega t - 120) + \alpha_n] \end{aligned} \quad (7.21)$$

$$\begin{aligned} (V_{C_4 C_2})_n &= \frac{N_{C_4 C_3}}{N_{c_2 c_1}} \cdot V_n \sin [n(\omega t - 240) + \alpha_n] + \frac{N_{C_1 C_2}}{N_{f_1 f_2}} \cdot 2V_n \\ &\quad \sin(60n) \sin(90n) \sin [n(\omega t - 120) + \alpha_n] \end{aligned} \quad (7.22)$$

It should be remembered that the transformer is designed so that

$$N_{A_4 A_3} = N_{A_1 A_2} = N_{B_4 B_3} = N_{B_1 B_2} = N_{C_4 C_3} = N_{C_1 C_2} = N,$$

and

$$\frac{N_{d_1 d_2}}{N_{a_2 a_1}} = \frac{N_{e_1 e_2}}{N_{b_2 b_1}} = \frac{N_{f_1 f_2}}{N_{c_2 c_1}} = \sqrt{3}.$$

It can be shown that for harmonics of order $h = 12k \pm 1$, equations (7.20), (7.21) and (7.22) reduce to three symmetrical equations which have equal magnitude of $2V_n$ and differ in their argument by $120n$. However, for harmonics of order $n = 12k \pm 5$, these equations become

$$\begin{aligned} (v_{A_4 A_2})_n &= \frac{N}{N_{a_2 a_1}} V_n \sin(n\omega t + \alpha_n) + \frac{N}{\sqrt{3} N_{a_2 a_1}} \cdot 2V_n \cdot \left(-\frac{\sqrt{3}}{2}\right) \\ &\quad \sin(n\omega t + \alpha_n) \\ &= 0 \end{aligned}$$

Likewise $(v_{B_4 B_2})_n = 0,$

$$(v_{C_4 C_2})_n = 0.$$

This interesting result demonstrates that when the h.v. winding sections are connected in series, their induced harmonic voltages of order $12k \pm 1$ are additive whereas harmonics of order $n = 12k \pm 5$ are of opposite sign. In other words, induced harmonic voltages in the h.v. winding sections cancel each others' effect and do not appear between line to neutral. Thus harmonic currents of order $12k \pm 5$ are suppressed from h.v. lines. Consequently, except for the effect of exciting current, these harmonic currents are also eliminated from l.v. winding lines. Therefore the equivalent circuit of Fig. 7.8(a)

reduces to that shown in Fig. 7.9(a), in which the h.v. side, though loaded, is considered effectively an open circuit for harmonic currents of order $n = 12k \pm 5$.

When the h.v. winding sections are connected in parallel, then

$$(V_{A_1 A_2})_n = (V_{A_4 A_2})_n,$$

$$(V_{B_1 B_2})_n = (V_{B_4 B_3})_n$$

and $(V_{C_1 C_2})_n = (V_{C_4 C_3})_n.$

It can be shown that the sum of induced voltages around the parallel connection is zero for harmonic of order $n = 12k \pm 1$, while the sum is double that of one section for harmonics of order $n = 12k \pm 5$. For example, the resultant voltages around phase A for harmonics of order $n = 12k \pm 5$ is,

$$(V_{A_4 A_3})_n - (V_{A_1 A_2})_n = 2 V_n \sin(n\omega t + \alpha_n)$$

This result shows that the parallel connection provides a closed path for harmonic currents of order $n = 12k \pm 5$ to circulate, and consequently their corresponding harmonic currents will appear on the l.v. side. However, under balanced conditions, the line currents on the h.v. side do not contain harmonic components of the above order, just as with the series connection. Therefore the equivalent circuit for this case, which is shown in Fig. 7.9(b), is the same as that of Fig. 7.9(a), but the h.v. side can now be considered effectively a short circuit for these harmonic currents. A test is developed in Section 7.5 to verify the equivalent circuit of Fig. 7.9(b).

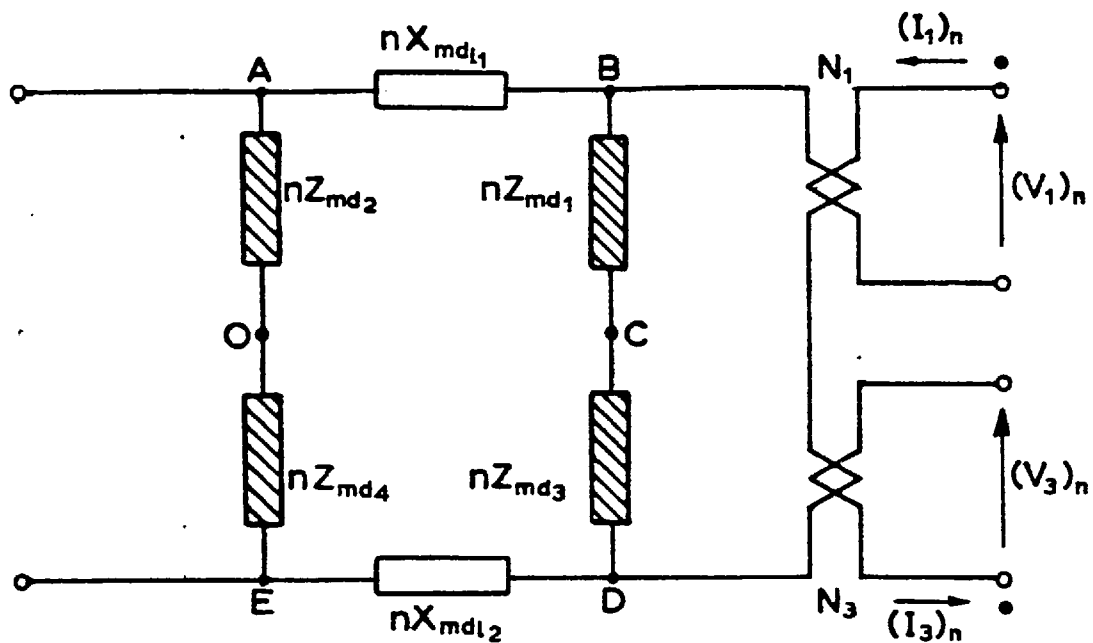
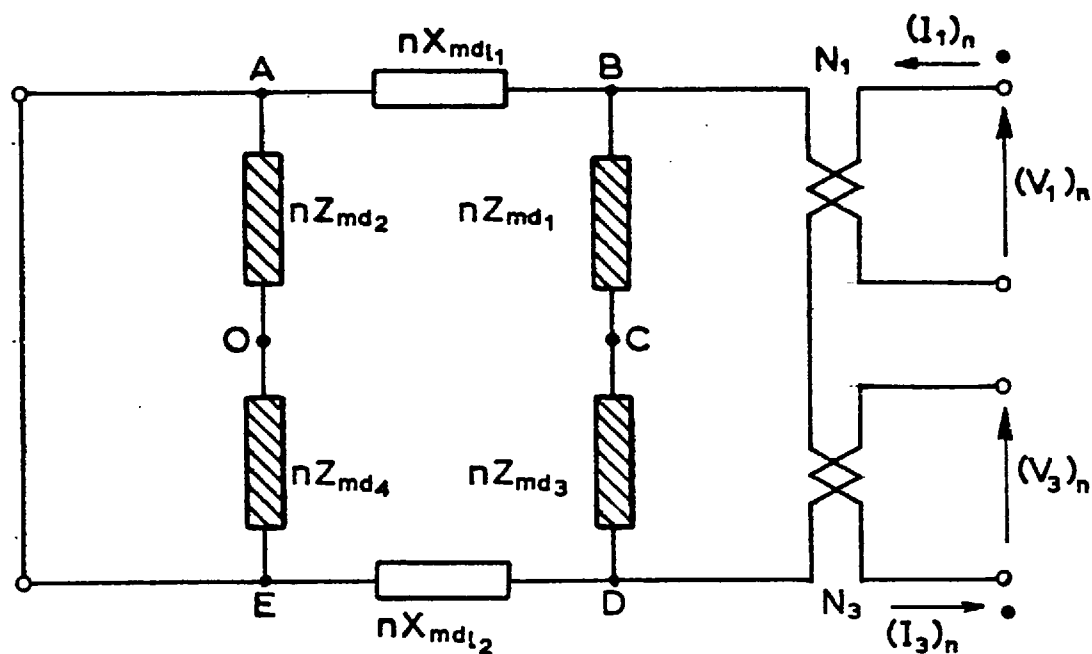
(a) $n = 12K \pm 5$ (b) $n = 12K \pm 5$

Fig. 7-9 Equivalent circuit with high voltage winding sections connected (a) in series (b) in parallel

In view of the above, it can be said that the presence of harmonic currents of order $12k \pm 5$ depends on the winding connections for the transformer under investigation. This is unlike the case of a 3-ph transformer bank in which the presence of these harmonics is not affected by the winding connection and can be treated in a way identical to that for harmonics of order $n = 12k \pm 1$.

Tests were made to support the above theoretical analysis, two of which are given here and the others given later. The first test was performed to confirm whether the induced harmonic voltages of order $n = 12k \pm 5$ and, in particular, the 5th and 7th were additive around the closed h.v. winding sections. A 3-ph switch was put between the parallel-connected h.v. winding sections and it was left open during the test. The transformer was energised and the harmonic components of the induced voltages were measured for each section, for example, $V_{C_1C_2}$ and $V_{C_4C_3}$, and across the switch $V_{C_1C_4}$. The wave analyser described in Section 4.3 was used for measuring the harmonic components and the results are given in Table 7.3. These results show that although the 5th and 7th harmonic voltages across any two sections are not equal, their sums are almost equal to the corresponding values of harmonic voltages across the switch. The inequality is probably caused by the presence of harmonic voltages generating from the transformer affecting the measurement.

The other test was performed to check whether the harmonic fluxes of order $n = 12k \pm 5$ are relatively greater in the outer limbs than in the yokes. This was achieved by first energising the three transformers and then comparing the harmonics content of the induced voltage waveforms in the search coils wound on the outer limbs with

TABLE 7.3

Harmonic components of induced voltages in
h.v. winding sections which are connected in
parallel through a 3-ph switch.

	1st	3rd	5th	7th
$V_{C_1C_2}$	105	.95	.4	.85
$V_{C_4C_3}$	104	48	2.1	.5
$V_{C_1C_4}$	2.4	49	2.3	1.4
$V_{A_1A_2}$	105	.85	0.6	.7
$V_{A_4A_3}$	104	48	3.3	1.6
$V_{A_1A_4}$	2	49	4	1.45

that wound on the yoke. The test was made with the tertiary winding closed to obtain identical flux distribution in the inner and outer limbs. Figure 7.10 shows the induced voltage waveform in the search coil wound on the yoke in which the harmonic contents of this waveform are:

$$V_f = 15.3 \text{ V}, V_{3^{\text{rd}}} = 2.7 \text{ V}, V_{5^{\text{th}}} = 2.3 \text{ V} \text{ and } V_{7^{\text{th}}} = .95\text{V}.$$

Comparison of Figs. (7.10) and (7.2(h)) shows that although the fundamental and the 3rd harmonic fluxes are higher in the yoke than in the outer limbs, the 5th and 7th harmonics are not. This indicates that, except for the iron non-linearity and the imbalance in magnetic circuit, the harmonic fluxes of order $n = 12k \pm 5$ are likely to flow only in the outer limbs.

7.5 EFFECT OF TRANSFORMER CONSTRUCTION ON THE HARMONIC CURRENTS AND FLUXES OF ORDER $n = 12k \pm 5$

The use of four-limb rather than two-limb transformer construction was justified in Section 5.3. The reduced height of the core overcomes the transportation problem. The comparison between these two types is considered here with respect to the harmonic currents and fluxes of order $12k \pm 5$ when the h.v. winding sections are connected in parallel or in series. Parallel connection is considered first.

Examination of the equivalent circuit in Fig. 7.9(b) shows that the harmonic circulating currents of order $12k \pm 5$ mainly flow in the leakage branches. In other words, the presence of the outer limbs, which are represented in the equivalent circuit by the impedances Z_{md_2} and Z_{md_4} , are immaterial. Therefore it is believed

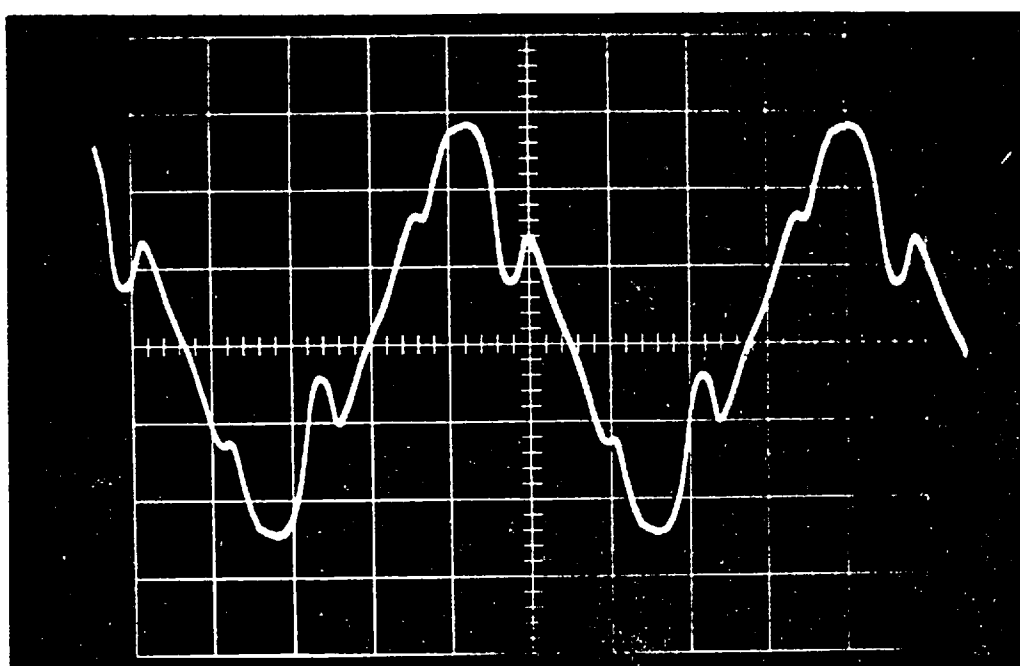


FIG. 7.10 Induced voltages in search coil wound on the yoke. Tertiary winding closed.

that the use of four- or two-limb transformer construction will not affect significantly the magnitude of these harmonic circulating currents.

A test was developed to simulate the behaviour of these harmonics in a four- and two-limb transformer, and to verify the equivalent circuit of Fig. 7.9(b). Consider Fig. 5.11 in which windings $3B_2-3B_1$ and $4B_2-4B_1$ have equal number of turns and connected in series, windings B_3-B_4 and B_1-B_2 have also equal number of turns but connected in parallel. First, it was ensured that windings B_3-B_4 and B_1-B_2 were connected properly in parallel by exciting the series winding so as to produce a flux pattern like that shown in Fig. 7.7(a) and measuring zero circulating current. Then windings $3B_2-3B_1$ and $4B_2-4B_1$ were reconnected and energised so as to obtain a flux pattern like that of Fig. 7.7(b) whereas the connection of windings B_3-B_4 and B_1-B_2 was not changed. Large circulating current was obtained from a relatively very small applied voltage because, in this case, the induced voltages in the parallel circuit are in antiphase. Also, very small induced voltages in the search coils were measured. This indicates that most of the flux emanating from the inner limbs is forced into the leakage paths, and thus preventing it from flowing in the outer limbs. This situation is identical to that in the short circuit test. Finally, the four-limb transformer was converted into two-limb type by short circuiting the search coils on the outer limbs. There was hardly any change in the magnitude of the circulating current, thus confirming that the presence of the outer limbs is ineffective.

When the h.v. winding sections are put in series, it was shown in Section 7.4 that the harmonic currents of order $n = 12k \pm 5$

do not appear in the lines on either side of the transformer. In other words, the transformer may be regarded as an open circuit for these harmonics and the flux pattern will be as shown in Fig. 7.7(b). If a two-, instead of a four-, limb transformer was used, then these harmonic fluxes must complete their magnetic circuit in air, thus increasing the stray losses. Also, they might cause a heating problem in the transformer tank. This situation is identical to the behaviour of triplen harmonic fluxes in a three-limb, 3-ph transformer core²¹. Therefore, it can be said that if the h.v. winding sections are put in series, a four-limb transformer construction is likely to produce less stray losses than a two-limb type.

7.6 HARMONICS BEHAVIOUR IN A SIX-PHASE GENERATOR DELIVERING POWER TO THREE-PHASE BUSBARS VIA 6-PH/3-PH TRANSFORMER BANK

To further appreciate the peculiar harmonic phenomena and to confirm the harmonic analysis made in Section 7.4, more tests were carried out but this time with the 6-ph generator loaded. The 6-ph generator was successfully synchronized to the 3-ph busbars through the transformer arrangement previously described in Section 5.3 and shown in Fig. 7.1. All tests were performed at half, and not full, rated generator power due to limitations on the magnitude of currents which could be safely drawn from the d.c. and a.c. mains. The programme of tests, as before, is subdivided according to whether the h.v. winding sections are connected in series or in parallel, and each case in turn is further subdivided into three parts depending on the type of loading. In each of the tests conducted, the waveforms of the following quantities were observed, photographed and the harmonic components measured using a wave analyser:

1. Generator terminal voltage,
2. Currents in l.v. and h.v. windings, and current per section for the case of parallel connection,
3. Terminal voltages of h.v. winding,
4. Induced voltages in the search coils wound on the outer limbs and on the upper yoke.

In order to make the synchronization of 6-ph generator to 3-ph busbars at two different voltages possible, i.e. once at 365 V line to line resulting from the series connection and once at 183 V line to line resulting from the parallel connection, a 3-ph variac was inserted between the h.v. side and the 3-ph busbars. For the sake of convenience, Wattmeters and power factor meter were inserted in the h.v. side. Six tests were performed, in each of which the active power delivered by the generator was kept constant at 1.5 kW. These tests are presented and studied in the following subsections.

7.6.1 Load Tests at unity, 0.8 Lagging and 0.8 Leading Power Factor and with the High Voltage Winding Sections connected in Series

Figures (7.11), (7.12) and (7.13) show the current and voltage waveforms when the 6-ph generator is half loaded at unity, 0.8 lagging and 0.8 leading power factor. Table 7.4 gives the magnitude of harmonic components of each waveform in these figures. The induced voltage waveforms in the h.v. winding and in search coils are not given here because they are nearly the same as the corresponding ones given in Figs. 7.2(e) to 7.2(h) inclusive. Also, the line currents of the six phases were found to be very nearly balanced. The following remarks can be made after studying Figs. (7.11), (7.12) and (7.13):

	Fig. No.	Tertiary connection	Parameters	Definitions	Star or Delta	1st	3rd	5th	7th	
Unity Power Factor	7.11	a	open	$i_{A_1 a_2}$	Gen. line currents	S	4.8	.06	.20	.06
	a	open	$i_{D_1 d_1}$	Gen. line currents	D	4.8	.08	.27	.04	
	b	closed	$i_{A_1 a_2}$	Gen. line currents	S	4.8	.03	.07	.03	
	b	closed	$i_{D_1 d_1}$	Gen. line currents	D	4.8	.04	.06	.02	
	c	open or closed	$v_{A_1 A_2}$	Gen. volt. L-N	S	53	5.0	.50	.40	
	c	open or closed	$v_{D_1 D_2}$	Gen. volt. L-N	D	53	4.6	.76	.48	
	d	open or closed	i_L	Line current on h.v. side	S	2.3	.035	.025	.005	
	0.8 Lagging Power Factor	7.12	a	open	$i_{A_1 a_2}$	Gen. line currents	S	6.6	.052	.22
a		open	$i_{D_1 d_1}$	Gen. line currents	D	6.6	.08	.28	.012	
b		closed	$i_{A_1 a_2}$	Gen. line currents	S	6.6	.04	.10	.03	
b		closed	$i_{D_1 d_1}$	Gen. line currents	D	6.6	.04	.06	.03	
c		open or closed	$v_{A_1 A_2}$	Gen. volt. L-N	S	54	6	.40	.75	
c		open or closed	$v_{D_1 D_2}$	Gen. volt. L-N	D	54	5.8	1.2	.40	
d		open or closed	i_L	Line current on h.v. side	S	3	.02	.03	.01	
0.8 Leading Power Factor		7.13	a	open	$i_{A_1 a_2}$	Gen. line currents	S	5.4	.06	
	a	open	$i_{D_1 d_1}$	Gen. line currents	D	5.4	.07			
	b	closed	$i_{A_1 a_2}$	Gen. line currents	S	5.4	.032			
	b	closed	$i_{D_1 d_1}$	Gen. line currents	D	5.4	.04			
	c	open or closed	$v_{A_1 A_2}$	Gen. volt. L-N	S	53	4.5			
	c	open or closed	$v_{D_1 D_2}$	Gen. volt. L-N	D	53	4			
	d	open or closed	i_L	Line current on h.v. side	S	2.6				

TABLE 7.4

Values of harmonic components in voltage and current waveforms of Figs. 7.11, 7.12 and 7.13. High voltage winding sections are connected in series. Harmonic voltages and currents are respectively given in V and A.

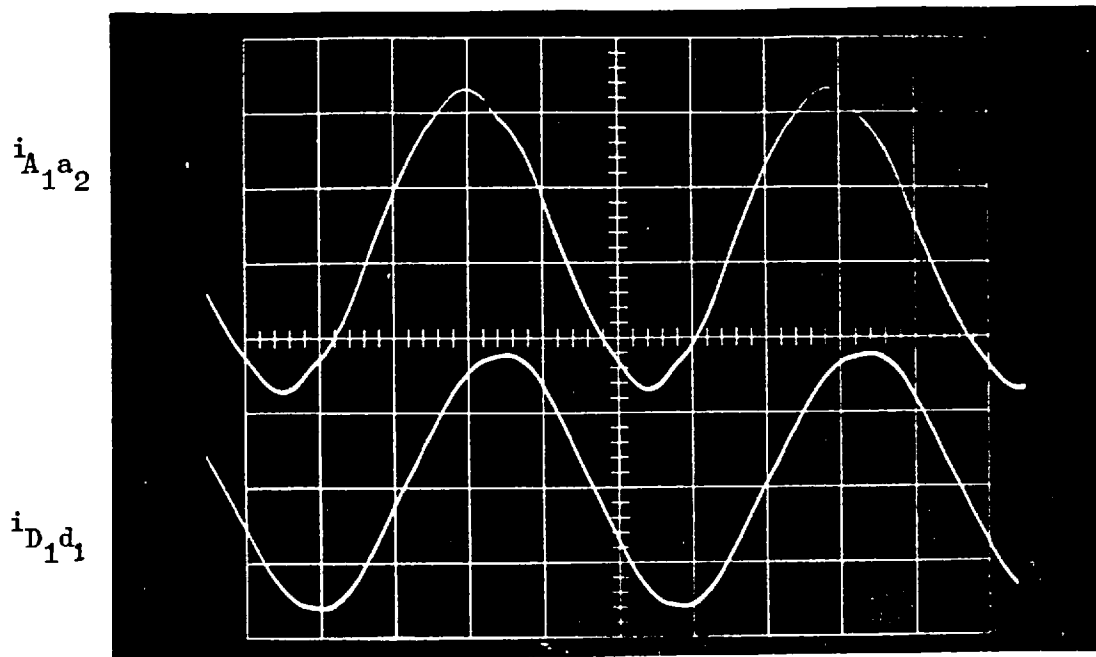


Fig. 7.11(b) The same, but tertiary winding closed.

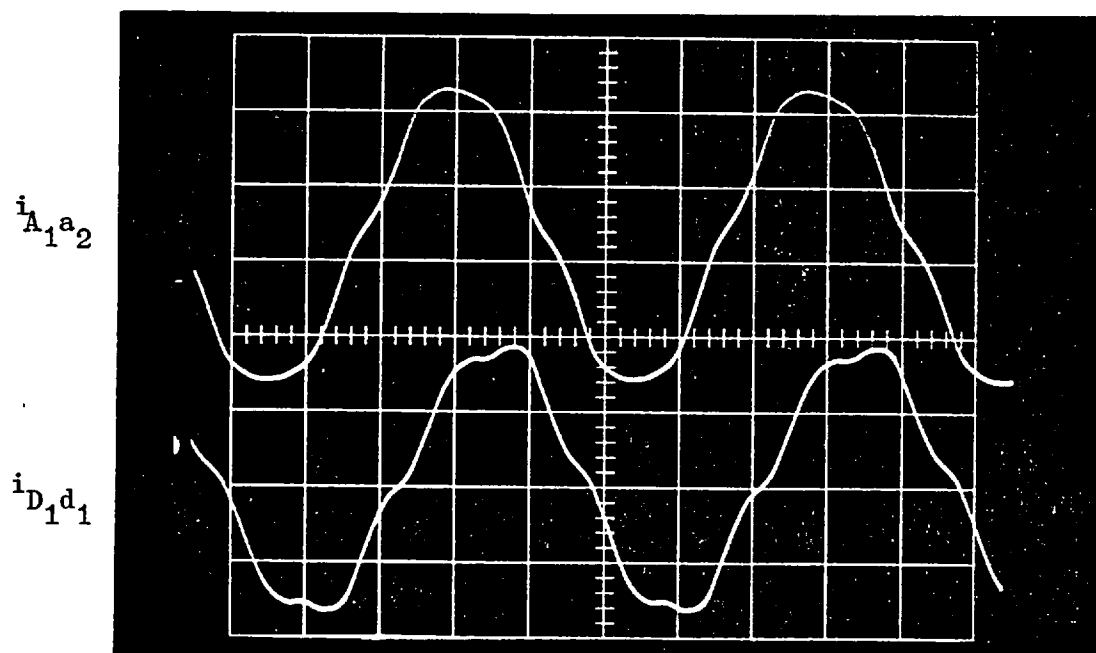


Fig. 7.11(a) Line currents in phase A and D.
Tertiary winding open.

FIG. 7.11 6-ph generator connected to 3-ph busbars via a 6-ph/3-ph transformer bank and is half loaded at unity power factor. High voltage winding sections connected in series.

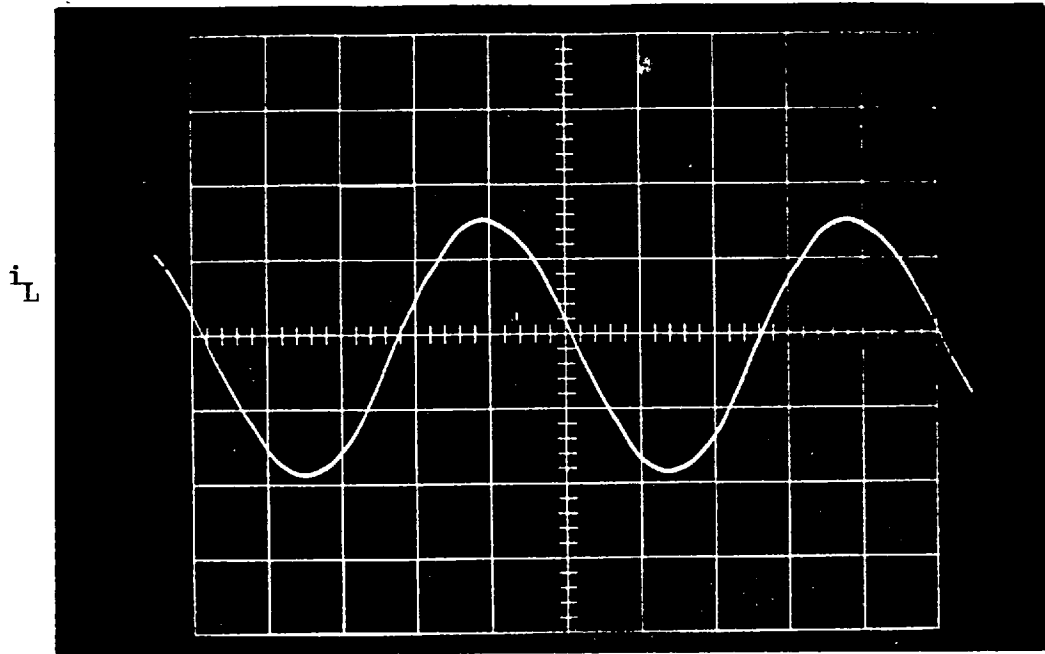


Fig. 7.11(d) Line current on high voltage side.
Tertiary winding is ineffective.

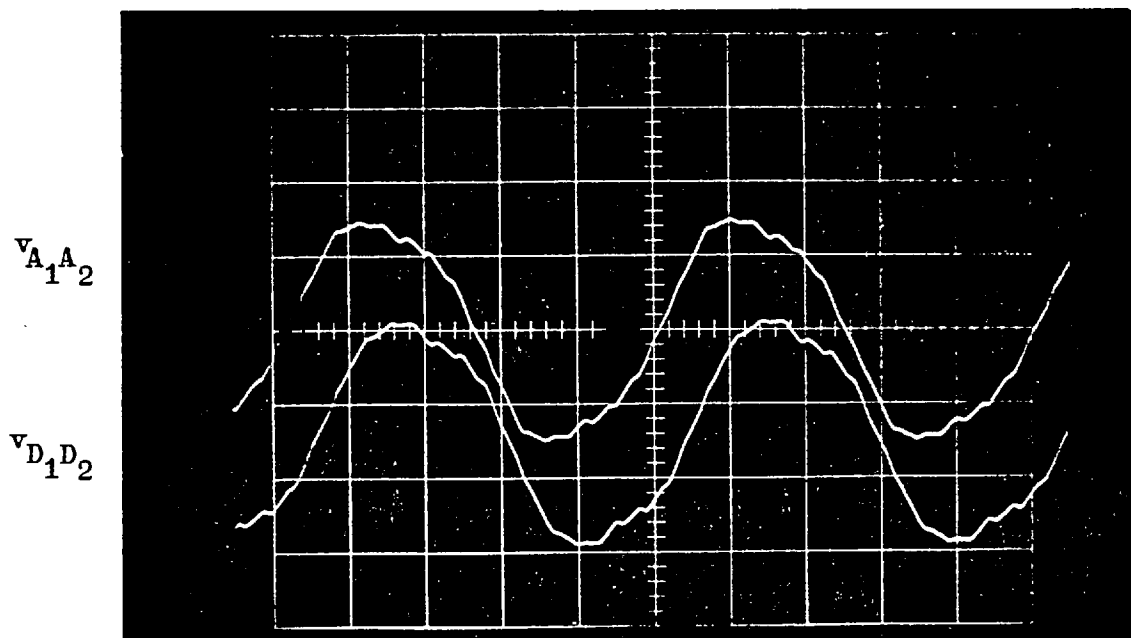


Fig. 7.11(c) Line to neutral generator voltages.

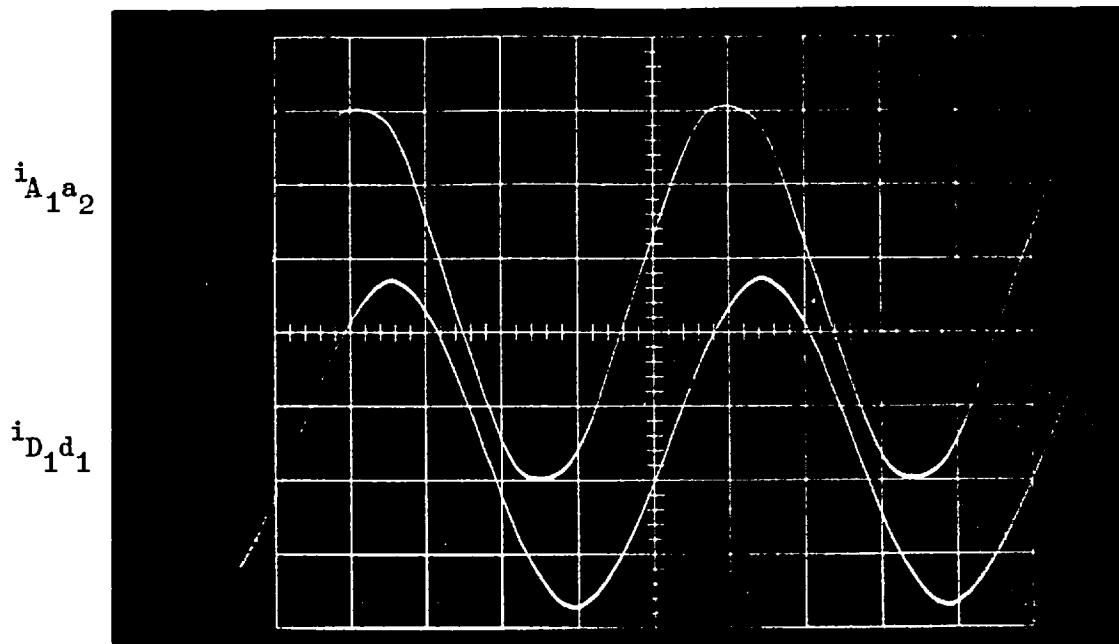


Fig. 7.12(b) The same, but tertiary winding closed.

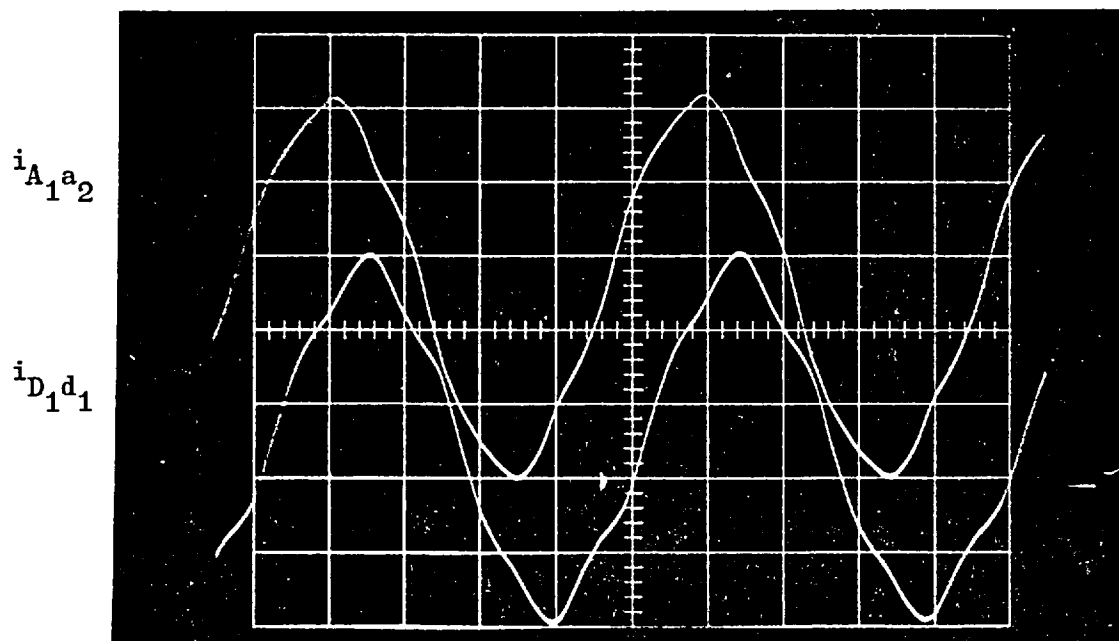


Fig. 7.12(a) Line current in phase A and D. Tertiary winding open.

FIG. 7.12 The same as Fig. 7.11, but at 0.8 Lagging Power Factor.

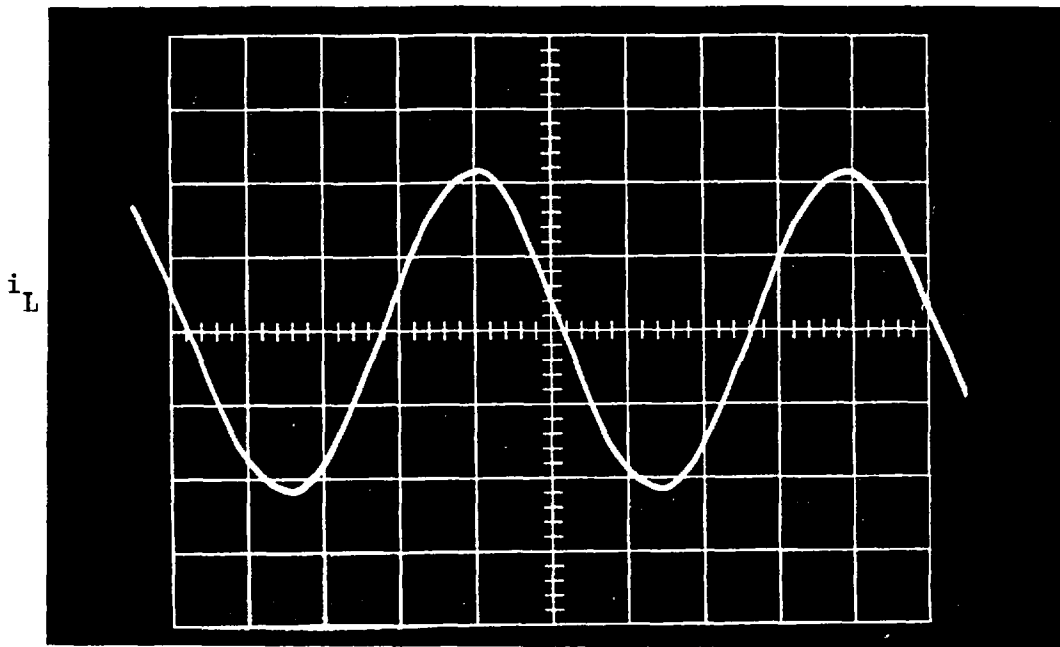


Fig. 7.12(d) Line current on high voltage side.
Tertiary winding is ineffective.

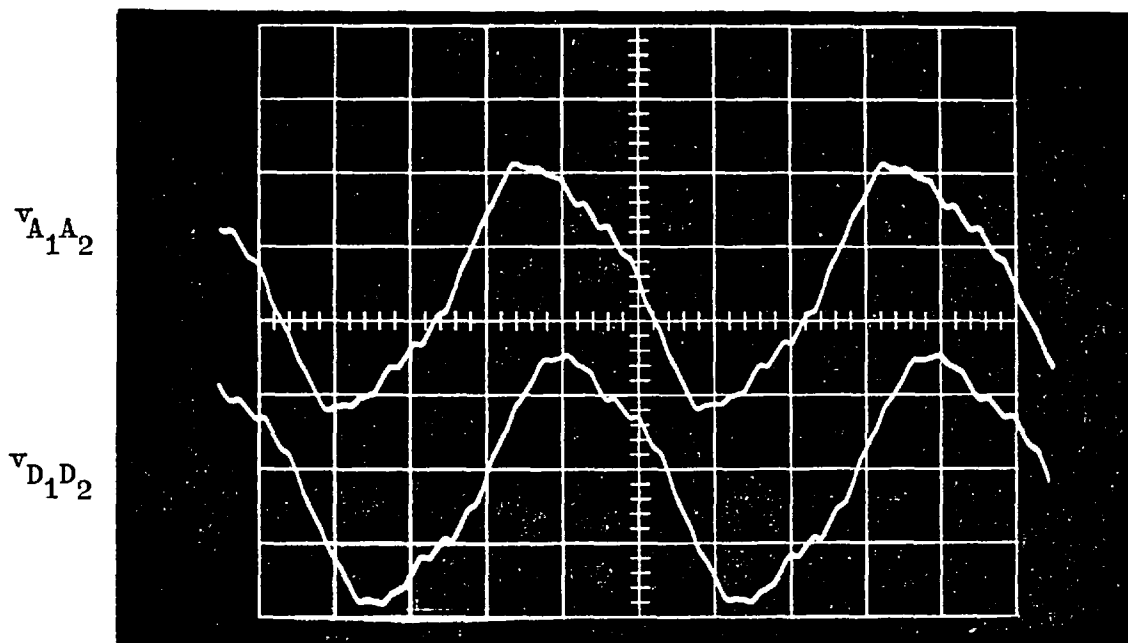


Fig. 7.12(c) Line to neutral generator voltages.

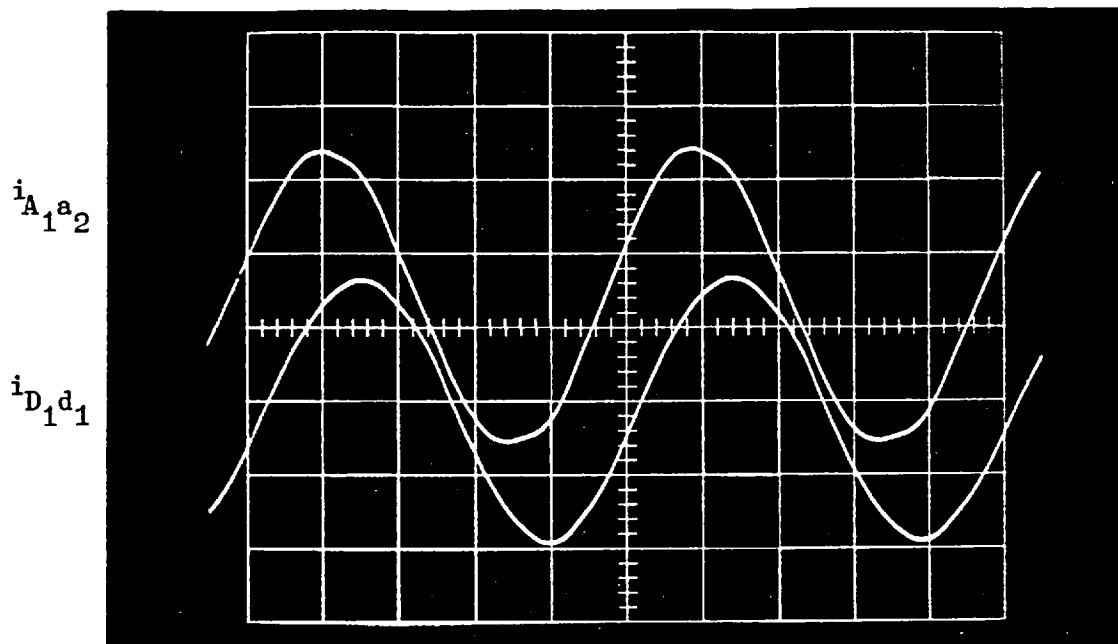


Fig. 7.13(b) The same, but tertiary winding closed.

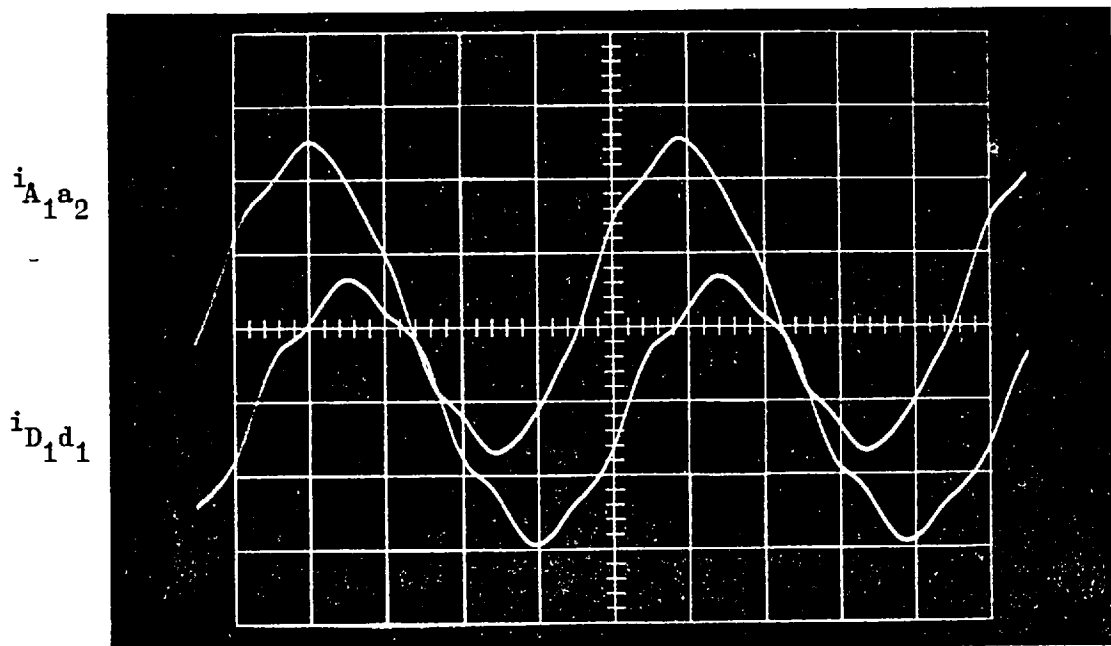


Fig. 7.13(a) Line current in phase A and D.
Tertiary winding open.

FIG. 7.13 The same as Fig. 7.11, but at 0.8 Leading Power Factor.

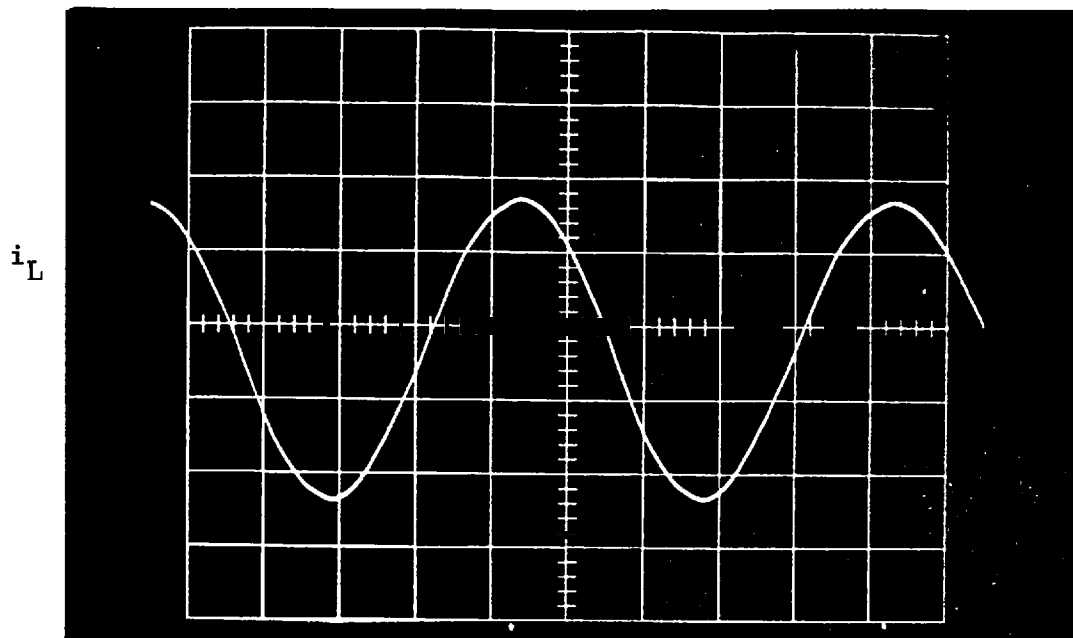


Fig. 7.13(d) Line current on the high voltage side.
Tertiary winding is ineffective.

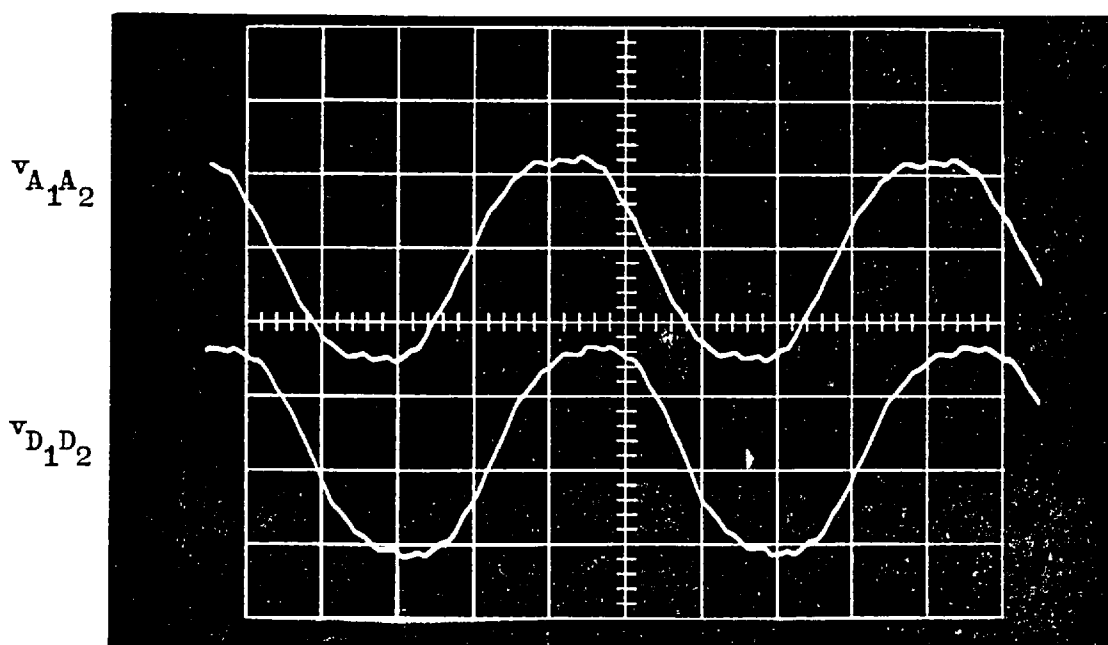


Fig. 7.13(c) Line to neutral generator voltages.

1. The waveforms of the line currents flowing in the l.v. side at all different loading conditions are improved when the tertiary is closed.
2. The line current waveforms on the h.v. side are more sinusoidal than those on the l.v. side when the tertiary winding is opened. The main reasons for this are thought to be:
 - (a) The harmonic currents flow through the transformer and load on the h.v. side, and through the transformer and the generator on the l.v. side. Since the load impedance is usually greater than that of the generator, the harmonic currents are limited on the h.v. side.
 - (b) The presence of harmonic currents of order $n = 12k \pm 5$ on the l.v. side are due to the transformer excitation characteristics because, as shown in Section 7.4, these harmonics do not originate in the generator under balanced conditions.

It should be noted that the 3rd harmonic currents are eliminated from line currents on both sides of the transformer because of the nature of the winding connections.

3. The harmonic content of the currents and voltages for the three load conditions is greatest in Fig. 7.12, which corresponds with the greatest generator excitation.

7.6.2 Load Tests at Unity, 0.8 Lagging and 0.8 Leading Power Factor and with the High Voltage Winding Sections connected in Parallel

These tests are similar to those given in Section 7.6.1 except that the h.v. winding sections were connected in parallel. Figures 7.14, 7.15 and 7.16 show the current waveforms obtained from these tests, and Table 7.5 gives their harmonics content. The induced voltage waveforms are not given because they were found to be the same as those in Section 7.6.1. The following points, which mainly concern the circulating current, can be made after studying Figs. 7.14, 7.15 and 7.16:

1. When the tertiary winding is excluded, the current flowing in each h.v. winding section is distorted, whereas the line currents on the h.v. side are not. The major reasons for this difference are thought to be:
 - (a) Third harmonic currents can only flow in the parallel-connected h.v. winding sections and are eliminated from the lines. The circulating third harmonic currents result from the difference between the induced voltage waveforms in the high voltage sections prior to the parallel connection (see Section 7.2.2).
 - (b) The harmonic currents of order $n = 12k \pm 5$ are, under balanced conditions, suppressed from the lines but circulate in the closed loop of the parallel connection (see Section 7.4).
 - (c) Because of (a) and (b), the only harmonic currents that might be present in the h.v. lines are of order $12k \pm 1$

	Fig. No.	Tertiary Winding	Parameters	Definitions	Star or Delta	1st	3rd	5th	7th
7.14 Unity power factor	a	open or closed	$i_{A_1 a_2}$	Gen. line current	S	5.14	.027	.14	.11
	a	open or closed	$i_{D_1 d_1}$	Gen. line current	D	4.56	.026	.083	.083
	b	open	i_L	Line current on h.v. side	S	4.3	.05	.05	.016
	b	open	i_{S_1}	Current per section		2.4	.33	.07	.04
	c	closed	i_L	Line current on h.v. side	S	4.3	.05	.052	.016
	c	closed	i_{S_1}	Current per section		2.4	.06	.072	.042
	d	open	i_{S_2}	Current per section		2.1	.30	.05	.044
e	closed	i_{S_2}	Current per section		2.1	.05	.062	.046	
7.15 0.8 Lagging Power Factor	a	open or closed	$i_{A_1 a_2}$	Gen. line current	S	7.15	.022	.174	.116
	a	open or closed	$i_{D_1 d_1}$	Gen. line current	D	6.1	.048	.052	.135
	b	open	i_L	Line current on h.v. side	S	5.86	.05	.024	.028
	b	open	i_{S_1}	Current per section		3.04	.42	.056	.082
	c	closed	i_L	Line current on h.v. side	S	5.8	.05	.016	.026
	c	closed	i_{S_1}	Current per section		3.0	.074	.062	.078
	d	open	i_{S_2}	Current per section		2.86	.38	.08	.056
e	closed	i_{S_2}	Current per section		2.8	.02	.086	.054	
7.16 0.8 Leading Power Factor	a	open or closed	$i_{A_1 a_2}$	Gen. line current	S				
	a	open or closed	$i_{D_1 d_1}$	Gen. line current	D				
	b	open	i_L	Line current on h.v. side	S	5.04		.032	.013
	b	open	i_{S_1}	Current per section		2.5		.062	.032
	c	closed	i_L	Line current on h.v. side	S	5.04		.038	.013
	c	closed	i_{S_1}	Current per section		2.46		.066	.034
	d	open	i_{S_2}	Current per section		2.6		.032	.044
e	closed	i_{S_2}	Current per section		2.6		.03	.046	

TABLE 7.5 Values of harmonic components in voltage and current waveforms of Figs. 7.14, 7.15 and 7.16. High voltage winding sections are connected in parallel. Harmonic voltages and currents are respectively given in V and A.

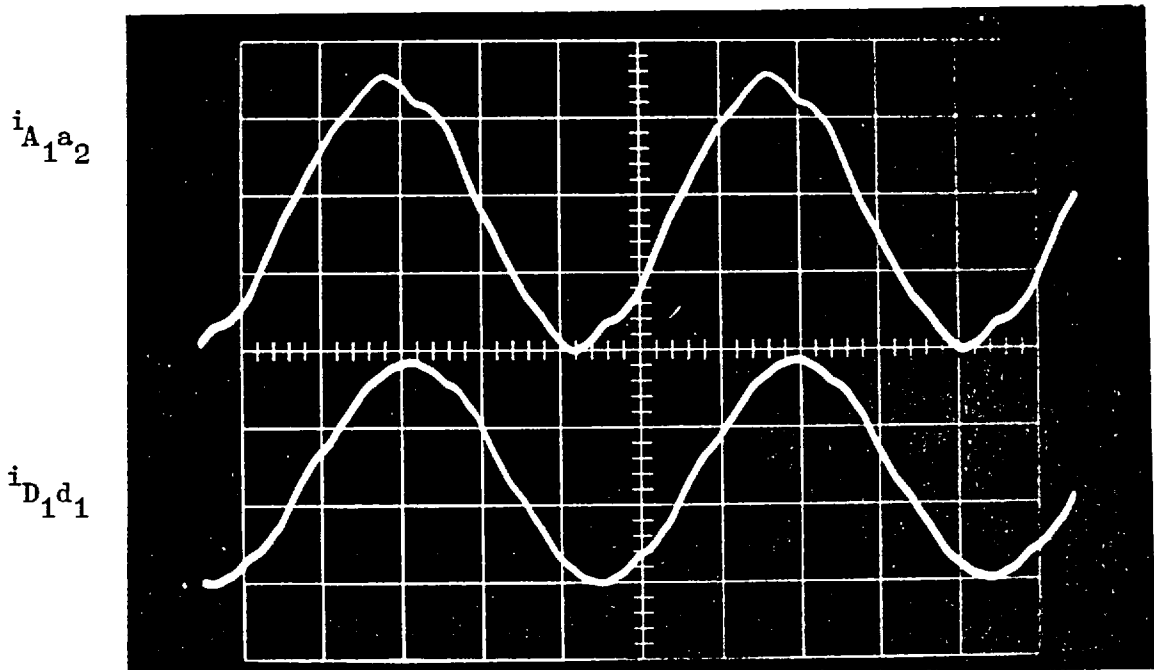


Fig. 7.14(a) Line currents in phase A and D.
Tertiary winding is ineffective.

FIG. 7.14

6-ph generator connected to 3-ph busbars via a 6-ph/3-ph transformer bank and its half loaded at unity power factor. High voltage winding sections connected in parallel.

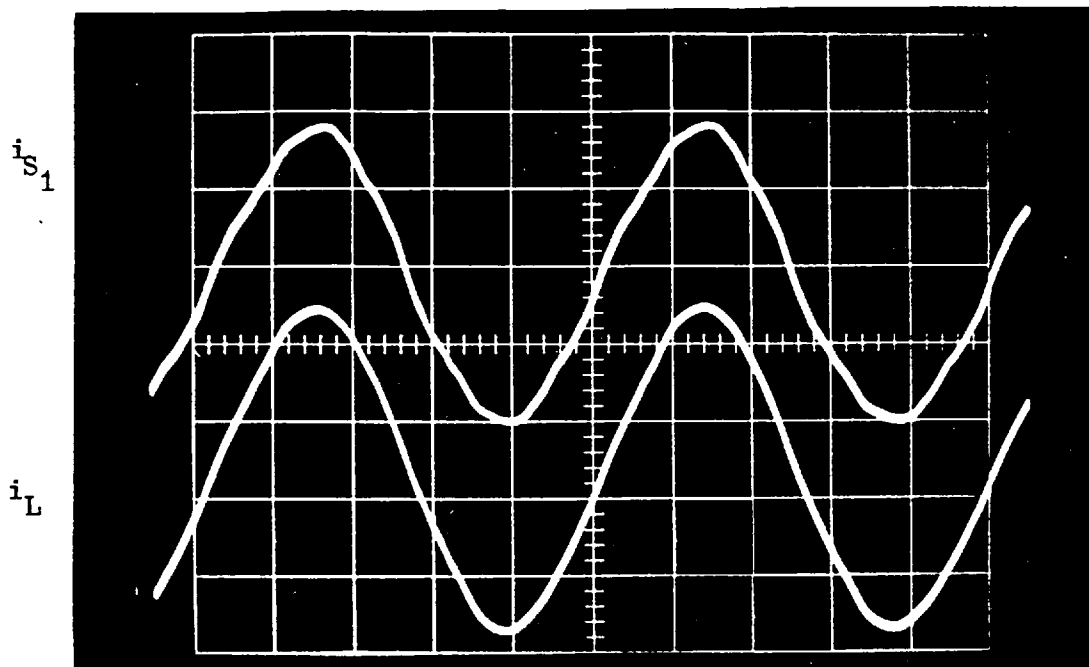


Fig. 7.14(c) The same, but tertiary winding closed.

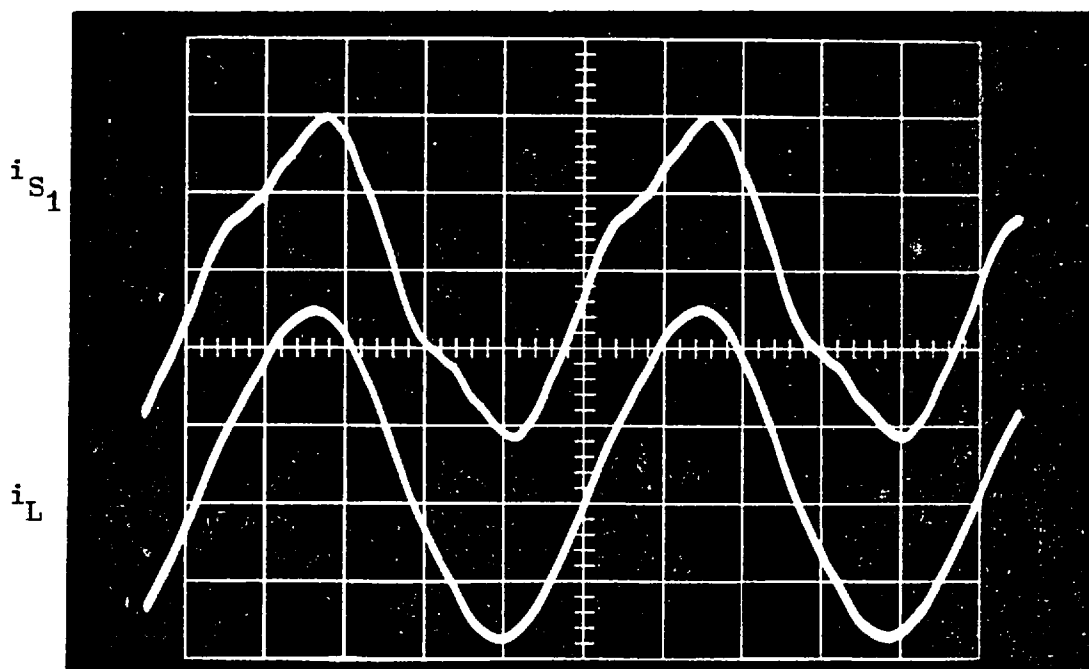


Fig. 7.14(b) Line and section currents in high voltage winding. Tertiary winding open. $i_{S_1} = i_{C_3 C_4}$.

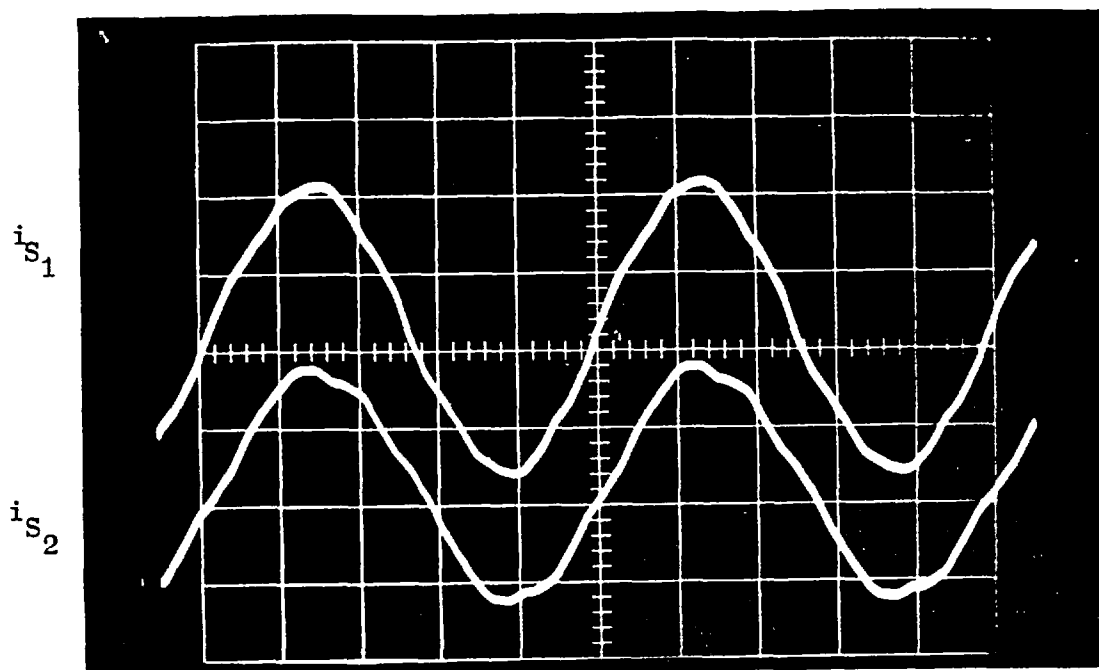


Fig. 7.14(e) The same, but tertiary winding closed.

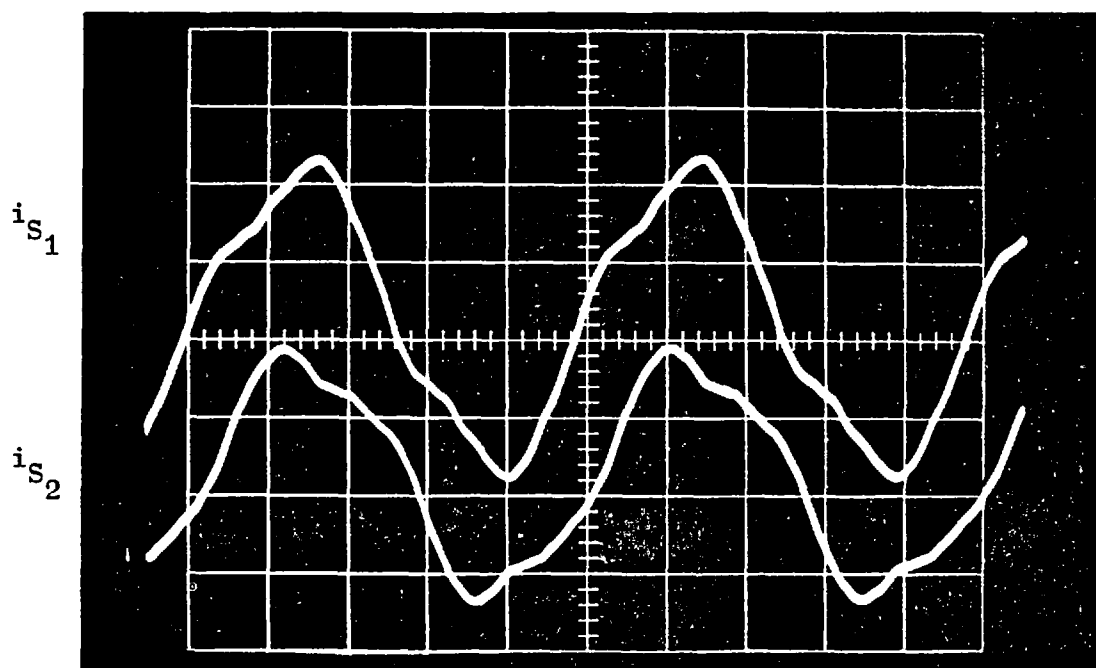


Fig. 7.14(d) Section currents in high voltage winding.
Tertiary winding open. $i_{S1} = i_{C_3 C_4}$, $i_{S2} = i_{C_1 C_2}$.

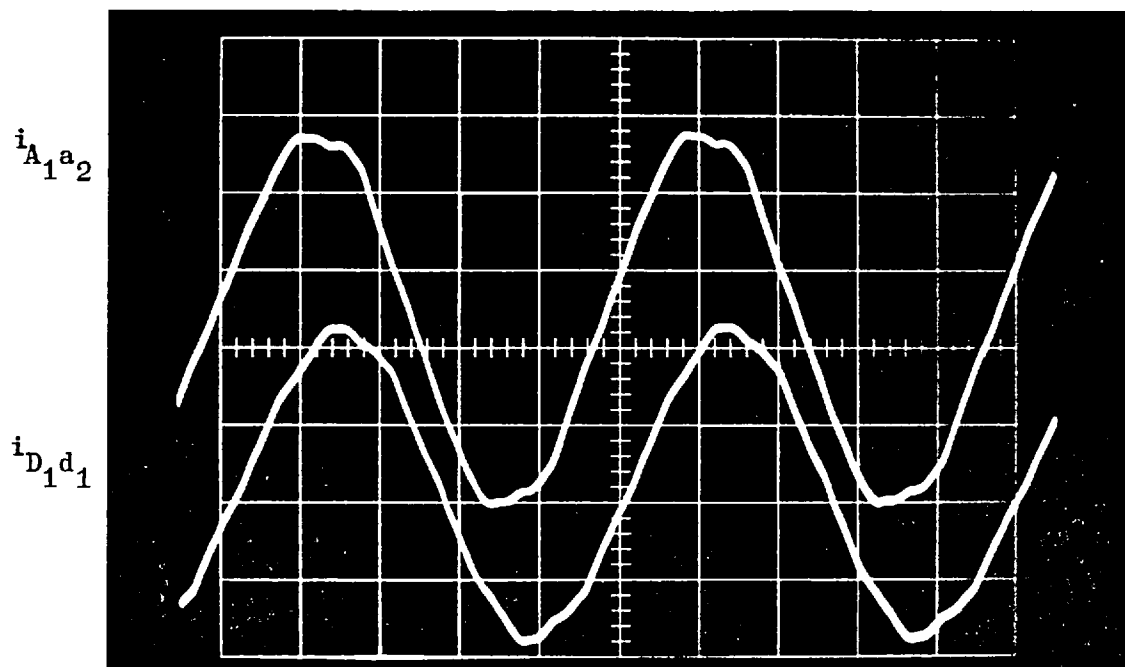


Fig. 7.15(a) Line currents in phase A and D.
Tertiary winding is ineffective.

FIG. 7.15 The same as Fig. 7.14, but at
0.8 Lagging Power Factor.

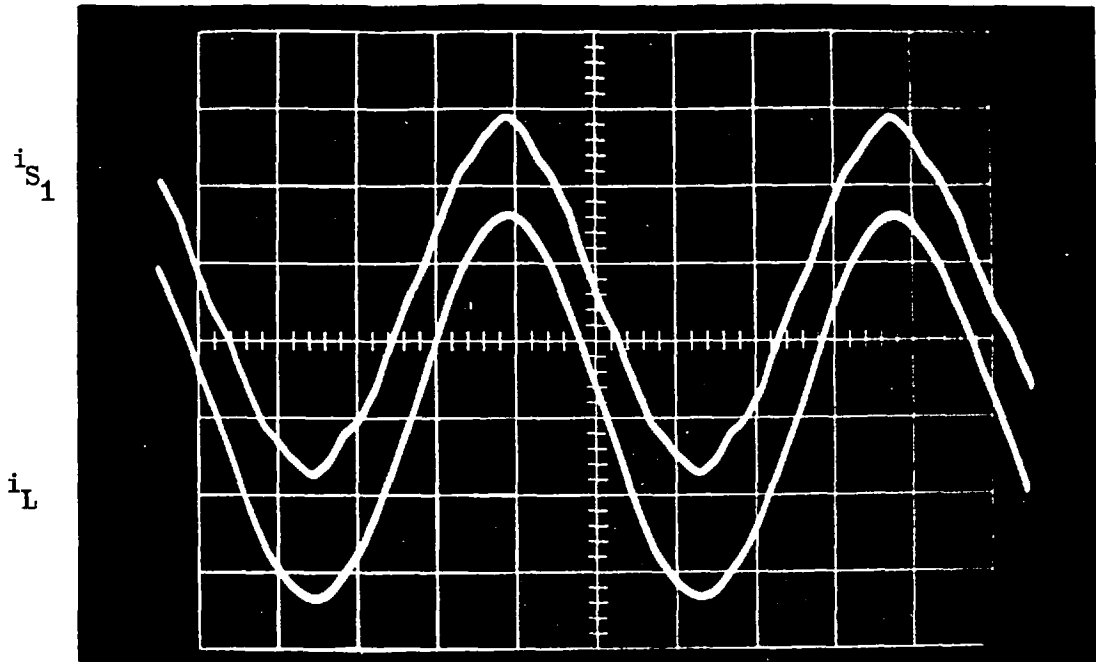


Fig. 7.15(c) The same, but tertiary winding closed.

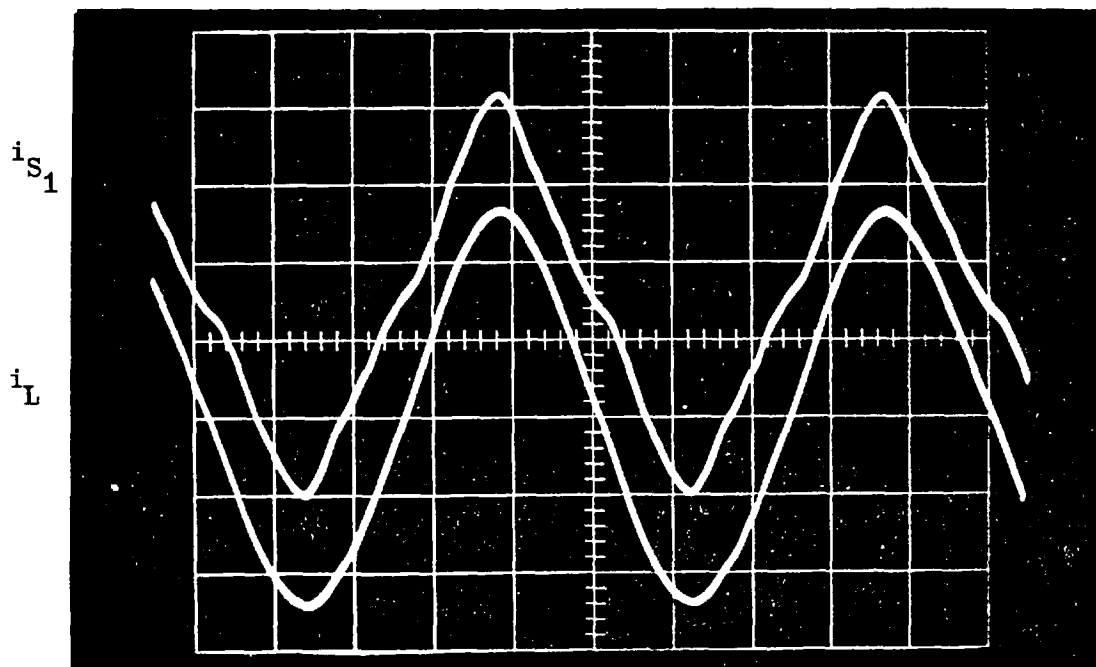


Fig. 7.15(b) Line and section currents in high voltage winding. Tertiary winding open. $i_{S1} = i_{C_3 C_4}$.

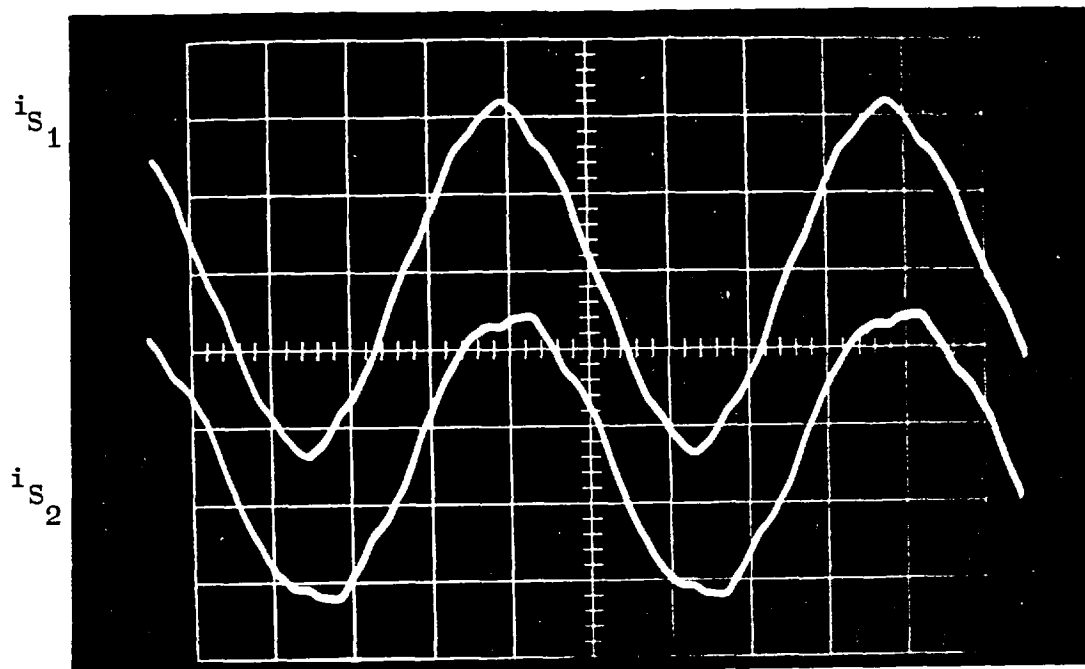


Fig. 7.15(e) The same, but tertiary winding closed.

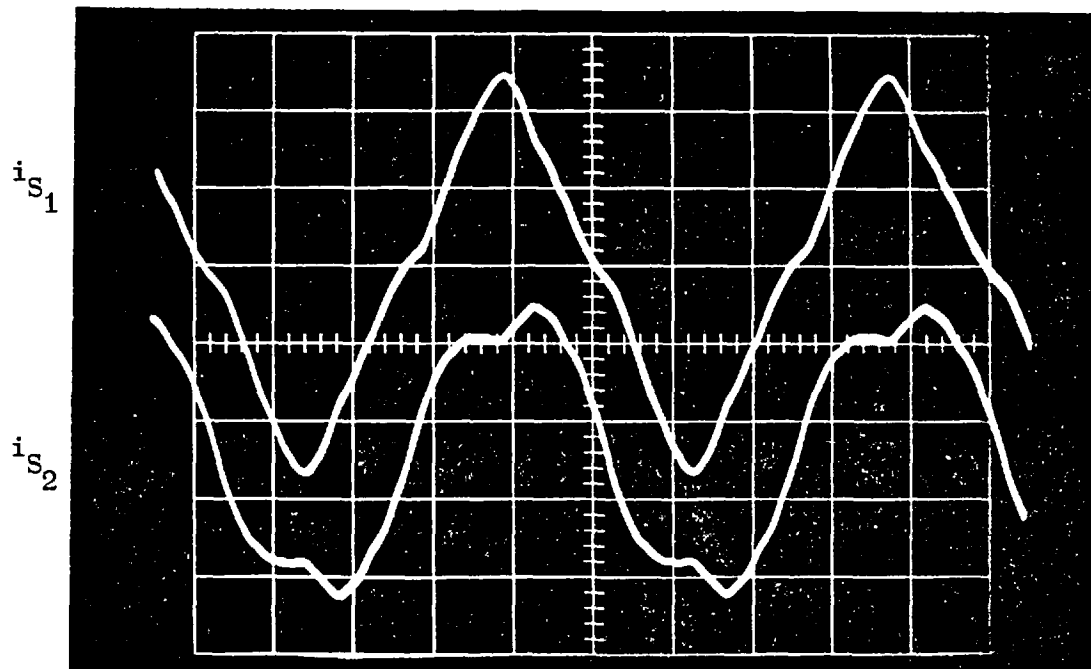


Fig. 7.15(d) Section currents in high voltage winding.
Tertiary winding open. $i_{S1} = i_{C3C4}$, $i_{S2} = i_{C1C2}$.

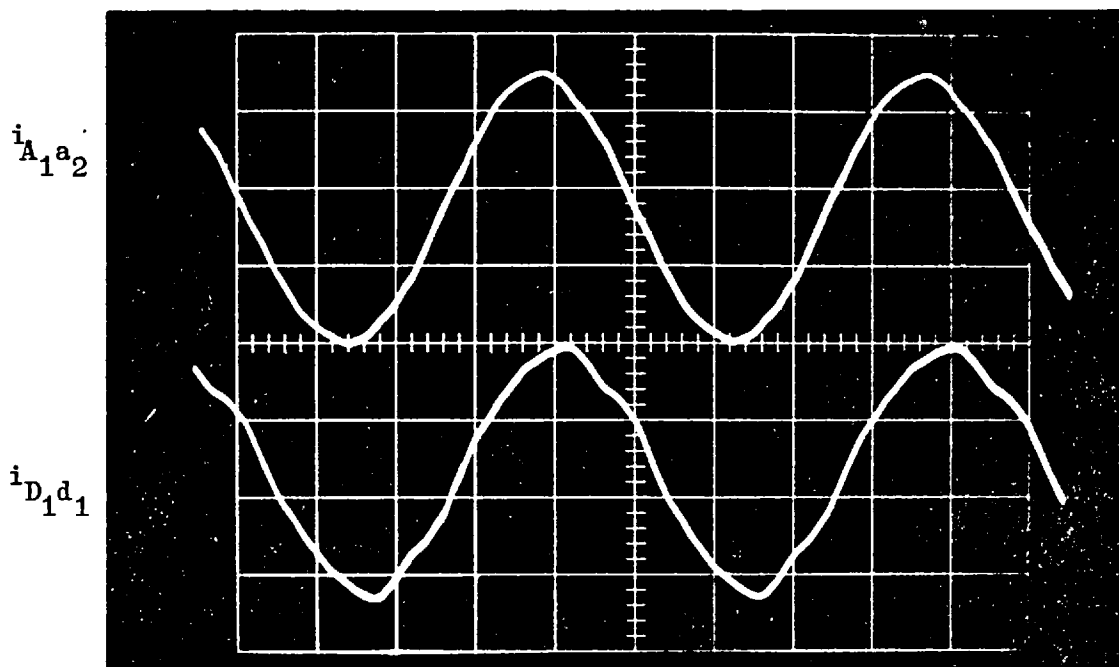


Fig. 7.16(a) Line currents in phase A and D.
Tertiary winding is ineffective.

FIG. 7.16 The same as Fig. 7.14, but at
0.8 Leading Power Factor.

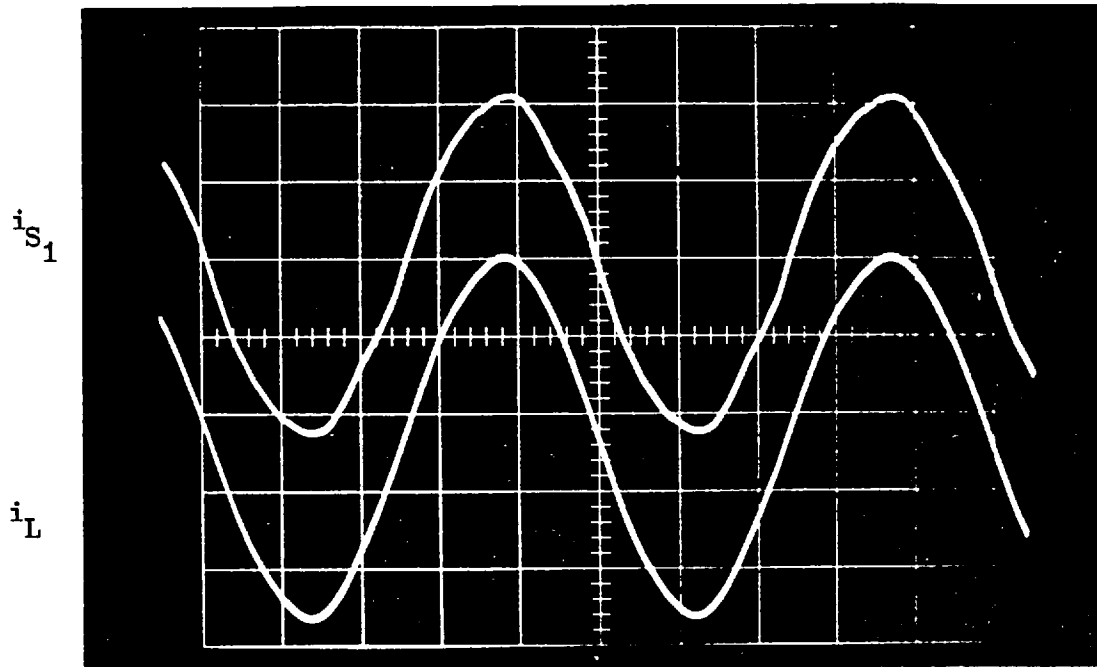


Fig. 7.16(c) The same, but tertiary winding closed.

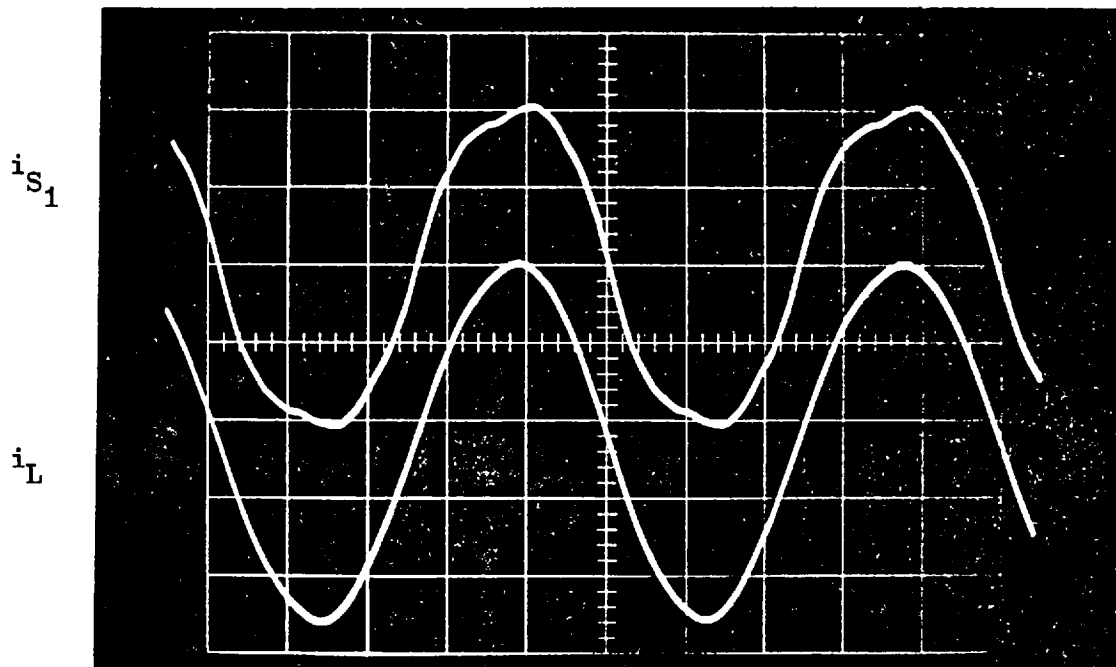


Fig. 7.16(b) Line and section currents in high voltage winding. Tertiary winding open. $i_{S_1} = i_{C_3 C_4}$.

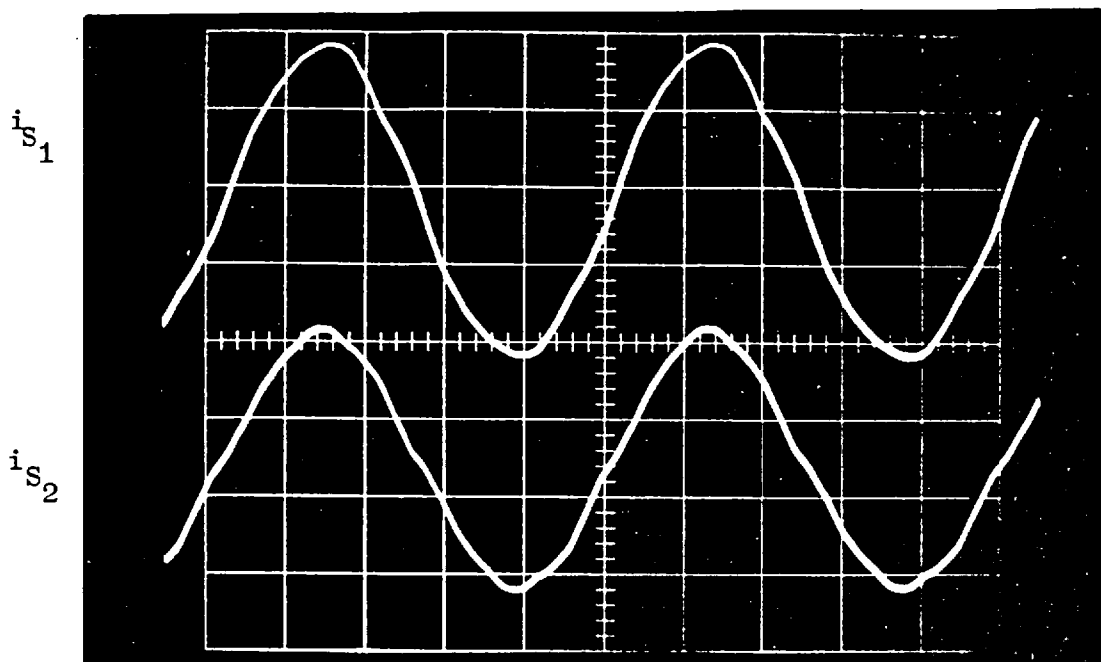


Fig. 7.16(e) The same, but tertiary winding closed.

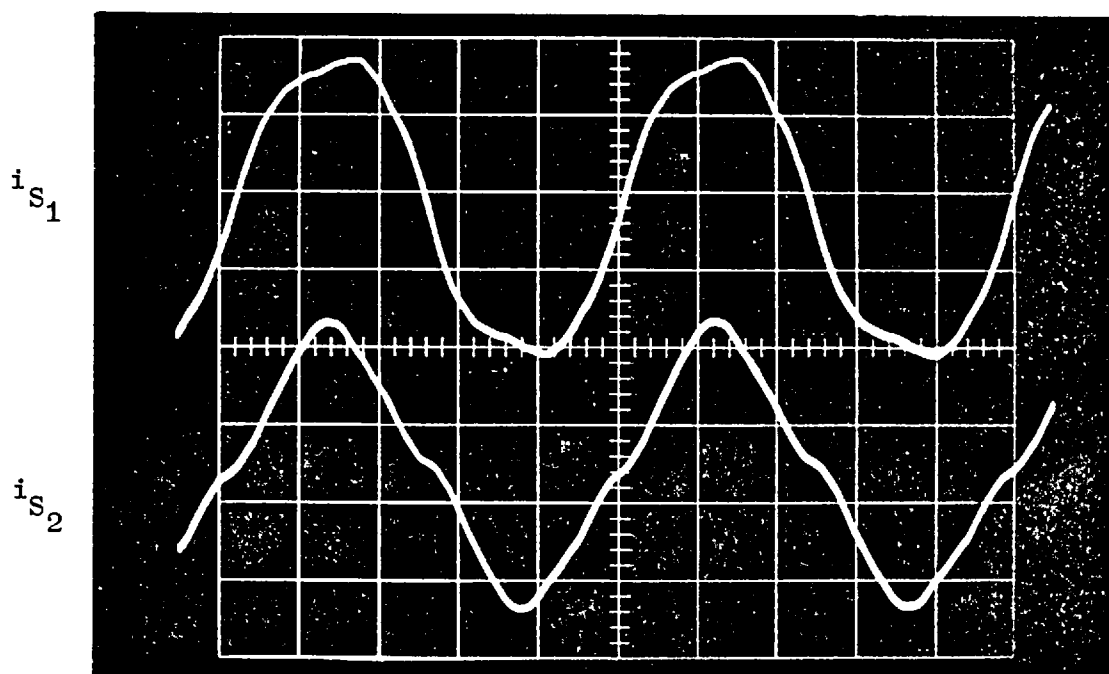


Fig. 7.16(d) Section currents in high voltage winding.
Tertiary winding open. $i_{S1} = i_{C3C4}$, $i_{S2} = i_{C1C2}$.

but these are normally small and damped by the load impedance.

2. The currents flowing in h.v. winding sections are greatly improved by the presence of a tertiary winding. This is because the tertiary winding provides an alternative path with lower impedance for the third harmonic currents which are the dominant component of the circulating current. It can be seen that, for example, when the generator is operating at unity power factor and when the tertiary winding is opened, the percentage of third harmonic current to the fundamental is 14%. This percentage, however, drops to 2.5% when the tertiary winding is closed.
3. The line currents on the l.v. side are less sinusoidal than those on the h.v. side, and the difference is mainly in harmonic components of order $12k \pm 5$. This is because the line current on the l.v. side is the phasor sum of the load and exciting current and both of them contain these harmonics as discussed earlier.

7.7 CONCLUSIONS

The behaviour of harmonics in a 6-ph generator and its associated transformer have been investigated with the transformer both on open circuit and when delivering power to 3-ph busbars. The study was quite general and covered not only the harmonics generated within the transformer due to iron non-linearity but also those supplied by the 6-ph generator.

In considering the excitation phenomena of the transformer with its h.v. winding sections connected in series, it was shown that the presence of a tertiary winding is important in providing a path for the third harmonic current necessary to maintain a nearly sinusoidal variation of voltages in the star connected l.v. winding and its associated h.v. winding. On the other hand, the advantage of including the tertiary winding with the parallel connection of h.v. winding sections is merely to provide an alternative path for the relatively large third harmonic current already circulating in the closed path formed by this connection.

The effect of the transformer winding arrangement and the core construction on the harmonics produced by the 6-ph generator connected to 3-ph busbars were studied. These harmonic voltages were of three types, $n = 12k \pm 1$, $n = 12k \pm 5$ and $n = 6k + 3$, each of which determines its own flux pattern in the transformer core and must therefore be treated separately. The study mainly concentrated on the harmonics of order $12k \pm 5$ because their behaviour was uncommon and of great interest. It was shown that except for the exciting current, the harmonic components of order $12k \pm 5$ were suppressed from the line current waveforms on both sides of the transformer when its h.v. winding sections were connected in series. On the other hand, it was shown that the parallel connection, unfortunately, provides a closed path for these harmonics to circulate, and consequently they are also present on the l.v. side. However, under balanced conditions, these harmonic currents are eliminated from the line current waveform on h.v. side as in the series connection.

It was shown that in so far as the harmonics of order $12k \pm 5$ are concerned, a four-limb construction has no significant advantage over a two-limb one if the h.v. winding sections were connected in parallel. This is because the flux emanating from the inner limbs will be forced into the leakage path and is prevented from flowing in the outer limbs. If, however, they were put in series, then the stray losses are likely to be smaller in a four-limb type.

From the overall studies made in this chapter regarding the comparison between the series and parallel connection of h.v. winding sections from the harmonic point of view, it can be said that the series connection is preferable.

CHAPTER EIGHTCONCLUSIONS8.1 GENERAL COMMENTS

The design and performance of 6-ph machines have been studied with particular regard to steady state behaviour. These investigations covered:

1. The behaviour of a 6-ph machine, as compared to a 3-ph one, when carrying non-sinusoidal current.
2. The design of a 6-ph/3-ph transformer to couple a 6-ph machine to a 3-ph busbar, and to represent the transformer in an electric network by an equivalent circuit.
3. The behaviour of the harmonics in a 6-ph generator and its associated 6-ph/3-ph transformer bank when on open circuit and when delivering power to 3-ph busbars.

Test results showed that, although the steady state short circuit current waveform of the machine connected as 3-ph is sinusoidal, that of the 6-ph machine is highly distorted, the 3rd, 5th and 7th being the principal harmonics. When the 3rd harmonic current was suppressed by isolating the neutral point of each 3-ph group, the current waveform slightly changed, and the magnitude of the 5th and 7th harmonic currents remained the same. An analytical method was developed to explain and predict the behaviour of these harmonic currents in a synchronous machine connected in 6 and 3 phases. The method was based on the conventional synchronous machine equivalent circuit but includes modifications to the conventional

theory necessary to account for time harmonic effects. These modifications involve recalculating the open circuit voltages, leakage and magnetizing reactances with respect to different harmonics. Correlation between individual measured and computed values of harmonic currents was acceptable over a range of excitation. These results gave some assurance of the validity of the method used to calculate the harmonic currents. In view of these studies the main reasons why the 5th and 7th harmonic components are so pronounced in the current waveform of a 6-ph machine, when compared with a 3-ph one, were shown to be:

1. The slot leakage reactance of a 3-ph machine with respect to harmonic current of order $n = 6k \pm 1$ ($k = 0, 1, 2, 3, \dots$) is n times that of the fundamental current ($X_{\text{slot}_n} = nX_{\text{slot}_1}$). Since this reactance normally represents the main component of the leakage reactance, then the higher the order of harmonic the higher is the leakage reactance and this results in lower harmonic currents. In a 6-ph machine, however, this relationship is only correct for harmonic currents of order $n = 12k \pm 1$, and requires some modifications for those of order $n = 12k \pm 5$. This is because the curves relating the slot leakage factor (K_{s_n}) versus the coil pitch with respect to the harmonic currents of order $n = 12k \pm 5$ and those of order $n = 12k \pm 1$ differ in a 6-ph machine, but are the same in a 3-ph one. The laboratory 6-ph machine has a $5/6$ coil pitch at which it was shown that the value of K_{s_n} with respect to harmonic currents of order $n = 12k \pm 5$ is minimum, and so is the slot leakage reactance. Consequently, the corresponding harmonic currents tend to be very large.

2. The open circuit harmonic voltages are larger in a 6-ph winding, as compared to a 3-ph one, because of the poor distribution factors for harmonics. A machine connected in 6 phases may have a distribution factor with respect to harmonics of order $h = 12k \pm 5$, which is nearly four times that for 3-ph connection.

The main conclusions arrived at on the basis of the studies made regarding the behaviour of harmonic currents in a 6-ph machine are:

1. Excessive 5th and 7th harmonic currents tend to flow if it is designed to have a 5/6 coil pitch. The effect of these harmonic currents is to increase the copper loss in the winding and the stray loss in the rotor surface.
2. The 5th and 7th harmonic currents in a 6-ph machine can be appreciably reduced if coil pitch of 11/12 is selected.
3. The existence of triplen harmonic currents (the third and its odd multiples) depends on the way in which the two 3-ph winding sets of a 6-ph machine are connected. The slot leakage factor for triplen harmonic currents is the same in 6-ph and 3-ph machines.

The main methods so far proposed to couple a 6-ph generator to a 3-ph system were surveyed critically. In addition, a new transformer bank which has a star-delta/star winding arrangement was described and the detail of the design work for a "micro" version was given. As a micro-generator is designed to have small per unit copper loss and high reactances to model a large turbo-generator, so

a micro-transformer must also be designed to have per unit parameters similar to those of a large one. Several design attempts were made to simulate a 1200 MW generator transformer having a 0.25% copper loss and 15% leakage reactance. It was shown that it is not economical and may not be possible to design a micro-transformer with these parameters. Therefore, instead, a micro-transformer of 0.6% copper loss and 9% leakage reactance was designed and built. Tests were made to verify the detail of the design work. The measured and calculated values of per unit copper loss and leakage reactance, and the specific total loss agreed reasonably with each other, but there was a large deviation in the magnetizing current. A typical measured value of the magnetizing current required to produce a flux density of 1.7 T in the inner limbs of any transformer was found to be 20% of full rated current, whereas the design value was 5.5%. The main reasons for such a discrepancy were found to be:

1. The method of calculating the magnetizing current from the design curves was not very accurate because the flux density was assumed equal in all parts of the iron core. The flux in this transformer is not confined to a single path but divides according to the reluctances of the magnetic circuit. It tends to be higher in the yoke than in the outer limbs. Therefore, the yokes saturate before the other parts, causing higher magnetizing current to be drawn from the supply.
2. The effect of the joints between the laminations on the calculation of magnetizing current in a micro-transformer is significant as compared with a large one. This is because both transformers operate at the same flux density level but the

micro-transformer has much shorter lamination lengths. In addition, the laminations were supplied unperforated, which made their assembly difficult.

Consequently, to reduce the harmonic effect introduced by the transformer core saturation, it was decided to work at 1.5 T, and not 1.7 T, flux density as originally designed. This also permits the study of the effect of the transformer winding arrangement on the harmonic voltages produced by the 6-ph generator on their own.

An equivalent circuit was built up for a four-limb, four-winding transformer which contains as many branches as may be necessary for determining the transformer performance in the steady state. The main feature of the approach used is that the non-linear elements in the magnetic circuit are represented by equivalent elements in the electric circuit. Moreover, it was shown that any variation in the transformer construction or in the method of excitation of the two input l.v. windings can easily be recognised. Although this method allows the derivation of equivalent circuits of varying accuracy and complexity, it was shown that its magnetizing impedances cannot always be determined in a simple and direct way. This problem was encountered in the case of the four-winding transformer and an approximate solution was obtained. It is felt that the equivalent circuits derived are adequate for qualitative studies.

Having explained the harmonic behaviour in a 6-ph generator and constructed a 6-ph/3-ph transformer, the next step was to study their behaviour when coupled together. First the excitation phenomena of the transformer bank were considered. It was shown that if the h.v. winding sections are connected in series, the presence of

a tertiary winding is important in providing a path for the third harmonic current necessary to maintain a nearly sinusoidal variation of voltages in the star-connected l.v. winding and its corresponding h.v. winding. On the other hand, if they are put in parallel the inclusion of the tertiary winding is only necessary when the third harmonic current circulating between the h.v. winding sections would otherwise be excessive.

The effect of the transformer winding arrangement and the core construction on the harmonics produced by the 6-ph generator connected to 3-ph busbars were studied. In making these studies the harmonics generated within the transformer due to iron non-linearity were ignored. It was shown that the harmonic voltages and currents of order $n = 12k \pm 5$ ($k = 0, 1, 2, 3, \dots$) originating in the generator need special treatment because they behave differently from the fundamental and those of order $n = 12k \pm 1$. Harmonic voltages of order $12k \pm 5$ produce a flux pattern in the transformer which is confined to the outer limbs, and the corresponding harmonic currents are dependent on the connection mode of the h.v. winding sections. If the sections are connected in series, these harmonic currents do not appear in the lines on either side of the transformer. However, parallel connection provides a closed circulating path for them; thus they also appear in the generator-transformer lines, but not in the h.v. output lines. Consequently, the equivalent circuit of the transformer derived with respect to the fundamental frequency cannot be directly used for harmonic current of order $12k \pm 5$ by only multiplying its impedances by the order of the harmonic, but it also requires certain modifications.

A comparison was made which showed that a four-limb transformer construction has no significant advantage over a two-limb one in limiting the circulating harmonic currents of the above-mentioned order. This is because their magnitudes depend on the leakage reactance between the windings and not on the magnetizing impedances. On the other hand, it was argued that the stray losses are likely to be smaller in four-limb transformer with its h.v. winding sections connected in series.

From the studies made regarding the comparison of the series and parallel connection of h.v. winding sections from the harmonic point of view it can be said that the series connection is preferable.

It is important to point out that since when the h.v. winding sections are connected in parallel, the harmonic voltages of order $12k \pm 5$ give rise to harmonic currents flowing in the generator-transformer side, then their magnitude must be considered. If their space harmonic m.m.f.'s are large they are likely to increase the stray losses in the rotor surface. The most usual and effective way to minimise these harmonic voltages is to choose a coil pitch of $5/6$. However, the work carried out in this thesis concerning the harmonic behaviour in 6-ph generator alone showed that it is better to use a coil pitch of $11/12$. In comparing these two coil pitches it is still considered better to select a coil pitch of $11/12$ for the following main reasons:

1. Although, on the one hand, the harmonic voltages are minimised when a coil pitch of $5/6$ is selected, on the other hand it was shown that the leakage reactance to these harmonics

is also minimal at this coil pitch. Therefore, if the transformer leakage reactance to these harmonics is insufficient large harmonic currents would result from small generator harmonic voltages. Use of 11/12 will increase the machine reactance and help to limit the magnitude of the harmonic circulating current.

2. Since the strongest space harmonic components, the 5th and 7th, are suppressed from the armature m.m.f. waveform produced by a sinusoidal armature current a coil pitch of 11/12 can be used. Therefore, for the same machine size, the output power is increased by 6%.

On the basis of the work done in this thesis the following recommendations may be made for the designers of the 6-ph machine and its associated transformer:

This work shows that the 6-ph generator is a practical proposition from the point of view of harmonic circulating currents. The only harmonic voltages liable to produce circulating currents are of order $n = 5, 7, \dots, 12k \pm 5$, and they occur when the transformer h.v. winding sections are connected in parallel. Nevertheless, these harmonic currents in a 6-ph winding, as compared with a 3-ph one, produce no fundamental space harmonic (see Table 2.1). Therefore, the most serious effect for the 5th and 7th harmonic currents in a 6-ph winding will arise from the space harmonics travelling with respect to the stator at $-7/5$ and $-5/7$ times synchronous speed and having 7 and 5 times the fundamental pole number respectively. The voltages that both these space harmonics induce in the rotor circuit are of 12 times fundamental frequency.

The magnitude of the harmonic circulating current (n) depends directly on the internal voltage (h) which is produced by rotor space harmonic (v) where $n = h = v$. It is also inversely dependent on the sum of the machine leakage reactance X_{l_n} and the transformer leakage reactance $X_{l_t_n}$ and the machine magnetizing reactance X_{m_n} for harmonic current (n). Thus

$$I_n = \frac{E_h}{j(X_{l_n} + X_{l_t_n} + X_{m_n})} \quad n = h$$

For the model 6-ph machine connected to a 3-ph system the harmonic currents are not large and it seems likely that they would not be important in a large 6-ph machine. However, in designing it their magnitude should be calculated, and this thesis has shown how this may be done. If they were shown to be excessive, a change of coil pitch to 11/12 from 5/6 might make them acceptable.

The transformer arrangement used appears to be suitable but three two-limb transformers would be equally acceptable. This, however, might have slightly higher stray losses. Tertiary windings should be used if the h.v. winding sections are connected in series otherwise fluxes in the transformer core become unbalanced.

If a short circuit test is performed to simulate the heat produced under load, the two sets of three phases must not be short-circuited by a common tie because this will provide a path for third harmonic current to circulate.

8.2 FUTURE WORK

The work presented in this thesis was concentrated on the design and performance of 6-ph machines operating in the steady state region. The next step is to investigate the unbalanced and transient operating conditions. A recent American paper³⁴ has developed a method to transform the 6-ph variables, abcdef, into equivalent d-q-0 representation, $d_1q_1^0$ and $d_2q_2^0$. It is thought that the material in this thesis, together with that in the paper, could provide a useful start to continue with fault studies. The theoretical analysis then developed could be verified by experimental results obtained from the 6-ph micro-machine coupled to 3-ph busbars via a 6-ph/3-ph transformer. First, however, the transient reactances must be determined.

It was shown that the joints in the micro-transformer have significant effects on the magnetic circuit calculation. To reduce this problem in future micro-transformers, it may well be better to assemble it in a manner similar to an "Epstein square" specimen using the fully lapped, instead of overlapped, joints. The advantages of this are twofold:

1. The core thickness at the joints is double the other sections and thus their effects would be reduced appreciably.
2. The per unit leakage reactance between a pair of windings would be higher because the core area is reduced by a factor of one-half.

The gap between the laminations should be filled in by press board having the same thickness as the laminations and hence maintaining strong core structure in all parts of the transformer.

1. Holley, C.H. and Willyoung, D.M.: "Stator winding systems with reduced vibratory forces for large turbine-generators", IEEE Trans. on Power App. and System. Vol. PAS-89, pp. 1922-1934 (1970).
2. Hawley, R. and Thomas, D.L.: "Definition, investigation and resolution of design limitations for large turbo-type generators", CIGRE, Paper 11-01 (1974).
3. Alger, P.L., Freiburghouse, E.H. and Chase, D.D.: "Double windings for turbine alternators", Trans. AIEE, pp. 226-244 (January 1930).
4. McElligot, J.E.: "Six-phase two-circuit generator", U.S. Patent 2 731 576 (1956).
5. Willyoung, D.M.: "Multiple-circuit winding patterns for poly-phase dynamo-electric machines", U.S. Patent 3 408 517 (1968).
6. "USSR to build 1200 MW generator", Electrical Review, pp. 195 (11 August 1972).
7. Robert, R., Dispaux, J. and Dacier, J.: "Improvement of turbo-alternator efficiency", CIGRE Meeting, 8-18 June (1966).
8. Chutorezkij, G.M. and Woronov, G.G.: "Six-phase windings for turbo-generators", Elektrotechnika, Moskow 39, pp. 1-6, 6b (1968).
9. Harley, R.G. and Adkins, B.: "Stability of synchronous machine with divided-winding rotor", Proc. IEE, Vol. 117, pp. 933-947 (1970).
10. Langsdorf, A.S.: "Theory of alternating current machinery", 2nd Edition, (McGraw-Hill, 1955).
11. Say, M.G.: "Alternating current machines", 4th Edition (Pitman, 1976).
12. Bewley, L.V.: "Alternating current machinery", (McGraw-Hill, 1949).
13. Alger, P.L.: "Induction Machines", 2nd Edition (Gordon & Breach, 1970).
14. Liwschitz, M.: "Alternating current machines", 2nd Edition (Van Nostrand, 1961).
15. Liwschitz, M.: "Differential leakage with respect to the fundamental wave and to the harmonics", AIEE Trans., Vol. 63, pp. 1139-1150 (1944).

16. Klingshirn, E.A. and Jordan, H.E.: "Polyphase induction motor performance and losses on non-sinudoidal voltage sources", IEEE Trans., PAS-87, (3), pp. 624-631 (1968).
17. Chalmers, B.J. and Sarkar, B.R.: "Induction motor losses due to non-sinusoidal supply waveforms", Proc. IEE, Vol. 115, No. 12, pp. 1777-1782 (Dec. 1968).
18. Richardson, P. and Young, N.: "Improvements in and relating to multi-phase alternating current apparatus", British Patent 1 104 844 (1968).
19. Hartill, E.R.: "Improvements in and relating to electrical generator and transformer arrangements", British Patent 1 107 704 (1968).
20. Allen, P.G.H. and Macdonald, D.C.: "Generator transformers for divided stator alternators", to be published in Electrical Times.
21. E.E. Staff of M.I.T.: "Magnetic circuits and transformers", 15th Printing (The M.I.T. Press, 1965).
22. Langley London Limited, Lantex Tubes (Catalogue, Sept. 1973).
23. British Steel Corporation, Unisil/Alphasil, Grain Oriented Electric Steel (Catalogue).
24. Carpenter, C.J.: "A network approach to the numerical solution of eddy-current problems", IEEE Trans. on Magnetic, Vol. MAG-11, No. 5, pp. 1517-1522 (Sep. 1975).
25. Slemon, C.R.: "Magnetolectric devices", (Wiley, 1966).
26. Carpenter, C.J.: "Magnetic equivalent circuit", Proc. IEE, Vol. 115, No. 10, pp. 1503-1511 (1968).
27. Cherry, E.C.: "The duality between interlinked electric and magnetic circuits and the formation of transformer equivalent circuits", Proc. of the Physical Society B, 62, p. 101-111 (1949).
28. Skilling, H.H.: "Electric Network", (Wiley, 1974).
29. Stigant, S.A. and Franklin, A.C.: "J and P transformer book", (Newnes-Butterworths, 1973, 10th Edition).

30. Blume. L.F.: "Transformer engineering", (Wiley, 1938).
31. Langlois-Berthelot, R.: "Transformer and generator for power system", (Macdonald, 1960).
32. Saklatvala, R.: "High voltage power transformers for 735 kV", Student Quarterly Journal, IEE, Vol. 36, No. 141, pp. 42-46 (Sept. 1965).
33. Kerchner, R.M. and Corcoran, G.F.: "Alternating current circuits", (Wiley, 1965).
34. Fuchs, E.F. and Rosenberg, L.T.: "Analysis of an alternator with two displaced stator windings", IEEE Trans. on Power Apparatus and Systems, PAS-93, pp. 1776-1786 (1974).

APPENDIX ACALCULATION OF THE EFFECTIVE AIRGAP LENGTH AND THE SALIENCY EFFECTS ON THE M.M.F. WAVEFORM

(a) The effective airgap length G is equal to the actual airgap g (namely the clearance between stator and rotor) multiplied by a factor dependent on the Carter's coefficient K_o which takes into account the effect of slots or other openings in the stator or rotor surfaces bounding the gap.

Let W_o = slot opening, τ_s = slot pitch, and subscripts 1 and 2 indicate stator and rotor quantities, respectively. The effective "contracted" width of stator slot pitch is¹¹

$$\tau'_{s1} = \tau_{s1} - K'_{o1} W_{o1}$$

where, K'_{o1} : a function of the ratio W_o/g .

Likewise

$$\tau'_{s2} = \tau_{s2} - K'_{o2} W_{o2} \quad (A.1)$$

The ratio of the reluctances of slotted armature to smooth core can be expressed as

$$K_{g1} = \frac{\tau_{s1}}{\tau'_{s1} - K'_{o1} W_{o1}} \quad (A.2)$$

Similarly,

$$K_{g2} = \frac{\tau_{s2}}{\tau'_{s2} - K'_{o2} W_{o2}} \quad (A.3)$$

A curve relating K_o and W_o/g for semi-closed slots is given in ref. 11, from which at $W_{o1}/g = 1.53/.7 = 2.185$, $K_{o1} = .39$, and at $W_{o2}/g = 2.54/.7 = 3.63$, $K_{o2} = .53$.

On substituting these values in equations (A.2) and (A.3), and for τ_{s1} and τ_{s2} from Fig. A.1,

$$K_{g_1} = \frac{13.33}{13.33 - .39 \times 1.53} = 1.047$$

and,

$$K_{g_2} = \frac{22.2}{22.2 - .53 \times 2.54} = 1.065$$

On the d-axis of the machine tested, only one side of the gap surface is slotted, hence

$$G_d = K_{g_1} \times g = 1.047 \times .7 = .733 \text{ mm}$$

and on the q-axis both sides are slotted, then

$$G_q = K_{g_1} \times K_{g_2} \times g = 1.047 \times 1.065 \times .7 = .78 \text{ mm}$$

(b) Saliency effects on the flux density waveform:

Having found the effective airgap length on both axes, the machine may be regarded as if it has two uniform airgaps, as shown in Fig. A.2. The flux density distribution will, therefore, not be similar to the m.m.f. waveform. In this analysis, only the fundamental component of m.m.f. is considered, from which the flux density waveform is obtained as given in Fig. A.3. For simplicity, it is assumed that the amplitude of the flux density under the pole is unity, and hence may be described as follows:

$$\begin{aligned} B(\theta) &= \frac{1}{K_{g_2}} \sin \theta & 0 \leq \theta \leq \alpha \\ &= \sin \theta & \alpha \leq \theta \leq \pi - \alpha \\ &= \frac{1}{K_{g_2}} \sin \theta & \pi - \alpha \leq \theta \leq \pi \end{aligned}$$

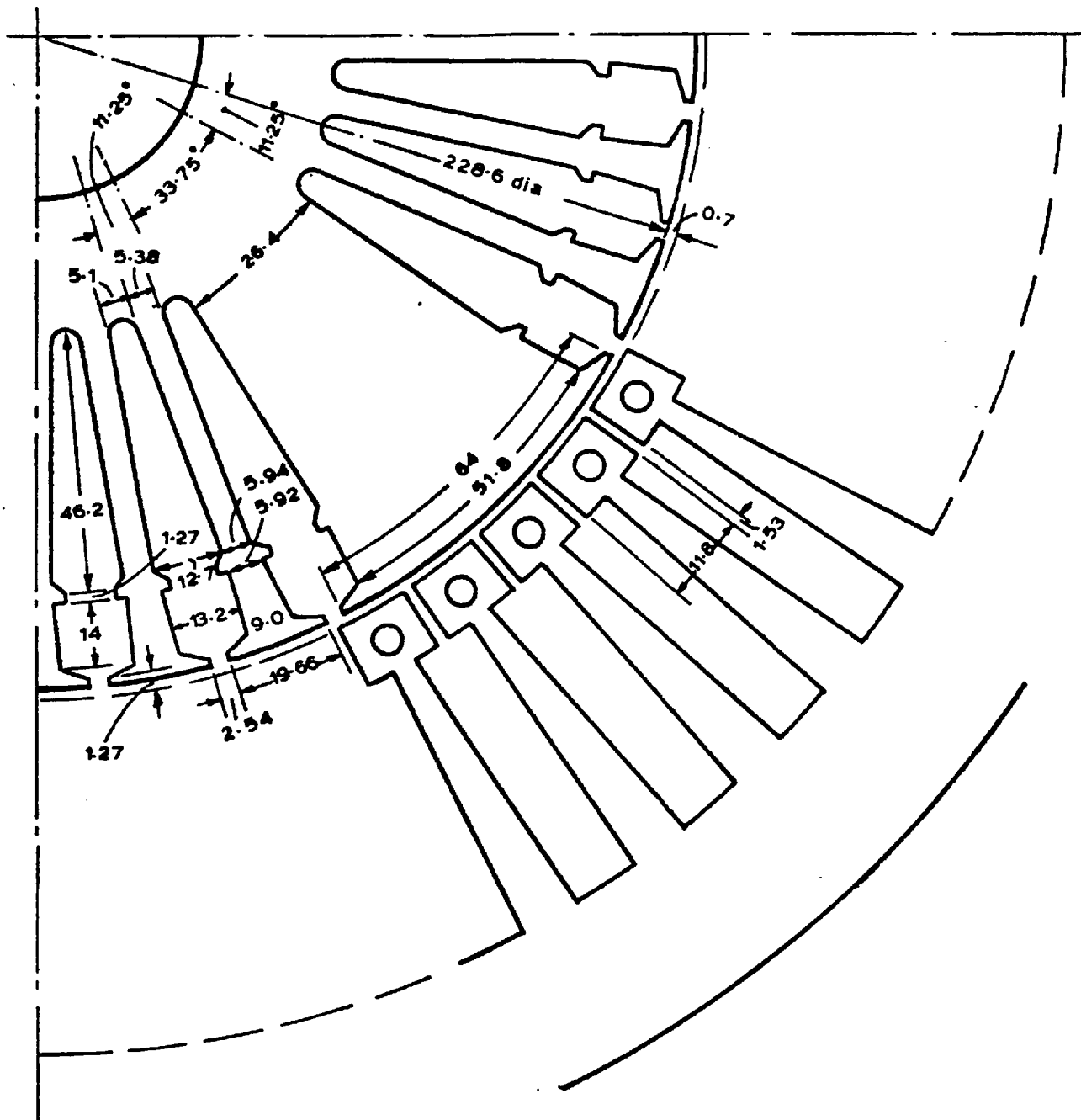


Fig. A1 *Constructional details in a 2-dimensional cross-sectional area of the laboratory micro-generator. Dimensions in mm.*

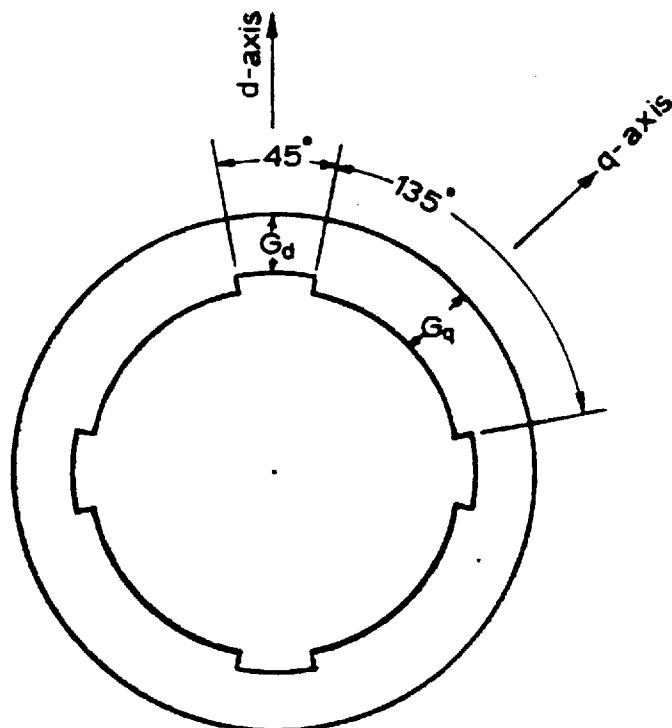
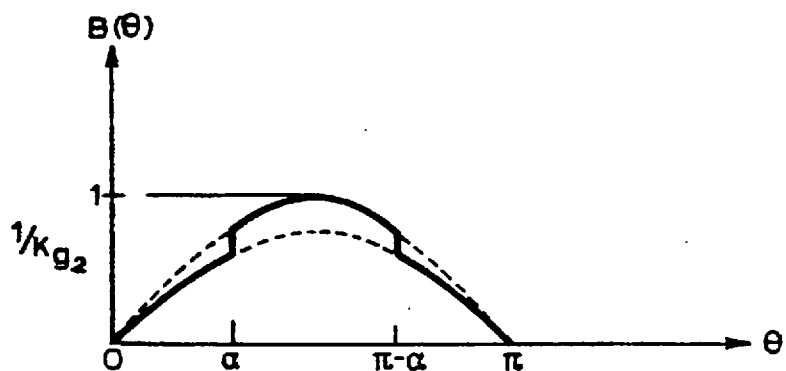
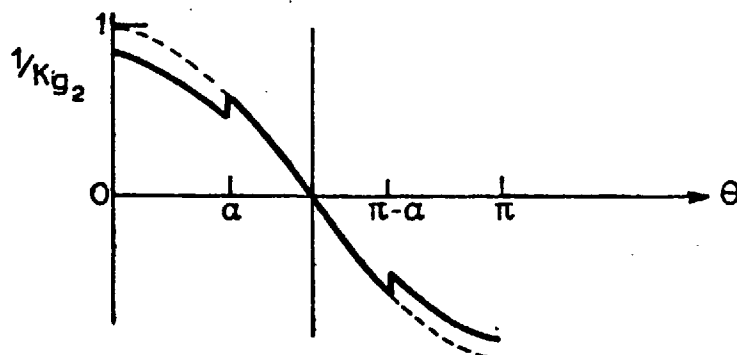


Fig.A2 Representation of cylindrical rotor



(a) m.m.f. along D-axis : maximum flux and inductance



(b) m.m.f. along Q-axis : minimum flux and inductance

Fig.A3 Flux density patterns produced by distributed winding.

The Fourier analysis of the waveform yields no cosine terms because of symmetry, and moreover it is enough to integrate over the period from $0 \rightarrow \pi/2$ to evaluate the coefficients of sine terms. Consider only the fundamental component, then

$$C_{d_1} = \frac{4}{\pi} \int_0^{\pi/2} B(\theta) \sin(\theta) d\theta$$

On substituting for $B(\theta)$, and performing the integration, the expression for C_{d_1} becomes

$$C_{d_1} = 1 - \left(\frac{2\alpha - \sin 2\alpha}{\pi} \right) \left(\frac{K_{g_2} - 1}{K_{g_2}} \right) \quad (\text{A.4})$$

When the m.m.f. axis is along the q-axis as shown in Fig. A.3(b), the coefficient of the fundamental component of the flux density may be found as above, and is equal to

$$C_{q_1} = 1 - \left(\frac{2\alpha + \sin 2\alpha}{\pi} \right) \left(\frac{K_{g_2} - 1}{K_{g_2}} \right) \quad (\text{A.5})$$

The rotor of the laboratory micro-machine has 8 slots and the pole face covers two slots; the value of α can therefore be given as

$$\alpha = \frac{1}{2} \left(180 \times \frac{6}{8} \right) = 67.5^\circ \text{ elec.}$$

Inserting the values of α and K_{g_2} into equations (A.4) and (A.5), thus

$$C_{d_1} = 0.97$$

and
$$C_{q_1} = 0.94$$

Every harmonic component of m.m.f. will have its own C_d and C_q , and may be derived in a similar manner to the method described above.

However, it can be seen that the ratio G_q/G_d is close to unity

because the machine has cylindrical rotor. Therefore it can be

assumed that the airgap is uniform, i.e. $C_{d_h} = C_{d_q} = 1$ and hence the flux density waveform is similar to the m.m.f. waveform.

APPENDIX BLISTING OF ALTERNATIVE MICRO-TRANSFORMER DESIGNSDESIGN NO. 1

The following specifications were first suggested to initiate the design:

1. A core with square cross-sectional area of $30 \times 30 \text{ mm}^2$.
2. A rectangular conductor of dimensions $1.25 \text{ mm} \times 10 \text{ mm}$.

Listing of the Design:

Voltage per turn = 0.326,

$N_1 = 184$, $N_2 = N_4 = 368$, $N_3 = 319$,

$a_1 = 12.29 \text{ mm}^2$, with dimensions of $1.25 \text{ mm} \times 10 \text{ mm}$,

$a_2 = a_4 = 6.035 \text{ mm}^2$ with dimensions of $1.25 \text{ mm} \times 5 \text{ mm}$,

$a_3 = 6.785 \text{ mm}^2$ with dimensions of $1.25 \text{ mm} \times 5.6 \text{ mm}$,

$J_1 = 0.68 \text{ A/mm}^2$, $J_2 = J_4 = 0.69 \text{ A/mm}^2$ and $J_3 = 0.71 \text{ A/mm}^2$.

The number of layers for each winding was chosen to be = 8, height of window = 260 mm, $r_{1i} = 30.2 \text{ mm}$, $r_{10} = 43.66 \text{ mm}$, $t_1 = 13.5 \text{ mm}$, $r_{2i} = x + 43.66 \text{ mm}$, $r_{20} = x + 57.16 \text{ mm}$, $t_2 = 13.5 \text{ mm}$. The spacing needed between any low voltage and its corresponding high voltage winding in order to have a leakage reactance of 11% is = 32.3 mm. $R_1 = 0.06 \Omega$, $R_2 = R_4 = 0.57 \Omega$ and $R_3 = 0.188 \Omega$. The percentage copper loss is therefore = 2.85%. It can be seen that the copper loss is too high and unacceptable as compared with the desired value of .25%. Hence the design was repeated for larger conductor size.

DESIGN NO. 2

The core size was kept as above, and hence the number of turns remained unchanged. The conductor sizes selected for all windings are the same as those given in Section 5.5.

The height of the window = 400 mm, $r_{1i} = 33.3$ mm, $r_{10} = 62$ mm, $t_1 = 28.7$ mm, $r_{2i} = x + 62$ mm, $r_{20} = x + 90.74$ mm. The spacing required to obtain 11% leakage reactance is 30 mm.

$R_1 = 0.0191 \Omega$, $R_2 = R_4 = 0.172 \Omega$, $R_3 = 0.059 \Omega$, the percentage copper loss = 0.871%. For this design the copper loss has considerably reduced but is still higher than the desired value. Moreover, the ratio of window height to the limb width is $400/30 = 13.3$, which means a very narrow and long limb.

APPENDIX CSHORT CIRCUIT AND OPEN CIRCUIT TEST
RESULTS FOR THE MICRO-TRANSFORMERC.1 TURNS RATIO

Design	Measured
$N_2/N_3 = 1.15$	1.14
$N_2/N_1 = 2$	1.97
$N_3/N_1 = \sqrt{3}$	1.73
$N_1/N_{ter} = 4$	4
$N_3/N_{ter} = 6.9$	6.80

C.2 D.C. RESISTANCE AND LEAKAGE REACTANCE

Design	Measured
$R_1 = .0122 \Omega$	$.013 \Omega$
$R_2 = R_4 = .117 \Omega$	$.118 \Omega$
$R_3 = .038 \Omega$	$.04 \Omega$

Design leakage reactance = 9.25%

Measured leakage reactance = 8.33%

C.3 OPEN CIRCUIT TEST

A low power factor wattmeter was used to measure the core loss which had compensation for the power loss in the voltage coil. Thus, the net core loss is equal to the wattmeter reading after allowing for the copper loss. Since the induced voltages in the search coils were non-sinusoidal, a mean value voltmeter calibrated to r.m.s. was used. The detailed explanation of the distorted induced voltage waveforms is discussed in Subsection 7.2.1.4. The experimental results are given in Table C.3(a)

TABLE C.3(a)

Test results for micro-transformer B

$V_{B_2B_4}$	I_m	V_{s_1}	V_{s_2}	$V_{b_1b_2}$	$V_{e_1e_2}$	W
270	1.56	32	34.8	66.5	118	29.1
260	1.29	30.2	33	64	114	26.2
250	1.07	29	32	62	110	23.8
240	0.86	28	30	59.5	105	21.5
230	.7	26.5	29	57	101	19.5
220	0.58	25	27.8	54.6	96.5	17.5
210	0.46	24	26.5	52	92	15.9
200	.369	23	25	49.5	87	14.1
180	.225	21	23	44.3	77.8	11.5
160	.129	18	20	39.2	68.3	9.2
140	.1	14	15.5	33.7	56.1	7.0
120	.077	10	10.8	28.5	45	5.25
100	.062	7	7.5	23.5	36.3	3.65

From Table C.3(a) the peak flux density in each limb was computed using equation (5.3). These values together with specific apparent power (VA/Kg) and specific total loss (W/Kg) are given in Table C.3(b).

TABLE C.3(b)

Calculated results for micro-transformer B

$V_{B_2 B_4}$	B_{s_1}	B_{s_2}	$B_{b_1 b_2}$	$B_{e_1 e_2}$	VI/Kg	W_i /Kg
270	1.8	1.96	1.875	1.92	25.1	1.7
260	1.71	1.86	1.81	1.856	20	1.536
250	1.64	1.8	1.75	1.79	15.93	1.4
240	1.58	1.69	1.68	1.71	12.3	1.268
230	1.49	1.64	1.61	1.64	9.59	1.154
220	1.41	1.57	1.54	1.57	7.6	1.04
210	1.35	1.49	1.47	1.5	5.75	0.944
200	1.3	1.41	1.4	1.42	4.39	0.837
180	1.18	1.3	1.25	1.26	2.4	0.684
160	1.02	1.13	1.11	1.11	1.23	0.548
140	0.79	.874	0.95	.914	.834	.42
120	.564	.609	.804	.733	0.55	0.313
100	.395	.423	.663	.590	0.37	0.217

APPENDIX DDETERMINATION OF THE IRON RELUCTANCES
OF THE MICRO-TRANSFORMER

The open circuit test described in Appendix C.3 was repeated, a wave analyser being used to measure the fundamental components of the induced voltages and the magnetizing current. The test results of a typical micro-transformer were:

$$I_m = 0.46 \text{ A} \quad , \quad V_{s_1} = 22.5 \text{ V} \quad , \quad V_{s_2} = 23.5 \text{ V}$$

$$V_{a_1 a_2} = 53.2 \text{ V} \quad \text{and} \quad V_{d_1 d_2} = 92.5 \text{ V}.$$

From these test results the reluctance of the iron paths can be calculated in the following steps:

1. The flux density in each limb was calculated by using equation (5.3).
2. The flux density as a function of time was drawn for each limb and projected on the B-H curve (see Fig. D.1) supplied by the steel manufacturer²³ to find H as a function of time. The fundamental component of H was extracted from the waveform³³. The iron permeability μ_i was obtained from the ratio of flux density and magnetic field strength.
3. Knowing the geometry of the micro-transformer (see Fig. 5.7), the reluctance of each iron element was then found using the formula

$$R_i = \frac{l_i}{\mu_i A_i}$$

where,

l_i : mean length of the flux path in each section

A_i : net cross-sectional area.

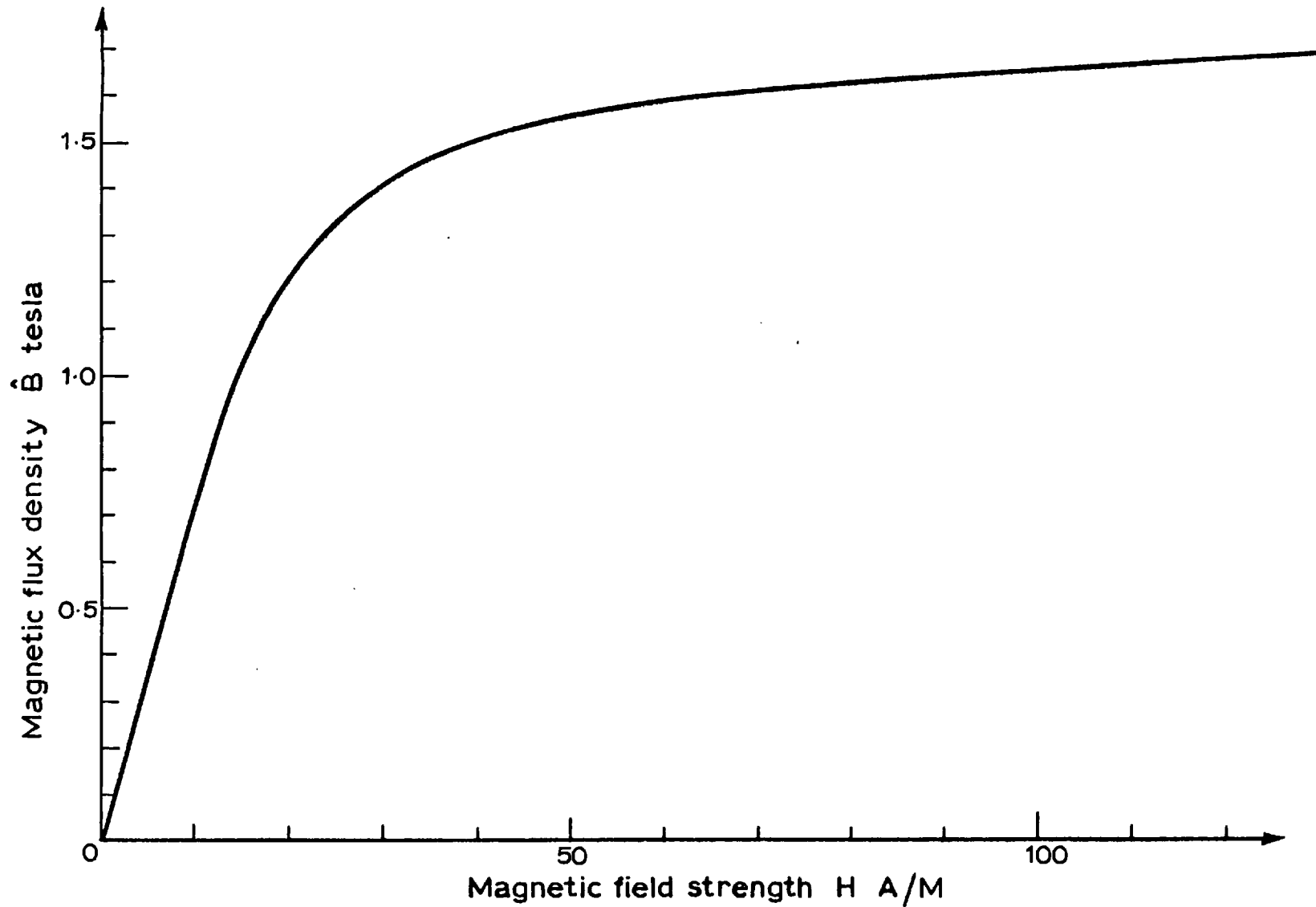


Fig. D1 Normal magnetization curve for Unisil/Alphasil 30 M 5

Thus the values of the iron reluctances to be inserted in the equivalent circuit shown in Fig. 6.5(b) are:

$$\begin{aligned} \mathcal{R}_{i1} &= 3319 \quad , \quad \mathcal{R}_{i2} = 11649 \quad , \quad \mathcal{R}_{i3} = 3319, \\ \mathcal{R}_{i4} &= 12189 \quad \text{and} \quad \mathcal{R}_{i5} = 37412. \end{aligned}$$